

1. Report No. 6.1		2. Government Accession No.		3. Recipient's Catalog No.	
4. Title and Subtitle Resilient Behavior of Asphalt Treated Base Course Material				5. Report Date August 1972	
				6. Performing Organization Code	
7. Author(s) R. L. Terrel/I. S. Awad				8. Performing Organization Report No.	
9. Performing Organization Name and Address University of Washington Department of Engineering Seattle, Washington 98195				10. Work Unit No.	
				11. Contract or Grant No. Y-1206	
				13. Type of Report and Period Covered Final Report	
12. Sponsoring Agency Name and Address Washington State Highway Commission Department of Highways Highway Administration Building				14. Sponsoring Agency Code	
15. Supplementary Notes Study was conducted in cooperation with the U.S. Department of Transportation, Federal Highway Administration.					
16. Abstract <p>This study was aimed at defining resilient properties (resilient modulus, Poisson's ratio) of asphalt treated base (ATB) under repeated loading. A brief program of testing these materials as found in the Washington State University test track and several in-service pavements in Western Washington was included. The purpose of these tests was to assist in defining the properties of field constructed ATB materials.</p> <p>A very sophisticated dynamic triaxial testing system was designed, constructed and utilized. Testing parameters for a wide range of conditions. were determined and analyzed. The resilient modulus was correlated with conventional tests and this approach shows promise for the transition from empirical to more basic engineering tests.</p>					
17. Key Words Asphalt Treated Base - Treated Base - Triaxial Testing - Base - Structural Design of Pavement - ATB Strength - ATB Design - ATB Flexure				18. Distribution Statement	
19. Security Classif. (of this report) Unclassified		20. Security Classif. (of this page) Unclassified		21. No. of Pages 213	22. Price



The contents of this report reflect the views of the authors who are responsible for the facts and the accuracy of the data presented herein. The contents do not necessarily reflect the official views or policies of the Washington State Department of Highways or the Federal Highway Administration. This report does not constitute a standard, specification, or regulation.

TABLE OF CONTENTS

<u>Chapter</u>	<u>Page</u>
CHAPTER I - INTRODUCTION	1
CHAPTER II - THEORETICAL BACKGROUND	9
Introduction	9
The Concept of Continuum Mechanics	10
The Theory of Elasticity	13
The Theory of Linear Viscoelasticity	15
The Viscoelastic Response	18
Permanent Deformations	23
CHAPTER III - THE TRIAXIAL TESTING SYSTEM	25
The Load Application System	26
Temperature Control System	29
The Measurement and the Monitoring Systems	30
CHAPTER IV - MATERIALS AND PROCEDURES	32
Asphalt	32
Aggregate	33
Sample Preparation	35
Laboratory Experimental Program	36
Conventional Tests	37
Triaxial Tests	38
Laboratory Tests of Core Specimens	40
CHAPTER V - TEST RESULTS AND DISCUSSION	42
The Resilient Modulus Tests	47
Correlation with Conventional Tests	52
The Modulus of Total Deformations	53
Creep Tests	55
Permanent Deformations	58
The Dynamic Modulus Tests	60
Time-Temperature Superposition	62
Core Sample Tests and Deflection Prediction	63
CHAPTER VI - SUMMARY, CONCLUSIONS AND RECOMMENDATIONS	65
REFERENCES	71
TABLES	75
FIGURES	109

LIST OF TABLES

<u>Table</u>	<u>Page</u>
1. Test Results on Asphalt Cement	32
2. Physical Description of Aggregate	33
3. Gradation of the Aggregate	34
4. Specific Gravity Test Results	35
5. Summary of Resilient Modulus Tests for 0.1 and 1.0 sec. Stress Durations	75
6. Summary of Resilient Modulus Tests for 0.1 and 1.0 sec. Stress Durations	76
7. Summary of Resilient Modulus Tests for 0.1 and 1.0 sec. Stress Durations	77
8. Summary of Modulus of Total Deformations for 0.1 and 1.0 sec. Stress Durations	78
9. Summary of Modulus of Total Deformations for 0.1 and 1.0 sec. Stress Durations	79
10. Summary of Modulus of Total Deformations for 0.1 and 1.0 sec. Stress Durations	80
11. Summary of the Coefficients in Equation 56 - $\epsilon = \sigma \alpha (\Delta t)^\beta$	81
12. Summary of the Coefficients in Equation 56 - $\epsilon = \sigma \alpha (\Delta t)^\beta$	82
13. Summary of the Coefficients in Equation 56 - $\epsilon = \sigma \alpha (\Delta t)^\beta$	83
14. Summary of the Creep Tests	84
15. Summary of the Creep Tests	85
16. Summary of the Creep Tests	86
17. Summary of the Complex Modulus Tests	87
18. Summary of the Complex Modulus Tests	88
19. Summary of the Complex Modulus Tests	89
20. Summary of the Complex Modulus Tests	90

<u>Table</u>		<u>Page</u>
21.	Summary of the Complex Modulus Tests	91
22.	Summary of the Complex Modulus Tests	92
23.	Summary of the Complex Modulus Tests	93
24.	Summary of the Complex Modulus Tests	94
25.	Summary of the Complex Modulus Tests	95
26.	Summary of the Complex Modulus Tests	96
27.	Summary of the Complex Modulus Tests	97
28.	Summary of the Complex Modulus Tests	98
29.	Summary of the Complex Modulus Tests	99
30.	Summary of the Complex Modulus Tests	100
31.	Summary of the Complex Modulus Tests	101
32.	Summary of the Complex Modulus Tests	102
33.	Summary of the Complex Modulus Tests	103
34.	Summary of the Complex Modulus Tests	104
35.	Dynamic Modulus /E*/ and Phase Lag ϕ for Class F Asphalt Treated and Hot-Mix Sand Asphalt Bases, Ring 4, WSU Test Track	105
36.	Dynamic Modulus /E*/ and Phase Lag ϕ for Class F Asphalt Treated and Hot-Mix Sand Asphalt Bases, Ring 4, WSU Test Track, (after the Asphalt Institute)	106
37.	Resilient Properties for Class F Asphalt Treated and Hot-Mix Asphalt Bases, Ring 4, WSU Test Track	107

LIST OF FIGURES

<u>Figure</u>		<u>Page</u>
1.	The Concept of Stress at Point P	109
	Components of the Stress Tensor	109
3.	Simple Linear Viscoelastic Models	110
4.	The Triaxial Chamber	111
4a.	Overall View of Dynamic Triaxial Testing System	112
4b.	Test Frame and Triaxial Chamber Showing Electro-Hydraulic Servo-Ram at Bottom	113
4c.	Close-Up of 4" Diameter by 8" High Asphalt Concrete Specimen in Triaxial Cell Prior to Connecting Lead Wires. Note Internal Frame that Permits Access to Specimens without Disassembly.	114
5.	Vertical Stress Functions Used by Various Investigators	115
6.	Variation of Calculated Vertical Compressive Stress Pulse Shape with Depth	116
7.	Axial Strains Resulting from Different Stress Pulse Shapes and Durations	117
8.	The Load Cell Used Inside the Triaxial Chamber	118
9.	Axial and Radial Stress Distribution Under Moving Load	119
10.	The System Used in Pulsing the Chamber Pressure	120
11.	The Temperature Control System	121
12.	Gradation Chart	122
12a.	Samples of Laboratory-Compacted Mixtures Illustrating Different Gradations	123
13.	Stress States Applied in the Triaxial Tests	124
13b.	Comparison of Benkelman Beam Deflections with Road Rater and Dynaflect for NE 124th Street	125
13c.	Comparison of Benkelman Beam Deflections with Road Rater and Dynaflect for Sign Route 167 Highway	126

<u>Figure</u>		<u>Page</u>
13d.	Comparison of Benkelman Beam Deflections with Road Rater and Dynaflect for Interstate 405	127
14.	Stress-Strain States Under Sustained Confining Pressures	128
15.	Stress-Strain States Under Sustained Confining Pressures	129
16.	Stress-Strain States Under Sustained Confining Pressures	130
17.	Stress-Strain States Under Sustained Confining Pressures	131
18.	Stress-Strain States Under Sustained Confining Pressures	132
19.	Stress-Strain States Under Sustained Confining Pressures	133
20.	Stress-Strain States Under Sustained Confining Pressures	134
21.	Stress-Strain States Under Sustained Confining Pressures	135
22.	Stress-Strain States Under Cyclic Axial and Radial Stresses	136
23.	Stress-Strain States Under Cyclic Axial and Radial Stresses	137
24.	Stress-Strain States Under Cyclic Axial and Radial Stresses	138
25.	Stress-Strain States Under Cyclic Axial and Radial Stresses	139
26.	Stress-Strain States Under Cyclic Axial and Radial Stresses	140
27.	Stress-Strain States Under Cyclic Axial and Radial Stresses	141
28.	Resilient and Total Strains Under Repeated Stress	142
29.	Coefficient B ₁ Versus Asphalt Content at 25, 45, 70 and 90°F	143
30.	Coefficient B ₁ Versus Asphalt Content at 25, 45, 70 and 90°F	144

<u>Figure</u>		Page
31.	Coefficient B2 Versus Asphalt Content at 25, 45, 70 and 90°F	145
32.	Coefficient B2 Versus Asphalt Content at 25, 45, 70 and 90°F	146
33.	Coefficient B3 Versus Asphalt Content at 25, 45, 70 and 90°F	147
34.	Coefficient B3 Versus Asphalt Content at 25, 45, 70 and 90°F	148
35.	Coefficient B4 Versus Asphalt Content at 25, 45, 70 and 90°F	149
36.	Coefficient B4 Versus Asphalt Content at 25, 45, 70 and 90°F	150
37.	Ratio B3/B2 Versus Asphalt Content at 25, 45, 70 and 90°F	151
38.	Ratio B3/B2 Versus Asphalt Content at 25, 45, 70 and 90°F	152
39.	Resilient Modulus Versus Asphalt Content at 25, 45, 70 and 90°F	153
40.	Resilient Modulus Versus Asphalt Content at 25, 45, 70 and 90°F	154
41.	Poisson's Ratio Versus Asphalt Content at 25, 45, 70 and 90°F	155
42.	Poisson's Ratio Versus Asphalt Content at 25, 45, 70 and 90°F	156
43.	Resilient Modulus Computed from Test Data, Equation 52, and Heukelom and Klomp	157
44.	Resilient Modulus Computed from Test Data, Equation 52, and Heukelom and Klomp	158
45.	Resilient Modulus Computed from Test Data, Equation 52, and Heukelom and Klomp	159
46.	Variation of Poisson's Ratio of Different Mixtures with Temperature	160
47.	Variation of Poisson's Ratio of Different Mixtures with Temperature	161
48.	Correlation Between the Stability Value and the Resilient Modulus	162

<u>Figures</u>		<u>Page</u>
49.	Correlation Between the Stability Value and the Resilient Modulus	163
50.	Log Axial Strain Versus Log Stress Duration at Different Temperatures	164
51.	Log Axial Strain Versus Log Stress Duration at Different Temperatures	165
52.	Log Axial Strain Versus Log Stress Duration at Different Temperatures	166
53.	Log Axial Strain Versus Log Stress Duration at Different Temperatures	167
54.	Log Axial Strain Versus Log Stress Duration at Different Temperatures	168
55.	Log Axial Strain Versus Log Stress Duration at Different Temperatures	169
56.	Log Axial Strain Versus Log Stress Duration at Different Temperatures	170
57.	Log Axial Strain Versus Log Stress Duration at Different Temperatures	171
58.	Log Axial Strain Versus Log Stress Duration at Different Temperatures	172
59.	Coefficient α Versus Temperature for Different Asphalt Contents	173
60.	Coefficient α Versus Temperature for Different Asphalt Contents	174
61.	Coefficient α Versus Temperature for Different Asphalt Contents	175
62.	Coefficient β Versus Temperature for Different Asphalt Contents	176
63.	Coefficient β Versus Temperature for Different Asphalt Contents	177
64.	Coefficient β Versus Temperature for Different Asphalt Contents	178
65.	Equation 59 Plotted Against Temperature for Different Asphalt Contents	179

<u>Figure</u>		<u>Page</u>
66.	Equation 59 Plotted Against Temperature for Different Asphalt Contents	180
67.	Equation 59 Plotted Against Temperature for Different Asphalt Contents	181
68.	Equation 59 Plotted Against Temperature for Different Asphalt Contents	182
69.	Equation 59 Plotted Against Temperature for Different Asphalt Contents	183
70.	Equation 59 Plotted Against Temperature for Different Asphalt Contents	184
71.	Variation of the Four-Element Model Parameters with Temperature	185
72.	Variation of the Four-Element Model Parameters with Temperature	186
73.	Variation of the Four-Element Model Parameters with Temperature	187
74.	Variation of the Four-Element Model Parameters with Temperature	188
75.	Variation of the Four-Element Model Parameters with Temperature	189
76.	Variation of the Four-Element Model Parameters with Temperature	190
77.	Creep Stress Versus Rate of Constant Creep at Different Temperatures	191
78.	Complex Modulus Versus Frequency at Different Temperatures	192
79.	Complex Modulus Versus Frequency at Different Temperatures	193
80.	Complex Modulus Versus Frequency at Different Temperatures	194
81.	Complex Modulus Versus Frequency at Different Temperatures	195
82.	Complex Modulus Versus Frequency at Different Temperatures	196
83.	Complex Modulus Versus Frequency at Different Temperatures	197

<u>Figures</u>	<u>Page</u>
84. Complex Modulus Versus Frequency at Different Temperatures	198
85. Complex Modulus Versus Frequency at Different Temperatures	199
86. Complex Modulus Versus Frequency at Different Temperatures	200
87. Axial Lag Angle ϕ_1 Versus Frequency at Different Temperatures	201
88. Axial Lag Angle ϕ_1 Versus Frequency at Different Temperatures	202
89. Axial Lag Angle ϕ_1 Versus Frequency at Different Temperatures	203
90. Axial Lag Angle ϕ_1 Versus Frequency at Different Temperatures	204
91. Axial Lag Angle ϕ_1 Versus Frequency at Different Temperatures	205
92. Axial Lag Angle ϕ_1 Versus Frequency at Different Temperatures	206
93. Axial Lag Angle ϕ_1 Versus Frequency at Different Temperatures	207
94. Axial Lag Angle ϕ_1 Versus Frequency at Different Temperatures	208
95. Axial Lag Angle ϕ_1 Versus Frequency at Different Temperatures	209
96. Shift Factor Versus Temperature (Reference Temperature = 70°F)	210
97. Master Complex Modulus $ E^* $ at Reference Temperature = 70°F	211
98. Master Complex Modulus $ E^* $ at Reference Temperature = 70°F	212
99. Master Complex Modulus $ E^* $ at Reference Temperature = 70°F	213
100. Comparison of Laboratory Prepared Mixtures with Cores of ATB Sampled from WSU Test Track and In-Service Pavements	214

<u>Figure</u>		<u>Page</u>
101.	Summary of Material Properties and Deflections for WSU Test Track Comparison	215

CHAPTER I

INTRODUCTION

In many parts of the world, the design of flexible pavement is still based on empirical methods which have been developed from engineering experience. These empirical methods cannot be extrapolated beyond their limits without full scale road trials to prove their applicability. In recent years, however, the increase of traffic, both in volume and axle loads, has led to the failure of many roads previously considered well designed. For this reason, therefore, researchers realized that a closer look at the pavement materials was desirable in order to develop a rational design procedure.

Due to the complexity of characterizing pavement materials, and the limitations of instrumentation, much of the reported work offered little help in changing design practice. This is, perhaps, due to the many simplifying assumptions which had to be introduced in the experimental procedure as well as the interpretation of the test results. Recently, however, there has been a sharp advancement in test instrumentation and an outstanding progress in processing the experimental results. This has been reflected through many fine investigations and has increased the demand for more improvements.

An asphalt pavement is a complex structure whose function is to provide a suitable surface for a highway, an airport, or other off-highway facility. The load of a vehicle or an aircraft is transmitted through the multilayered system of processed materials which have different mechanical properties. The stress distribution within this system is highly complex and to a large extent is dependent on the relative stiffnesses of the individual layers.

A rational structural design of a pavement section is inevitably complicated. This is due to the presence of many variables whose effects are not clearly understood. Nevertheless, it is still feasible to proportion a pavement section based upon the fundamental engineering properties of the materials. This approach does not necessarily suggest that we abandon the functional approach which is based on performance, but rather, to be the governing criterion.

Before one could develop a rational design method, the behavior of the pavement materials have to be well understood according to the laws of physics for different environments. It is apparent that many assumptions must be introduced because of the complex nature of the problem. The usefulness of such a method and its ability to predict the performance of the pavement structure will be a function of the validity of the assumptions used, and the degree of idealization introduced.

The relationship between stress and strain may be simple or complex depending upon the material itself and the environment in which it is used. For asphalt treated materials, this relationship in general takes the form:

$$\underline{\sigma}(\underline{x},t) = \int_{t=0}^t F [\underline{\epsilon}(\underline{x},t), T(\underline{x},t), a/c, \gamma, \underline{x},t]$$

where:

- \underline{x} = spacial coordinate matrix
- $\underline{\sigma}$ = induced or observed stress matrix
- $\underline{\epsilon}$ = induced or observed strain matrix
- T = temperature
- t = time at which the stress or strain is observed
- a/c = asphalt content
- γ = unit weight of sample (degree of compaction and/or air voids)

A number of experimental methods have been developed to describe the relationship between stress and strain for asphalt mixes. Two of these methods, the dynamic complex modulus and the modulus of resilient deformation, are similar. The concept and definition of the dynamic complex modulus for asphalt concrete, have been presented by Papazian (38). Seed, Chan, and Lee (43) developed the background and the concept of the modulus of resilient deformation. In both tests, vertical stresses are applied to a specimen and the resultant vertical strains measured. A modulus is calculated as the ratio of stress to the recoverable or resilient strain under repeated loading conditions. By the complex modulus test procedure, inelastic as well as elastic behavior may be measured.

The stiffness modulus is another concept for describing the relationship between stress and strain for asphalt mixes. Deacon, (12) presented the stiffness concept and calculated it from repeated beam flexure tests by measuring the beam's central deflection. Deacon measured the total deflection (recoverable and permanent), from which he computed the stiffness modulus. It is expected, therefore, that the stiffness modulus would differ from both the modulus of resilient deformation and the complex modulus.

The tests discussed above, are expensive, complicated, and, therefore, may not be available for different pavement design agencies. For this reason, and in order to effectively evaluate the modulus or strength properties of the paving materials, researchers have often attempted to correlate these properties to some standard or conventional tests. Many of these attempts were unsuccessful, and some showed some degree of correlation with a wide scatter. This scatter is expected and is due to either the inconsistency of the properties of the specimen tested or the experimental inaccuracies associated with the conventional tests. It should be recognized that these correlations

should be used for estimating only when actual test data are not available.

The following brief discussion of some of these approaches at least indicates that there is some potential for such correlation.

Nijboer (37) has suggested a method for predicting or estimating the asphalt mixture stiffness as correlated to the ratio of the Marshall stability and the Marshall flow value. Nijboer's formula was limited to a loading time of four seconds at high service temperatures (60°C). McLeod (30) also developed a similar procedure and suggested that the stiffness-Marshall correlation was valid for a range of mixtures.

Finn, et al, (17) working with data obtained from extracted cores of emulsion treated base layers have developed an expression relating the sand fraction of the aggregate and the penetration of the asphalt to the dynamic modulus.

Shook and Kallas (47) investigated the relationship between the flexural modulus and several routine or standard tests including the Marshall stability, Marshall flow value, Hveem stability, Hveem cohesiometer value, ultimate tensile strength, elongation in direct tension, and elongation in indirect tension or the split-tension test. Even though several corrections were made in regard to air-voids in the specimens, no practical degree of correlation was found between the resilient modulus and most of these other conventional test values. However, fairly good correlations were obtained using the results of the ultimate tensile strength of the Marshall stability/flow ratio as related to the resilient modulus.

Hadley, et al, (20) investigated possible correlations between the stiffness or resilient modulus and Poisson's ratio determined for the indirect tension test at 75°F and a standard beam test at 140°F . They found reasonable

correlations for a general range of test conditions for the modulus of elasticity and cohesimeter values, and for Poisson's ratio and stability.

One of the more useful as well as convenient methods for estimating resilient modulus of asphalt treated mixtures is based on the stiffness concept of van der Poel (50). By this method the stiffness or resilient modulus of pure asphalts can be estimated from nomographs. The penetration and ring and ball softening point of the asphalt in the mix are needed as input for this estimate.

Heukelom and Klomp (21) extended the work of van der Poel to estimate the stiffness of asphalt treated mixtures. In addition to the penetration and ring and ball softening point data, the volume concentration of the aggregate C_v , must be determined. Heukelom and Klomp's semi-empirical equation for mixture stiffness is reliable for mixtures with approximately 3% air-voids. Subsequently, van Draat and Sommer have modified this relationship to include the effects of different air voids.

The nomograph suggested by Heukelom and Klomp seems to indicate a fairly good approach to predicting stiffness over a range of temperatures and times of loading, at least for a range of conventional mixes. However, there have been incidences where this nomograph fails to predict experimental data with any reasonable degree of certainty. There may be some asphalt cementing materials which do not follow the stiffness concepts originally developed by van der Poel. These may be based on different viscosity relationships, sources of the asphalt, or other factors. Also, the low asphalt content as used in some of the leaner asphalt treated bases may cause the stiffness to deviate somewhat from that predicted by Heukelom and Klomp.

The analysis of the asphalt medium is most commonly done by the theory of elasticity. In this theory, the asphalt mix is assumed to be linear or

non-linear elastic, homogeneous and isotropic. The system to be analyzed is considered to consist of "n" layers, the nth of which is the subgrade. All layers are assumed to be of infinite horizontal extent, and the nth layer is assumed to be semi-infinite in depth.

The finite element method is the latest technique utilizing the theory of elasticity. One major advantage of this method is that the material properties can be varied within each layer in the horizontal direction.

The effects of non-linear material response on the behavior of pavement have been investigated (13). The iterative solution by the finite element method was employed. In each iterative cycle, the material properties were adjusted according to predetermined laboratory relationship between stresses and strains.

The theory of linear viscoelasticity has also been used to describe the behavior of asphalt pavements. Huang represented the layered pavement by a series of Kelvin models with a spring and a dashpot added in series. He produced surface and interfacial stresses and deflections as functions of time and modular ratios for multilayer systems.

The use of a linear elastic, non-linear elastic, or a linear viscoelastic theory to describe the behavior of asphalt pavement depends largely on the relative change in loads, temperature, and the speed of traffic. For a change in the load intensity from 10 to 50 psi, for example, the stiffness of the pavement might be reduced by less than 5 percent. A change in temperature from 40 to 70°F reduces the stiffness to one-quarter of its original value. Moreover, at low temperatures, the asphalt pavements behave elastically. This is due to the rapid increase in the viscosity of the bituminous binder as the temperature decreases.

The frequency at which the repeated load is applied (traffic speed) greatly influences the behavior of the material. Papazian (38) found that the material complex modulus increases as the frequency increases up to a certain value, after which it remains constant. This stable value of the complex modulus was found to be the value of the material instantaneous elasticity. This is because at high frequencies the viscous elements "do not have time" to react, and the material behaves elastically.

The investigations briefly discussed in the preceding paragraphs, and the various relationships for relating the mechanical characteristics of asphalt mixtures, have essentially been confined to conventional, high-quality surfacing materials. Asphalt treated base (ATB) is a lower quality treated base material used in the State of Washington, as well as numerous other states. This material has several advantages over untreated bases, such as reduced thickness, waterproofing, frost resistance, etc. Originally, the Washington Highway Department utilized ATB primarily as a working platform which was placed directly on the subgrade. This ATB layer acts as a covering mat to protect the subgrade from early autumn rains and construction traffic, and often served as the temporary pavement through the winter. Finally, the ATB was overlain with the usual asphalt concrete or portland cement concrete pavement.

ATB, as used in the State of Washington, is a well-graded, crushed rock or natural gravel mixed with paving grade asphalt. Generally, the mixtures contain relatively low asphalt percentages (2.5 to 4.5), while the required Hveem stabilometer value of 20 to 40 approach those of conventional mixtures.

One of the major questions in current procedures is the advisability of using low asphalt contents in ATB materials. In order to more fully utilize the attributes of ATB, it may be feasible to increase the asphalt content.

It has been suggested that this would increase the tensile strength and ultimately improve the fatigue characteristics. Little work has been done on the influence of asphalt content on the behavior of treated bases. Low asphalt contents increase the stress dependency and reduce the temperature susceptibility, so that the material is best treated as non-linear elastic. Excessive amounts of asphalt, on the other hand, increase the thickness of the asphalt film between the aggregate particles, and thus increase the tendency towards a more viscous behavior.

The objective of the research described herein is to better define the properties of ATB. This includes investigating the basic stress-strain relationships of this material in order to obtain the required parameters which can be used in a rational design procedure.

CHAPTER II

THEORETICAL BACKGROUND

Introduction

Matter as described by physicists is not continuous. The molecular concept shows that solids, liquids, and gases differ in the average spacing of molecules, with solids being more closely packed than liquids or gases. In practice, however, the discrete discontinuity is ignored, and the material is treated as continuous with no gaps. Molecules exist in a vast variety of structures and sizes ranging from very simple to large and highly complex. These molecules, if no boundary forces exist, are in a state of equilibrium under the internal forces of attraction and repulsion. The physical properties of a material depends largely on the arrangement of the atoms which can be classified as: (1) molecular structure or grouping of atoms, (2) crystal structure, i.e. a repetitious pattern of atoms, and (3) amorphous structure with no specific formation.

Upon the application of external forces, a redistribution of the resultant molecular forces take place throughout the body. This causes changes in the configurational arrangement of the molecules. If this change is reversible under the applied load, the behavior is described as elastic. If the applied loads are high enough to cause permanent change or slip in the molecular arrangement, then the behavior is plastic. Some materials, show a pronounced influence of the rate of loading, creep, and relaxation. Such materials are called viscoelastic and they include metals at elevated temperature, concrete, asphalts, and plastics.

An asphalt mixture is a combination of a non-linear elastic matrix (aggregate) (27) cemented by a non-linear viscoelastic binder (asphalt). The behavior

of the mixture, therefore, is neither elastic nor viscoelastic but rather a non-linear combination of both depending on the mixture ingredient as well as environmental factors. Furthermore, due to the enormous stiffness of the aggregate particles relative to the asphalt binder, the distribution of strains and deformations at a finite point are highly complex. Strains due to low stresses, in effect, are limited to shear due to sliding between adjacent aggregate particles. This suggests, phenomenologically, the idealization of the mixture as a series of solid particles connected by a system of springs and dashpots (28). Such idealization, is more complicated due to the internal friction provided by the interlocking of the aggregate particles.

Finally, since most problems confronting engineers in pavement analysis involve boundary distances and loaded areas which are large compared with individual particles, it appears reasonable to invoke the assumptions of the theory of continuum mechanics as a basis for analytical consideration of these problems.

The Concept of Continuum Mechanics

Consider a body under the action of a system of forces F_i which are in equilibrium (Fig. 1). Consider, further, a planar surface area ΔS oriented by the unit normal vector n_i . Let ΔF_i be the total force that the material on the $+n_i$ side exerts on the material on the $-n_i$ side, the stress vector σ_i at the point P corresponding to the direction n_i is defined as (10):

$$\sigma_i = \lim_{\Delta S \rightarrow 0} \frac{\Delta F_i}{\Delta S} = \frac{dF_i}{dS} \quad (1)$$

The stress σ_i has three components σ_{1i} , σ_{2i} , and σ_{3i} acting on the surface elements whose normals are in the positive x_1 , x_2 , and x_3 directions. The three stresses σ_{1i} , σ_{2i} , and σ_{3i} have a total of nine components, they

are called the stress tensor σ_{ij} and shown in Figure (2).

$$\sigma_{ij} \Rightarrow \begin{bmatrix} \sigma_{11} & \sigma_{12} & \sigma_{13} \\ \sigma_{21} & \sigma_{22} & \sigma_{23} \\ \sigma_{31} & \sigma_{32} & \sigma_{33} \end{bmatrix} \quad (2)$$

If no body moments are acting, then it can be easily proven that the shearing components of the stress tensor are symmetric, thus:

$$\sigma_{ij} = \sigma_{ji}$$

and of the nine components of the stress tensor, only six are independent.

The equilibrium of a volume V of a continuum subjected to a system of surface forces F_i , body forces b_i , and inertia forces $\rho\ddot{u}$ requires that the resultant force and moment be zero; or:

$$\sigma_{ij,j} + b_i = \rho\ddot{u} \quad (3)$$

The entity of all strains occurring at a point form a strain tensor, ϵ_{ij} . If u_i are the components of the displacements, a_j are the components of the initial position, then the Lagrangian nonlinear strain tensor is:

$$\epsilon_{ij} = \frac{1}{2} \left[\frac{\partial u_i}{\partial a_j} + \frac{\partial u_j}{\partial a_i} + \frac{\partial u_r}{\partial a_i} \frac{\partial u_r}{\partial a_j} \right] \quad (4)$$

Assuming that the derivatives of the displacements to be small, $\frac{\partial u_i}{\partial a_j} \ll 1$, the term involving the product of these derivatives in Equation 4 can be neglected in comparison with the other two terms, so that:

$$\epsilon_{ij} = \frac{1}{2} \left[\frac{\partial u_i}{\partial a_j} + \frac{\partial u_j}{\partial a_i} \right] \quad (5)$$

The nonlinear as well as the linear strain tensors are symmetric and, therefore, have six independent components. Since these six components are derived from three displacements u_i , then they cannot be prescribed arbitrarily and, therefore, have to be connected by a corresponding number of restrictions. These restrictions are referred to as the compatibility equations:

$$\epsilon_{ij,kl} + \epsilon_{kl,ij} = \epsilon_{ik,jl} + \epsilon_{jl,ik} \quad (6)$$

The physical meaning of the strain compatibility is that deformed pieces of a continuum fit together properly with no gaps or overlaps.

In order to solve a boundary problem more equations are needed in addition to Equations 3 and 5. The required additional equations should be a functional relationship between the stress, the density, and the state of motion. This additional relationship should be an invariant and not a function of configuration. It is provided by the kinetic equations of state which are referred to as the constitutive equations. The characterization of a material is basically the selection of the constitutive equations to represent the material behavior, and in the evaluation of the parameters in these equations.

For asphalt mixes, the stress at a point x , at a time t is a function of the histories of strain (ϵ), temperature (T), as well as of the position and age. It was suggested (13) that such a relationship can be expressed by the following statement:

$$\sigma(x,t) = \int_{t=0}^t F [\epsilon(x,t), T(x,t), x,t] \quad (7)$$

For isothermal behavior, this relationship can be expressed in the most general form:

$$\sum_{i=0}^n p_i D^i \sigma_{ij} = \sum_{r=0}^m q_r D^r \epsilon_{ij} \quad (8)$$

where D^i and D^r are the i^{th} and r^{th} linear time derivatives, p_i and q_r are the material parameters which can be evaluated experimentally. These parameters can be either constants in a linear behavior, or functions of some variables in which case the behavior is characterized as nonlinear.

Nonlinearity of the material response can take any of the following forms:

- a) Geometric nonlinearity due to increasing strains beyond the limits of validity of infinitesimal strain theory, Equation (4).
- b) Material nonlinearity due to nonlinear properties of the material or material components.
- c) A combination of (a) and (b).

The Theory of Elasticity

As was discussed before, the response of asphalt mixes is time dependent and consequently should be analyzed as such. Under some special conditions, however, this behavior can be approximately considered as elastic and reasonable solutions of stresses and deformations can be obtained. It is, therefore, justified to look into this theory and indicate the usefulness as well as the limitations of its applicability.

In the classical theory of linear elasticity, the temperature effects are neglected. Therefore, the stress components σ_{ij} are to be uniquely related to the strain components. Assuming the absence of stress components in the undeformed state, Equation (8) takes the general form:

$$\epsilon_{ij} = B_{ijkl} \sigma_{kl} \quad (9)$$

Equation (9) is the generalized Hook's law for a linear elastic solid.

B_{ijkl} is the modulus tensor and has 81 constants. However, since σ_{ij} and

ϵ_{ij} are both symmetrical, and due to the existence of strain energy, it can be shown that there are only 21 independent constants for the general case of complete anisotropy.

It is likely that pavement material as they exist in layered structure will have cross-isotropy, with the axis of elastic symmetry coinciding with the vertical axis. If in addition the stress is axisymmetric about the vertical axis, then using the cylindrical notation, and τ and γ for shear stresses and strains,

$\tau_{r\theta} = \tau_{z\theta} = \gamma_{r\theta} = \gamma_{z\theta} = 0$, Equation (9) becomes:

$$\begin{Bmatrix} \epsilon_{rr} \\ \epsilon_{\theta\theta} \\ \epsilon_{zz} \\ \gamma_{rz} \end{Bmatrix} = \begin{bmatrix} B_{11} & B_{12} & B_{13} & 0 \\ B_{21} & B_{22} & B_{23} & 0 \\ B_{31} & B_{32} & B_{33} & 0 \\ 0 & 0 & 0 & B_{44} \end{bmatrix} \begin{Bmatrix} \sigma_{rr} \\ \sigma_{\theta\theta} \\ \sigma_{zz} \\ \tau_{rz} \end{Bmatrix} \quad (10)$$

In the triaxial test, the radial and the vertical stresses are principal stresses, $\tau_{rz} = \gamma_{rz} = 0$, and since $\sigma_{rr} = \sigma_{\theta\theta}$, $\epsilon_{rr} = \epsilon_{\theta\theta}$, then:

$$\begin{Bmatrix} \epsilon_{rr} \\ \epsilon_{zz} \end{Bmatrix} = \begin{bmatrix} (B_{11} + B_{12}) & B_{13} \\ (B_{31} + B_{32}) & B_{33} \end{bmatrix} \begin{Bmatrix} \sigma_{rr} \\ \sigma_{zz} \end{Bmatrix}$$

or:

$$\begin{Bmatrix} \epsilon_{rr} \\ \epsilon_{zz} \end{Bmatrix} = \begin{bmatrix} B_1 & B_2 \\ B_3 & B_4 \end{bmatrix} \begin{Bmatrix} \sigma_{rr} \\ \sigma_{zz} \end{Bmatrix} \quad (11a,b)$$

If we define E_z and E_r as Young's moduli in the vertical and the radial directions, $\nu_{r\theta}$ and ν_{rz} as the ratio of circumferential and axial strain to radial strain, ν_{zr} as the ratio of radial strain to axial strain, then Equation 11 becomes:

$$\begin{Bmatrix} \epsilon_{rr} \\ \epsilon_{zz} \end{Bmatrix} = \begin{bmatrix} \frac{1}{E_r} (1 - \nu_{r\theta}) & \frac{-\nu_{rz}}{E_z} \\ \frac{-2\nu_{zr}}{E_r} & \frac{1}{E_z} \end{bmatrix} \begin{Bmatrix} \sigma_{rr} \\ \sigma_{zz} \end{Bmatrix} \quad (12)$$

For an isotropic material, $E_z = E_r = E$, and $\nu_{r\theta} = \nu_{rz} = \nu_{zr} = \nu$

$$\begin{Bmatrix} \epsilon_{rr} \\ \epsilon_{zz} \end{Bmatrix} = \begin{bmatrix} \frac{1}{E} (1 - \nu) & \frac{-\nu}{E} \\ \frac{-2\nu}{E} & \frac{1}{E} \end{bmatrix} \begin{Bmatrix} \sigma_{rr} \\ \sigma_{zz} \end{Bmatrix} \quad (13)$$

E and ν in Equation 13 are the only two constants needed to characterize an isotropic linear elastic material.

The Theory of Linear Viscoelasticity

Certain materials may exhibit combined solidlike and liquidlike characteristics even under infinitesimal strains or strain rates. If such material is subjected to a constant stress, it continues to deform slowly with time, or creeps; if it is constrained at a constant deformation, on the other hand, the required constraining stress diminishes gradually, or relaxes. When the applied stress on such a material oscillates sinusoidally, the resulting

oscillating strain is not in phase with the stress, but lags with an angle somewhere between zero and 90 degrees. The behavior of this material shows spectacular dependency on the temperature; its consistency, in fact, ranges between glasslike at low temperatures and rubber or fluidlike at higher temperatures. Materials whose behavior exhibit such characteristics are referred to as viscoelastic.

The behavior of viscoelastic materials in a uniaxial direction can be represented by mechanical models composed of springs (Hookian elements) and dashpots (Newtonian elements). These basic elements are combined in different models to best fit a certain material response. Model representation, however, is limited to a combination that yields the desired accuracy without complicating the analytical manipulation beyond practical feasibility. Therefore, considerable judgement must be exercised in selecting a model which may adequately represent some given response, such as creep for example. It should be noted, at this point, that this same model may not necessarily represent some different response for the same material. In other words, it may be necessary to use different models to describe different components of a material's response, such as shear and dilatation. Figure (3) shows typical linear viscoelastic models which are used in theoretical analysis of idealized material response. The differential equation of any of Kelvin or Maxwell or a combination of both has the general form:

$$\sum_{i=0}^n p_i D^i \sigma = \sum_{r=0}^m q_r D^r \epsilon \quad (14)$$

p_i , D^i , q_r , and D^r were defined earlier.

Equation 14 may also be written as:

$$P\sigma = Q\epsilon \quad (15)$$

where

$$P = \sum_{i=0}^n p_i D^i, \quad Q = \sum_{r=0}^m q_r D^r \quad (16)$$

If a viscoelastic material is isotropic, a hydrostatic stress must produce a dilatation and no distortion. A shear stress, on the other hand, produces shear strains and no dilatation. This suggests an approach where Equation 15 is separated into dilatation and shear as follows:

$$P'\sigma_{ii} = Q'\epsilon_{ii} \quad (17)$$

$$P''s_{ij}^* = Q''e_{ij}^{**} \quad (18)$$

Equations 17, and 18 can be transformed into algebraic relationships by applying the Laplace transformation.^{***} These algebraic relations, then, become identical with the following elastic counterparts:

$$\sigma_{ii} = 3K \epsilon_{ii} \quad (19)$$

$$s_{ij} = 2G e_{ij} \quad (20)$$

where K and G are the bulk and the shear moduli respectively.

This approach leads to a general principle of correspondence between the elastic solution and the viscoelastic one. This principle is usually expressed in terms of the viscoelastic substitutes for the elastic constants

* s_{ij} is the deviatoric stress tensor

** e_{ij} is the deviatoric strain tensor

*** The Laplace transform of $F(t)$ denoted by $\mathcal{L}\{F(t)\}$ or $f(s)$ is defined by:

$$\mathcal{L}\{F(t)\} = f(s) = \int_0^{\infty} \exp(-st) F(t) dt$$

in order to obtain the viscoelastic solution. These substitutions are as follows:

$$3K \rightarrow \frac{Q'(s)}{P'(s)} \quad , \quad 2G \rightarrow \frac{Q''(s)}{P''(s)} \quad (21a,b)$$

$$E \rightarrow \frac{3Q''(s)Q'(s)}{2P''(s)Q'(s) + Q''(s)P'(s)} \quad , \quad \nu \rightarrow \frac{P''(s)Q'(s) - Q''(s)P'(s)}{2P''(s)Q'(s) + Q''(s)P'(s)} \quad (22a,b)$$

The Viscoelastic Response

It has been demonstrated (35), (42), that the four-element model could provide a general approximation of the behavior of asphalt treated material over a wide range of load and ambient conditions. It should be emphasized, however, that this modeling was limited to describe the material behavior in a uniaxial direction. In order to study the behavior under the triaxial conditions, a more general approach would be to separate the material behavior in shear and dilatation.

It is believed that the four-element model represents within reasonable approximation the shear behavior of asphalt treated materials. It is also believed that such material, at low void contents, can adequately be considered to behave elastically in dilatation.* At this point, it is important to realize that in order to truly model a material response, it is necessary to utilize more than one combination of the models displayed in Figure (3).

For the four-element model, Equation 14 becomes:

$$[1 + p_1D + p_2D^2] \sigma = [q_1D + q_2D^2] \epsilon \quad (23)$$

*This assumption was not verified experimentally, and a more acceptable model, is perhaps, the Kelvin model.

This differential equation can now be solved for any particular stress $\sigma = \sigma(t)$.

Consider the creep test, where $\sigma = \sigma_0 H(t)$, in which $H(t)$ is the Heaviside unit step function,* and σ_0 is the magnitude of the uniaxial creep stress. In this case, the expression for the axial and the lateral strains ϵ_1 and ϵ_3 are:

$$\epsilon_1(t) = \sigma_0 \left[\frac{1}{9K} - \frac{2q_2}{3q_1^2} + \frac{2p_1}{3q_1} \right] + \left[\frac{2}{3q_1} \right] t + \frac{2}{3} \left[\frac{p_2}{q_2} - \frac{p_1}{q_1} + \frac{q_2}{q_1^2} \right] \exp\left(-\frac{q_1}{q_2} t\right) H(t)$$

(24)

and:

$$\epsilon_3(t) = \sigma_0 \left[\frac{1}{9K} - \frac{q_2}{3q_1^2} - \frac{p_1}{3q_1} \right] - \left[\frac{1}{3q_1} \right] t - \frac{1}{3} \left[\frac{p_2}{q_2} - \frac{p_1}{q_1} + \frac{q_2}{q_1^2} \right] \exp\left(-\frac{q_1}{q_2} t\right) H(t)$$

(25)

If in a creep test, the vertical as well as the lateral strains were recorded at the same time intervals t , then a curve fitting technique was employed, $\epsilon_1(t)$ and $\epsilon_3(t)$ would be determined. The curve fitting functions in this case will be:

$$\epsilon_1(t) = \sigma_0 \{C_1 + C_2 t + C_3 \exp(-C_4 t)\} \quad (26)$$

and

$$\epsilon_3(t) = \sigma_0 \{C_1 + C_2 t + C_3 \exp(-C_4 t)\} \quad (27)$$

where C_i , and C_i' are constants to be determined from the curve fitting.

The material constants q_i , p_i , and K can then be computed.

*The Heaviside unit step functions, $H(t)$ is defined by:

$$H(t) = \begin{cases} 0, & t \leq 0 \\ 1, & t > 0 \end{cases}$$

Consider now the case where the stress is an oscillating function of time, $\sigma(t) = \sigma_0 \sin \omega t$, where ω is the angular frequency in rad/sec. If we assume that the viscoelastic deformations are slow enough that accelerations are very small, then the inertia effects can be neglected. In this case, if the material is linear viscoelastic, then the resulting steady state response will be also a sinusoidal oscillating strain of the same frequency but out of phase with the stress by the lag angle ϕ :

$$\epsilon(t) = \epsilon_0 \sin(\omega t - \phi) \quad (28)$$

The complex modulus $|E^*|$ is defined as the magnitude of the ratio of the oscillating vertical stress to the oscillating vertical strain:

$$|E^*| = \frac{\sigma_0}{\epsilon_0} \quad (29)$$

E^* is a complex quantity which can be put in the form:

$$E^* = E_1 + iE_2 \quad (30)$$

E_1 and E_2 are the in-phase (storage) and the out-of-phase (loss) moduli respectively. E_1 and E_2 may also be computed from:

$$E_1 = |E^*| \cos \phi_1 \quad (31)$$

and

$$E_2 = |E^*| \sin \phi_1 \quad (32)$$

The transverse modulus $|T^*|$ is also defined as the magnitude of the ratio of the oscillating vertical stress to the oscillating lateral strain:

$$|T^*| = \frac{\sigma_0}{\epsilon_0^3} \quad (33)$$

The lateral strain in this case lags behind the stress by an angle ϕ_3 which is not necessarily equal to the axial shift angle ϕ_1 .

The complex Poisson's ratio $|\nu^*|$ is defined as:

$$|\nu^*| = \frac{\epsilon_3^0}{\epsilon_1^0} \quad (34)$$

Other terms can be defined as the shear complex modulus G^* , the shear complex compliance J^* , the bulk complex modulus K^* , the bulk complex compliance B^* , and axial complex compliance D^* as follows:

$$G^* = \frac{E^*}{2(1 + \nu^*)} \quad (35)$$

$$J^* = \frac{1}{G^*} \quad (36)$$

$$K^* = \frac{E^*}{3(1 - 2\nu^*)} \quad (37)$$

$$B^* = \frac{1}{K^*} \quad (38)$$

and
$$D^* = \frac{1}{E^*} \quad (39)$$

Equations 29-39 suggest that if two independent complex moduli were determined for a homogeneous, isotropic, and linear viscoelastic material it is possible to write the stress-strains relationships in the frequency domain. These relationships are identical to the elastic counterparts in the time domain:

$$\epsilon_{11}^* = \frac{1}{E^*} [\sigma_{11}^* - \nu^*(\sigma_{22}^* + \sigma_{33}^*)] \quad \dots \text{and two others}^\dagger \quad (40)$$

$^\dagger \sigma^*$ is the Fourier transform of $\sigma(t)$

$$\sigma^* = \int_{-\infty}^{\infty} \sigma(t) \exp(-i\omega t) dt = \frac{\sigma_0}{i\omega} \quad \text{for a constant stress } \sigma_0.$$

$$\epsilon^*_{13} = \frac{1}{2G^*} \sigma^*_{13} \quad \dots \text{ and two others} \quad (41)$$

In order to phenomenologically obtain the response of the models displayed in Figure (3), consider for convenience the stress as

$$\sigma = \sigma_0 \exp(i\omega t) = \sigma_0 (\cos \omega t + i \sin \omega t) \quad (42)$$

If this stress is introduced in Equation 14, we find that the strain must have a factor $\exp(i\omega t)$

$$\epsilon = \epsilon_0 \exp(i\omega t) \quad (43)$$

Equation 14 then becomes:

$$\sigma_0 \sum_{\ell=0}^n p_{\ell}(i\omega)^{\ell} \exp(i\omega t) = \epsilon_0 \sum_{r=0}^m q_r(i\omega)^r \exp(i\omega t) \quad (44)$$

or

$$\epsilon_0 = \sigma_0 \frac{\sum_{\ell=0}^n p_{\ell}(i\omega)^{\ell}}{\sum_{r=0}^m q_r(i\omega)^r} = \sigma_0 \frac{P(i\omega)}{Q(i\omega)} \quad (45)$$

Since $E^* = \frac{\sigma_0}{\epsilon_0}$, then:

$$E^* = \frac{Q(i\omega)}{P(i\omega)} = E_1 + iE_2 \quad (46)$$

With little mathematical manipulation an expression can be obtained for E^* by substituting $(i\omega)$ for (D) . The real part of E^* is E_1 and the imaginary part is E_2 .

For a real material, there are two distinct experimental methods for obtaining the complex modulus. One method is based on a series of sinusoidally oscillating stresses over a wide range of frequencies. For each frequency, the complex modulus is completely defined by magnitude and phase. The second method is based on a static test $\sigma(t)$ whose transform in the frequency domain is $\sigma^*(i\omega)$. Mathematically then, it is conceivable to transform the static response $\epsilon(t)$ into the frequency domain $\epsilon^*(i\omega)$, and the ratio of the transformed stress to the transformed strain yields the desired modulus:

$$E^* = \frac{\sigma^*(i\omega)}{\epsilon^*(i\omega)} \quad (47)$$

Permanent Deformations

Permanent deformations due to moving traffic loads can take place in one or all layers in a pavement section. This permanent deformation can be interpreted as a result of time-dependent deformations or volume changes due to material densification. Excessive permanent deformation is a sign of failure from the standpoint of highway serviceability and little work has been invested in studying it.

Several attempts have been made to characterize permanent deformations in the subgrade as well as the asphalt concrete surface materials. The most significant of these are, perhaps, the quasi-elastic approach by Romain (40) and the viscoelastic approach by Moavenzadeh (32) and Griggs (19).

In the quasi-elastic approach, the theory of elasticity is used to obtain the strain distribution in the layered system. If, then, a pre-existing relationship between the permanent strain and the elastic strain is utilized, the permanent strain can be integrated over the effective thickness of a layer to obtain the total rut depth. This method, in spite of its simplicity, is based

on the existence of deformation laws which characterize the permanent strain in terms of the elastic stress or strain and the number of stress applications. Such laws, if they can be obtained, require an extensive program of testing different materials at different stress and environmental conditions.

The second approach utilizes the theory of linear viscoelasticity in accumulating the permanent strains as the traffic load moves from $-\infty$ to $+\infty$ at a certain speed v . Griggs obtained a general expression of the surface deformation of any viscoelastic model due to a point load moving on a semi-infinite medium. His formulation, however, does not yield a realistic value for the surface deformation. All solid viscoelastic models yielded no deformations, and all fluid viscoelastic models resulted in infinite deformations. It is for this reason that Moavenzadeh considered only finite rebound time for the Kelvin model after which deformations cease and become permanent.

The theory of linear viscoelasticity while requiring many approximations, has a sounder theoretical basis and a greater potential as a tool for future research than the quasi-elastic approach. The fact that this theory does not yield an answer at the present time does not necessarily disqualify it, it only displays another example of the complex behavior of asphalt mixtures.

In conclusion, in order to combat the unrealistic answers obtained by the theory of linear viscoelasticity, it is perhaps necessary to investigate the time as well as the stress non-linearity of permanent deformations. This can be accomplished by an extensive test program that includes creep tests as well as repeated triaxial tests.

CHAPTER III

THE TRIAXIAL TESTING SYSTEM

In the search for a "rational" design method of asphalt pavements, much of the work reported in recent years emphasized the importance of laboratory testing. Research into the response of asphalt pavement materials is now extensive as well as intricate.

In order to characterize asphalt materials in the laboratory, the specimen has to be subjected to environments simulating the field conditions. This can be achieved in many different ways, of which the slab tests and the triaxial tests are the most common.

The dynamic bending tests are widely used, particularly to evaluate the fatigue resistance of pavement materials. Due to limitations in the testing facilities, however, this type of test has been limited to either small slab thicknesses, or beams of actual thicknesses. This would limit the test to a particular aggregate size and introduces the model effects, or unrealistic boundary conditions in the case of beams. The subgrade effects are usually either ignored or substituted with springs or rubber layers.

The triaxial test, despite its limitations, can adequately simulate the conditions of any point in the pavement or subsoil. Repeated load triaxial tests have been successfully used in the determination of permanent rutting characteristics of both stabilized and unstabilized pavement materials.

Figures (4a, 4b, and 4c) illustrate the main features of the triaxial testing system designed to carry out the proposed investigation. The cell itself, unlike those of conventional design, provides continuous circulation of silicone oil at a constant temperature and under the required

pressure (Fig. 4d). This can be accomplished by having the entire temperature control system under the same pressure. For this purpose, therefore, the heating tank and the chamber are equipped with belloframs connected to two pressure reservoirs which provide two levels of pressure, static and pulsating.

A special type bellofram is provided on the bottom of the chamber to act as a seal and a separation between the triaxial chamber and a "sub-chamber." This "sub-chamber" can be either vented or connected to the same pressure as the chamber by a shut-off valve. By doing this, it is possible to separate or isolate the vertical and lateral stresses.

The testing system was designed for testing soils as well as asphalt mixes. With this in mind, it was essential that the system should have an accurate control over the following components:

1. The load application system.
2. The temperature control system.
3. The measurement and the monitoring systems.

The Load Application System:

As traffic moves on a highway pavement, the vertical and the lateral stresses change for a period of time such that each wheel pass can be considered as a stress pulse. The magnitude, shape and duration of these pulses vary with the wheel load, its speed, and the depth in the pavement at which the stress is considered.

Little information is available concerning the actual shape of the vertical stress pulse and its variation with depth. Most researchers used the data obtained from full scale test tracks (Fig. 5). The shape of the stress pulse can also be theoretically computed by the elastic

theory knowing the speed of the moving load for different depths (Fig. 6). It is clear that there is little correspondence between the actual observed pulses and those used in the laboratory, and that the full sine stress pulse is the closest to the in situ conditions. Due to limitations in the experimental as well as the theoretical interpretation, however, this pulse is replaced by either a triangular or a square shape.

In order to select a pulse shape, an experimental investigation was carried out which included the full sine, the square, and the triangular stresses. In this experiment, a stress of 30 psi was applied in the sinusoidal and triangular modes for 0.1, 1.0, and 10 seconds. The specimen was then subjected to combinations of percentages of both the stress duration and magnitude. The result of this investigation is shown in Fig. (7) and the following are the conclusions:

1. There is no significant difference in the magnitude of the total or the resilient strains between the triangular or the sinusoidal stress pulses.
2. An equivalent square pulse can be obtained by:
 - a) applying the same stress but for a duration of 33% of the equivalent sinusoidal, or
 - b) applying 66% of the stress with the same duration as the equivalent sinusoidal.

It was also concluded that a square vertical stress pulse is a reasonable approximation of the actual conditions within a pavement layer. This approximation certainly simplifies the model fitting and the subsequent analysis of the data.

The axial load is controlled by a load cell which is fixed to the upper side of the test specimen inside the triaxial cell. By doing this, problems resulting from friction are essentially eliminated. Moreover, in designing the load cell, it was important to isolate the effects of the chamber pressure and the vertical stress. In other words, to have a load cell that is insensitive to chamber pressure variations. Fig. (8) shows the load cell used in this experimental study.

The axial load is applied to the test specimen by a closed loop servo-hydraulic system (MTS). This system has the following main features:

- a) Stress or strain controlled
- b) Load capacity = 12,000 lbs.
- c) Hydraulic power supply = 20 gpm at 3000 psi
- d) Maximum stroke = 5 inches
- e) Frequency range = 0.001 - 1100 cps.
- f) Load mode = 12 modes with special control on individual pulse spacing (0.1 - 22 seconds).

The n-layer computer program was used to plot the variation of the lateral pressure as a result of a moving load. Figure (9) shows the variation of both the vertical and lateral stresses. The relative magnitude of these stresses depends on the intensity and geometry of the load as well as the depth at which this stress is considered.

It is most difficult to duplicate the variation of the lateral stress in the laboratory for obvious reasons. In this experimental work, therefore, a more simplified form of the lateral stress was adopted. The lateral stress was pulsed in a square shape and controlled to coincide with the vertical stress.

Pulsing the lateral pressure is a more difficult task than pulsing the vertical stress. This is due to the fact that lateral pressure is in general pneumatically applied where the shape of the pulse is hard to control, particularly for small durations.

Figure (10) shows the system designed to pulse the chamber pressure. In this system, the pressure is kept constant in two tanks (σ_3 and $\Delta\sigma_3$). The pressure σ_3 is equivalent to the in situ lateral pressure and alternatively applied with $\Delta\sigma_3$ which corresponds to the total lateral pressure during the load pulse. A special circuit was designed to synchronize the vertical and the lateral pulses, and to control the time duration of the lateral pressure. In this circuit, the command signal to the lateral pressure directional valve is adjusted to correspond to the signal applying the vertical stress (MTS). It also has the capability of expanding and shifting the lateral pressure independently from the vertical one.

Temperature Control System:

There has been an increasing awareness that the test temperature plays the major role in the behavior of asphalt treated materials. It is, therefore, highly important that the testing system should have the capability of controlling and maintaining a constant temperature throughout the experiment.

Experimental studies conducted at the University of Washington indicated that it takes 4-5 hours to bring the temperature of a 4 x 8 inch specimen from 75°F to 40°F in air. A similar test was conducted when the specimen was immersed in water, the comparative time for this test was only from 1.5-2 hours. This was one of the reasons that a liquid (silicone oil) was selected to be used inside the triaxial chamber.

Figure (11) diagrammatically shows the main features of the closed loop temperature control system. In this system, the refrigerator and the heating unit work opposite to each other to obtain a constant temperature in the tank. The silicone oil at this temperature is then circulated through a centrifugal pump to the triaxial chamber where the temperature is measured by three sensors located at different elevations. In order to obtain the required temperature, the heating coil or the refrigerator are activated by a thermostat to compensate for any heat losses or gains.

The following items are used in the temperature control system:

- a) One H. P. Copelametic refrigeration unit using an R-12 refrigerant.
- b) 4,000 watts Calrod Merchant heater
- c) Thermac power controller 6000, Model D30.

The Measurement and the Monitoring Systems:

It was originally planned to use linear, variable, differential transformers (LVDT) to measure the axial and diametrical displacements. This method of measurement, however, was unsatisfactory due to slippage between the rubber membranes and the test specimen. Furthermore, continuous drifts in the LVDTs were observed and were interpreted as drifts due to contaminations associated with the use of silicone oil in the chamber. For this reason, therefore, the LVDT's were replaced by two axial and two circumferential strain gages to measure the strains. SR-4, A-1 wire gages 0.75 inches in length and M.M.EA-13-19CDK foil gages 2.0 inches long produced satisfactory results. It was later decided to use the 2.0 inch long gages since the maximum size aggregate was limited to 3/4 inches.

The vertical load is controlled by a 4-inch diameter load cell inside the triaxial chamber and continuously checked against a special load cell in the MTS loading frame.

The triaxial chamber pressure is measured by a pressure transducer located at the bottom of the cell. The pressure at this point is slightly higher than that at the center of the specimen due to the hydrostatic pressure of the oil.

From the description of the instrumentation it is clear that in testing asphalt mixes four sets of data are obtained. These comprise the axial load, the lateral pressure, the axial and the circumferential strains. The number of pulses applied to the specimen is directly read from the MTS machine.

During each test, continuous recording of data are made using an ultra-violet recorder. The necessary information is then read from this recording using a magnifying lense and an accurate scale.

The following components are used in conjunction with the monitoring system:

- a) A digital voltmeter, Model 251-A
- b) Tectronix - 564 memo-oscilloscope with 3A6 vertical amplifier and type 2B67 time base.
- c) Dixson Southern 10-212 light beam ultra-violet oscillograph recorder.
- d) Daytronic 300D carrier amplifier with type 93 input module, and type P output module.
- e) Daytronic 870 data module.

CHAPTER IV

MATERIALS AND PROCEDURES

In order to study the behavior of the asphalt treated base material, a relatively large range of mixtures had to be considered. This range, however, was restricted to the mixtures of practical significance. The State of Washington Specifications (54) were used as a guide in selecting material combinations.

Asphalt

The asphalt binder used in this study was 85-100 penetration asphalt cement supplied by the Chevron Asphalt Company. The results of standard tests on this asphalt are presented in Table (1). Three asphalt contents were selected: 2.5%, 3.5% and 4.5% by total weight of mixture. These fall within the range of the Washington specification for asphalt treated base.

TABLE 1
TESTS RESULTS ON ASPHALT CEMENT

Test	Result
Specific Gravity (ASTM D70)	0.990
Penetration (ASTM D5)	88 dmm
Recovered Penetration (ASTM)	67 dmm
Flash Point (ASTM D93)	480°F
R & B Softening Pt. (ASTM D36)	108°F
Ductility (ASTM D113)	100 + cm

Aggregate

The coarse and fine aggregate (passing 3/4" but retained on #200 sieve) was natural "pit-run" gravel supplied by the Civil Engineering Department's Asphalt and Concrete Lab at the University of Washington. The -#200 material was manufactured of 50% crushed rock and 50% KT clays - Mayfield, Ky. The physical descriptions of the aggregate are presented in Table (2).

Because the aggregate gradation would be subject to considerable variation in the field, it was felt that a wide range of gradations should be studied. Therefore, it was decided to study each extreme of the Washington specification for ATB and also a third gradation midway between the extremes. In this manner, three gradations ("coarse," "middle" and "fine") were examined. Each gradation was combined with each of the three selected asphalt contents, and thus, a total of nine different paving mixtures were included.

TABLE 2
PHYSICAL DESCRIPTION OF AGGREGATE

ITEM	DESCRIPTION
Source	Naturally occurring glacial gravels from Puget Sound region, State of Washington.
Mineralogy	Larger particles composed mainly of andesite porphyries, dacite porphyries, metaandesites, quartzites, metasandstones, diorites, aplites and monzonites. Finer sand fractions predominantly individual grains of quartz and feldspar. (12)
Size and Distribution	3/4" maximum size through -#200. See gradation chart.
Shape	Well rounded to sub-angular for larger sizes; sub-rounded to sub-angular particles for smaller sizes. (#10 - #200).
Surface texture	Smooth in most cases.
Porosity	Aggregate absorbed 1.1% to 1.8% asphalt. (Percent of total sample weight)

The three gradations used are presented in Table (3) and plotted in Figure (12). Also Table (4) shows the results of the specific gravity tests performed on the aggregate.

TABLE 3
GRADATION OF THE AGGREGATE

Sieve	Fine cumulative % passing	Individual % retained
3/4"	100	0
1/2"	100	0
1/4"	78	22
#10	57	21
#40	32	25
#200	9	23
-#200	0	9
Sieve	Middle cumulative % passing	Individual % retained
3/4"	100	0
1/2"	83	16
1/4"	61	23
#10	36	25
#40	18	18
#200	8	10
-#200	0	8
Sieve	Coarse cumulative % passing	Individual % retained
3/4"	100	0
1/2"	56	44
1/4"	40	16
#10	22	18
#40	8	14
#200	2	6
-#200	0	2

TABLE 4
SPECIFIC GRAVITY TEST RESULTS

	GRADATION	B.S.G.	B.S.G. (SSD)	A.S.G.
+ 1/4 Agg.	Fine	2.64	2.66	2.69
	Middle	2.66	2.67	2.69
	Coarse	2.69	2.70	2.71
- 1/4 Agg.	Fine	2.52	2.56	2.66
	Middle	2.54	2.60	2.69
	Coarse	2.62	2.66	2.72
Combined Aggregate	Fine	2.54	2.59	2.67
	Middle	2.58	2.63	2.69
	Coarse	2.66	2.69	2.71

Sample Preparation

A total of 27 samples representing nine different mixes were required for this study. All specimens were manufactured at 230°F using a mechanical mixer and the Triaxial Institute kneading compactor. The proper quantities from all pre-oven dried-aggregates were weighed and combined. The aggregate and the asphalt were then heated to 300°F then mixed mechanically. The mixture was cured for 15 hours at 140 degrees F. It was then divided into three equal amounts (for the three 8" x 4" specimens) and stored within plastic bags at room temperature until compacted.

The compaction procedure was essentially the same as the Hveem method recommended by the Asphalt Institute. In order to compact an 8" specimen,

however, a special mold was used. This mold was tapered on the inside and fitted with two counter-tapered sleeves of semi-circular cross-section. In order to duplicate the Asphalt Institute compaction procedure, it was felt that the 8" specimen should be compacted in three or four lifts. Several density/voids experiments were conducted varying the number of tamps on each lift. Little difference was found in the results of three and four lifts. Therefore, the three lift compaction was adapted with 130, 140 and 150 tamps of 500 psi on the bottom, middle and top lifts respectively.

After compaction, each specimen was placed in the oven at 140°F for 1½ hours and then was subjected to a static pressure of 1000 psi at the rate of 0.05" per minute. The specimens then were placed in plastic bags and stored at 40°F until testing.

A photograph of the compacted fine, medium and coarse specimen is shown in Fig. 12a.

Laboratory Experimental Program

Many of the laboratory tests currently used to characterize paving materials are empirical in nature, and consequently supply no fundamental engineering properties of these materials. In recent years, as newer theoretical techniques have become available, it has become increasingly evident that "better" tests must be provided to characterize the material layer within the pavement. In other words, the theoretical aspects of pavement design have progressed somewhat further than the conventional tests ability to provide suitable parameters to complete the design.

Characterization of paving materials is a complex problem. It is not only important to simulate the pavement conditions in the laboratory, but also to take into consideration the effect of the environment over a long

period of time. Thus, the laboratory tests and the conditions under which they are performed must be chosen with great care to represent realistic conditions of the materials in service.

In order to conduct an extensive study on the asphalt treated base material, it was necessary to design an experimental program which includes conventional as well as unconventional tests. The conventional tests were performed following the Washington State Highway specifications. The unconventional tests, on the other hand, were performed in the triaxial testing apparatus.

Conventional Tests

The triaxial tests, are necessarily somewhat specialized, and therefore, require considerable effort and equipment. In order to effectively characterize the asphalt treated base materials, therefore, it would appear that a procedure whereby a correlation of the newly recognized material parameters with more conventional tests would be desirable.

The correlation included: a) stability, b) cohesion, c) specific gravity, and d) air voids. The test specimens were tested in the following order:

1. Bulk specific gravity (saturated surface dry)
2. Hveem stability
3. Hveem cohesiometer
4. Maximum theoretical specific gravity ASTM D2041-64T

The bulk and maximum specific gravities were used in determining the amount of asphalt lost by absorption into the aggregate, effective asphalt content, voids in the mineral aggregate and percent air voids.

The Cohesimeter test was slightly modified in that the shot loading mechanism was replaced by an equivalent water-loading device in order to surmount difficulties in operating the shot loader.

It should also be noted that some of the stability values may be slightly higher than they should be. It is possible that these samples were not maintained at 140°F long enough for them to attain this temperature throughout their respective masses. Due to this uncertainty a letter "Q" (for questionable data) has been inserted next to these particular points in both the data listing and the plots of stability.

Stability and cohesimeter tests were also performed on specimens used in the triaxial tests. The test temperature of these being 45°, 70°, and 90°F.

Triaxial Tests

In designing the triaxial experimental program for this investigation, it was considered important that the test results would shed more light on the following questions:

- 1) How does the asphalt content influence the behavior of the material?
- 2) How does the aggregate gradation and the percent air voids affect the mix properties?
- 3) How do different mixes behave at different temperatures?
- 4) Does the asphalt treated base material show any stress non-linearity, and how is that influenced when both the vertical and the lateral stresses are repetitive in nature?

and finally

- 5) How can the behavior of this material be modeled, and what are the limitations of such modeling?

The range of stress, temperature, stress durations, and some other variables to be encountered in conducting this research were selected so that they

fall within the service conditions of a base layer. This selection was partly made by utilizing the Chevron n-layer computer program and partly by the extensive data published on similar subjects (1), (26), (29). As a result, the following conclusions were reached:

- 1) The magnitude of the vertical stress depends on the axle load as well as the tire pressure. This stress is always compressive and decreases very rapidly with depth. The radial stress, on the other hand, can vary from tensile to compressive with considerably lower magnitude. In this research the vertical stress was varied up to 50 psi, the radial stress was varied up to 20 psi, both being compressive (see Fig. 13a).
- 2) The pavement surface temperature varies from sub-freezing to temperatures as high as 140°F in the State of Washington. Within a base layer with an asphalt concrete surface, however, the temperature drops sharply and a range of temperature from freezing to 90°F is adequately justified.
- 3) The duration of a stress pulse depends largely on the speed of the moving load and the depth at which it is considered. Within a base layer, therefore, a range of stress duration from 0.1 sec. to 1000 sec. covers rapid as well as very slow moving loads. The long duration of stresses (creep tests) are particularly important if temperature induced stresses and strains are to be considered.

The tests conducted in the triaxial apparatus fall into the following three categories:

- a) The repeated or resilient modulus tests
- b) Creep tests
- c) Dynamic modulus tests

In addition to the resilient modulus tests in which the vertical and the lateral stresses were pulsed simultaneously, another test was performed to study the effects of the confining pressure. In this test, a hydrostatic pressure σ_c was applied on the specimen for a relatively long time. On top of this pressure axial pulses were applied with the axial and lateral strains recorded.

In order to minimize the effects of the stress history, the test procedure was such that lower stresses, shorter durations, and higher frequencies were applied first at lower temperatures. The resilient modulus tests were performed first, followed by the dynamic modulus tests, and finally the creep tests.

These tests will be discussed in detail in a subsequent chapter.

Laboratory Tests of Core Specimens

As part of the overall investigation, several cores of asphalt treated base material were obtained from field projects for comparison with the laboratory fabricated material. Ring 4 of the Washington State University test track contained several sections with ATB. Since these were also tested independently by the Asphalt Institute, they provided a good reference point.

In addition to the WSU material, three in-service pavements were sampled in Western Washington. Two of these projects, I-405 northeast of Seattle, and SR-167 southeast of Seattle, were constructed with ATB layers.

Deflection measurements of all three pavements were also made utilizing a Benkelman beam, Dynaflect, and Road Rater. The three instruments were used at several identical points in each roadway, on the same day, in an attempt to correlate them. The results of this correlation was not entirely satisfactory as seen in Figs. 13b, 13c, and 13d. The correlation for N.E. 124th St. (east of Seattle) appears to be best, but this pavement was

considerably thinner in terms of asphalt treated material, averaging only 2.5 inches. For the pavements with ATB, correlation with the Benkelman was not particularly good for the Dynaflect, and practically non-existent for the Road Rater. However, it should be pointed out that calibration of the Road Rater was suspect and this factor was reported by the operators of the Road Rater following these tests.

Data and analysis of the materials from these field projects is included in the following chapter.

CHAPTER V

TEST RESULTS AND DISCUSSION

It was discussed in a previous chapter that this experimental study was designed to answer a few questions pertaining to the behavior of asphalt treated base materials. One basic question in the characterization of such material is the linearity of its behavior, and in particular the linearity due to stress.

Pavement materials, in general, show some degree of non-linearity. This phenomenon has been investigated by many workers and is very well documented. The following is a brief review of some pertinent findings:

- 1) Most of the work done on unbound granular materials was performed in the triaxial apparatus under repeated loading (29), (43), (13) (44). These tests led to the conclusion that the resilient modulus of such materials increases with confining pressure, and is essentially unaffected by the magnitude of the repeated deviator stress, provided this stress is not high enough to induce shear failure. No clear variation of the resilient Poisson's ratio was noticed with either confining pressure or deviator stress.
- 2) All studies on cohesive soils showed that the resilient modulus was only slightly affected by the confining pressure, and it decreases with increasing the deviator stress.
- 3) A series of laboratory investigations of the behavior of cement-treated sands and clays in triaxial compression was carried out by Mitchell et al. In general, the resilient modulus decreased as the repeated deviator stress increased.
- 4) Terrel (49), conducted repetitive triaxial compression tests on

emulsion treated aggregate. This material showed an increase in the resilient modulus with increasing the confining pressure soon after compaction, this dependency became less marked at long curing times. A reduction of modulus with increasing deviator stress was observed at all curing times, and became the dominant non-linear factor.

It appears from this brief review that non-linearity in asphalt bound material is more influenced by the deviator stresses rather than confining pressures. Non-linearity of unbound material, on the other hand, was dominated by the confining pressure. Asphalt treated base material with a relatively low asphalt content, therefore, falls somewhere between these two categories and, perhaps, shows very little non-linearity with respect to both the deviator stress as well as the confining pressure.

It should be noted, at this point, that most of the tests discussed above were performed under a condition where the confining pressures were constant. The axial stress was then repeatedly applied and the corresponding strains recorded. This procedure is far from the actual changes in stress which take place in a pavement section under a moving load. For this reason, and in order to investigate the stress linearity of asphalt treated material, it was decided to run two separate series of tests: a) utilizing the constant confining stress approach at different stress levels and durations, and b) subjecting the same samples to simultaneous axial and confining stresses compatible to those under a.

Figures 14-17 show plots of the axial strains against the axial stress for the coarse gradation. These results were obtained from the constant confining pressure series for the 2.5% and the 4.5% asphalt at the 0.1 sec. stress duration, under different temperatures.

At low temperatures and relatively high asphalt contents, the confining pressures have no significant effects on the behavior of the mix (Fig. 14 and 15). As the asphalt content decreases, these effects become more noticeable even at low temperatures (Fig. 16), and increased with temperature. Figures 18-21 show the same plots for 1.0 sec. stress durations. Similar results were obtained with the exception that the dependency on the confining pressure was observed at relatively lower temperatures. This dependency increased rather sharply at higher temperatures (Fig. 21).

Figures 22 and 23 show samples of the stress-strain plots for the case when the axial stress σ_1 as well as the lateral stress σ_3 were cycled simultaneously. In this case, the response consists of parallel lines each representing a different lateral stress σ_3 . The results of this test show no change in the response due to the cycled lateral stress. This does not necessarily contradict with the dependency of the response on the constant confining pressure, but rather indicates the fallacy in considering that result to characterize the material.

The confining pressure, for the unbound aggregate, increases the interlocking between individual particles and thus results in a media with a stiffness directly related to the confining pressure. If these particles are coated with a thick film of asphalt, the effects of the confinement would be much slower. These effects become more significant as the asphalt film becomes thinner i.e. at lower asphalt contents. At low temperatures, the asphalt film is stiff enough to behave as a solid. As the temperature increases, however, the asphalt becomes less viscous and eventually loses its function as a cementing agent. This condition resembles the untreated aggregate with a stiffness that is influenced to a greater degree by the confining pressure. Terrel (49), reported an analogous condition with emulsion treated

aggregate. The stiffness of the mix had greater dependency on the confining pressure soon after mixing. This dependency diminished gradually as the asphalt film hardened.

Under the cycled axial and lateral stresses, and due to the short duration of the confining pressure, no significant effects due to the confining pressure were observed. This leads to the conclusion that such materials should be tested under these conditions and in general should be characterized as insensitive to confining pressures under the conditions simulating those of the field.

The stress-strain relationships represented in Fig. 14-23, are quite linear with respect to the deviator stresses. This is particularly true under the environmental conditions which justify the use of the theory of elasticity (low temperatures and short stress durations). In fact, since the range of stresses within a base are likely to be low, it is reasonable to assume that the behavior is linear whenever the theory of elasticity is utilized. Once these conditions are violated, however, a more appropriate approach should be employed.

One common approach to characterize stress non-linear behavior is to assume that the strain can be described as a polynomial of the stresses. The order of this polynomial depends on the degree of non-linearity. Least squares fitting is then employed to obtain the constants in the polynomial. The physical meaning of this representation is that the strain is described by a three dimensional curved surface in terms of the stresses. In order to determine the coefficients in Equation 11 at a selected reference stress, the polynomials are differentiated to obtain the slope of the surface in a particular direction.

This type of approach is often found unsatisfactory and cannot adequately describe the response of the material in practice. This may be due to fitting the experimental data by the least squares which frequently yield relations inconsistent with the behavior of the same material in practice.

In linear elasticity, the curved surfaces mentioned above become planes. The radial and axial strains, in this case described in Equation 11b can be put in the form:

$$\begin{aligned}\epsilon_r &= B_1 \sigma_r + B_2 \sigma_z \\ \epsilon_z &= B_3 \sigma_r + B_4 \sigma_z\end{aligned}\tag{48}$$

the constants $B_1 - B_4$ can be obtained from linearly fitting the experimental data.

Figures 24-27 show samples of the stress-strain relationships plotted in order to obtain the coefficients $B_1 - B_4$. Curve fitting was not employed in this case, in order to allow for some judgement in excluding some of the undesirable experimental points. This process was quite tedious since it was repeated in processing 432 plots.

Since most of the available elastic solutions utilize the isotropic conditions, an approximate value for the modulus and Poisson's ratio are required. These values can be obtained by comparing Equations 11b and 13.

$$E \approx \frac{2}{B_1 + B_4} + \frac{2}{3} \frac{(B_2 + B_3)}{\left[(B_1 + B_4) - \frac{(B_2 + B_3)}{3} \right] (B_1 + B_4)}\tag{49}$$

$$\nu \approx -\frac{2}{3} \frac{(B_2 + B_3)}{(B_1 + B_4) - \frac{(B_2 + B_3)}{3}}$$

The Resilient Modulus Tests

Although the concept of the resilient modulus was introduced for untreated materials, it was adopted to characterize asphalt mixes as well. In this concept, the resilient modulus is defined as the ratio of the applied axial stress to the recoverable or resilient axial strain (see Figure 28):

$$M_R = \frac{\sigma_o}{\epsilon_R} \quad (50)$$

Under a single repetition of stress of duration Δt , the recorded strains (axial or lateral) consist of the following components:

- a) Instantaneous elastic strain that is a function of the mix properties as well as the temperature and the applied stress.
- b) A time-dependent response that is a function of all the variables in (a) and the duration of the applied stress Δt .
- c) Upon the removal of the stress, an instantaneous elastic rebound will take place. This part is in general not equal to the response mentioned above under (a).
- d) The magnitude of the recovered strain is a function of all the variables mentioned above and the rebound time.
- e) Part of the total strain is not recoverable (permanent). This part, however, is small and hard to measure under single stress repetitions.

It should be clear from the preceding analysis that the resilient strain depends largely on the time it is measured after the stress is removed. If a stress is repeatedly applied every n seconds, therefore, the measured resilient strain would be a characteristic of that particular frequency. Under very short stress durations and at low temperatures, the material behaves almost elastically. This fact simplified the problem, and a loading pattern in which

the stress is applied for a 0.1 sec. and then repeated every 3 seconds, is very common. This practice, however, should be modified in case the loading time is relatively longer and when testing at elevated temperatures.

Some asphalt mixes under special environments (saturated samples at high temperature, for example[†]) result in very little or even no resilient strain. These materials, if the concept of the resilient modulus is applied, have an extraordinarily high modulus. It should be recognized, therefore, that the resilient modulus is not an adequate measure of the stiffness or the quality of a certain mix. Instead, in order to fully characterize a material, it is important to add to the resilient modulus an additional modulus relating the stress and the total strains:

$$M_T = \frac{\sigma_0}{\epsilon_T} \quad (51)$$

where M_T is the modulus of total deformations.

In conducting the resilient modulus tests, it has been the practice to subjecting the specimen to an initial period of conditioning by applying a certain stress for a large number of repetitions. The main objective of this conditioning is to bring the specimen to the in situ or service conditions. Increments of stress are then applied in a specified pattern for a smaller number of times before the required "stable" strain readings are recorded. If this procedure is repeated for every stress increment it may induce undesirable excessive permanent strains. If each test is to be performed on a "fresh" sample, on the other hand, a very large number of samples has to be manufactured.

[†]This test was performed at the University of Washington in an investigation of the asphalt stripping phenomenon.

In this study, due to the large number of tests to be performed on each sample, the conditioning was limited to 50 repetitions of all possible combinations of the vertical and lateral stresses. This eliminated the undesirable initial responses in the specimen after long storage and temperature changes. The specimen then was subjected to a series of single repetitions to cover all desired combinations of the vertical and the lateral stresses. Adequate time was allowed for rebound between individual stress pulses.

Two sets of parameters were obtained based on: a) the resilient strains, and b) the total strains. Equations 49 together with Equations 50 and 51 were utilized for this purpose. These parameters are the approximate values of the resilient modulus, the modulus of total deformation, and the corresponding Poisson's ratios. Tables 5-7 summarize the parameters based on the resilient strains for the 0.1 sec. and 1.0 sec. stress durations. Shown in these tables also are the coefficients B_1 , B_2 , B_3 , and B_4 . Figures 29-42 show plots of these parameters and the ratio B_3/B_2 against the asphalt content at different temperatures. All parameters which are based on total strains were not plotted and are only presented in tabulated forms (see Tables 8-10).

In studying Figures 29-42, as well as the data based on the total strains, following observations were made:

- a) Coefficient B_1 , B_2 , and B_3 showed a greater scatter than B_4 .
This may be due to the close ties between these coefficients and Poisson's ratio.
- b) All coefficients $B_1 - B_4$ had a low value at low temperatures short stress durations.

- c) The value of coefficient B_1 did not show any clear minimum with respect to the asphalt content for the fine gradation. For both the medium and coarse gradation, however, it had a minimum at 3.5% asphalt content. This minimum shifted gradually towards lower asphalt content at higher temperatures.
- d) The value of coefficient B_2 was influenced very little by the asphalt content for all gradations at low temperatures. At a high temperature, on the other hand, its value increased more rapidly as the asphalt content increased.
- e) For all gradations, B_3 and B_4 had clear minimum values with respect to the asphalt content even at low temperatures. These minimum values moved towards lower asphalt contents at higher temperatures.
- f) The significance of the ratio B_3/B_2 is that this ratio should have a value of 2 in order to verify the condition of cross-isotropy. This ratio had extraordinarily high values at low asphalt contents. These values, however, were converging towards the value of 2 at higher asphalt contents. This convergence, furthermore, was more rapid at higher temperatures. The general trend was such that mixes with lower air voids were closer to agreement with the condition of cross-isotropy.
- g) The average value of the resilient modulus decreased sharply with temperature and stress durations. This value seemed to have a definite maximum for the fine and medium gradations with respect to the asphalt content. This maximum shifted toward lower asphalt contents as the temperature increased. The coarse gradation was only slightly influenced by the asphalt content at low temperatures.

This trend was changed at elevated temperatures under which the resilient modulus dropped sharply after reaching a maximum at about 3.0 percent asphalt content.

- h) The average value of Poisson's ratio increased with temperature. At low temperatures, this ratio was very little influenced by the asphalt content or the gradation. At high temperature, on the other hand, it had greater scatter and had values enveloping the limiting value of 0.5.
- i) At low temperatures, no appreciable difference was noticed between the values of the parameters based on the resilient strains and those based on the total strains. This difference increased with temperature due to permanent strains.

In addition to the preceding notes, it was also observed, that when total strains rather than resilient strains were used, the values of the computed parameters were more consistent. This may be due to the fact that resilient strains are more affected by the stress history than total strains. Furthermore, in some rare occasion, resilient strains were hard to measure due to very small changes in the triaxial cell pressure.

The Stepwise Linear Regression of the statistical Biomedical Computer Programs (14) was utilized in order to describe the resilient modulus and Poisson's ratio in terms of the temperature, the asphalt content, and the air voids. It has to be realized, at this point that such curve fitting is entirely empirical and should not be extrapolated beyond the experimental data. On one hand such curve fitting helps in understanding how different variables affect a certain parameter. This fitting, on the other hand, supplies fair approximations of the behavior of different mixes at different environments.

The curve fitting equations for the resilient modulus for the 0.1 sec. and 1.0 sec. stress durations are:

$$\begin{aligned} \text{LOG}_{10} M_R(0.1 \text{ sec.}) = & 6.8203 - 0.0000029944(a/c)^2(T)^2 - 0.00011927(T) \\ & - 1.414(\% \text{ air})/(T) \end{aligned} \quad (52)$$

$$\begin{aligned} \text{LOG}_{10} M_R(1.0 \text{ sec.}) = & 6.98798 - 0.001765(a/c)(T) - 0.01165(T) \\ & - 0.0022964(\% \text{ air})^2 - 0.973085(\% \text{ air})^2/(T)^2 \end{aligned} \quad (53)$$

where:

a/c = asphalt content - percent

T = temperature - °F

% air = air void - percent

Equation 52 is plotted in Figures 43-45. Plotted in the same figure also are the expected values from the Heukelom and Klomp nomograph. Good agreement with the Heukelom and Klomp was observed at low temperatures. As the temperature increased, however, Equation 52 predicted higher stiffnesses, particularly for low asphalt contents.

No acceptable fitting was obtained for Poisson's ratio. This is perhaps due to the very large scatter in the experimental data as shown in Figures 46 and 47.

Correlation with Conventional Tests

It was indicated earlier that the main objectives of this type of correlation are not to substitute for the actual testing of a certain material. It only helps the designer to have an equivalency between the conventional parameters and the newer ones whenever direct testing is not available. With this in mind, several attempts were made to correlate the resilient modulus or Poisson's ratio with Hveem stability, cohesion, density, and several other

arbitrary formulae which utilize the data obtained from these tests (41). Due to many uncertainties in the conventional tests, such correlations were extremely poor. The only correlation that is worth reporting is that between the resilient modulus and the Hveem stability:

$$\text{LOG}_{10}M_R(0.1 \text{ sec.}) = [5196240 + 1.697 S^3] \times 10^{-6} \quad (54)$$

$$\text{LOG}_{10}M_R(1.0 \text{ sec.}) = [4457240 + 214.13 S^2] \times 10^{-6} \quad (55)$$

where S is the Hveem stability value obtained at the same temperature as that of the resilient modulus.

Figures 48 and 49 show Equations 54, 55 and the experimental data of this test program. Also shown in the same plots are the test results of some ATB and asphalt concrete samples obtained from two sites in the Seattle area. Some results of the work of Shook and Kallas (47) are also plotted in the 0.1 sec. stress durations. It is clear that Equation 54 does not closely represent this additional data. This may be due to the fact that the modulus in the Shook and Kallas data was obtained from a dynamic modulus value by a conversion factor. It is conceivable that through this process of double correlation the value of the modulus was underestimated.

The Modulus of Total Deformations

The importance of the modulus of total deformations was discussed earlier in this chapter and was defined by Equation 51. The value of this modulus is more consistent than the resilient modulus and certainly completes the characterization of any material. An alternative approach is perhaps to characterize the material by either the resilient modulus or the modulus of total strains together with the permanent strains.

Upon plotting the total strains due to different stress levels at different temperatures against the time duration of the stresses on a log-log scale,

straight and parallel lines were obtained for each temperature. Figures 50-58 show these curves for the fine, medium, and coarse gradations, the three asphalt contents, and at the three stress levels applied in this study. From these figures the following observations were made:

- a) This straight line relationship is only valid through stress durations up to 10 seconds. This is particularly true at high temperatures.
- b) The slope of these straight lines increases with both temperature and asphalt content. This slope, however, is constant for different stress levels.
- c) The intercept at a certain stress duration is linear with stress, and increased with temperature. This intercept decreased, however, as the asphalt content increased.

The general equation of these straight lines is:

$$\epsilon = \sigma \alpha (\Delta t)^\beta \quad (56)$$

where α is the intercept at a stress duration equals 1.0 sec. per unit stress, β is the slope of these lines, and Δt is the duration of stress.

The coefficients α and β were curve fitted as functions of the temperature, the asphalt content, and the air voids. These empirical relationships are:

$$\begin{aligned} \text{LOG}_{10} \alpha = & -0.61054 + 0.003919(\% \text{ air})^2 + 0.00007582(T)^2 \sqrt{a/c} \\ & + 0.000001037(T) (a/c) \quad \text{(Microstrains/psi)} \quad (57) \end{aligned}$$

$$\begin{aligned} \beta = & 0.03052 - 2.08(a/c)^2/(T)^2 + 0.002525(a/c)^2/(\% \text{ air})^2 \\ & + 0.001325(T)(a/c) \quad (58) \end{aligned}$$

Equations 57 and 58 as well as the experimental data are plotted in Figures 59-64 against temperature. If the exponent β in Equation 56 equals zero, the strain becomes no longer a function of time, and the response can be characterized as elastic. Figures 62-64 indicate that this exponent β is converging towards a zero value at a temperature between 10 and 20°F. This temperature is perhaps the equivalent transition between elastic and viscoelastic behavior.

The modulus of total deformation, due to the linear nature with respect to stress, is the inverse of Equation 56.

$$M_T = \frac{1}{\alpha (\Delta t)^\beta} \quad (59)$$

Equation 59 together with Equations 57 and 58 are plotted in Figures 65-70 for the 0.1 and the 1.0 sec. stress durations, for the different asphalt mixtures tested.

Creep Tests

Due to time limitations, and because of the non-destructive nature of this test program, the creep tests were limited to 1000 sec. only. This test was performed at the same stress levels as the resilient modulus tests (10, 30, and 50 psi) and at the same temperatures (25, 45, 70, and 90°F). Continuous recording of the axial and circumferential strains were obtained. At this time, however, the discussion will focus on the behavior in the axial direction only.

Creep tests are perhaps the least complicated, and, if performed over a wide range of temperatures, supply valuable information concerning the rheological behavior of a mix. From the practical point of view, it is important

to understand how the material responds to slow or static loading (e.g. parking areas, or thermal stresses).

Equation 26 describes the response of the 4-element model in the axial direction. A computer program based on a least square regression technique was then employed in obtaining the coefficients C_i in Equation 26. These coefficients are summarized in Tables 14-16.

Since this study, at this point, is limited to the response in the axial direction only, it would be of some interest to discuss how the parameters of the 4-element model change for different mixes at different temperatures. These parameters for the case of uniaxial compression are E_1 , E_3 , η_2 , and η_3 . For this purpose, therefore, the parameters were curve fitted as functions of temperature, asphalt content, and the air voids. The results of this curve fitting is as follows:

$$\begin{aligned} \text{LOG}_{10} E_1(\text{psi}) = & 7.00455 - 0.00974(T) - 0.0036193(\% \text{ air})^2 \\ & - 0.002266(T)(a/c) \end{aligned} \quad (60)$$

$$\begin{aligned} \text{LOG}_{10} E_3(\text{psi}) = & 2.621 + 148.64(1/T) + 33574.5(1/T^3) \\ & + 0.0007861(T)^2/(a/c)^2 - 0.00238(\% \text{ air})^2 \end{aligned} \quad (61)$$

$$\begin{aligned} \text{LOG}_{10} \eta_2(\text{lb. sec./in}^2) = & 8.5237 + 36.743(1/t) - 0.04454(a/c)^2 \\ & - 0.04577(\% \text{ air}) \end{aligned} \quad (62)$$

$$\begin{aligned} \text{LOG}_{10} \eta_3(\text{lb. sec./in}^2) = & 10.194 - 0.02222(T) - 9.08498 \times 10^{-6}(T)^2(a/c)^2 \\ & - 0.0472 (\% \text{ air}) \end{aligned} \quad (63)$$

Figures 71-76 show plots of these empirically fitted functions as well as the experimental data. The following observations were made concerning these plots:

- a) At low temperatures, the coefficients of the Kelvin model (E_3 and η_3) have such high values that the material can be modeled by the Maxwell body. For short stress applications, therefore, the computed stiffnesses by either the resilient modulus or the modulus of total deformations reasonably equal E_1 . For the matter of fact, under 0.1 sec. stress durations, the stiffness of the mix can be described as equivalent to E_1 over the experimental range of temperature.
- b) It is of some interest, perhaps, to indicate that E_3 becomes equal to E_1 and η_3 becomes equal to η_2 at some temperature between 45 and 55°F for all mixtures. This temperature corresponds closely to the point of maximum curvature of the modulus-temperature curve.
- c) The curve fitted functions are entirely empirical and are not intended to represent the true behavior. These functions, however, indicate approximately how different variables influence the parameters E_1 , E_3 , η_2 , and η_3 . Temperature, by far, is the most important factor followed by the asphalt content and then the air voids. For different aggregate gradations, the coarse gradation is the least influenced by the asphalt content. This is possibly due to the fact that the asphalt films which coat the aggregate are the thickest for this gradation. Consequently, small changes in the asphalt content do not reflect considerable change in the overall behavior.

Permanent Deformations

It was discussed before that permanent strains take place even under single stress applications. Since both the total and resilient strains were found to be linear with respect to the applied stress, it is reasonable to assume that permanent strains in a certain mix at a certain temperature are only a function of the stress duration. This means that if the material is linear viscoelastic, all permanent strains are linear with loading time and are attributed only to the free dash pot in the 4-element model. In this case, the permanent strain is described as:

$$\epsilon^P = \sigma_1 C_2 t \quad (64)$$

where t is the duration of stress, and C is one of the constants in the creep compliance (Equation 26). If, therefore, n stress applications each of duration t were imposed on a specimen, then the permanent strain will be:

$$\epsilon^P = n \sigma_1 C_2 t \quad (65)$$

A specimen of the medium gradation with an asphalt content of 3.5% was selected to check the validity of Equation 65. This specimen was tested under uniaxial stress of 30 psi at 70°F at various numbers of applications and stress durations. The results of this investigation were extremely inconsistent and in some cases even contradictory and, therefore, will not be reported. Few conclusions, however, were drawn from this unsuccessful attempt:

- a) Larger number of samples and tests are necessary in order to obtain adequate data that may indicate the general trend for modeling permanent strains.
- b) The stress history is an important factor in the material response, particularly, with respect to permanent strains.

- c) Permanent strains result in a process of densification that changes the material properties. This densification is possibly responsible for the non-linear character of permanent strains.
- d) More information concerning the nature of radial strains within the pavement is needed in order to develop an experimental procedure which utilizes the triaxial apparatus in investigating permanent strains. An alternative approach is full-scale slab tests.
- e) Although the theory of linear viscoelasticity has been successfully used in analyzing pavement deformations, non-linear viscoelastic approaches are perhaps necessary in order to describe permanent deformations.

The viscoelastic solution to permanent deformations as suggested by Moavenzadeh (32), implies an empirical restriction on the rebound time after which strains become permanent. This inspired a different approach to attack the same problem. Figure 77 is a plot of the creep stress against the constant rate of creep ($\sigma_1 C_2$) at different temperatures. This relationship tends to be linear with an intercept $\sigma_{c\ell}$ on the stress axis. This means that uniaxial stresses of magnitude equal or less than $\sigma_{c\ell}$, result in no continuous creep and consequently cause no permanent strains. If this concept is proven to be true, therefore, permanent deformations under a moving load take place only in the locations where the stress exceeds $\sigma_{c\ell}$. This limiting value of the stress is termed "creep limit" (46).

It is realized that the creep limit concept may not be the answer to the complex phenomenon of permanent strains. It is also realized that such a limit may not even exist. It was felt, however, that this approach has some potential, and a great deal of work is needed to prove its merits.

The Dynamic Modulus Tests

In addition to their fundamental use in finding the stress-strain relationship of viscoelastic material, the dynamic modulus tests provide a good basis for evaluating and comparing various materials in terms of their rheological properties. In addition to their potential use in developing mix design criteria, the complex moduli may prove very helpful in evaluating the performance of the material in the road.

This test series was conducted under no confining pressures at the same temperatures and axial stress levels as those of the resilient modulus tests (10, 30, 50 psi). The sinusoidal axial load was provided by the MTS so that the stress is always in the compression mode. The stress frequency was varied from 0.01-20 cps. Stresses, strains, and phase angles were obtained from the continuous recordings as described in Chapter III.

Due to time limitations, presentation of the test data will be confined to the complex modulus (E^*) and the axial phase lag ϕ_1 . The complex Poisson's ratio $|\nu^*|$ and the radial phase lag ϕ_3 will only be included in the analysis without any plots.

Figure 78-86 show plots of the complex modulus versus frequency for different mixtures at the three stress levels within the experimental range of temperatures. Figures 87-95, on the other hand, show plots of the axial phase lag versus frequency over the same range of variables. The following observations were drawn concerning this test:

- a) The value of the complex modulus drops considerably as the temperature increases and as the frequency decreases. At low temperatures, the value of this modulus is in close agreement with both the resilient modulus and the modulus of total deformations. Furthermore, this value is also equivalent to the stiffness of the free elastic

- parameter in the 4-element model computed from the creep tests.
- b) The value of the complex modulus is quite influenced by the asphalt content. As the asphalt content increases the effect of temperature becomes more significant and the value of the complex modulus becomes less and less affected by the frequency. This result is expected, since unbound material ($a/c = 0$) is not at all influenced by temperature and possibly very little by frequency. Pure asphalt ($a/c = 100\%$), on the other hand, is quite viscous and its response is very much dependent on both temperature and asphalt content.
 - c) As a result of (b), different gradations have different asphalt film thicknesses. The coarse gradation, then, which has the thickest asphalt films has the highest temperature and/or frequency susceptibility.
 - d) The value of the complex Poisson's ratio has very low values at low temperatures and at high frequencies. This value, however, tends to approach the limiting value of 0.5 at high temperature and at low frequency. This was more prominent in mixtures with high asphalt contents and coarser gradations.
 - e) In general, the axial phase lag angle is smaller than that in the radial or circumferential directions. The difference is more noticeable at high temperatures and under low frequencies.
 - f) The phase lag, ϕ_1 or ϕ_3 , increases with temperature and decreases with frequency. The measured values of ϕ at high frequencies may be slightly in error because of the difficulties involved in reading them. The phase lag also increases with thickness of the asphalt film coating the aggregate. This was noticed particularly in the coarse gradation at 4.5% asphalt.

As the frequency approaches small values ($\omega \rightarrow 0$), the phase lag does not decrease towards a zero value. As the frequency approaches high values ($\omega \rightarrow \infty$), on the other hand, this phase approaches a zero value. From the viewpoint of viscoelastic modeling, this means that such material is fluid viscoelastic. This, together with the results of the creep tests, reinforce the assumption that the 4-element model can adequately describe the behavior of asphalt treated materials.

Time-Temperature Superposition

It is very difficult to analyze the temperature dependence by seeking an analytical form for the complex parameters at a constant frequency. Instead, the method of reduced variables or viscoelastic corresponding states was utilized. This method affords a valuable simplification in separating the two principal variables of time and temperature on which the viscoelastic properties depend, and expressing the properties in terms of a single function of each. In principal, this method is based on an empirical basis which essentially assumes that time/or frequency and temperature are interchangeable for linear viscoelastic materials.

Figure 96 illustrates the shift functions ϕ_T for different mixtures with 70°F as reference temperature. For ideally elastic materials with no temperature susceptibility, time shifts equal zero, and the material response is unchanged regardless of the test temperature. Untreated aggregate, for all practical purposes falls within this category. As the asphalt content increases, the temperature susceptibility and the shift factor increase indicating more tendencies towards viscous behavior.

Figures 97-99 show the master curves of the complex modulus versus reduced frequencies for the asphalt mixtures tested. At low asphalt content,

little difference was observed between the medium and the coarse gradations. The fine gradation, however, assumed considerably lower values even at high frequencies. This may be due to the high air voids associated with this gradation. As the asphalt content increases, no appreciable difference between the three gradations was noticed at high frequencies. At low frequencies, however, coarse gradation which has the thickest asphalt films, resulted in low values of the complex modulus.

Core Sample Tests and Deflection Prediction

In the previous chapter, mention was made of comparing the properties of laboratory specimens and cores obtained from field sites. Although complete tests on each core were conducted, Fig. 100 was prepared to show the range of moduli for the cores as compared to laboratory specimens when tested under similar conditions. Since some deterioration of the field materials should be expected, their lower moduli is probably not unusual. Tables 35-37 includes more complete data for the WSU test track cores.

As one step toward the rational design approach, the two field projects which include ATB were further analyzed. Using laboratory determined modulus values for each of the asphalt bound layers and estimating them for the subgrade, deflections for the layers were computed using the Chevron n-layer computer program. Input for the surface loading was of two configurations: (1) two 4,500 lb. tires spaced for normal dual tires, and (2) two 500 lb. loads spaced the same as for the Dynaflect machine. Contact areas for each situation were adjusted accordingly. Fig. 101 shows a summary of the measured and computed deflections along with appropriate material properties. Results show that the computed values for Benkelman beam deflections are low, while the Dynaflect deflections are overestimated in one case and underestimated in the other. Also of interest is the percentage of total deflection that

occurs in each layer--according to computations. The loading from the Dynaflect induces nearly all of the deflection in the subgrade, while the heavier truck loading used with the Benkelman beam shows a better distribution. The actual field deflection values used for this comparison are noted in Figs. 13c and 13d.

CHAPTER VI

SUMMARY, CONCLUSIONS AND RECOMMENDATIONS

This research project was initiated in an attempt to define the resilient or elastic properties of asphalt treated base (ATB) as used in the State of Washington. The Highway Department originally used ATB as a working platform in order to expedite construction activities. With success in this endeavor came the practice of incorporating the ATB into the thickness design by assigning an equivalency factor whereby a given thickness in terms of gravel (gravel equivalent) could be related to ATB of a thickness that should give equal performance.

As part of the overall study of ATB to better utilize this material in pavements, two phases could be recognized:

- (1) Phase I, to evaluate the resilient or stiffness properties of ATB for future incorporation into a rational design procedure such as one utilizing elastic layer theory,
- (2) Phase II, to evaluate the design life characteristics of ATB such as resistance to cracking (fatigue) and rutting (permanent deformation).

The study reported herein is that of Phase I.

A very brief evaluation of ATB as constructed in the field included cores from the Washington State University test track and from two in-service highways in Western Washington. In addition, a few deflection measurements of these latter pavements were made to provide an opportunity for prediction from laboratory tests.

The primary study was the behavior of ATB materials under repeated load or dynamic load triaxial stress conditions. A sophisticated triaxial test

system was designed and constructed to provide a wide range of stress-temperature conditions in order to simulate in-situ properties. Specimens were fabricated to represent the full range of materials representative of ATB as used in Washington, including three aggregate gradations and three asphalt contents. These 4-in. diameter by 8-in. high specimens were subjected to a full complement of stresses, including repeated load, sinusoidal, creep, and a variety of frequencies. Also, the temperature was varied from 25° to 90°F, representing the range expected within a base course, i.e., several inches below the pavement surface.

It should be emphasized that the primary objective of this study was to evaluate the behavior of ATB under a range of test conditions in the laboratory. As pointed out above, the behavior in and the design life of pavements constructed with ATB goes beyond the scope of this project. In order to predict design life of these pavements, information on the fatigue, permanent deformation and other properties will be necessary. The results of this study indicate that the modulus or stiffness of ATB is comparable to that of high quality surface mixtures. In this regard, base courses constructed of ATB will perform equally well with surface courses in reducing deflection of the pavement structure under moving wheel loads. However, it should be recognized that the performance of the ATB will be directly related to conditions that exist in the field during and following construction. There is considerable damage to an ATB layer that is placed as a working platform for heavy construction equipment, and the ultimate performance will be reduced once the pavement is completed and placed in service.

The results of findings and observations in this study are summarized below in the form of conclusions derived directly from the laboratory investigation.

- (1) Stiffness properties of the ATB cores from the WSU test track and in-service pavements were similar, but were slightly lower than the laboratory fabricated specimens.
- (2) The stress-strain relationship of asphalt treated base material was found to be linear within the practical range of axial stresses and temperatures. It is recommended that no further testing should be invested in this aspect.
- (3) The stiffness of this material as defined by the resilient modulus was unaffected by the practical range of confining pressure at low temperatures. At high temperature, however, this stiffness was quite dependent not only on temperature but also on the asphalt content. Low asphalt contents do not provide adequate cementation of the aggregate particles particularly if high percentages of fines are used. The behavior of these mixtures, therefore, was close to the unbound aggregate with considerable dependency on confining pressures. High asphalt contents beyond the quantity of asphalt needed to cement the aggregate particles together, increase the dependency on long lasting confining pressures.
- (4) The conclusion under (3) is basically applied to rounded uncrushed aggregate. If crushed aggregate is used, the interlocking of the particles will influence the behavior of the material by changing its shear behavior. The effects of asphalt contents and temperature on the material non-linearity may be slightly altered.
- (5) Investigation of the condition of isotropy is important when characterizing an unknown material. Cross-isotropy was verified by checking the ratio (B_3/B_2) which should have a value of 2.

Mixtures having low asphalt contents assumed very high values for this ratio. For higher asphalt contents, however, this ratio was very near 2. The convergence of the behavior towards the cross-isotropic assumption was very much affected by temperature. It was also concluded that, in general, mixtures with low air voids satisfy the condition of cross-isotropy better than mixtures with high air void content.

- (6) The general behavior of ATB mixtures can be treated as elastic under some special conditions. These conditions include low temperatures and short stress durations or high speed loading. These two conditions are obviously interchangeable such that as long as the viscous elements which are represented by the asphalt cement are frozen, the behavior can be characterized as elastic. At high temperatures, or due to slowly applied stresses, these viscous elements will creep and result in a tendency toward the viscoelastic behavior. ATB mixtures considered in this research have a temperature limiting value between 10° and 20° F below which the behavior is elastic.
- (7) As a result of utilizing photoelastic coating to observe the strain pattern and distribution between the aggregate and the asphalt matrix, it was concluded that the deformations are largely due to shear strains in the asphalt. Strains within the gravel particles were minimal.
- (8) Although some differentiation was made between the resilient modulus and the modulus of total deformations, little difference was encountered between their values for ATB. This differentiation, however, should be retained and utilized whenever permanent strains become a considerable fraction of the total response.

- (9) Air voids have a small influence on the overall behavior of the material. This is, perhaps, due to the fact that temperature and asphalt contents dominated the material response. The influence of air voids, however, should be well investigated whenever permanent deformation is an important factor.
- (10) Although the influence of the asphalt content is very well taken care of as far as the stress-strain law is concerned, the optimum asphalt content for the modulus may not be optimum for some other phenomenon such as fatigue for example. This may prove to be dependent on the temperature.
- (11) Temperature plays the biggest role in the behavior of asphalt mixtures. Temperature susceptibility for different gradations and asphalt contents was discussed in several occasions and was presented in many figures within the report.
- (12) As a comparison with conventional tests, the resilient modulus was correlated with the Hveem stability value. This correlation, however, should not be used as a substitute for actual material testing. It may only be used for estimating whenever actual test data are not available.
- (13) Asphalt mixtures, as are all viscoelastic materials, are sensitive to stress histories. This certainly presents a serious problem, and in particular, from the standpoint of permanent deformation. Considerable work is still needed in order to characterize this phenomenon in both the theoretical as well as the experimental fields. The concept of creep limit was presented as a potential approach to solve the problems encountered by using the theory of viscoelasticity.

- (14) As a result of utilizing strain gages in this study, it is recommended that this technique may only be used within the framework of small deformations. It is suggested that LVDT's be utilized if large deformations of test specimens are to be encountered.
- (15) In completing this research, it is of some importance to question the reproducibility of the test results. The test data presented in this research were obtained from two specimens representing each mix. In terms of statistical considerations, this is not totally adequate. It is strongly recommended, therefore, that in any future testing on similar subjects that fewer tests and more samples be tested. This does not, however, disqualify the test data presented herein. These data were quite consistent considering the many uncertainties involved in the sample preparation as well as the general heterogeneity of the material caused by random distribution of the aggregate particles.

REFERENCES

1. Barksdale, R. D., "Compressive Stress Pulse Times in Flexible Pavements for Use in Dynamic Testing" The 50th Annual Meeting of the Highway Research Board, Wash. D.C. 1971.
2. Bazin, P. and Saunier, J. B., "Deformability, Fatigue and Healing Properties of Asphalt Mixes," Proceedings, Second International Conference on the Structural Design of Asphalt Pavements, University of Michigan, Ann Arbor, Michigan, 1967, pp. 553-569.
3. Bland, D. R., "The Theory of Linear Viscoelasticity" Pergamon Press, London, 1960.
4. Brown, S. F. and Pell, P. S. "An Experimental Investigation of the Stresses, Strains, and Deflections in a Layered Pavement Structure Subjected to Dynamic Loads," Proceedings, Second International Conference on the Structural Design of Asphalt Pavements, 1967.
5. Burmister, D. M. "The Theory of Stresses and Displacements in Layered Systems and Application to Design of Airport Runways," Proceedings, Highway Research Board, Vol. 23, 1943.
6. Burmister, D. M., "The General Theory of Stresses and Displacements in Layered Systems," Journal of Applied Physics, Vol. 16, 1945.
7. Bush, D. I., "Behavior of Flexible Pavements Subjected to Dynamic Load," Ph.D. Dissertation, University of Nottingham, 1969.
8. Chen, J. T., "A Rheological Stress-Strain-Time Relationship for Seattle Soils," Ph.D. Dissertation, University of Washington, 1969.
9. Cragg, R. and Pell, P. S., "The Dynamic Stiffness of Bituminous Road Materials."
10. Daniel, F. and Chang, T.S., "Continuum Mechanics" Allyn and Bacon, Inc., Boston, 1965.
11. Deacon, J. A., "Materials Characterization-Experimental Behavior," in HRB Special Report 126, Structural Design of Asphalt Concrete Pavement Systems, Proceedings of a Workshop, Austin, Texas, 1970.
12. Deacon, J. A., "Fatigue of Asphalt Concrete," Ph.D. Dissertation, University of California, Berkeley, 1965.
13. Dehlen, G. L. "The Effect of Non-Linear Material Response on the Behavior of Pavements Subjected to Traffic Loads," Ph.D. Dissertation, University of California, Berkeley, 1969.
14. Dixon, W. J., Editor, "Biomedical Computer Programs," University of California Press, Berkeley and Los Angeles, 1967.

15. Duncan, J. M. and C. L. Monismith and Wilson, E. L., "Finite Element Analyses of Pavements," Highway Research Record 228, HRB, 1968.
16. Ferry, J. D. "Viscoelastic Properties of Polymers," John Wiley and Sons, 1970.
17. Finn, F. N., Hicks, R. G., Kari, W. J. and Coyne, L. D., "Design of Emulsified Asphalt Treated Bases," Highway Research Record No. 239, Highway Research Board, Washington, D.C., 1968.
18. Flügge, Wilhelm, "Viscoelasticity," Blaisdell Publishing Co., Waltham, Mass., 1967.
19. Griggs, G. E., "Permanent Deformation Subsystems - Quasi-Elastic and Viscoelastic Approaches."
20. Hadley, W. O., Hudson, W. and Kennedy, T. W., "Correlation of Tension Properties with Stability and Cohesimeter Values for Asphalt Treated Materials," Center for Highway Research, University of Texas at Austin, Austin, Texas, June 1970, pp. 10, 19-30.
21. Heukelom, W. and Klomp, A. J. G., "Road Design and Dynamic Loading," Proceedings of the AAPT, Dallas, Texas, 1964.
22. Holubec, I. and Wilson, K. H., "A Cyclic Creep Study of Pavement Material," D.H.O. Report No. RR163, June 1970.
23. Hveem and Vallerga, as presented in: National Cooperative Highway Research Program, Report 39, "Factors Involved in the Design of Asphaltic Pavement Surfaces," Highway Research Board, Washington, D.C., 1967, pp. 3-4.
24. Kallas, B. F., "Dynamic Modulus of Asphalt Concrete in Tension and Tension-Compression," AAPT, 1970.
25. Kallas, B. F. and Riley, J. C., "Mechanical Properties of Asphalt Pavement Materials," Proceedings, Second International Conference on the Structural Design of Asphalt Pavements, 1967.
26. Kasianchuk, D. A., "Fatigue Considerations in the Design of Asphalt Concrete Pavements," Ph.D. Dissertation, University of California, Berkeley, California.
27. Kenis, W. J., "A Comparative Examination Between Prototype Pavements and Rational Design Concepts."
28. Krokosky, E. M., "Rheological Properties of Asphalt/Aggregate Compositions," Research Report R62-32, Part II, School of Civil Engineering, M.I.T., Cambridge, Mass., Aug. 1962.

29. Material Research and Development, Inc., "Translating AASHO Road Test Findings Basic Properties of Pavement Components," Project Nos. 1-10 and 1-10/1, Oakland, 1970.
30. McLeod, N. W., "The Asphalt Institute's Layer Equivalency Program," Research Series No. 15 (RS-15), The Asphalt Institute, College Park, Maryland, March 1967, p. 18.
31. Mitchell, J. K. and Monismith, C. L., "Behavior of Stabilized Soils Under Repeated Loading," Report No. 2 for U.S. Army Material Command, University of California, Berkeley, 1966.
32. Moavenzadeh, F. and Elliot, J. F., "Moving Load on Viscoelastic Layered System, Phase II," Research Report R69-64 of Civil Engineering, M.I.T., 1969.
33. Monismith, C. L., "Design Considerations for Asphalt Pavements," Seminar, University of Washington, 1970.
34. Monismith, C. L., Alexander, R. L. and Secor, K. E., "Rheologic Behavior of Asphalt Concrete," Proceedings, AAPT, 1966, Vol. 35.
35. Monismith, C. L., and Secor, K. E., "Viscoelastic Behavior of Asphalt Concrete Pavements," International Conference on the Structural Design of Asphalt Pavements, Michigan 1962.
36. Monismith, C. L., "Asphalt Paving Mixtures," Short Course in Asphalt Paving Technology, University of California, Berkeley, 1961.
37. Nijboer, L. W., "Einige Betrachtungen über das Marshallverfahren zur Untersuchung Bituminöser Massen," Strasse und Autobahn, 8-1957, p. 210.
38. Papazian, H. S., "The Response of Linear Viscoelastic Materials in the Frequency Domain with Emphasis on Asphaltic Concrete," International Conference on the Structural Design of Asphalt Pavements, Michigan, 1962.
39. Pendakur, V. S., "Viscoelastic Response of Flexible Pavements in Relation to Pavement Performance-Serviceability," Ph.D. thesis, University of Washington, 1964.
40. Romain, J. E., "Rut Depth Prediction in Asphalt Pavements," Research Report No. 150/JER/1969, Centre De Recherches Routieres, Bruxelles.
41. Rutz, F. R., "Correlation of Resilient Properties with Conventional Test Values for Asphalt Treated Materials," M.Sc. Thesis, University of Washington, 1971.
42. Secor, K. E., and Monismith, C. L., "Analysis of Triaxial Test Data on Asphalt Concrete Using Viscoelastic Principles," Proceedings, Highway Research Board, V. 40, 1961.

43. Seed, H. B., Chan, C. K., and Lee, C. E., "Resilience Characteristics of Subgrade Soil and Thin Relation to Fatigue Failure in Asphalt Pavements," Proceedings, First International Conference on the Structural Design of Asphalt Pavements, Ann Arbor, 1962.
44. Seed, H. B., Mitry, F. G., Monismith, C. L., and Chan, C. K., "Prediction of Pavement Deflection from Laboratory Repeated Load Tests," Report No. Te 65/6, University of California, Berkeley, 1965.
45. Shackel, B., "A Research Apparatus for Subjecting Pavement Materials to Repeated Triaxial Loading," Australian Road Research, Vol. 4, June 1970.
46. Sherif, M. A., "Flow and Fracture Properties of Seattle Clays," Engineering Research Series No. 1, University of Washington, 1965.
47. Shook, J. F., and Kallas, B. F., "Factors Influencing Dynamic Modulus of Asphalt Concrete," Proceedings, Association of Asphalt Paving Technologists, Vol. 38, 1969, pp. 162-164.
48. Sokolnikoff, I. S., "Mathematical Theory of Elasticity," McGraw-Hill Book Co., Inc., New York 1956.
49. Terrel, R. L., "Factors Influencing the Resilient Characteristics of Asphalt Treated Aggregates," Ph.D. Dissertation, University of California, Berkeley 1967.
50. Van der Poel, C., "A General System Describing the Viscoelastic Properties of Bitumins and its Relation to Routine Test Data," Journal of Applied Chemistry, May 1954.
51. van Draat, W. E. F., and Sommer, P., "Ein Gerät Zur Bestimmung der Dynamischen Elastizitätsmoduln von Asphalt," Strasse und Autobahn, Vol. 35, 1966.
52. Varanasi, S. R., "Wave Propagation and Dynamic Stress Analysis of a Viscoelastic Cylinder," Ph.D. Dissertation, University of Washington, 1968.
53. Van Vlack, L. H., "Elements of Materials Science," Addison-Wesley, London 1960.
54. Washington State Highway Commission, Department of Highways, "Standard Specifications for Road and Bridge Construction," Washington State Highway Commission, Olympia, Washington, 1969, Section 9-03.6.
55. Westman, R. A., "Fundamentals of Material Characterization," Special Report 126 HRB, 1970.

TABLE 5 - Summary of Resilient Modulus Tests for 0.1 and 1.0 sec. Stress Durations

GRADATION	ASPHALT CONTENT	EFFECTIVE ASPHALT CONTENT	PERCENT VOIDS	PERCENT AIR	TEMPERATURE	COEFFICIENT B1	COEFFICIENT B2	COEFFICIENT B3	COEFFICIENT B4	RESILIENT MODULUS-PSI	POISSON'S RATIO
FINE	2.5	2.25	15.37	13.71	25	.600	-.070	-.752	1.112	1.007E+06	.276
FINE	2.5	2.25	15.37	13.71	45	1.000	-.212	-1.100	1.530	1.017E+06	.445
FINE	2.5	2.25	15.37	13.71	70	1.700	-.490	-4.600	4.000	3.127E+05	.530
FINE	2.5	2.25	15.37	13.71	90	4.360	-1.475	-4.900	5.450	2.531E+05	.529
FINE	3.5	2.37	11.70	7.18	25	.440	-.105	-.195	.300	2.390E+06	.231
FINE	3.5	2.37	11.70	7.18	45	.450	-.118	-.320	.528	1.779E+06	.260
FINE	3.5	2.37	11.70	7.18	70	.970	-.354	-.825	.980	8.917E+05	.350
FINE	3.5	2.37	11.70	7.18	90	2.350	-.900	-1.900	3.270	4.392E+05	.410
FINE	4.5	2.46	9.46	1.97	25	.142	-.060	-.150	.268	4.138E+06	.303
FINE	4.5	2.46	9.46	1.97	45	.220	-.123	-.200	.406	2.726E+06	.294
FINE	4.5	2.46	9.46	1.97	70	.680	-.445	-.910	1.020	9.295E+05	.420
FINE	4.5	2.46	9.46	1.97	90	1.720	-1.410	-3.400	3.370	3.513E+05	.563
FINE	2.5	2.25	15.37	13.71	25	.780	-.105	-.900	1.410	7.921E+05	.265
FINE	2.5	2.25	15.37	13.71	45	1.390	-.344	-1.910	2.320	5.778E+05	.434
FINE	2.5	2.25	15.37	13.71	70	3.800	-1.140	-6.800	7.080	1.900E+05	.503
FINE	2.5	2.25	15.37	13.71	90	9.800	-3.130	-9.750	10.400	1.291E+05	.554
FINE	3.5	2.37	11.70	7.18	25	.440	-.134	-.208	.370	2.165E+06	.247
FINE	3.5	2.37	11.70	7.18	45	.450	-.172	-.430	.735	1.443E+06	.290
FINE	3.5	2.37	11.70	7.18	70	1.700	-.795	-1.900	2.140	5.350E+05	.481
FINE	3.5	2.37	11.70	7.18	90	6.200	-2.670	-5.500	8.270	1.787E+05	.487
FINE	4.5	2.46	9.46	1.97	25	.182	-.097	-.185	.325	3.328E+06	.313
FINE	4.5	2.46	9.46	1.97	45	.270	-.207	-.500	.625	1.759E+06	.417
FINE	4.5	2.46	9.46	1.97	70	1.550	-1.170	-1.450	2.270	5.415E+05	.473
FINE	4.5	2.46	9.46	1.97	90	5.900	-4.120	-8.400	8.940	1.437E+05	.600

TABLE 6 - Summary of Resilient Modulus Tests for 0.1 and 1.0 sec. Stress Durations

GRADATION	ASPHALT CONTENT	EFFECTIVE ASPHALT CONTENT	PERCENT VOIDS	PERCENT AIR	TEMPERATURE	COEFFICIENT B1	COEFFICIENT B2	COEFFICIENT B3	COEFFICIENT B4	RESILIENT MODULUS-PSI	POISSON'S RATIO
MEDIUM 2.5	2.36	12.69	9.94	25	.332	-.068	-.385	.720	1.663E+06	.251	
MEDIUM 2.5	2.36	12.69	9.94	45	.655	-.104	-.450	1.050	1.058E+05	.195	
MEDIUM 2.5	2.36	12.69	9.94	70	1.100	-.264	-1.070	1.540	9.594E+05	.427	
MEDIUM 2.5	2.36	12.69	9.94	90	1.720	-.450	-1.600	3.480	4.096E+05	.280	
MEDIUM 3.5	2.49	8.71	2.43	25	.125	-.085	-.100	.240	4.687E+06	.289	
MEDIUM 3.5	2.49	8.71	2.43	45	.133	-.090	-.170	.356	3.474E+06	.301	
MEDIUM 3.5	2.49	8.71	2.43	70	.255	-.256	-.640	.940	1.435E+06	.429	
MEDIUM 3.5	2.49	8.71	2.43	90	1.440	-.960	-2.000	2.430	5.186E+05	.512	
MEDIUM 4.5	2.50	9.32	1.03	25	.255	-.070	-.150	.284	3.266E+06	.240	
MEDIUM 4.5	2.50	9.32	1.03	45	.375	-.200	-.205	.288	2.506E+06	.338	
MEDIUM 4.5	2.50	9.32	1.03	70	1.250	-.960	-1.520	2.020	6.459E+05	.534	
MEDIUM 4.5	2.50	9.32	1.03	90	4.600	-5.930	-10.700	12.100	1.098E+05	.605	
MEDIUM 2.5	2.36	12.69	9.94	25	.520	-.092	-.490	.840	1.287E+06	.250	
MEDIUM 2.5	2.36	12.69	9.94	45	.600	-.107	-.450	1.400	9.151E+05	.170	
MEDIUM 2.5	2.36	12.69	9.94	70	1.680	-.448	-1.200	2.360	5.572E+05	.306	
MEDIUM 2.5	2.36	12.69	9.94	90	3.550	-1.060	-3.300	6.000	2.499E+05	.363	
MEDIUM 3.5	2.49	8.71	2.43	25	.180	-.086	-.360	.266	3.363E+06	.500	
MEDIUM 3.5	2.49	8.71	2.43	45	.310	-.130	-.338	.490	2.092E+06	.326	
MEDIUM 3.5	2.49	8.71	2.43	70	.860	-.720	-1.880	1.880	5.545E+05	.481	
MEDIUM 3.5	2.49	8.71	2.43	90	4.520	-3.000	-5.650	6.600	1.999E+05	.576	
MEDIUM 4.5	2.50	9.32	1.03	25	.275	-.096	-.235	.360	2.683E+06	.296	
MEDIUM 4.5	2.50	9.32	1.03	45	.650	-.390	-.450	.880	1.105E+06	.309	
MEDIUM 4.5	2.50	9.32	1.03	70	9.400	-4.100	-13.100	7.900	1.435E+05	.823	
MEDIUM 4.5	2.50	9.32	1.03	90	30.200	-36.300	-39.500	48.250	2.713E+04	.686	

TABLE 7 - Summary of Resilient Modulus Tests for 0.1 and 1.0 sec. Stress Durations

GRADATION	ASPHALT CONTENT	EFFECTIVE ASPHALT CONTENT	PERCENT VOIDS	PERCENT AIR	TEMPERATURE	COEFFICIENT B1	COEFFICIENT B2	COEFFICIENT B3	COEFFICIENT B4	RESILIENT MODULUS-PSI	POISSON'S RATIO
COARSE 2.5	2.41	12.80	9.21	25	.320	-.086	-.130	.362	2.653E+06	.191	
COARSE 2.5	2.41	12.80	9.21	45	.431	-.140	-.372	1.000	1.249E+06	.213	
COARSE 2.5	2.41	12.80	9.21	70	.947	-.485	-.682	1.530	6.978E+05	.271	
COARSE 2.5	2.41	12.80	9.21	90	2.140	-.850	-1.785	4.120	3.892E+05	.342	
COARSE 3.5	2.43	12.99	5.79	25	.200	-.085	-.182	.390	2.946E+06	.262	
COARSE 3.5	2.43	12.99	5.79	45	.400	-.124	-.290	.384	2.169E+06	.299	
COARSE 3.5	2.43	12.99	5.79	70	.750	-.384	-.773	1.480	7.646E+05	.295	
COARSE 3.5	2.43	12.99	5.79	90	2.350	-1.610	-3.370	3.500	3.630E+05	.603	
COARSE 4.5	2.47	12.42	3.50	25	.304	-.125	-.100	.265	3.106E+06	.233	
COARSE 4.5	2.47	12.42	3.50	45	.241	-.174	-.361	.522	2.125E+06	.379	
COARSE 4.5	2.47	12.42	3.50	70	1.030	-.532	-1.446	1.280	9.987E+05	.692	
COARSE 4.5	2.47	12.42	3.50	90	5.110	-5.050	-12.000	10.320	1.241E+05	.705	
COARSE 2.5	2.41	12.80	9.21	25	.416	-.100	-.239	.460	2.022E+06	.229	
COARSE 2.5	2.41	12.80	9.21	45	.642	-.176	-.550	1.200	9.597E+05	.232	
COARSE 2.5	2.41	12.80	9.21	70	2.830	-1.580	-2.450	4.170	3.153E+05	.424	
COARSE 2.5	2.41	12.80	9.21	90	4.200	-1.520	-4.000	5.120	2.441E+05	.457	
COARSE 3.5	2.43	12.99	5.79	25	.300	-.100	-.192	.444	2.377E+06	.231	
COARSE 3.5	2.43	12.99	5.79	45	.449	-.222	-.496	.562	1.600E+06	.383	
COARSE 3.5	2.43	12.99	5.79	70	1.800	-1.020	-2.040	3.930	3.540E+05	.361	
COARSE 3.5	2.43	12.99	5.79	90	7.300	-4.670	-10.100	10.100	1.305E+05	.643	
COARSE 4.5	2.47	12.42	3.50	25	.372	-.113	-.181	.344	2.457E+06	.241	
COARSE 4.5	2.47	12.42	3.50	45	.410	-.374	-.781	.900	1.180E+06	.454	
COARSE 4.5	2.47	12.42	3.50	70	1.650	-1.940	-2.810	3.620	3.417E+05	.541	
COARSE 4.5	2.47	12.42	3.50	90	28.000	-26.900	-59.700	54.000	2.201E+04	.635	

TABLE 8 - Summary of Modulus of Total Deformations for 0.1 and 1.0 sec. Stress Durations

	GRADATION	EFFECTIVE ASPHALT CONTENT	ASPHALT CONTENT	PERCENT ASPHALT CONTENT	PERCENT AIR	TEMPERATURE	COEFFICIENT B1	COEFFICIENT B2	COEFFICIENT B3	COEFFICIENT B4	MODULUS OF TOTAL DEFORMATIONS	POISSON'S RATIO
FINE	2.5	2.25	15.37	13.71	25	.600	-.070	-.752	1.112	1.007E+06	.276	
FINE	2.5	2.25	15.37	13.71	45	1.000	-.212	-1.250	1.550	6.585E+05	.321	
FINE	2.5	2.25	15.37	13.71	70	2.160	-.520	-5.330	5.200	2.148E+05	.419	
FINE	2.5	2.25	15.37	13.71	90	4.960	-1.735	-5.500	6.250	1.468E+05	.354	
FINE	3.5	2.37	11.70	7.18	25	.440	-.105	-.185	.300	2.390E+06	.231	
FINE	3.5	2.37	11.70	7.18	45	.450	-.118	-.320	.528	1.779E+06	.260	
FINE	3.5	2.37	11.70	7.18	70	1.020	-.380	-.920	1.030	8.054E+05	.349	
FINE	3.5	2.37	11.70	7.18	90	2.600	-1.140	-2.250	3.670	2.703E+05	.305	
FINE	4.5	2.46	9.46	1.97	25	.142	-.060	-.160	.258	4.138E+06	.303	
FINE	4.5	2.46	9.46	1.97	45	.220	-.123	-.200	.420	2.675E+05	.288	
FINE	4.5	2.46	9.46	1.97	70	.810	-.675	-1.160	1.255	7.472E+05	.457	
FINE	4.5	2.46	9.46	1.97	90	2.420	-1.840	-3.630	3.900	2.456E+05	.448	
FINE	2.5	2.25	15.37	13.71	25	.780	-.105	-.900	1.410	7.921E+05	.265	
FINE	2.5	2.25	15.37	13.71	45	1.510	-.376	-2.000	2.400	4.254E+05	.337	
FINE	2.5	2.25	15.37	13.71	70	4.320	-1.290	-10.000	9.000	1.171E+05	.441	
FINE	2.5	2.25	15.37	13.71	90	11.500	-4.030	-10.500	11.301	7.235E+04	.350	
FINE	3.5	2.37	11.70	7.18	25	.440	-.134	-.208	.370	2.165E+06	.247	
FINE	3.5	2.37	11.70	7.18	45	.450	-.180	-.430	.760	1.415E+06	.288	
FINE	3.5	2.37	11.70	7.18	70	2.040	-.915	-2.350	2.370	3.637E+05	.396	
FINE	3.5	2.37	11.70	7.18	90	7.900	-3.330	-7.100	9.750	9.467E+04	.329	
FINE	4.5	2.46	9.46	1.97	25	.182	-.097	-.185	.325	3.328E+06	.313	
FINE	4.5	2.46	9.46	1.97	45	.292	-.223	-.500	.650	1.691E+06	.407	
FINE	4.5	2.46	9.46	1.97	70	2.400	-1.800	-3.000	3.220	2.770E+05	.443	
FINE	4.5	2.46	9.46	1.97	90	8.600	-6.630	-12.000	11.401	7.631E+04	.474	

TABLE 10 - Summary of Modulus of Total Deformations for 0.1 and 1.0 sec. Stress Durations

GRADATION	ASPHALT CONTENT	EFFECTIVE ASPHALT CONTENT	PERCENT VOIDS	PERCENT AIR	TEMPERATURE	COEFFICIENT B1	COEFFICIENT B2	COEFFICIENT B3	COEFFICIENT B4	MODULUS OF TOTAL DEFORMATIONS	POISSON'S RATIO
MEDIUM 2.5	2.36	12.69	9.94	25	.332	-.068	-.385	.720	1.663E+06	.251	
MEDIUM 2.5	2.36	12.69	9.94	45	.655	-.104	-.450	1.050	1.058E+06	.195	
MEDIUM 2.5	2.36	12.69	9.94	70	1.100	-.264	-1.075	1.580	6.397E+05	.286	
MEDIUM 2.5	2.36	12.69	9.94	90	1.850	-.465	-1.700	3.650	3.215E+05	.232	
MEDIUM 3.5	2.49	8.71	2.43	25	.125	-.085	-.100	.240	4.687E+06	.289	
MEDIUM 3.5	2.49	8.71	2.43	45	.133	-.090	-.180	.370	3.373E+06	.304	
MEDIUM 3.5	2.49	8.71	2.43	70	.285	-.256	-.660	.860	1.379E+06	.421	
MEDIUM 3.5	2.49	8.71	2.43	90	1.550	-1.090	-2.300	2.620	3.774E+05	.426	
MEDIUM 4.5	2.50	9.32	1.03	25	.255	-.070	-.185	.284	3.205E+06	.272	
MEDIUM 4.5	2.50	9.32	1.03	45	.420	-.208	-.300	.320	2.199E+06	.372	
MEDIUM 4.5	2.50	9.32	1.03	70	1.380	-1.070	-2.000	2.200	4.345E+05	.445	
MEDIUM 4.5	2.50	9.32	1.03	90	5.500	-6.500	-14.400	16.600	6.881E+04	.479	
MEDIUM 2.5	2.36	12.69	9.94	25	.520	-.092	-.490	.840	1.287E+06	.250	
MEDIUM 2.5	2.36	12.69	9.94	45	.600	-.107	-.470	1.440	8.959E+05	.172	
MEDIUM 2.5	2.36	12.69	9.94	70	1.750	-.460	-1.300	2.400	4.222E+05	.248	
MEDIUM 2.5	2.36	12.69	9.94	90	3.900	-1.150	-4.200	6.600	1.628E+05	.290	
MEDIUM 3.5	2.49	8.71	2.43	25	.180	-.086	-.360	.266	3.363E+06	.500	
MEDIUM 3.5	2.49	8.71	2.43	45	.350	-.134	-.380	.500	1.958E+06	.336	
MEDIUM 3.5	2.49	8.71	2.43	70	1.000	-.748	-2.000	2.000	5.107E+05	.468	
MEDIUM 3.5	2.49	8.71	2.43	90	5.100	-3.450	-6.650	7.370	1.263E+05	.425	
MEDIUM 4.5	2.50	9.32	1.03	25	.275	-.096	-.250	.370	2.630E+06	.303	
MEDIUM 4.5	2.50	9.32	1.03	45	.690	-.446	-.700	.960	9.843E+05	.376	
MEDIUM 4.5	2.50	9.32	1.03	70	9.500	-4.160	-13.900	8.350	8.379E+04	.504	
MEDIUM 4.5	2.50	9.32	1.03	90	31.500	-37.300	-46.500	52.600	1.785E+04	.499	

TABLE 11 - Summary of the Coefficients in Equation 56 - $\epsilon = \sigma \alpha (\Delta t)^B$

GRADATION	ASPHALT CONTENT	TEMPERATURE	PERCENT AIR	AXIAL STRESS	COEFFICIENT α /PSI	COEFFICIENT B
FINE	2.5	25	13.71	10	1.55	.1285
FINE	2.5	25	13.71	30	1.48	.1285
FINE	2.5	25	13.71	50	1.44	.1310
FINE	2.5	45	13.71	10	2.25	.2150
FINE	2.5	45	13.71	30	2.45	.2150
FINE	2.5	45	13.71	50	2.56	.2180
FINE	2.5	70	13.71	10	6.90	.2380
FINE	2.5	70	13.71	30	8.55	.2380
FINE	2.5	70	13.71	50	9.25	.2330
FINE	2.5	90	13.71	10	9.87	.2640
FINE	2.5	90	13.71	20	11.50	.2600
FINE	2.5	90	13.71	30	13.00	.2580
FINE	3.5	25	7.18	10	.40	.1120
FINE	3.5	25	7.18	30	.37	.1120
FINE	3.5	25	7.18	50	.37	.1180
FINE	3.5	45	7.18	10	.76	.1890
FINE	3.5	45	7.18	30	.80	.1900
FINE	3.5	45	7.18	50	.79	.1930
FINE	3.5	70	7.18	10	2.13	.3680
FINE	3.5	70	7.18	30	2.35	.3680
FINE	3.5	70	7.18	50	2.46	.3680
FINE	3.5	90	7.18	10	8.50	.3880
FINE	3.5	90	7.18	20	8.55	.3730
FINE	3.5	90	7.18	30	8.90	.3750
FINE	4.5	25	1.97	10	.31	.1590
FINE	4.5	25	1.97	30	.34	.1410
FINE	4.5	25	1.97	50	.32	.1430
FINE	4.5	45	1.97	10	.68	.2250
FINE	4.5	45	1.97	20	.67	.2230
FINE	4.5	45	1.97	30	.69	.2250
FINE	4.5	70	1.97	10	3.10	.4330
FINE	4.5	70	1.97	20	3.35	.4300
FINE	4.5	70	1.97	30	3.33	.4370
FINE	4.5	90	1.97	10	11.00	.4780
FINE	4.5	90	1.97	20	11.25	.4830
FINE	4.5	90	1.97	30	12.33	.4790

TABLE 12 - Summary of the Coefficients in Equation 56 - $\epsilon = \sigma \alpha (\Delta t)^{\beta}$

	GRADATION	ASPHALT CONTENT	TEMPERATURE	PERCENT AIR	AXIAL STRESS	COEFFICIENT α /PSI	COEFFICIENT β
MEDIUM	2.5	25	9.94	10	.88	.0633	
MEDIUM	2.5	25	9.94	30	.85	.0675	
MEDIUM	2.5	25	9.94	50	.82	.0760	
MEDIUM	2.5	45	9.94	10	1.46	.1560	
MEDIUM	2.5	45	9.94	30	1.44	.1600	
MEDIUM	2.5	45	9.94	50	1.46	.1490	
MEDIUM	2.5	70	9.94	10	2.37	.2070	
MEDIUM	2.5	70	9.94	30	2.58	.2210	
MEDIUM	2.5	70	9.94	50	2.56	.2030	
MEDIUM	2.5	90	9.94	10	5.84	.2410	
MEDIUM	2.5	90	9.94	20	6.15	.2630	
MEDIUM	2.5	90	9.94	30	6.45	.2520	
MEDIUM	3.5	25	2.43	10	.31	.0800	
MEDIUM	3.5	25	2.43	30	.29	.0910	
MEDIUM	3.5	25	2.43	50	.28	.0780	
MEDIUM	3.5	45	2.43	10	.58	.1460	
MEDIUM	3.5	45	2.43	30	.55	.1820	
MEDIUM	3.5	45	2.43	50	.55	.1750	
MEDIUM	3.5	70	2.43	10	1.95	.3820	
MEDIUM	3.5	70	2.43	30	2.09	.4030	
MEDIUM	3.5	70	2.43	50	2.17	.4020	
MEDIUM	3.5	90	2.43	10	7.00	.4240	
MEDIUM	3.5	90	2.43	20	7.15	.4500	
MEDIUM	3.5	90	2.43	30	7.33	.4340	
MEDIUM	4.5	25	1.03	10	.37	.1500	
MEDIUM	4.5	25	1.03	30	.38	.1480	
MEDIUM	4.5	25	1.03	50	.38	.1480	
MEDIUM	4.5	45	1.03	10	1.04	.3190	
MEDIUM	4.5	45	1.03	30	1.06	.3190	
MEDIUM	4.5	45	1.03	50	1.05	.3190	
MEDIUM	4.5	70	1.03	10	8.22	.5780	
MEDIUM	4.5	70	1.03	30	8.15	.5770	
MEDIUM	4.5	70	1.03	50	8.04	.5770	
MEDIUM	4.5	90	1.03	10	32.00	.6100	
MEDIUM	4.5	90	1.03	20	44.00	.5470	
MEDIUM	4.5	90	1.03	30	42.00	.5600	

TABLE 13 - Summary of the Coefficients in Equation 56 - $\epsilon = \sigma \alpha (\Delta t)^\beta$

	GRADATION	ASPHALT CONTENT	TEMPERATURE	PERCENT AIR	AXIAL STRESS	COEFFICIENT α /PSI	COEFFICIENT β
COARSE	2.5	25	9.21	10	.47	.0930	
COARSE	2.5	25	9.21	30	.48	.1100	
COARSE	2.5	25	9.21	50	.48	.1050	
COARSE	2.5	45	9.21	10	1.38	.1710	
COARSE	2.5	45	9.21	30	1.35	.1710	
COARSE	2.5	45	9.21	50	1.28	.1710	
COARSE	2.5	70	9.21	10	4.10	.5000	
COARSE	2.5	70	9.21	30	4.28	.4560	
COARSE	2.5	70	9.21	50	4.30	.4300	
COARSE	2.5	90	9.21	10	10.50	.3800	
COARSE	2.5	90	9.21	20	10.50	.3820	
COARSE	2.5	90	9.21	30	10.00	.3820	
COARSE	3.5	25	5.79	10	.53	.0550	
COARSE	3.5	25	5.79	30	.45	.0780	
COARSE	3.5	25	5.79	50	.43	.1350	
COARSE	3.5	45	5.79	10	.68	.1000	
COARSE	3.5	45	5.79	30	.60	.1440	
COARSE	3.5	45	5.79	50	.56	.1940	
COARSE	3.5	70	5.79	10	4.36	.4430	
COARSE	3.5	70	5.79	30	4.30	.4140	
COARSE	3.5	70	5.79	50	4.16	.4130	
COARSE	3.5	90	5.79	10	11.60	.4500	
COARSE	3.5	90	5.79	20	12.50	.4500	
COARSE	3.5	90	5.79	30	11.67	.4250	
COARSE	4.5	25	3.50	10	.44	.1220	
COARSE	4.5	25	3.50	30	.35	.1640	
COARSE	4.5	25	3.50	50	.36	.1340	
COARSE	4.5	45	3.50	10	1.08	.3300	
COARSE	4.5	45	3.50	30	1.06	.3290	
COARSE	4.5	45	3.50	50	1.07	.3290	
COARSE	4.5	70	3.50	10	5.10	.4820	
COARSE	4.5	70	3.50	30	5.33	.4800	
COARSE	4.5	70	3.50	50	5.20	.4800	
COARSE	4.5	90	3.50	10	57.00	.6350	
COARSE	4.5	90	3.50	20	57.00	.6805	
COARSE	4.5	90	3.50	30	57.50	.6838	

TABLE 14 - Summary of the Creep Tests

GRADATION	ASPHALT CONTENT	TEMPERATURE	AXIAL STRESS-PSI	COEFFICIENT C ₁	COEFFICIENT C ₂	COEFFICIENT C ₃	COEFFICIENT C ₄
FINE	2.5	25	10	3.174	.000965	-1.0350	.000935
FINE	2.5	25	30	2.779	.001626	-1.5113	.001139
FINE	2.5	25	50	2.660	.001854	-1.3488	.000541
FINE	2.5	45	10	6.462	.003013	-4.4290	.002804
FINE	2.5	45	30	7.453	.003560	-5.4900	.001094
FINE	2.5	45	50	7.262	.003928	-5.1480	.000635
FINE	2.5	70	10	19.780	.006979	-14.9200	.005078
FINE	2.5	70	30	18.480	.005643	-12.4400	.002123
FINE	2.5	70	50	16.796	.006946	-10.5560	.001227
FINE	2.5	90	10	22.930	.010060	-15.7600	.007059
FINE	2.5	90	20	23.640	.007840	-15.2200	.002614
FINE	2.5	90	30	21.407	.005620	-12.5500	.002423
FINE	3.5	25	10	.553	.000393	-.3635	.042090
FINE	3.5	25	30	.568	.000419	-.2499	.002866
FINE	3.5	25	50	.627	.000389	-.2814	.000723
FINE	3.5	45	10	2.609	.002382	-1.7830	.002001
FINE	3.5	45	30	2.757	.002710	-1.9583	.000510
FINE	3.5	45	50	3.044	.002678	-2.2160	.000258
FINE	3.5	70	10	12.860	.005731	-10.5200	.001927
FINE	3.5	70	20	19.180	.008925	-15.7400	.001419
FINE	3.5	70	30	19.293	.008583	-15.3600	.001369
FINE	3.5	90	10	28.730	.007860	-21.8000	.007449
FINE	3.5	90	30	25.470	.010837	-19.0430	.003610
FINE	4.5	25	10	.759	.000331	-.4342	.001532
FINE	4.5	25	30	.692	.000427	-.3713	.000546
FINE	4.5	25	50	.644	.000481	-.3496	.000512
FINE	4.5	45	10	2.259	.003249	-1.6370	.001804
FINE	4.5	45	20	2.462	.004209	-1.8500	.000748
FINE	4.5	45	30	2.655	.004637	-2.0220	.000518
FINE	4.5	70	10	14.220	.005121	-11.7800	.002973
FINE	4.5	70	20	14.185	.004599	-11.7950	.001787
FINE	4.5	70	30	13.643	.004543	-11.2870	.001404
FINE	4.5	90	10	29.190	.008590	-24.3200	.012060
FINE	4.5	90	20	25.015	.008285	-19.5800	.008065
FINE	4.5	90	30	24.770	.005197	-20.1900	.007317

TABLE 15 - Summary of the Creep Tests

GRADATION	ASPHALT CONTENT	TEMPERATURE	AXIAL STRESS-PSI	COEFFICIENT C ₁	COEFFICIENT C ₂	COEFFICIENT C ₃	COEFFICIENT C ₄
MEDIUM	2.5	25	10	1.264	.00372	-.4806	.004257
MEDIUM	2.5	25	30	1.303	.00474	-.5320	.001074
MEDIUM	2.5	25	50	1.227	.00440	-.4950	.006738
MEDIUM	2.5	45	10	3.105	.001494	-1.7590	.002695
MEDIUM	2.5	45	30	3.209	.001645	-1.8997	.000716
MEDIUM	2.5	45	50	3.184	.002178	-1.8942	.000479
MEDIUM	2.5	70	10	6.118	.002178	-4.2030	.004304
MEDIUM	2.5	70	30	5.993	.002514	-4.2167	.001523
MEDIUM	2.5	70	50	5.790	.002968	-3.9120	.000996
MEDIUM	2.5	90	10	13.550	.005098	-9.1330	.005168
MEDIUM	2.5	90	20	14.195	.006060	-8.9500	.001836
MEDIUM	2.5	90	30	14.393	.005987	-9.1533	.001334
MEDIUM	3.5	25	10	.520	.00373	-.2194	.003361
MEDIUM	3.5	25	30	.482	.00284	-.2271	.001066
MEDIUM	3.5	25	50	.473	.00313	-.2174	.000543
MEDIUM	3.5	45	10	1.618	.001293	-1.1280	.002111
MEDIUM	3.5	45	30	1.770	.001849	-1.3133	.000579
MEDIUM	3.5	45	50	1.864	.002174	-1.3508	.000329
MEDIUM	3.5	70	10	13.410	.005320	-11.6700	.002099
MEDIUM	3.5	70	30	12.903	.005567	-11.2700	.000924
MEDIUM	3.5	70	50	11.828	.004316	-10.1460	.000631
MEDIUM	3.5	90	10	20.900	.006235	-16.5200	.007266
MEDIUM	3.5	90	20	28.950	.010550	-23.6650	.002838
MEDIUM	3.5	90	30	20.157	.007333	-15.1370	.002943
MEDIUM	4.5	22	10	1.101	.001772	-.7394	.002151
MEDIUM	4.5	22	30	1.046	.001507	-.6787	.000512
MEDIUM	4.5	22	50	.931	.001418	-.5720	.000426

TABLE 16 - Summary of the Creep Tests

GRADATION	ASPHALT CONTENT	TEMPERATURE	AXIAL STRESS-PSI	COEFFICIENT C ₁	COEFFICIENT C ₂	COEFFICIENT C ₃	COEFFICIENT C ₄
COARSE	2.5	25	10	.942	.00564	-.5167	.001653
COARSE	2.5	25	30	.877	.00729	-.4517	.000700
COARSE	2.5	25	50	.944	.00874	-.5284	.000423
COARSE	2.5	45	10	4.103	.003275	-2.9710	.002414
COARSE	2.5	45	30	3.667	.003160	-2.5053	.000764
COARSE	2.5	45	50	3.594	.003108	-2.4380	.000392
COARSE	2.5	70	10	31.830	.011000	-28.3500	.002441
COARSE	2.5	70	30	27.977	.008927	-24.3530	.001124
COARSE	2.5	70	50	19.875	.006766	-16.3980	.001083
COARSE	2.5	90	10	20.590	.004831	-15.1800	.011120
COARSE	2.5	90	20	18.255	.005965	-13.0550	.007365
COARSE	2.5	90	30	18.137	.005140	-10.9570	.002552
COARSE	3.5	25	10	.919	.005999	-.4171	.001908
COARSE	3.5	25	30	.900	.006664	-.4900	.000707
COARSE	3.5	25	50	.894	.007709	-.4932	.000359
COARSE	3.5	45	10	2.878	.003977	-2.2940	.001227
COARSE	3.5	45	30	2.968	.003700	-2.4273	.000436
COARSE	3.5	45	50	2.944	.003494	-2.3920	.000294
COARSE	3.5	70	10	28.050	.007633	-24.6600	.003003
COARSE	3.5	70	30	20.107	.005263	-16.8100	.001708
COARSE	3.5	70	50	17.266	.004250	-14.8600	.001647
COARSE	4.5	25	10	.885	.007790	-.5128	.001590
COARSE	4.5	25	30	.842	.009755	-.5527	.000605
COARSE	4.5	25	50	.819	.001222	-.5348	.000429
COARSE	4.5	45	10	8.228	.010530	-7.3900	.001042
COARSE	4.5	45	30	10.713	.016913	-9.7800	.000271
COARSE	4.5	45	50	14.376	.014825	-13.2980	.000129
COARSE	4.5	70	10	37.450	.022520	-32.4700	.001893
COARSE	4.5	70	30	24.640	.019840	-20.2500	.000918
COARSE	4.5	70	50	20.260	.010504	-17.2480	.001294

TABLE 17 - Summary of the Complex Modulus Tests

GRADATION	ASPHALT CONTENT	TEMPERATURE - °F	FREQUENCY - CPS	STRESS-PSI	AXIAL LAG-DEG.	CIRCUMFERENTIAL LAG-DEG.	COMPLEX MODULUS $ E^* $ - PSI	COMPLEX MODULUS $ T^* $ - PSI	COMPLEX POISSON'S RATIO ν^*
FINE	2.5	25	.01	10.00	16.20	20.30	5.263E+05	6.667E+06	.079
FINE	2.5	25	.01	30.00	17.90	12.70	5.882E+05	5.455E+06	.108
FINE	2.5	25	.01	50.00	18.20	19.10	6.452E+05	4.762E+06	.135
FINE	2.5	25	.10	10.00	13.10	18.30	7.143E+05	8.333E+06	.086
FINE	2.5	25	.10	30.00	12.90	15.60	7.653E+05	7.500E+06	.102
FINE	2.5	25	.10	50.00	13.50	15.80	8.547E+05	6.667E+06	.128
FINE	2.5	25	1.00	10.00	10.60	12.90	8.850E+05	1.000E+07	.088
FINE	2.5	25	1.00	30.00	10.30	12.60	1.000E+06	8.824E+06	.113
FINE	2.5	25	1.00	50.00	10.10	12.50	1.064E+06	8.621E+06	.123
FINE	2.5	25	10.00	10.00	7.90	8.20	1.176E+06	1.250E+07	.094
FINE	2.5	25	10.00	30.00	7.60	8.60	1.261E+06	1.500E+07	.084
FINE	2.5	25	10.00	50.00	7.70	8.90	1.344E+06	1.000E+07	.134
FINE	2.5	25	20.00	10.00	6.90	7.20	1.333E+06	2.000E+07	.067
FINE	2.5	25	20.00	30.00	6.90	7.40	1.364E+06	1.667E+07	.082
FINE	2.5	25	20.00	50.00	5.90	6.40	1.429E+06	1.111E+07	.129
FINE	2.5	45	.01	10.00	18.70	26.50	3.704E+05	2.000E+06	.185
FINE	2.5	45	.01	30.00	26.70	33.40	3.304E+05	1.622E+06	.204
FINE	2.5	45	.01	50.00	25.40	31.60	3.704E+05	1.453E+06	.255
FINE	2.5	45	.10	10.00	15.90	20.60	5.556E+05	3.333E+06	.167
FINE	2.5	45	.10	30.00	20.00	23.30	5.217E+05	2.857E+06	.183
FINE	2.5	45	.10	50.00	19.00	23.00	5.774E+05	2.632E+06	.219
FINE	2.5	45	1.00	10.00	11.20	12.50	8.000E+05	4.000E+06	.200
FINE	2.5	45	1.00	30.00	14.50	18.70	7.634E+05	4.615E+06	.165
FINE	2.5	45	1.00	50.00	14.80	18.70	8.065E+05	4.098E+06	.197
FINE	2.5	45	10.00	10.00	12.00	13.50	1.053E+06	5.556E+06	.189
FINE	2.5	45	10.00	30.00	11.70	15.10	1.079E+06	6.522E+06	.165
FINE	2.5	45	10.00	50.00	10.00	12.60	1.104E+06	5.814E+06	.190
FINE	2.5	45	20.00	10.00	8.40	12.40	1.205E+06	7.143E+06	.169
FINE	2.5	45	20.00	30.00	7.10	9.10	1.224E+06	6.977E+06	.176
FINE	2.5	45	20.00	50.00	6.70	12.40	1.232E+06	6.024E+06	.204

TABLE 18 - Summary of the Complex Modulus Tests

GRADATION	ASPHALT CONTENT	TEMPERATURE-°F	FREQUENCY-CPS	STRESS-PSI	AXIAL LAG-DEG.	CIRCUMFERENTIAL LAG-DEG.	COMPLEX MODULUS E* - PSI	COMPLEX MODULUS T* - PSI	COMPLEX POISSON'S RATIO ν*
FINE	2.5	70	.01	10.00	25.60	33.30	7.837E+04	3.279E+05	.239
FINE	2.5	70	.01	30.00	24.10	33.00	1.144E+05	3.550E+05	.322
FINE	2.5	70	.01	50.00	23.00	33.50	1.351E+05	3.546E+05	.381
FINE	2.5	70	.10	10.00	25.00	31.00	1.316E+05	6.897E+05	.191
FINE	2.5	70	.10	30.00	24.00	31.10	1.685E+05	6.316E+05	.267
FINE	2.5	70	.10	50.00	22.20	30.40	1.812E+05	5.155E+05	.351
FINE	2.5	70	1.00	10.00	23.20	30.40	2.247E+05	1.333E+06	.169
FINE	2.5	70	1.00	30.00	21.20	27.90	2.641E+05	1.200E+06	.220
FINE	2.5	70	1.00	50.00	20.20	27.40	2.700E+05	9.328E+05	.289
FINE	2.5	70	10.00	10.00	20.60	28.90	3.846E+05	2.632E+06	.146
FINE	2.5	70	10.00	30.00	19.50	22.90	4.348E+05	2.222E+06	.196
FINE	2.5	70	10.00	50.00	17.80	22.70	3.931E+05	1.634E+06	.241
FINE	2.5	70	20.00	10.00	20.00	25.50	4.762E+05	3.333E+06	.143
FINE	2.5	70	20.00	30.00	15.50	19.80	5.455E+05	2.727E+06	.200
FINE	2.5	70	20.00	50.00	15.90	18.50	4.630E+05	1.953E+06	.237
FINE	2.5	90	.01	10.00	23.40	31.40	6.868E+04	2.128E+05	.323
FINE	2.5	90	.01	20.00	23.80	34.00	7.519E+04	1.761E+05	.427
FINE	2.5	90	.01	30.00	25.20	35.20	9.180E+04	1.779E+05	.516
FINE	2.5	90	.10	10.00	24.00	30.00	9.921E+04	3.509E+05	.283
FINE	2.5	90	.10	20.00	23.60	32.60	1.078E+05	2.985E+05	.361
FINE	2.5	90	.10	30.00	23.80	33.80	1.200E+05	2.752E+05	.436
FINE	2.5	90	1.00	10.00	25.30	28.90	1.667E+05	6.757E+05	.247
FINE	2.5	90	1.00	20.00	23.90	30.00	1.695E+05	5.405E+05	.314
FINE	2.5	90	1.00	30.00	23.30	32.20	1.752E+05	4.870E+05	.360
FINE	2.5	90	10.00	10.00	22.80	27.40	3.205E+05	1.333E+06	.240
FINE	2.5	90	10.00	20.00	25.30	29.30	3.063E+05	1.143E+06	.268
FINE	2.5	90	10.00	30.00	25.80	30.30	3.000E+05	1.017E+06	.295
FINE	2.5	90	20.00	10.00	22.50	27.00	4.082E+05	1.667E+06	.245
FINE	2.5	90	20.00	20.00	23.20	27.80	3.968E+05	1.481E+06	.268
FINE	2.5	90	20.00	30.00	22.80	28.30	3.704E+05	1.304E+06	.284

TABLE 19 - Summary of the Complex Modulus Tests

GRADATION	ASPHALT CONTENT	TEMPERATURE - °F	FREQUENCY - CPS	STRESS-PSI	AXIAL LAG-DEG.	CIRCUMFERENTIAL LAG-DEG.	COMPLEX MODULUS E* - PSI	COMPLEX MODULUS T* - PSI	COMPLEX POISSON'S RATIO ν*
FINE	3.5	25	10.00	12.50	17.10	2.083E+06	5.882E+06	.354	
FINE	3.5	25	30.00	11.50	13.50	2.143E+06	7.059E+06	.304	
FINE	3.5	25	50.00	12.40	15.50	2.212E+06	7.246E+06	.305	
FINE	3.5	25	10.00	9.10	11.50	2.941E+06	8.333E+06	.353	
FINE	3.5	25	30.00	10.10	11.20	2.857E+06	9.375E+06	.305	
FINE	3.5	25	50.00	8.90	10.50	2.778E+06	9.615E+06	.289	
FINE	3.5	25	1.00	7.40	8.50	3.077E+06	7.692E+06	.400	
FINE	3.5	25	1.00	7.30	9.00	3.333E+06	1.154E+07	.289	
FINE	3.5	25	1.00	6.50	7.70	3.333E+06	1.190E+07	.280	
FINE	3.5	25	10.00	6.22	6.50	3.571E+06	1.000E+07	.357	
FINE	3.5	25	30.00	4.90	5.00	3.947E+06	1.200E+07	.329	
FINE	3.5	25	50.00	4.53	4.70	4.000E+06	1.316E+07	.304	
FINE	3.5	25	10.00	5.65	6.00	3.704E+06	1.667E+07	.222	
FINE	3.5	25	30.00	2.90	3.00	3.947E+06	1.364E+07	.289	
FINE	3.5	25	50.00	1.83	2.00	4.167E+06	1.429E+07	.292	
FINE	3.5	45	10.00	21.50	24.50	7.143E+05	2.564E+06	.279	
FINE	3.5	45	30.00	24.00	28.70	7.595E+05	3.000E+06	.253	
FINE	3.5	45	50.00	25.40	29.60	8.403E+05	3.289E+06	.255	
FINE	3.5	45	10.00	16.60	17.50	1.176E+06	4.000E+06	.294	
FINE	3.5	45	30.00	17.20	19.80	1.250E+06	5.455E+06	.229	
FINE	3.5	45	50.00	17.40	20.00	1.292E+06	5.319E+06	.243	
FINE	3.5	45	1.00	12.00	14.50	1.538E+06	6.667E+06	.231	
FINE	3.5	45	1.00	12.10	15.80	1.818E+06	8.571E+06	.212	
FINE	3.5	45	1.00	12.30	15.00	1.838E+06	7.937E+06	.232	
FINE	3.5	45	10.00	7.70	8.00	1.923E+06	7.692E+06	.250	
FINE	3.5	45	30.00	7.50	9.50	2.308E+06	9.231E+06	.250	
FINE	3.5	45	50.00	7.40	10.50	2.439E+06	1.111E+07	.220	
FINE	3.5	45	10.00	5.90	6.00	2.439E+06	9.091E+06	.268	
FINE	3.5	45	30.00	6.90	7.20	2.564E+06	1.111E+07	.231	
FINE	3.5	45	50.00	6.00	6.90	2.632E+06	1.190E+07	.221	

TABLE 20 - Summary of the Complex Modulus Tests

GRADATION	ASPHALT CONTENT	TEMPERATURE - °F	FREQUENCY - CPS	STRESS-PSI	AXIAL LAG-DEG.	CIRCUMFERENTIAL LAG-DEG.	COMPLEX MODULUS E* - PSI	COMPLEX MODULUS T* - PSI	COMPLEX POISSON'S RATIO [ν*]
FINE	3.5	70	10.00	31.20	32.20	1.779E+05	4.878E+05	.365	
FINE	3.5	70	30.00	26.40	28.80	1.948E+05	4.511E+05	.432	
FINE	3.5	70	50.00	29.80	33.60	2.747E+05	6.944E+05	.396	
FINE	3.5	70	10.00	33.50	34.60	4.000E+05	1.087E+06	.368	
FINE	3.5	70	30.00	31.60	34.70	4.615E+05	1.200E+06	.385	
FINE	3.5	70	50.00	29.00	31.50	4.960E+05	1.282E+06	.387	
FINE	3.5	70	10.00	25.40	27.90	8.929E+05	2.381E+06	.375	
FINE	3.5	70	30.00	23.50	25.50	9.259E+05	2.609E+06	.355	
FINE	3.5	70	50.00	24.60	26.30	9.766E+05	2.500E+06	.391	
FINE	3.5	70	10.00	18.00	22.80	1.667E+06	3.846E+06	.433	
FINE	3.5	70	30.00	16.20	19.80	1.630E+06	4.839E+06	.337	
FINE	3.5	70	50.00	16.20	21.50	1.563E+06	4.717E+06	.331	
FINE	3.5	70	10.00	13.80	18.60	1.923E+06	5.000E+06	.385	
FINE	3.5	70	30.00	14.50	16.80	1.829E+06	6.000E+06	.305	
FINE	3.5	70	50.00	11.00	11.40	1.838E+06	5.682E+06	.324	
FINE	3.5	90	10.00	24.90	32.70	6.897E+04	1.575E+05	.438	
FINE	3.5	90	20.00	24.30	33.10	8.929E+04	2.105E+05	.424	
FINE	3.5	90	30.00	23.30	33.00	1.000E+05	2.281E+06	.044	
FINE	3.5	90	10.00	33.00	36.80	1.274E+05	3.390E+05	.376	
FINE	3.5	90	20.00	28.00	34.50	1.538E+05	4.255E+05	.362	
FINE	3.5	90	30.00	27.30	34.20	1.596E+05	4.286E+05	.372	
FINE	3.5	90	10.00	33.70	36.90	2.924E+05	8.475E+05	.345	
FINE	3.5	90	20.00	31.20	34.80	3.077E+05	9.302E+05	.331	
FINE	3.5	90	30.00	30.40	33.60	3.158E+05	9.091E+05	.347	
FINE	3.5	90	10.00	28.30	36.00	6.897E+05	2.174E+06	.317	
FINE	3.5	90	20.00	28.60	29.60	6.757E+05	2.105E+06	.321	
FINE	3.5	90	30.00	27.50	29.60	6.667E+05	2.222E+06	.300	
FINE	3.5	90	10.00	22.10	27.00	9.091E+05	2.632E+06	.345	
FINE	3.5	90	20.00	23.20	24.30	8.511E+05	2.667E+06	.319	
FINE	3.5	90	30.00	22.10	22.80	8.451E+05	2.857E+06	.296	

TABLE 21 - Summary of the Complex Modulus Tests

GRADATION	ASPHALT CONTENT	TEMPERATURE-°F	FREQUENCY-CPS	STRESS-PSI	AXIAL LAG-DEG.	CIRCUMFERENTIAL LAG-DEG.	COMPLEX MODULUS E* - PSI	COMPLEX MODULUS E* - PSI	COMPLEX POISSON'S RATIO ν*
FINE	4.5	25	.01	10.00	15.20	21.20	2.222E+06	5.000E+06	.4444
FINE	4.5	25	.01	30.00	16.50	20.00	2.400E+06	6.250E+06	.384
FINE	4.5	25	.01	50.00	16.00	20.50	2.326E+06	6.667E+06	.349
FINE	4.5	25	.10	10.00	10.60	14.00	2.857E+06	6.667E+06	.429
FINE	4.5	25	.10	30.00	10.20	16.90	3.158E+06	9.375E+06	.337
FINE	4.5	25	.10	50.00	10.30	14.70	3.125E+06	1.000E+07	.313
FINE	4.5	25	1.00	10.00	7.30	12.90	3.333E+06	7.143E+06	.467
FINE	4.5	25	1.00	30.00	6.10	12.80	3.614E+06	1.200E+07	.301
FINE	4.5	25	1.00	50.00	7.10	12.20	4.000E+06	1.351E+07	.296
FINE	4.5	25	10.00	10.00	5.10	8.00	4.000E+06	1.000E+07	.400
FINE	4.5	25	10.00	30.00	5.20	7.60	4.286E+06	2.000E+07	.214
FINE	4.5	25	10.00	50.00	4.10	8.60	4.545E+06	1.667E+07	.273
FINE	4.5	25	20.00	10.00	3.60	8.10	5.000E+06	1.429E+07	.350
FINE	4.5	25	20.00	30.00	2.70	7.60	5.000E+06	2.727E+07	.183
FINE	4.5	25	20.00	50.00	2.00	5.00	4.630E+06	1.923E+07	.241
FINE	4.5	45	.01	10.00	29.60	32.10	9.091E+05	2.222E+06	.409
FINE	4.5	45	.01	20.00	28.30	32.80	8.889E+05	2.381E+06	.373
FINE	4.5	45	.01	30.00	28.10	31.80	9.231E+05	2.362E+06	.391
FINE	4.5	45	.10	10.00	20.30	26.40	1.562E+06	3.846E+06	.406
FINE	4.5	45	.10	20.00	20.20	26.70	1.562E+06	4.444E+06	.352
FINE	4.5	45	.10	30.00	20.00	25.50	1.613E+06	4.615E+06	.349
FINE	4.5	45	1.00	10.00	16.70	25.70	2.128E+06	6.250E+06	.340
FINE	4.5	45	1.00	20.00	14.30	23.30	2.273E+06	6.061E+06	.375
FINE	4.5	45	1.00	30.00	12.90	19.00	2.344E+06	6.667E+06	.352
FINE	4.5	45	10.00	10.00	11.30	22.30	2.857E+06	9.091E+06	.314
FINE	4.5	45	10.00	20.00	11.00	21.70	2.857E+06	1.000E+07	.286
FINE	4.5	45	10.00	30.00	9.00	15.80	3.000E+06	1.154E+07	.260
FINE	4.5	45	20.00	10.00	9.00	19.30	3.333E+06	1.000E+07	.333
FINE	4.5	45	20.00	20.00	8.10	19.40	3.226E+06	1.111E+07	.290
FINE	4.5	45	20.00	30.00	8.60	12.20	3.448E+06	1.364E+07	.253

TABLE 22 - Summary of the Complex Modulus Tests

GRADATION	ASPHALT CONTENT	TEMPERATURE - °F	FREQUENCY - CPS	STRESS - PSI	AXIAL LAG - DEG.	CIRCUMFERENTIAL LAG - DEG.	COMPLEX MODULUS E* - PSI	COMPLEX MODULUS T* - PSI	COMPLEX POISSON'S RATIO ν*
FINE	4.4	70	10.00	34.30	33.90	1.733E+05	2.890E+05	.600	
FINE	4.5	70	20.00	32.60	39.00	2.286E+05	3.289E+05	.695	
FINE	4.5	70	30.00	31.40	37.40	2.212E+05	3.593E+05	.616	
FINE	4.5	70	10.00	34.50	38.50	3.922E+05	7.246E+05	.541	
FINE	4.5	70	20.00	32.80	37.60	4.149E+05	7.220E+05	.575	
FINE	4.5	70	30.00	31.60	36.70	4.225E+05	7.317E+05	.577	
FINE	4.5	70	10.00	29.60	34.70	8.696E+05	1.667E+06	.522	
FINE	4.5	70	20.00	28.60	34.40	9.217E+05	1.786E+06	.516	
FINE	4.5	70	30.00	28.50	34.60	9.146E+05	1.807E+06	.506	
FINE	4.5	70	10.00	21.60	33.30	1.538E+06	3.333E+06	.462	
FINE	4.5	70	20.00	20.80	32.90	1.639E+06	3.846E+06	.426	
FINE	4.5	70	30.00	20.60	32.20	1.714E+06	3.750E+06	.457	
FINE	4.5	70	10.00	17.80	28.70	1.818E+06	5.000E+06	.364	
FINE	4.5	70	20.00	15.40	26.80	2.000E+06	4.651E+06	.430	
FINE	4.5	70	30.00	16.60	25.20	2.000E+06	4.839E+06	.413	
FINE	4.5	90	10.00	27.90	33.50	5.411E+04	9.294E+04	.582	
FINE	4.5	90	20.00	24.80	31.70	6.887E+04	1.131E+05	.609	
FINE	4.5	90	30.00	24.10	32.00	7.194E+04	1.092E+05	.659	
FINE	4.5	90	10.00	33.20	36.20	1.057E+05	2.041E+05	.518	
FINE	4.5	90	20.00	29.30	34.40	1.220E+05	2.247E+05	.543	
FINE	4.5	90	30.00	27.80	34.50	1.225E+05	2.128E+05	.576	
FINE	4.5	90	10.00	36.80	39.50	2.577E+05	5.464E+05	.472	
FINE	4.5	90	20.00	34.40	37.90	2.695E+05	5.650E+05	.477	
FINE	4.5	90	30.00	33.80	37.30	2.568E+05	5.128E+05	.501	
FINE	4.5	90	10.00	32.80	35.40	6.536E+05	1.429E+06	.458	
FINE	4.5	90	20.00	34.60	38.40	6.667E+05	1.429E+06	.467	
FINE	4.5	90	30.00	33.80	38.60	6.250E+05	1.376E+06	.454	
FINE	4.5	90	10.00	29.10	39.60	8.333E+05	1.923E+06	.433	
FINE	4.5	90	20.00	30.20	34.70	8.511E+05	2.000E+06	.426	
FINE	4.5	90	30.00	29.70	32.00	8.333E+05	2.000E+06	.417	

TABLE 23 - Summary of the Complex Modulus Tests

GRADATION	ASPHALT CONTENT	TEMPERATURE-°F	FREQUENCY-CPS	STRESS-PSI	AXIAL LAG-DEG.	CIRCUMFERENTIAL LAG-DEG.	COMPLEX MODULUS E* - PSI	COMPLEX MODULUS T* - PSI	COMPLEX POISSON'S RATIO ν*
MEDIUM	2.5	25	10.00	11.70	16.00	9.524E+05	6.667E+06	.143	
MEDIUM	2.5	25	30.00	10.70	15.00	1.141E+06	8.333E+06	.137	
MEDIUM	2.5	25	50.00	12.50	13.00	1.168E+06	8.197E+06	.143	
MEDIUM	2.5	25	10.00	10.50	13.60	1.149E+06	9.091E+06	.126	
MEDIUM	2.5	25	30.00	9.30	13.30	1.376E+06	1.000E+07	.138	
MEDIUM	2.5	25	50.00	10.00	10.70	1.429E+06	1.042E+07	.137	
MEDIUM	2.5	25	10.00	8.90	12.90	1.333E+06	1.000E+07	.133	
MEDIUM	2.5	25	30.00	8.10	9.00	1.579E+06	1.071E+07	.147	
MEDIUM	2.5	25	50.00	7.10	10.00	1.645E+06	1.087E+07	.151	
MEDIUM	2.5	25	10.00	4.50	7.60	1.587E+06	1.429E+07	.111	
MEDIUM	2.5	25	30.00	6.00	7.90	1.840E+06	1.364E+07	.135	
MEDIUM	2.5	25	50.00	3.90	6.00	1.923E+06	1.282E+07	.150	
MEDIUM	2.5	25	10.00	1.40	4.50	1.852E+06	1.667E+07	.111	
MEDIUM	2.5	25	30.00	1.10	5.90	2.000E+06	1.500E+07	.133	
MEDIUM	2.5	25	50.00	1.40	4.30	2.066E+06	1.471E+07	.140	
MEDIUM	2.5	45	10.00	20.80	26.10	4.808E+05	5.556E+06	.087	
MEDIUM	2.5	45	30.00	20.50	23.80	5.236E+05	4.918E+06	.106	
MEDIUM	2.5	45	50.00	20.70	25.60	5.708E+05	4.167E+06	.137	
MEDIUM	2.5	45	10.00	13.40	14.60	6.897E+05	7.143E+06	.097	
MEDIUM	2.5	45	30.00	16.00	18.00	8.108E+05	7.895E+06	.103	
MEDIUM	2.5	45	50.00	15.70	17.90	8.547E+05	6.944E+06	.123	
MEDIUM	2.5	45	10.00	14.30	15.20	8.929E+05	1.000E+07	.089	
MEDIUM	2.5	45	30.00	11.10	11.40	1.060E+06	9.375E+06	.113	
MEDIUM	2.5	45	50.00	11.50	12.80	1.136E+06	1.000E+07	.114	
MEDIUM	2.5	45	10.00	8.25	10.00	1.190E+06	1.429E+07	.083	
MEDIUM	2.5	45	30.00	6.80	11.70	1.364E+06	1.200E+07	.114	
MEDIUM	2.5	45	50.00	7.60	8.00	1.445E+06	1.316E+07	.110	
MEDIUM	2.5	45	10.00	5.50	6.00	1.429E+06	2.000E+07	.071	
MEDIUM	2.5	45	30.00	4.00	4.50	1.538E+06	1.364E+07	.113	
MEDIUM	2.5	45	50.00	6.60	6.80	1.563E+06	1.389E+07	.113	

TABLE 24 - Summary of the Complex Modulus Tests

GRADATION	ASPHALT CONTENT	TEMPERATURE - °F	FREQUENCY - CPS	STRESS-PSI	AXIAL LAG-DEG.	CIRCUMFERENTIAL LAG-DEG.	COMPLEX MODULUS E* - PSI	COMPLEX MODULUS T* - PSI	COMPLEX POISSON'S RATIO ν*
MEDIUM	2.5	70	.01	10.00	22.90	26.60	2.667E+05	1.333E+06	.200
MEDIUM	2.5	70	.01	30.00	24.50	28.40	3.191E+05	1.250E+06	.255
MEDIUM	2.5	70	.01	50.00	25.00	30.50	3.650E+05	1.220E+06	.299
MEDIUM	2.5	70	.10	10.00	20.30	20.90	4.348E+05	2.222E+06	.196
MEDIUM	2.5	70	.10	30.00	21.50	23.00	5.000E+05	2.069E+06	.242
MEDIUM	2.5	70	.10	50.00	20.80	24.20	5.495E+05	2.000E+06	.275
MEDIUM	2.5	70	1.00	10.00	18.20	19.80	6.667E+05	3.704E+06	.180
MEDIUM	2.5	70	1.00	30.00	17.60	19.50	7.595E+05	3.488E+06	.218
MEDIUM	2.5	70	1.00	50.00	18.40	20.50	8.197E+05	3.226E+06	.254
MEDIUM	2.5	70	10.00	10.00	15.20	17.30	9.804E+05	4.545E+06	.216
MEDIUM	2.5	70	10.00	30.00	11.70	14.10	1.071E+06	5.000E+06	.214
MEDIUM	2.5	70	10.00	50.00	12.30	16.80	1.149E+06	5.000E+06	.230
MEDIUM	2.5	70	20.00	10.00	13.60	16.30	1.111E+06	5.000E+06	.222
MEDIUM	2.5	70	20.00	30.00	11.00	14.60	1.277E+06	5.455E+06	.234
MEDIUM	2.5	70	20.00	50.00	8.40	11.80	1.333E+06	5.882E+06	.227
MEDIUM	2.5	90	.01	10.00	26.50	34.50	1.099E+05	4.651E+05	.236
MEDIUM	2.5	90	.01	20.00	24.50	34.60	1.325E+05	4.878E+05	.272
MEDIUM	2.5	90	.01	30.00	23.50	34.10	1.397E+05	4.918E+05	.284
MEDIUM	2.5	90	.10	10.00	25.20	31.40	1.835E+05	9.346E+05	.196
MEDIUM	2.5	90	.10	20.00	24.30	31.60	2.083E+05	9.302E+05	.224
MEDIUM	2.5	90	.10	30.00	24.30	32.40	2.143E+05	9.231E+05	.232
MEDIUM	2.5	90	1.00	10.00	24.80	27.90	3.195E+05	1.818E+06	.176
MEDIUM	2.5	90	1.00	20.00	22.90	29.50	3.448E+05	1.852E+06	.186
MEDIUM	2.5	90	1.00	30.00	24.30	31.00	3.513E+05	1.786E+06	.197
MEDIUM	2.5	90	10.00	10.00	19.30	20.00	5.714E+05	3.846E+06	.149
MEDIUM	2.5	90	10.00	20.00	20.80	22.90	5.970E+05	3.448E+06	.173
MEDIUM	2.5	90	10.00	30.00	19.00	25.40	6.000E+05	3.614E+06	.166
MEDIUM	2.5	90	20.00	10.00	15.80	17.50	6.757E+05	4.348E+06	.155
MEDIUM	2.5	90	20.00	20.00	14.00	19.90	7.143E+05	4.255E+06	.168
MEDIUM	2.5	90	20.00	30.00	18.20	19.10	7.143E+05	4.762E+06	.150

TABLE 25 - Summary of the Complex Modulus Tests

GRADATION	ASPHALT CONTENT	TEMPERATURE - °F	FREQUENCY - CPS	STRESS - PSI	AXIAL LAG - DEG.	CIRCUMFERENTIAL LAG - DEG.	COMPLEX MODULUS [E*] - PSI	COMPLEX MODULUS [T*] - PSI	COMPLEX POISSON'S RATIO [V*]
MEDIUM	3.5	25	.01	10.00	13.80	17.00	2.857E+06	6.667E+06	.429
MEDIUM	3.5	25	.01	30.00	11.10	16.50	2.913E+06	9.375E+06	.311
MEDIUM	3.5	25	.01	50.00	11.90	16.20	2.907E+06	1.111E+07	.262
MEDIUM	3.5	25	.10	10.00	8.30	12.50	3.333E+06	6.667E+06	.500
MEDIUM	3.5	25	.10	30.00	8.40	13.50	3.750E+06	1.250E+07	.300
MEDIUM	3.5	25	.10	50.00	8.60	13.90	3.704E+06	1.515E+07	.244
MEDIUM	3.5	25	1.00	10.00	6.40	11.90	3.571E+06	7.692E+06	.464
MEDIUM	3.5	25	1.00	30.00	6.90	12.00	4.110E+06	1.364E+07	.301
MEDIUM	3.5	25	1.00	50.00	6.00	11.80	4.348E+06	1.667E+07	.261
MEDIUM	3.5	25	10.00	10.00	3.90	10.90	4.000E+06	1.000E+07	.400
MEDIUM	3.5	25	10.00	30.00	3.70	9.30	4.762E+06	1.667E+07	.286
MEDIUM	3.5	25	10.00	50.00	4.10	9.00	4.902E+06	1.852E+07	.265
MEDIUM	3.5	25	20.00	10.00	2.70	6.30	4.348E+06	1.667E+07	.261
MEDIUM	3.5	25	20.00	30.00	2.30	5.40	5.000E+06	1.765E+07	.283
MEDIUM	3.5	25	20.00	50.00	2.70	5.90	5.263E+06	2.000E+07	.263
MEDIUM	3.5	45	.01	10.00	24.30	31.30	1.176E+06	2.941E+06	.400
MEDIUM	3.5	45	.01	30.00	24.70	30.20	1.235E+06	3.226E+06	.383
MEDIUM	3.5	45	.01	50.00	25.00	30.00	1.250E+06	3.226E+06	.388
MEDIUM	3.5	45	.10	10.00	18.70	25.50	1.923E+06	5.000E+06	.385
MEDIUM	3.5	45	.10	30.00	18.20	24.50	2.000E+06	5.769E+06	.347
MEDIUM	3.5	45	.10	50.00	17.60	24.30	2.049E+06	5.882E+06	.348
MEDIUM	3.5	45	1.00	10.00	13.60	21.20	2.632E+06	7.143E+06	.368
MEDIUM	3.5	45	1.00	30.00	12.00	20.10	2.857E+06	8.571E+06	.333
MEDIUM	3.5	45	1.00	50.00	12.00	20.00	2.890E+06	1.000E+07	.289
MEDIUM	3.5	45	10.00	10.00	8.60	15.00	2.941E+06	1.000E+07	.294
MEDIUM	3.5	45	10.00	30.00	8.30	15.20	3.409E+06	1.071E+07	.318
MEDIUM	3.5	45	10.00	50.00	7.90	15.80	3.623E+06	1.250E+07	.290
MEDIUM	3.5	45	20.00	10.00	5.00	12.30	3.704E+06	1.667E+07	.222
MEDIUM	3.5	45	20.00	30.00	5.40	13.10	3.750E+06	1.304E+07	.287
MEDIUM	3.5	45	20.00	50.00	4.60	12.70	3.906E+06	1.351E+07	.289

TABLE 26 - Summary of the Complex Modulus Tests

GRADATION	ASPHALT CONTENT	TEMPERATURE - °F	FREQUENCY - CPS	STRESS-PSI	AXIAL LAG-DEG.	CIRCUMFERENTIAL LAG-DEG.	COMPLEX MODULUS $ E^* - \text{PSI}$	COMPLEX MODULUS $ T^* - \text{PSI}$	COMPLEX POISSON'S RATIO ν^*
MEDIUM	3.5	70	.01	10.00	34.40	35.90	2.597E+05	6.452E+05	.403
MEDIUM	3.5	70	.01	30.00	32.90	35.40	2.788E+05	6.912E+05	.403
MEDIUM	3.5	70	.01	50.00	30.70	34.20	2.809E+05	7.042E+05	.399
MEDIUM	3.5	70	.10	10.00	32.90	34.40	5.988E+05	1.429E+06	.419
MEDIUM	3.5	70	.10	30.00	33.30	34.20	6.148E+05	1.554E+06	.395
MEDIUM	3.5	70	.10	50.00	33.10	34.80	5.747E+05	1.493E+06	.385
MEDIUM	3.5	70	1.00	10.00	26.60	29.70	1.176E+06	3.030E+06	.388
MEDIUM	3.5	70	1.00	30.00	26.20	30.20	1.288E+06	3.529E+06	.365
MEDIUM	3.5	70	1.00	50.00	27.80	30.10	1.241E+06	3.497E+06	.355
MEDIUM	3.5	70	10.00	10.00	16.80	22.80	2.000E+06	5.000E+06	.400
MEDIUM	3.5	70	10.00	30.00	16.30	23.00	2.190E+06	6.250E+06	.350
MEDIUM	3.5	70	10.00	50.00	16.90	23.60	2.193E+06	6.410E+06	.342
MEDIUM	3.5	70	20.00	10.00	14.40	17.10	2.381E+06	8.333E+06	.286
MEDIUM	3.5	70	20.00	30.00	13.10	17.20	2.564E+06	7.143E+06	.359
MEDIUM	3.5	70	20.00	50.00	11.40	17.70	2.525E+06	7.692E+06	.328
MEDIUM	3.5	90	.01	10.00	26.30	33.20	7.364E+04	1.269E+05	.580
MEDIUM	3.5	90	.01	20.00	21.80	28.90	9.042E+04	1.555E+05	.581
MEDIUM	3.5	90	.01	30.00	20.50	27.60	1.042E+05	1.786E+05	.583
MEDIUM	3.5	90	.10	10.00	34.60	37.30	1.433E+05	2.809E+05	.510
MEDIUM	3.5	90	.10	20.00	31.40	35.10	1.672E+05	3.344E+05	.500
MEDIUM	3.5	90	.10	30.00	29.00	32.20	1.792E+05	3.546E+05	.505
MEDIUM	3.5	90	1.00	10.00	38.40	41.50	3.663E+05	7.812E+05	.469
MEDIUM	3.5	90	1.00	20.00	35.80	38.10	4.016E+05	8.511E+05	.472
MEDIUM	3.5	90	1.00	30.00	34.20	36.70	4.021E+05	8.523E+05	.472
MEDIUM	3.5	90	10.00	10.00	30.00	33.40	9.709E+05	2.000E+06	.485
MEDIUM	3.5	90	10.00	20.00	28.20	34.50	9.804E+05	2.299E+06	.426
MEDIUM	3.5	90	10.00	30.00	30.00	33.80	1.000E+06	2.273E+06	.440
MEDIUM	3.5	90	20.00	10.00	25.00	29.00	1.176E+06	3.030E+06	.388
MEDIUM	3.5	90	20.00	20.00	25.90	30.40	1.290E+06	3.030E+06	.426
MEDIUM	3.5	90	20.00	30.00	25.00	32.60	1.261E+06	3.000E+06	.420

TABLE 28 - Summary of the Complex Modulus Tests

GRADATION	ASPHALT CONTENT	TEMPERATURE-°F	FREQUENCY-CPS	STRESS-PSI	AXIAL LAG-DEG.	CIRCUMFERENTIAL LAG-DEG.	COMPLEX MODULUS E* - PSI	COMPLEX MODULUS T* - PSI	COMPLEX POISSON'S RATIO ν*
MEDIUM	4.5	70	.01	10.00	49.50	51.50	7.375E+04	1.437E+05	.513
MEDIUM	4.5	70	.01	30.00	45.00	46.00	1.076E+05	1.801E+05	.598
MEDIUM	4.5	70	.01	50.00	38.50	45.20	1.449E+05	1.866E+05	.777
MEDIUM	4.5	70	.10	10.00	45.50	47.30	1.866E+05	3.704E+05	.504
MEDIUM	4.5	70	.10	30.00	38.70	42.00	3.061E+05	5.769E+05	.531
MEDIUM	4.5	70	.10	50.00	37.80	42.30	3.717E+05	5.682E+05	.654
MEDIUM	4.5	70	1.00	10.00	40.20	44.50	5.682E+05	1.136E+06	.500
MEDIUM	4.5	70	1.00	30.00	33.20	38.00	7.895E+05	1.667E+06	.474
MEDIUM	4.5	70	1.00	50.00	31.60	37.80	8.929E+05	1.667E+06	.536
MEDIUM	4.5	70	10.00	10.00	29.70	34.70	1.282E+06	2.857E+06	.449
MEDIUM	4.5	70	10.00	30.00	23.50	28.50	1.554E+06	4.000E+06	.389
MEDIUM	4.5	70	10.00	50.00	23.00	30.70	1.724E+06	3.788E+06	.455
MEDIUM	4.5	70	20.00	10.00	18.80	19.30	1.667E+06	5.000E+06	.333
MEDIUM	4.5	70	20.00	30.00	15.20	21.50	1.899E+06	5.000E+06	.380
MEDIUM	4.5	70	20.00	50.00	18.50	24.40	2.174E+06	5.263E+06	.413
MEDIUM	4.5	90	.01	10.00	34.90	36.80	2.381E+04	5.176E+04	.460
MEDIUM	4.5	90	.01	10.00	34.90	36.80	2.381E+04	5.176E+04	.460
MEDIUM	4.5	90	.01	30.00	29.60	34.10	3.968E+04	7.317E+04	.542
MEDIUM	4.5	90	.10	10.00	44.50	47.00	7.353E+04	1.667E+05	.441
MEDIUM	4.5	90	.10	10.00	44.50	47.00	7.353E+04	1.667E+05	.441
MEDIUM	4.5	90	.10	30.00	37.80	41.70	9.894E+04	2.113E+05	.468
MEDIUM	4.5	90	1.00	10.00	48.00	51.20	2.632E+05	6.135E+05	.429
MEDIUM	4.5	90	1.00	10.00	48.00	51.20	2.632E+05	6.135E+05	.429
MEDIUM	4.5	90	1.00	30.00	44.50	47.50	3.030E+05	7.143E+05	.424
MEDIUM	4.5	90	10.00	10.00	44.10	45.00	9.091E+05	1.667E+06	.545
MEDIUM	4.5	90	10.00	10.00	44.10	45.00	9.091E+05	1.667E+06	.545
MEDIUM	4.5	90	10.00	30.00	37.30	44.70	1.010E+06	2.439E+06	.414
MEDIUM	4.5	90	20.00	10.00	42.30	45.00	1.493E+06	3.125E+06	.478
MEDIUM	4.5	90	20.00	10.00	42.30	45.00	1.493E+06	3.125E+06	.478
MEDIUM	4.5	90	20.00	30.00	32.40	33.30	1.429E+06	3.333E+06	.429

TABLE 29 - Summary of the Complex Modulus Tests

GRADATION	ASPHALT CONTENT	TEMPERATURE - °F	FREQUENCY - CPS	STRESS-PSI	AXIAL LAG-DEG.	CIRCUMFERENTIAL LAG-DEG.	COMPLEX MODULUS E* - PSI	COMPLEX MODULUS T* - PSI	COMPLEX POISSON'S RATIO ν*
COARSE	2.5	25	.01	10.00	14.60	20.70	1.587E+06	4.348E+06	.365
COARSE	2.5	25	.01	30.00	15.20	21.40	1.714E+06	6.250E+06	.274
COARSE	2.5	25	.01	50.00	16.10	22.20	1.742E+06	6.494E+06	.268
COARSE	2.5	25	.10	10.00	10.20	14.00	2.083E+06	5.000E+06	.417
COARSE	2.5	25	.10	30.00	10.00	13.80	2.273E+06	8.333E+06	.273
COARSE	2.5	25	.10	50.00	10.20	14.50	2.294E+06	9.434E+06	.243
COARSE	2.5	25	1.00	10.00	7.70	11.00	2.273E+06	6.250E+06	.364
COARSE	2.5	25	1.00	30.00	7.20	11.60	2.727E+06	1.000E+07	.273
COARSE	2.5	25	1.00	50.00	7.60	11.40	2.778E+06	1.190E+07	.233
COARSE	2.5	25	10.00	10.00	3.80	7.50	2.778E+06	8.333E+06	.333
COARSE	2.5	25	10.00	30.00	4.50	8.30	3.125E+06	1.111E+07	.281
COARSE	2.5	25	10.00	50.00	3.80	7.20	3.226E+06	1.316E+07	.245
COARSE	2.5	25	20.00	10.00	2.30	6.00	3.333E+06	1.429E+07	.233
COARSE	2.5	25	20.00	30.00	2.70	5.80	3.488E+06	1.500E+07	.233
COARSE	2.5	25	20.00	50.00	2.30	5.40	3.401E+06	1.515E+07	.224
COARSE	2.5	45	.01	10.00	25.20	30.00	9.091E+05	3.846E+06	.236
COARSE	2.5	45	.01	30.00	23.90	28.00	1.111E+06	5.455E+06	.204
COARSE	2.5	45	.01	50.00	23.80	30.20	1.244E+06	6.024E+06	.206
COARSE	2.5	45	.10	10.00	17.20	23.40	1.471E+06	6.250E+06	.235
COARSE	2.5	45	.10	30.00	17.50	24.20	1.695E+06	1.000E+07	.169
COARSE	2.5	45	.10	50.00	16.20	22.20	1.887E+06	1.087E+07	.174
COARSE	2.5	45	1.00	10.00	13.40	17.40	2.222E+06	7.143E+06	.311
COARSE	2.5	45	1.00	30.00	12.00	16.70	2.308E+06	1.304E+07	.177
COARSE	2.5	45	1.00	50.00	12.90	16.80	2.564E+06	1.515E+07	.169
COARSE	2.5	45	10.00	10.00	7.50	13.10	2.632E+06	9.091E+06	.289
COARSE	2.5	45	10.00	30.00	7.60	12.40	2.830E+06	1.500E+07	.189
COARSE	2.5	45	10.00	50.00	6.80	12.40	3.165E+06	2.174E+07	.146
COARSE	2.5	45	20.00	10.00	5.50	8.20	3.030E+06	1.250E+07	.242
COARSE	2.5	45	20.00	30.00	4.90	8.50	3.158E+06	2.143E+07	.147
COARSE	2.5	45	20.00	50.00	5.00	8.10	3.425E+06	2.381E+07	.144

TABLE 30 - Summary of the Complex Modulus Tests

GRADATION	ASPHALT CONTENT	TEMPERATURE - F	FREQUENCY - CPS	STRESS - PSI	AXIAL LAG - DEG.	CIRCUMFERENTIAL LAG - DEG.	COMPLEX MODULUS E* - PSI	COMPLEX MODULUS T* - PSI	COMPLEX POISSON'S RATIO ν*
COARSE	2.5	70	.01	10.00	28.30	37.50	1.538E+05	3.509E+05	.438
COARSE	2.5	70	.01	30.00	27.10	36.70	1.471E+05	3.074E+05	.478
COARSE	2.5	70	.01	50.00	23.30	34.10	1.656E+05	3.289E+05	.503
COARSE	2.5	70	.10	10.00	32.40	37.80	3.268E+05	8.621E+05	.379
COARSE	2.5	70	.10	30.00	31.80	37.10	3.000E+05	7.895E+05	.380
COARSE	2.5	70	.10	50.00	28.70	34.90	3.205E+05	8.475E+05	.378
COARSE	2.5	70	1.00	10.00	28.70	34.00	6.897E+05	1.818E+06	.379
COARSE	2.5	70	1.00	30.00	30.00	35.80	6.742E+05	1.935E+06	.348
COARSE	2.5	70	1.00	50.00	28.40	32.90	6.684E+05	1.961E+06	.341
COARSE	2.5	70	10.00	10.00	19.50	27.70	1.176E+06	3.125E+06	.376
COARSE	2.5	70	10.00	30.00	20.30	27.40	1.304E+06	4.054E+06	.322
COARSE	2.5	70	10.00	50.00	21.00	25.90	1.282E+06	4.098E+06	.313
COARSE	2.5	70	20.00	10.00	15.70	24.80	1.370E+06	4.000E+06	.342
COARSE	2.5	70	20.00	30.00	17.60	24.30	1.538E+06	5.000E+06	.308
COARSE	2.5	70	20.00	50.00	15.10	20.90	1.515E+06	5.000E+06	.303
COARSE	2.5	90	.01	10.00	22.30	30.30	1.462E+05	4.237E+05	.345
COARSE	2.5	90	.01	20.00	22.20	33.20	1.639E+05	4.082E+05	.402
COARSE	2.5	90	.01	30.00	21.00	31.90	1.852E+05	4.286E+05	.432
COARSE	2.5	90	.10	10.00	29.10	34.00	2.532E+05	8.696E+05	.291
COARSE	2.5	90	.10	20.00	27.50	35.50	2.717E+05	8.584E+05	.317
COARSE	2.5	90	.10	30.00	24.80	34.00	2.913E+05	8.955E+05	.325
COARSE	2.5	90	1.00	10.00	30.80	33.60	5.263E+05	1.818E+06	.289
COARSE	2.5	90	1.00	20.00	30.00	34.70	5.479E+05	2.041E+06	.268
COARSE	2.5	90	1.00	30.00	28.50	35.70	5.556E+05	2.000E+06	.278
COARSE	2.5	90	10.00	10.00	24.80	29.70	1.053E+06	3.704E+06	.284
COARSE	2.5	90	10.00	20.00	24.40	29.60	1.081E+06	4.762E+06	.227
COARSE	2.5	90	10.00	30.00	23.10	31.40	1.083E+06	4.615E+06	.235
COARSE	2.5	90	20.00	10.00	22.50	27.00	1.333E+06	5.882E+06	.227
COARSE	2.5	90	20.00	20.00	20.30	26.60	1.333E+06	6.250E+06	.213
COARSE	2.5	90	20.00	30.00	23.40	29.20	1.322E+06	5.455E+06	.242

TABLE 31 - Summary of the Complex Modulus Tests

GRADATION	ASPHALT CONTENT	TEMPERATURE - ° F	FREQUENCY - CPS	STRESS-PSI	AXIAL LAG-DEG.	CIRCUMFERENTIAL LAG-DEG.	COMPLEX MODULUS E* - PSI	COMPLEX MODULUS T* - PSI	COMPLEX POISSON'S RATIO ν*
COARSE	3.5	25	.01	10.00	14.90	20.10	1.667E+06	5.556E+06	.300
COARSE	3.5	25	.01	30.00	15.50	17.40	1.852E+06	7.143E+06	.259
COARSE	3.5	25	.01	50.00	15.00	20.00	1.818E+06	7.576E+06	.240
COARSE	3.5	25	.10	10.00	10.70	13.50	2.083E+06	6.667E+06	.312
COARSE	3.5	25	.10	30.00	10.20	11.50	2.381E+06	1.000E+07	.238
COARSE	3.5	25	.10	50.00	10.20	13.30	2.439E+06	1.064E+07	.229
COARSE	3.5	25	1.00	10.00	7.30	9.50	2.857E+06	7.692E+06	.371
COARSE	3.5	25	1.00	30.00	6.10	9.00	2.857E+06	1.111E+07	.257
COARSE	3.5	25	1.00	50.00	7.10	9.00	2.857E+06	1.429E+07	.200
COARSE	3.5	25	10.00	10.00	5.60	7.80	3.125E+06	1.000E+07	.312
COARSE	3.5	25	10.00	30.00	5.30	6.40	3.261E+06	1.304E+07	.250
COARSE	3.5	25	10.00	50.00	5.60	6.80	3.448E+06	1.562E+07	.221
COARSE	3.5	25	20.00	10.00	3.20	5.40	3.704E+06	1.667E+07	.222
COARSE	3.5	25	20.00	30.00	3.10	4.50	3.529E+06	1.364E+07	.259
COARSE	3.5	25	20.00	50.00	2.30	4.90	3.650E+06	1.786E+07	.204
COARSE	3.5	45	.01	10.00	28.40	34.80	9.524E+05	2.000E+06	.476
COARSE	3.5	45	.01	30.00	30.40	35.00	9.677E+05	2.143E+06	.452
COARSE	3.5	45	.01	50.00	30.60	35.00	9.804E+05	2.146E+06	.457
COARSE	3.5	45	.10	10.00	22.10	29.80	1.667E+06	4.000E+06	.417
COARSE	3.5	45	.10	30.00	21.60	26.00	1.796E+06	4.478E+06	.401
COARSE	3.5	45	.10	50.00	21.60	27.30	1.799E+06	3.333E+06	.540
COARSE	3.5	45	1.00	10.00	14.50	21.20	2.500E+06	5.882E+06	.425
COARSE	3.5	45	1.00	30.00	14.70	20.50	2.655E+06	7.500E+06	.354
COARSE	3.5	45	1.00	50.00	14.40	20.40	2.660E+06	7.576E+06	.351
COARSE	3.5	45	10.00	10.00	8.20	13.50	3.333E+06	6.667E+06	.500
COARSE	3.5	45	10.00	30.00	7.50	13.10	3.659E+06	1.000E+07	.366
COARSE	3.5	45	10.00	50.00	6.80	12.00	3.650E+06	1.111E+07	.328
COARSE	3.5	45	20.00	10.00	4.50	12.60	4.000E+06	1.250E+07	.320
COARSE	3.5	45	20.00	30.00	4.60	10.30	3.846E+06	1.250E+07	.308
COARSE	3.5	45	20.00	50.00	4.10	9.00	4.000E+06	1.351E+07	.296

TABLE 32 - Summary of the Complex Modulus Tests

GRADATION	ASPHALT CONTENT	TEMPERATURE - F	FREQUENCY - CPS	STRESS-PSI	AXIAL LAG-DEG.	CIRCUMFERENTIAL LAG-DEG.	COMPLEX MODULUS E* - PSI	COMPLEX MODULUS T* - PSI	COMPLEX POISSON'S RATIO v*
COARSE	3.5	70	.01	10.00	32.10	38.60	1.010E+05	3.195E+05	.316
COARSE	3.5	70	.01	30.00	26.70	33.20	1.410E+05	4.367E+05	.323
COARSE	3.5	70	.01	50.00	24.10	31.60	1.515E+05	4.440E+05	.341
COARSE	3.5	70	.10	10.00	38.80	41.30	2.513E+05	8.696E+05	.289
COARSE	3.5	70	.10	30.00	31.40	35.00	2.988E+05	1.034E+06	.289
COARSE	3.5	70	.10	50.00	30.70	33.30	2.976E+05	9.804E+05	.304
COARSE	3.5	70	1.00	10.00	33.50	36.40	6.250E+05	2.326E+06	.269
COARSE	3.5	70	1.00	30.00	30.60	34.40	6.696E+05	2.500E+06	.268
COARSE	3.5	70	1.00	50.00	29.80	32.00	6.460E+05	2.347E+06	.275
COARSE	3.5	70	10.00	10.00	19.60	27.50	1.250E+06	3.571E+06	.350
COARSE	3.5	70	10.00	30.00	21.00	26.60	1.364E+06	5.000E+06	.273
COARSE	3.5	70	10.00	50.00	22.90	28.50	1.299E+06	4.673E+06	.278
COARSE	3.5	70	20.00	10.00	16.80	23.60	1.639E+06	5.882E+06	.279
COARSE	3.5	70	20.00	30.00	14.90	23.10	1.622E+06	6.000E+06	.270
COARSE	3.5	70	20.00	50.00	16.20	22.10	1.553E+06	6.250E+06	.248
COARSE	3.5	90	.01	10.00	21.50	30.50	4.970E+04	8.651E+04	.575
COARSE	3.5	90	.01	20.00	19.60	30.00	5.917E+04	9.328E+04	.634
COARSE	3.5	90	.01	30.00	18.80	28.90	6.316E+04	9.375E+04	.674
COARSE	3.5	90	.10	10.00	2.10	35.20	9.246E+04	1.880E+05	.492
COARSE	3.5	90	.10	20.00	28.10	32.30	1.050E+05	1.980E+05	.530
COARSE	3.5	90	.10	30.00	25.40	31.10	1.111E+05	2.027E+05	.548
COARSE	3.5	90	1.00	10.00	39.40	41.20	2.381E+05	5.076E+05	.469
COARSE	3.5	90	1.00	20.00	36.40	40.70	2.451E+05	4.926E+05	.498
COARSE	3.5	90	1.00	30.00	34.00	37.10	2.439E+05	4.918E+05	.496
COARSE	3.5	90	10.00	10.00	32.20	44.30	6.803E+05	1.471E+06	.463
COARSE	3.5	90	10.00	20.00	32.30	38.60	6.757E+05	1.515E+06	.446
COARSE	3.5	90	10.00	30.00	35.30	41.30	6.667E+05	1.429E+06	.467
COARSE	3.5	90	20.00	10.00	31.50	40.50	9.709E+05	2.222E+06	.437
COARSE	3.5	90	20.00	20.00	27.90	38.70	9.259E+05	2.000E+06	.463
COARSE	3.5	90	20.00	30.00	28.80	35.10	8.902E+05	2.041E+06	.436

TABLE 33 - Summary of the Complex Modulus Tests

GRADATION	ASPHALT CONTENT	TEMPERATURE - °F	FREQUENCY - CPS	STRESS-PSI	AXIAL LAG-DEG.	CIRCUMFERENTIAL LAG-DEG.	COMPLEX MODULUS $ E^* $ - PSI	COMPLEX MODULUS $ T^* $ - PSI	COMPLEX POISSON'S RATIO ν^*
COARSE	4.5	25	.01	10.00	20.50	24.50	1.923E+06	5.000E+06	.385
COARSE	4.5	25	.01	30.00	18.80	25.00	2.041E+06	6.000E+06	.340
COARSE	4.5	25	.01	50.00	19.10	20.80	2.174E+06	5.952E+06	.365
COARSE	4.5	25	.10	10.00	13.10	17.50	2.632E+06	5.882E+06	.447
COARSE	4.5	25	.10	30.00	13.10	16.00	2.885E+06	7.895E+06	.365
COARSE	4.5	25	.10	50.00	13.80	17.60	3.067E+06	9.091E+06	.337
COARSE	4.5	25	1.00	10.00	9.80	11.80	3.571E+06	6.667E+06	.536
COARSE	4.5	25	1.00	30.00	8.90	11.30	3.750E+06	1.154E+07	.325
COARSE	4.5	25	1.00	50.00	8.90	10.50	3.846E+06	1.250E+07	.308
COARSE	4.5	25	10.00	10.00	3.00	9.00	4.348E+06	1.000E+07	.435
COARSE	4.5	25	10.00	30.00	2.60	8.30	4.286E+06	1.500E+07	.286
COARSE	4.5	25	10.00	50.00	3.80	9.40	4.237E+06	1.351E+07	.314
COARSE	4.5	25	20.00	10.00	1.10	6.30	4.762E+06	1.667E+07	.286
COARSE	4.5	25	20.00	30.00	.90	5.60	4.918E+06	1.667E+07	.295
COARSE	4.5	25	20.00	50.00	1.30	4.10	4.762E+06	2.000E+07	.238
COARSE	4.5	45	.01	10.00	43.40	46.00	4.082E+05	9.524E+05	.429
COARSE	4.5	45	.01	30.00	40.30	45.70	4.732E+05	1.010E+06	.468
COARSE	4.5	45	.01	50.00	35.40	40.50	5.230E+05	1.136E+06	.460
COARSE	4.5	45	.10	10.00	30.80	38.10	1.020E+06	2.381E+06	.429
COARSE	4.5	45	.10	30.00	28.70	34.70	1.111E+06	2.727E+06	.407
COARSE	4.5	45	.10	50.00	27.40	32.50	1.163E+06	2.907E+06	.400
COARSE	4.5	45	1.00	10.00	22.20	26.60	1.818E+06	4.348E+06	.418
COARSE	4.5	45	1.00	30.00	20.20	26.00	1.935E+06	5.455E+06	.355
COARSE	4.5	45	1.00	50.00	18.90	24.20	2.041E+06	6.024E+06	.339
COARSE	4.5	45	10.00	10.00	13.50	16.90	2.857E+06	7.143E+06	.400
COARSE	4.5	45	10.00	30.00	11.30	16.90	2.857E+06	8.824E+06	.324
COARSE	4.5	45	10.00	50.00	12.80	17.60	2.941E+06	8.621E+06	.341
COARSE	4.5	45	20.00	10.00	9.00	14.40	3.333E+06	1.429E+07	.233
COARSE	4.5	45	20.00	30.00	9.10	12.30	3.191E+06	9.375E+06	.340
COARSE	4.5	45	20.00	50.00	8.20	13.60	3.268E+06	1.000E+07	.327

TABLE 34 - Summary of the Complex Modulus Tests

GRADATION	ASPHALT CONTENT	TEMPERATURE - °F	FREQUENCY - CPS	STRESS - PSI	AXIAL LAG - DEG.	CIRCUMFERENTIAL LAG - DEG.	COMPLEX MODULUS E* - PSI	COMPLEX MODULUS T* - PSI	COMPLEX POISSON'S RATIO ν*
COARSE	4.5	70	.01	10.00	32.50	37.70	9.615E+04	1.462E+05	.658
COARSE	4.5	70	.01	30.00	30.30	34.80	9.004E+04	2.400E+05	.375
COARSE	4.5	70	.01	50.00	26.30	35.90	1.214E+05	1.689E+05	.718
COARSE	4.5	70	.10	10.00	39.30	43.10	2.326E+05	4.115E+05	.565
COARSE	4.5	70	.10	30.00	35.60	39.80	2.703E+05	4.747E+05	.569
COARSE	4.5	70	.10	50.00	34.30	39.80	2.509E+05	4.464E+05	.562
COARSE	4.5	70	1.00	10.00	36.90	42.80	6.452E+05	1.299E+06	.497
COARSE	4.5	70	1.00	30.00	34.30	39.20	6.865E+05	1.382E+06	.497
COARSE	4.5	70	1.00	50.00	34.50	40.00	6.410E+05	1.295E+06	.495
COARSE	4.5	70	10.00	10.00	27.70	34.10	1.351E+06	2.857E+06	.473
COARSE	4.5	70	10.00	30.00	24.40	31.20	1.485E+06	3.261E+06	.455
COARSE	4.5	70	10.00	50.00	26.20	31.90	1.441E+06	3.268E+06	.441
COARSE	4.5	70	20.00	10.00	21.60	29.20	1.562E+06	3.704E+06	.422
COARSE	4.5	70	20.00	30.00	20.10	30.10	1.765E+06	4.110E+06	.429
COARSE	4.5	70	20.00	50.00	20.00	29.00	1.761E+06	4.167E+06	.423
COARSE	4.5	90	.01	10.00	25.80	26.10	1.022E+04	1.887E+04	.542
COARSE	4.5	90	.01	20.00	21.60	23.90	1.709E+04	3.077E+04	.556
COARSE	4.5	90	.01	30.00	18.80	24.80	3.254E+04	4.298E+04	.757
COARSE	4.5	90	.10	10.00	34.00	38.90	2.801E+04	4.950E+04	.566
COARSE	4.5	90	.10	20.00	29.80	33.30	4.141E+04	7.485E+04	.553
COARSE	4.5	90	.10	30.00	25.10	31.10	5.906E+04	9.778E+04	.604
COARSE	4.5	90	1.00	10.00	45.30	48.80	9.208E+04	1.773E+05	.519
COARSE	4.5	90	1.00	20.00	39.50	42.00	1.104E+05	2.155E+05	.512
COARSE	4.5	90	1.00	30.00	35.40	39.20	1.307E+05	2.479E+05	.527
COARSE	4.5	90	10.00	10.00	46.50	47.70	3.390E+05	6.623E+05	.512
COARSE	4.5	90	10.00	20.00	44.00	45.00	3.472E+05	6.826E+05	.509
COARSE	4.5	90	10.00	30.00	40.80	42.00	3.597E+05	7.500E+05	.480
COARSE	4.5	90	20.00	10.00	41.40	51.30	4.831E+05	9.524E+05	.507
COARSE	4.5	90	20.00	20.00	37.80	43.10	5.076E+05	1.042E+06	.487
COARSE	4.5	90	20.00	30.00	36.90	40.10	5.051E+05	1.079E+06	.468

TABLE 36 - Dynamic Modulus $/E^*$ and Phase Lag ϕ For Class F Asphalt Treated and Hot-Mix Sand Asphalt Bases, Ring 4, WSU Test Track (After the Asphalt Institute)

PAVEMENT COURSE	TEMP. (°F)	LOADING FREQUENCY					
		$/E^*/$ PSI x 10 ⁵	ϕ (DEG.)	$/E^*/$ PSI x 10 ⁵	ϕ (DEG.)	$/E^*/$ PSI x 10 ⁵	ϕ (DEG.)
CLASS F ASPHALT TREATED BASE	40	15.1	12	17.8	8	20.7	12
	70	3.91	30	5.85	30	8.06	28
	100	0.77	30	1.28	34	2.07	38
HOT-MIX SAND ASPHALT BASE	40	6.47	12	7.26	10	8.14	12
	70	2.23	24	2.97	21	3.74	22
	100	0.70	26	1.01	24	1.32	31

TABLE 37 - Resilient properties for Class F Asphalt Treated
and Hot-Mix Asphalt Bases, Ring 4, WSU Test Track

PAVEMENT COURSE	TEMP. (F)	LOAD TIME SEC.	σ_1 PSI	σ_3 PSI	M_R PSI x 10^6	POISSON RATIO
CLASS F ASPHALT TREATED BASE	40	0.1	10		1.14	0.32
			20		1.07	0.278
			30		1.03	0.316
			40		1.1	0.307
			50		1.11	0.323
		1.0	10		0.71	0.284
			20		0.746	0.35
			30		0.738	0.368
			40		0.728	0.35
			50		0.72	0.333
		10	10		0.462	0.324
			20		0.416	0.345
			30		0.422	0.361
			40		0.409	0.362
			50		0.4	0.36
70	0.1	10		0.321	0.384	
		20		0.326	0.375	
		30		0.301	0.401	
		40		0.294	0.375	
		50		0.292	0.375	
	1.0	10		0.139	0.431	
		20		0.137	0.41	
		30		0.124	0.398	
		40		0.119	0.403	
		50		0.112	0.414	
	10	10		0.062	0.44	
		20		0.055	0.45	
		30		0.052	0.457	
		40		0.051	0.465	
		50		0.052	0.465	

TABLE 37 (CON'T)

PAVEMENT COURSE	TEMP. (°F)	LOAD TIME SEC.	σ_1 PSI	σ_3 PSI	M_R PSI x 10 ⁶	POISSON RATIO
CLASS F ASPHALT TREATED BASE	100	0.1	10		0.05	0.44
			20		0.047	0.448
			30		0.0472	0.498
			40		0.049	0.465
			50		0.049	0.46
		1.0	10		0.0219	0.506
			20		0.0235	0.537
			30		0.0244	0.568
			40		0.0247	0.58
10	10		0.0122	0.697		
	20		0.01425	0.747		
	30		0.0163	0.747		
	40		0.018	0.753		
	50		0.0198	0.737		
HOT-MIX SAND ASPHALT BASE	40	0.1	10		0.546	0.225
			20		0.54	0.257
			30		0.528	0.281
			40		0.515	0.283
			50		0.512	0.282
		1.0	10		0.365	0.336
	20			0.345	0.31	
	30			0.335	0.329	
	40			0.32	0.316	
	50			0.305	0.291	
	70	0.1	10		0.16	0.365
			20		0.154	0.39
			30		0.143	0.371
40				0.143	0.351	
50				0.139	0.37	
1.0		10		0.069	0.359	
		20		0.063	0.385	
		30		0.0625	0.395	
40		0.0615	0.405			
50		0.0612	0.424			

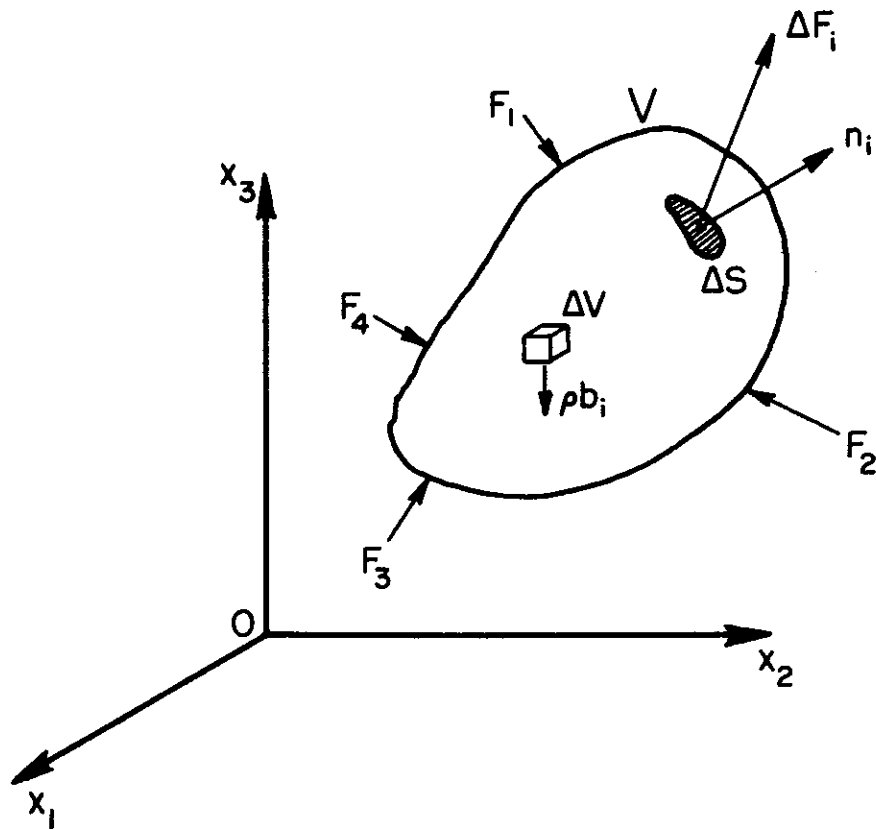


FIGURE 1 - The Concept of Stress at Point P

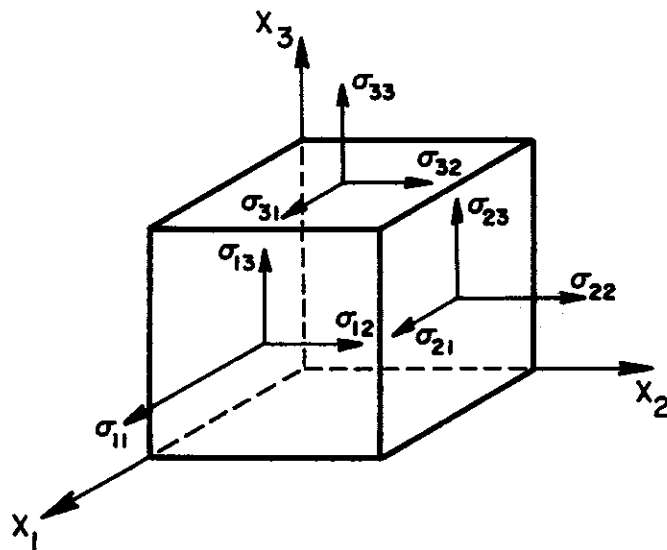
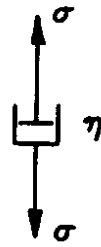


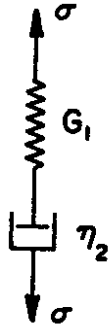
FIGURE 2 - Components of the Stress Tensor



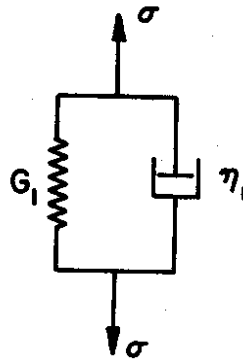
HOOKEAN ELEMENT



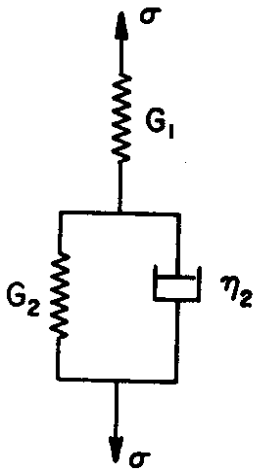
NEWTONIAN ELEMENT



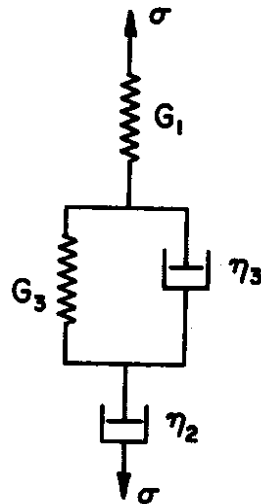
MAXWELL ELEMENT



KELVIN-VOIGT ELEMENT



THREE-ELEMENT MODEL



FOUR-ELEMENT MODEL

FIGURE 3 - Simple Linear Viscoelastic Models

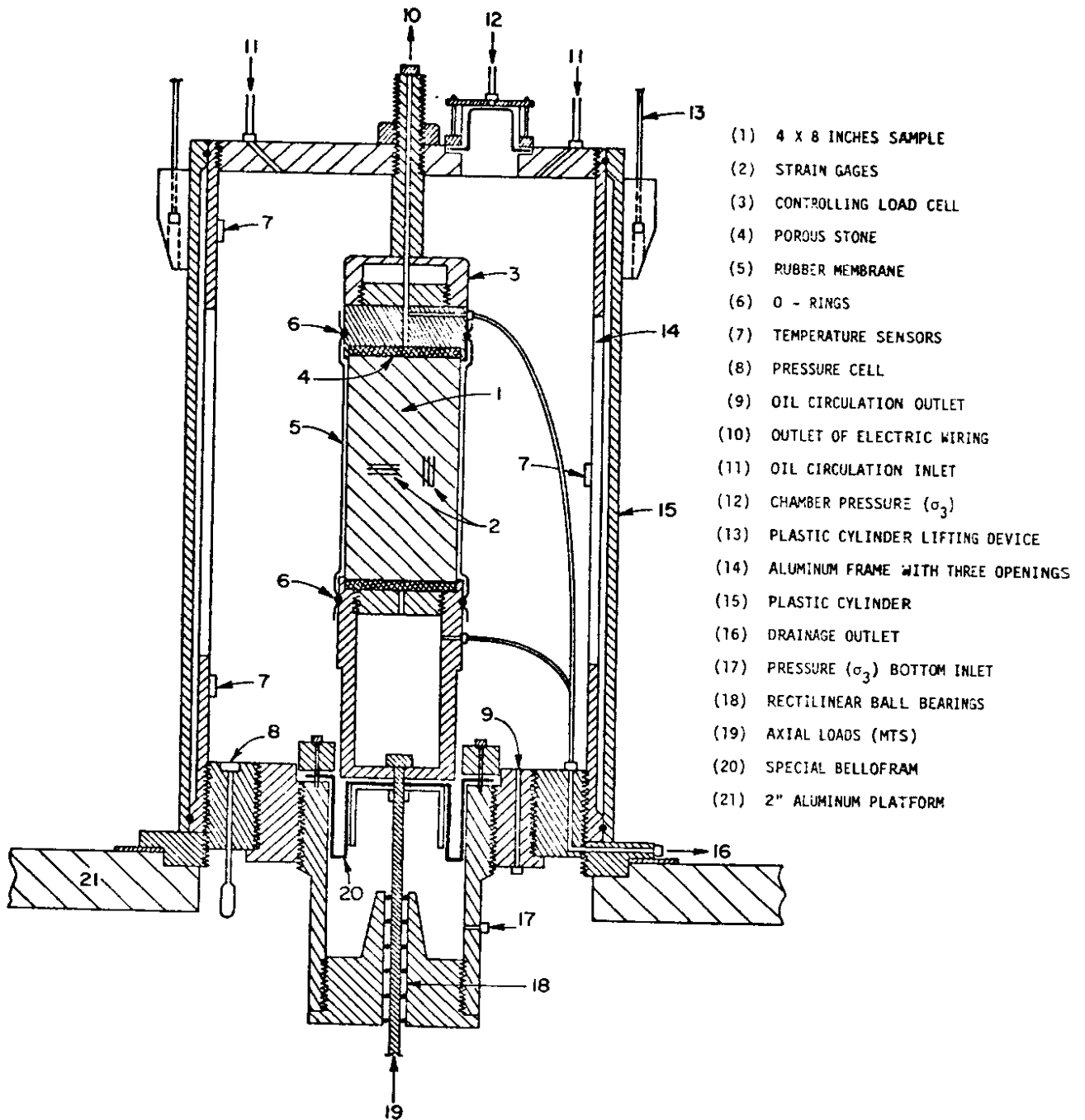


FIGURE 4d - The Triaxial Chamber

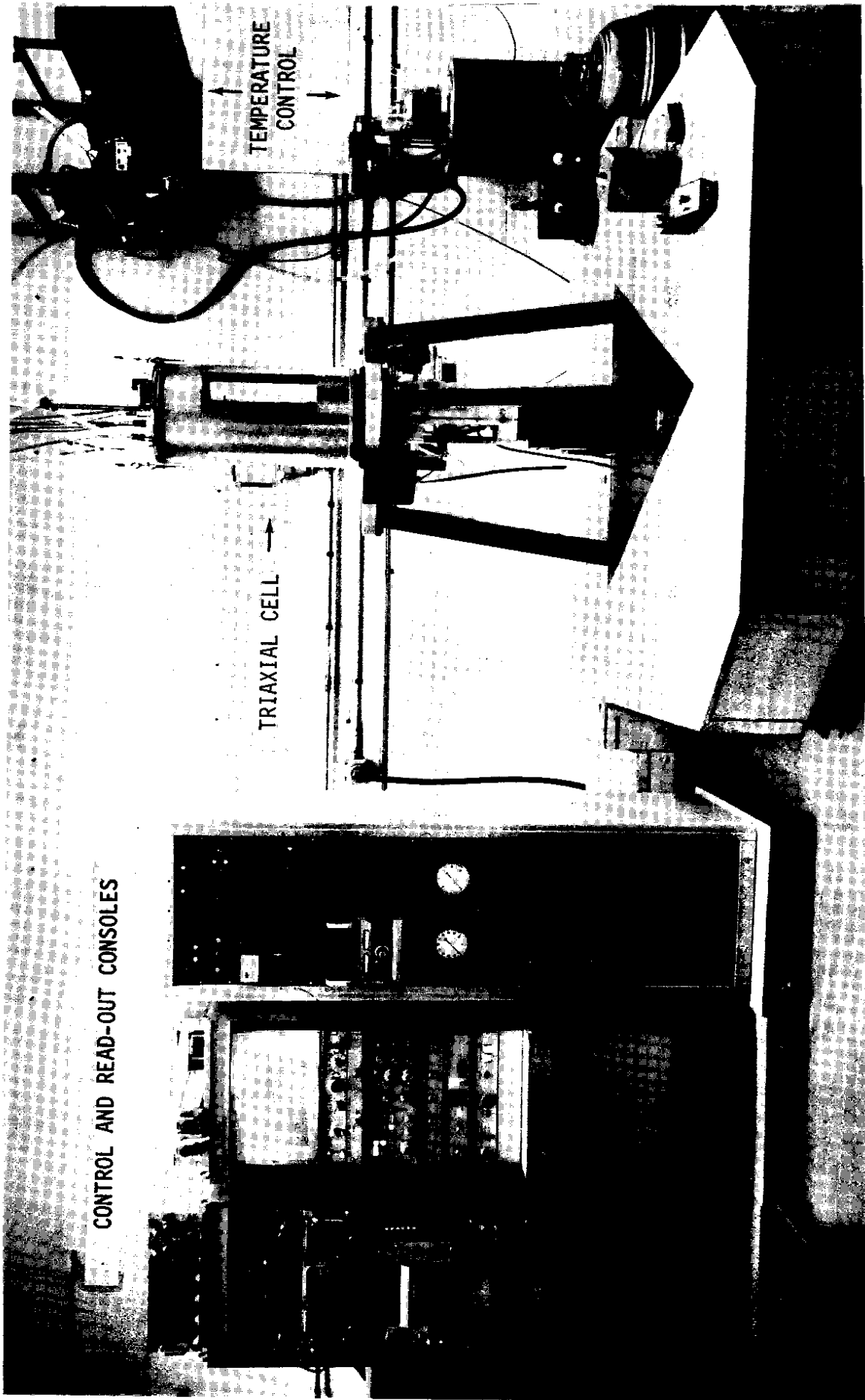


FIGURE 4a - Overall View of Dynamic Triaxial Testing System

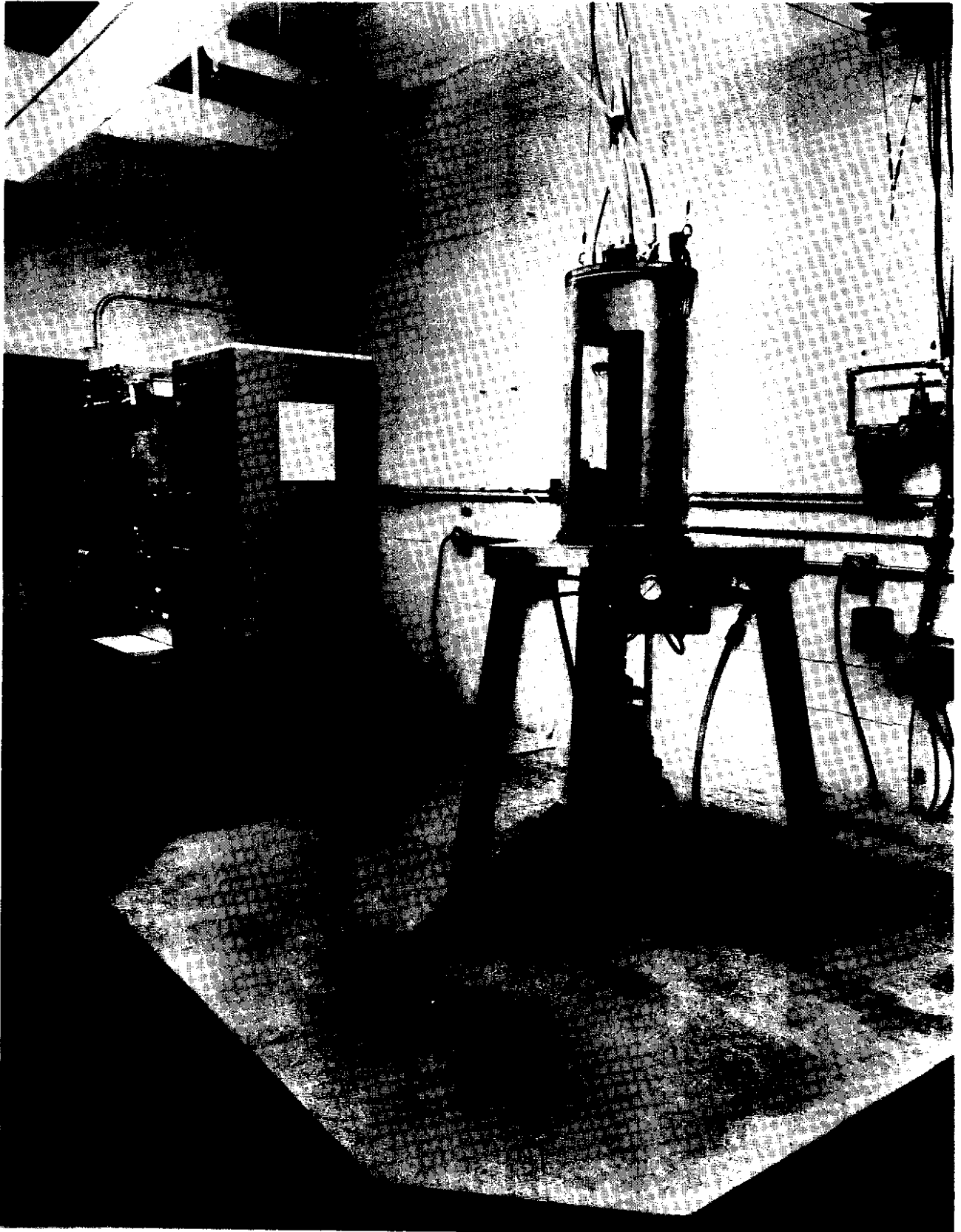


FIGURE 4b - Test Frame and Triaxial Chamber Showing Electro-Hydraulic Servo-Ram at Bottom

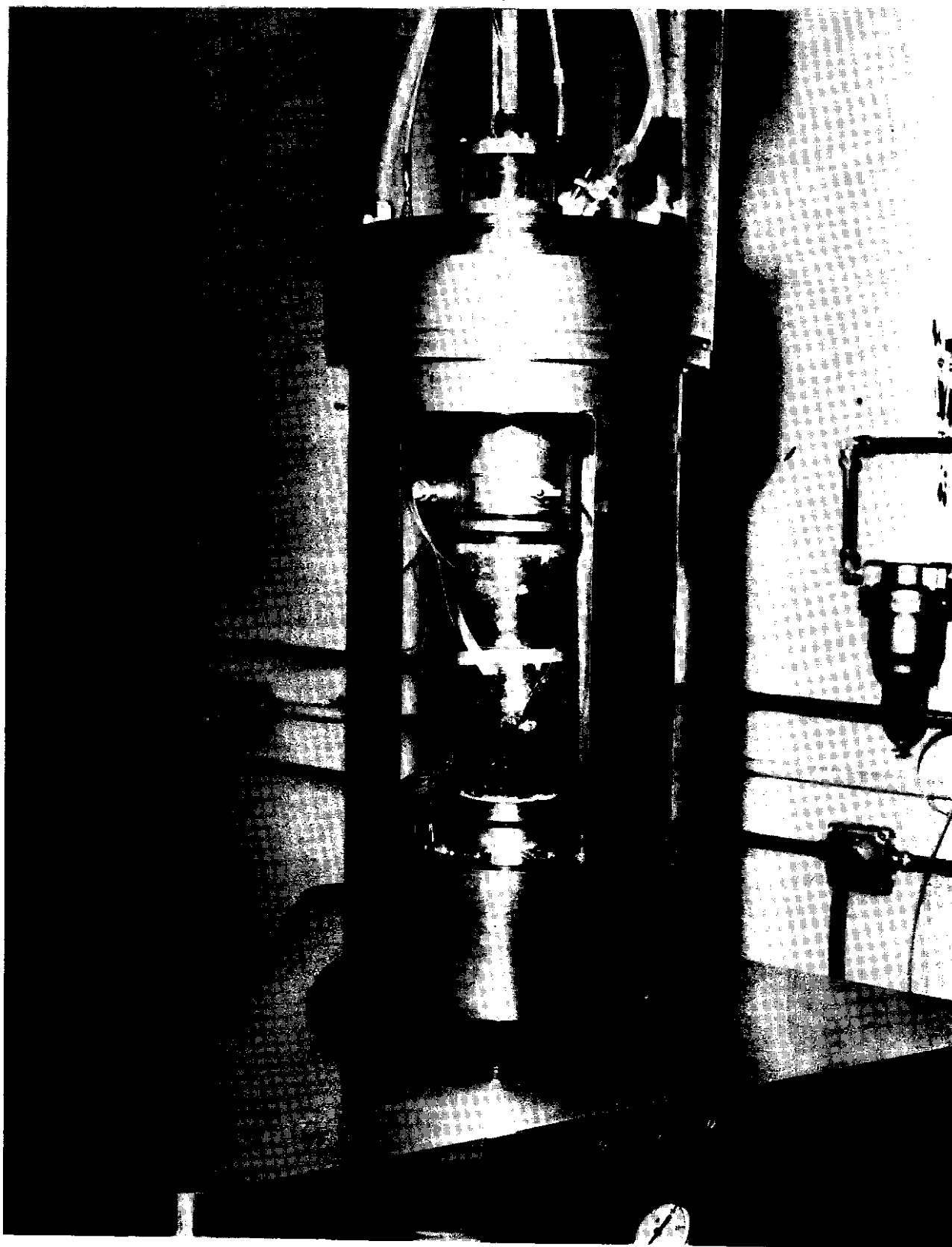


FIGURE 4c - Close-Up of 4" Diameter by 8" High Asphalt Concrete Specimen in Triaxial Cell Prior to Connecting Lead Wires. Note Internal Frame that Permits Access to Specimens Without Disassembly.

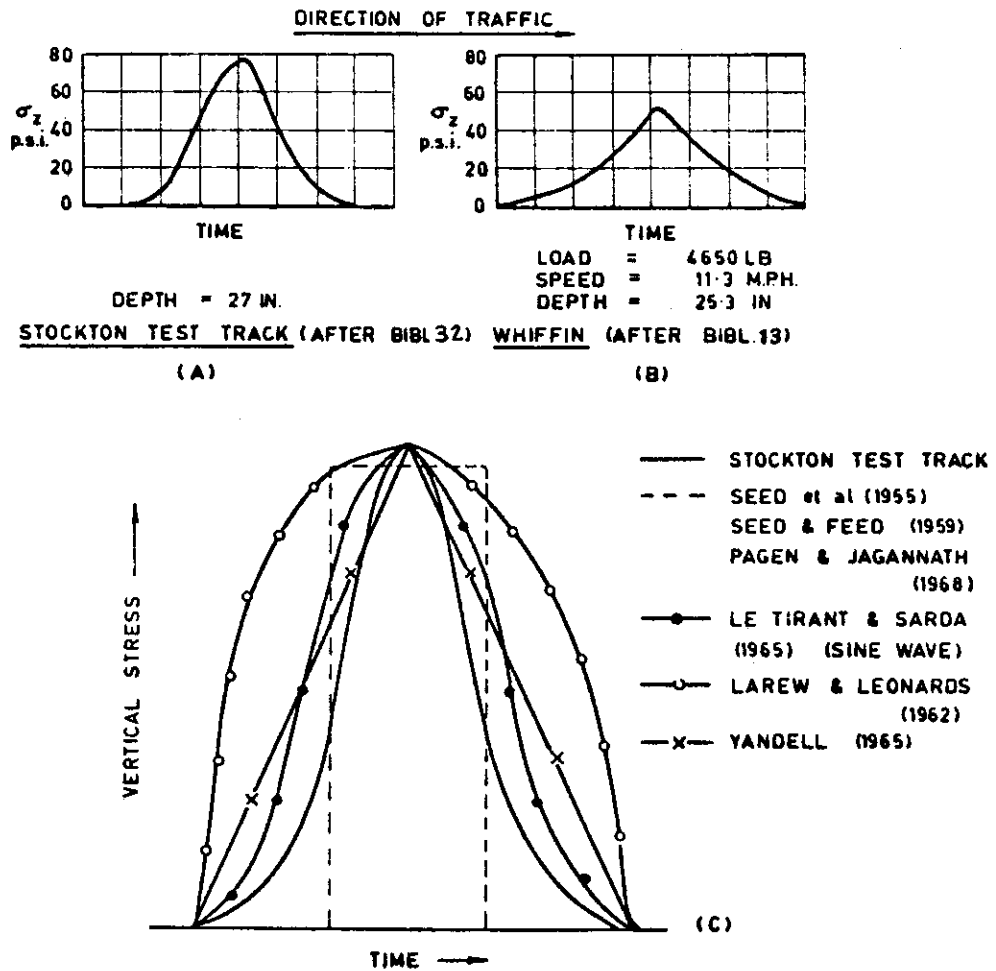


FIGURE 5 - Vertical Stress Functions Used by Various Investigators (After Shackel)

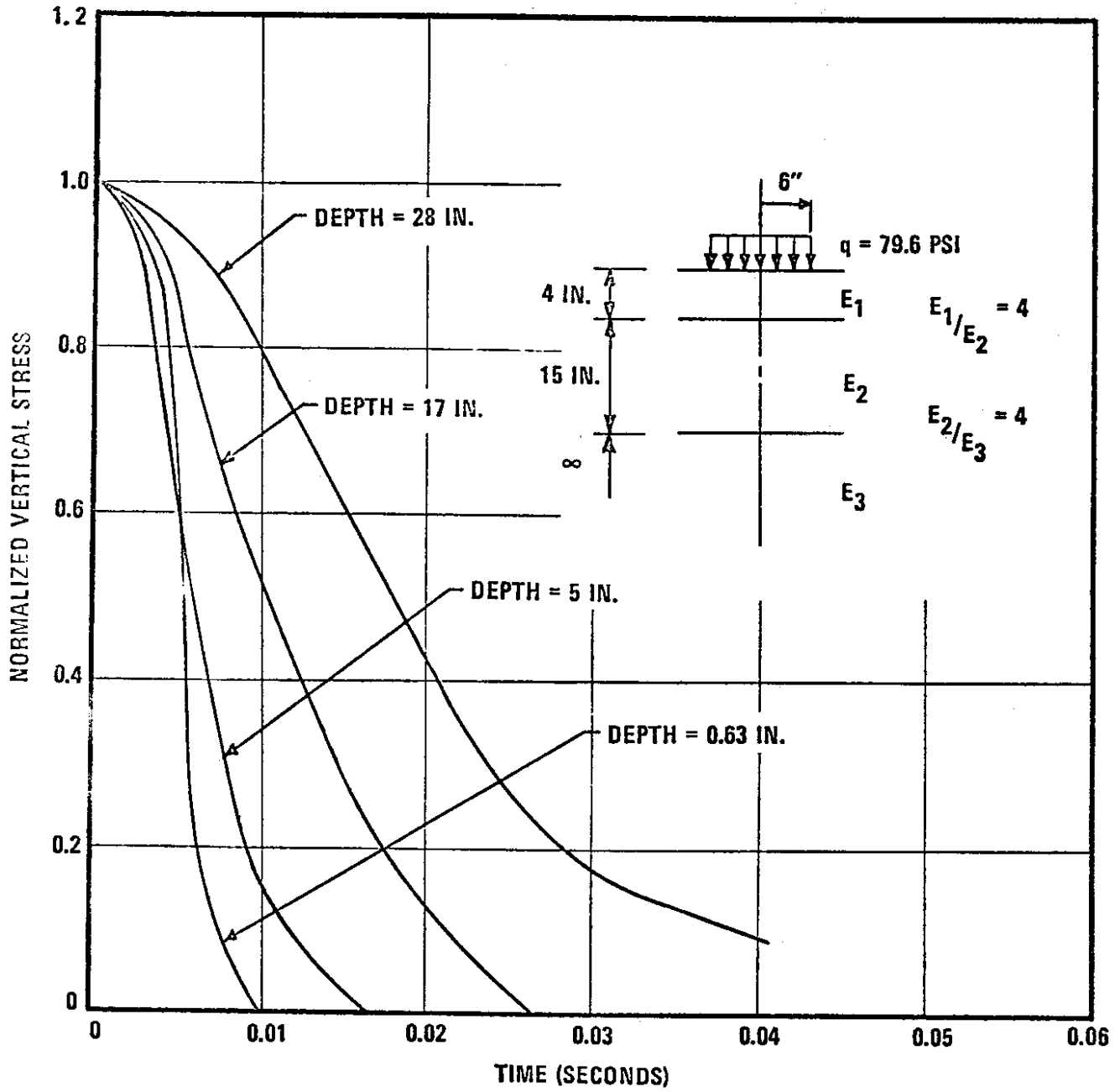


FIGURE 6 - Variation of Calculated Vertical Compressive Stress Pulse Shape with Depth (After Barksdale)

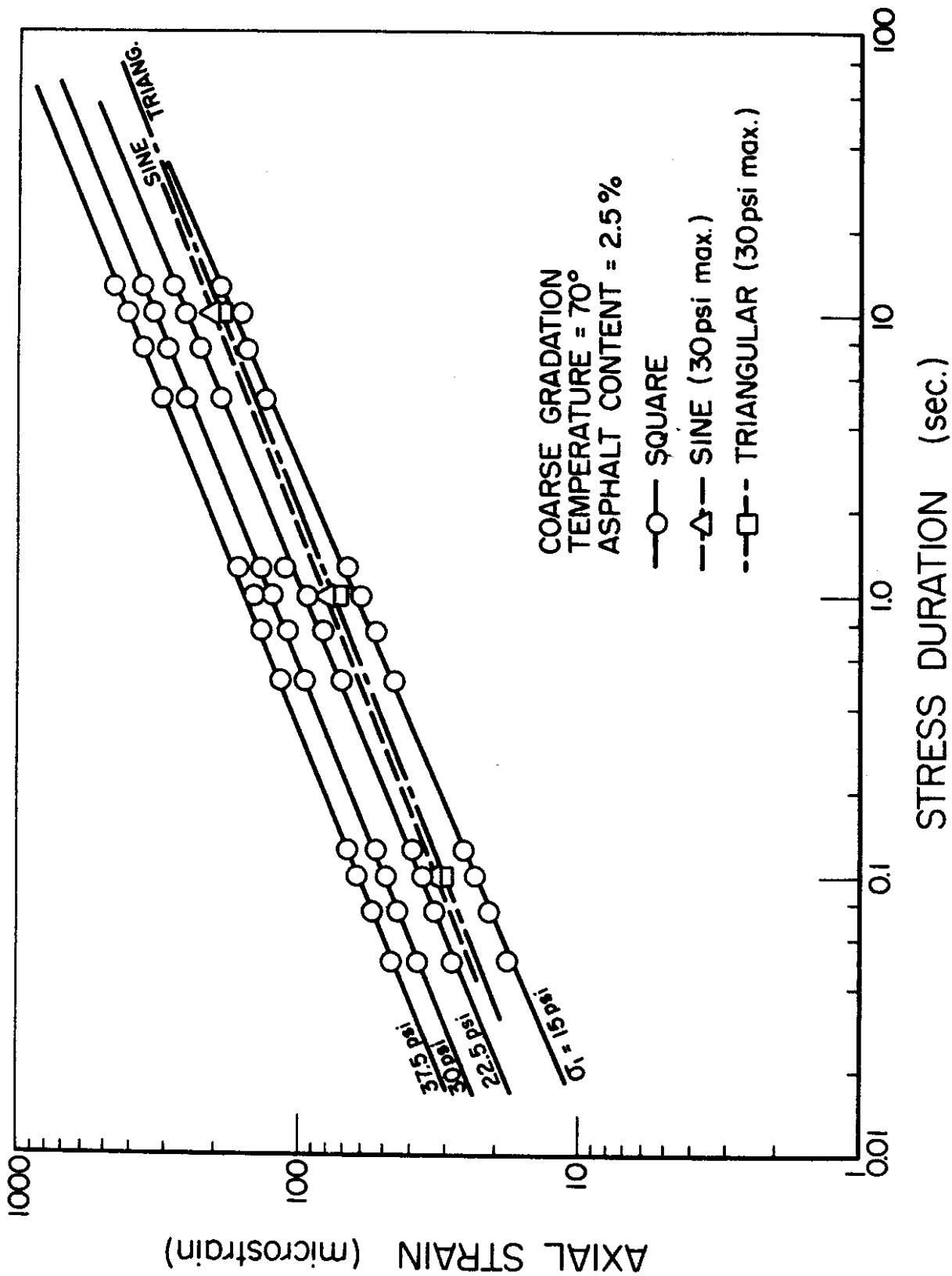


FIGURE 7 - Axial Strains Resulting from Different Stress Pulse Shapes and Durations

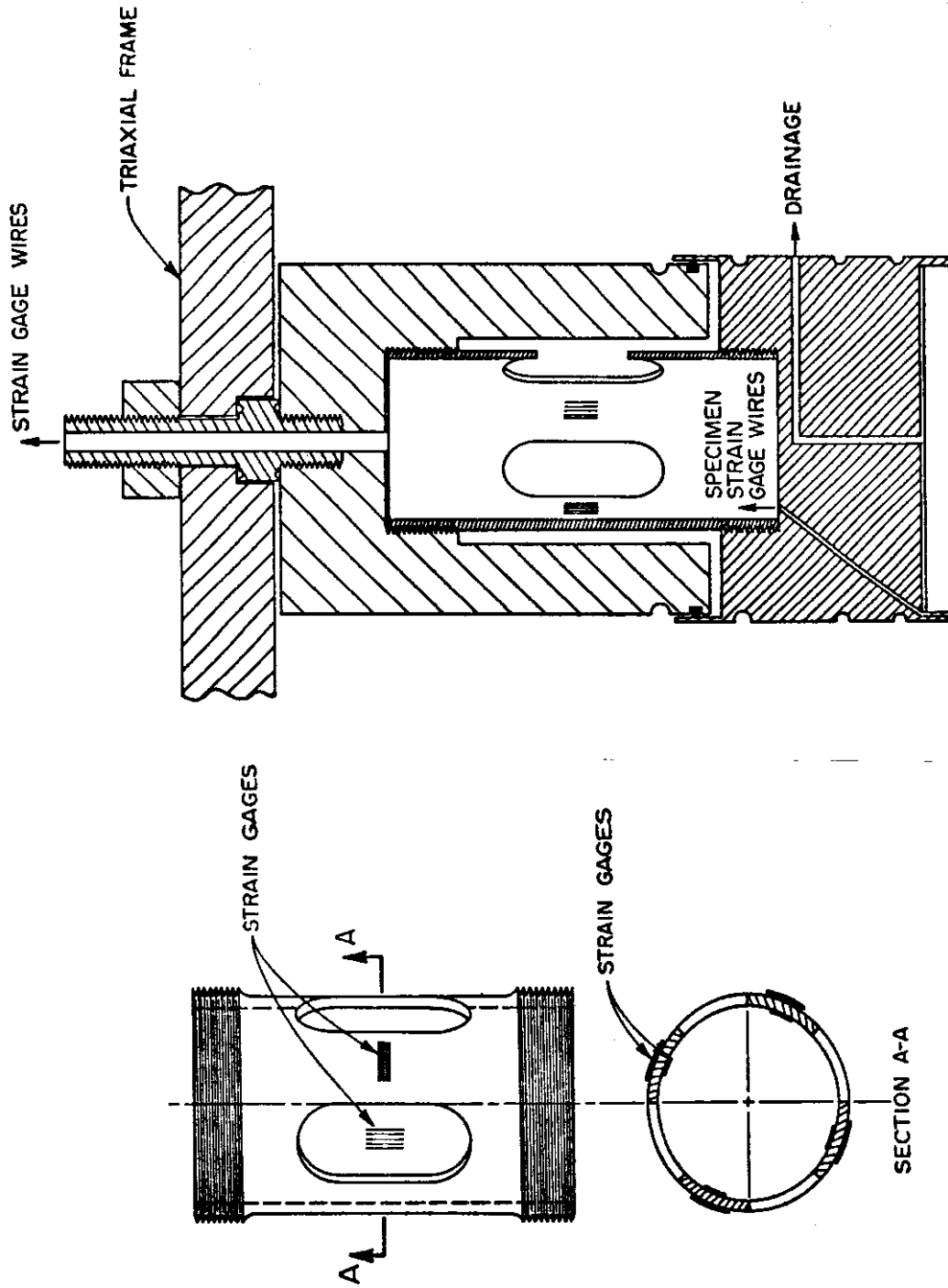


FIGURE 8 - The Load Cell Used Inside the Triaxial Chamber

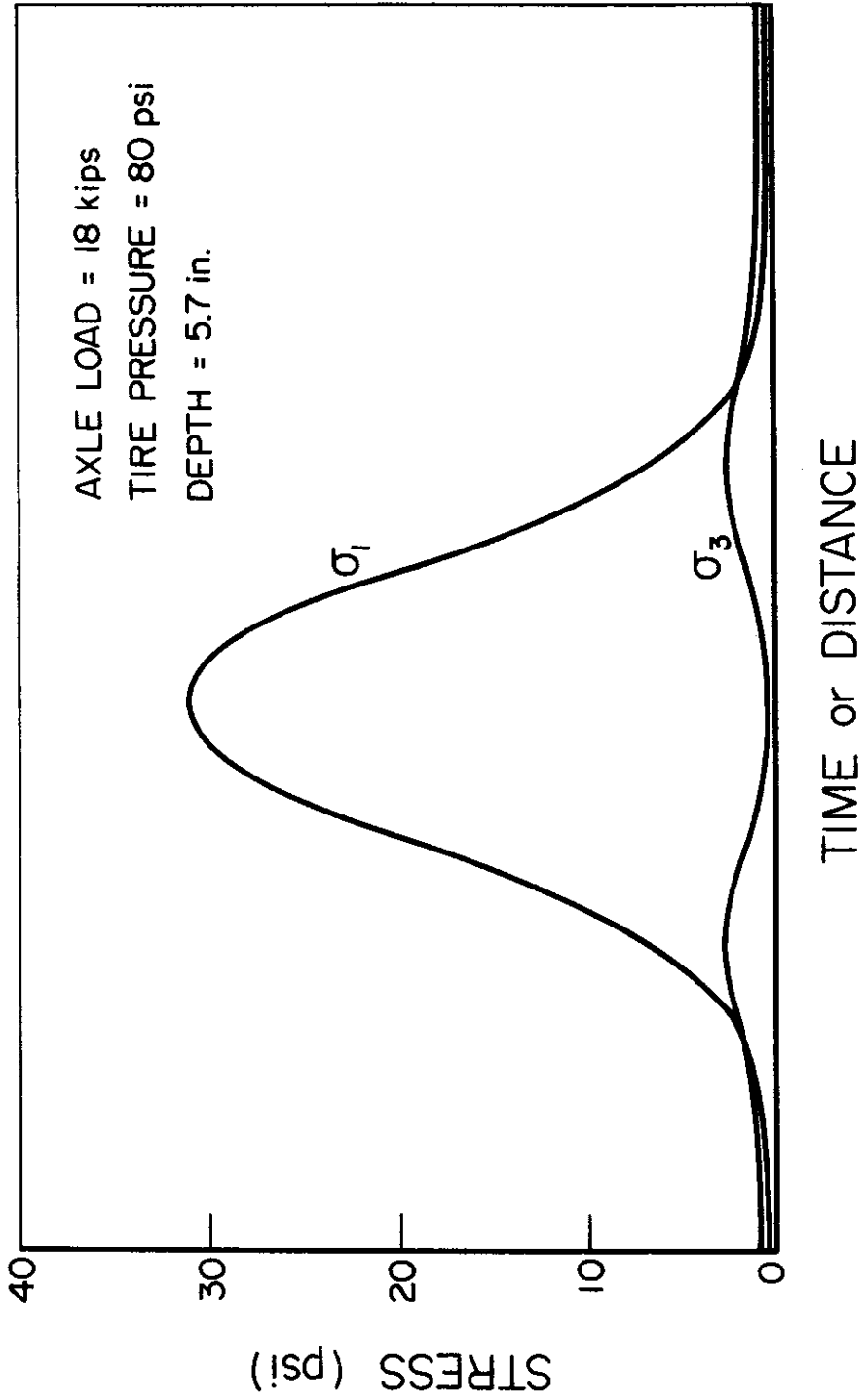


FIGURE 9 - Axial and Radial Stress Distribution Under Moving Load (From n-Layer Computer Program)

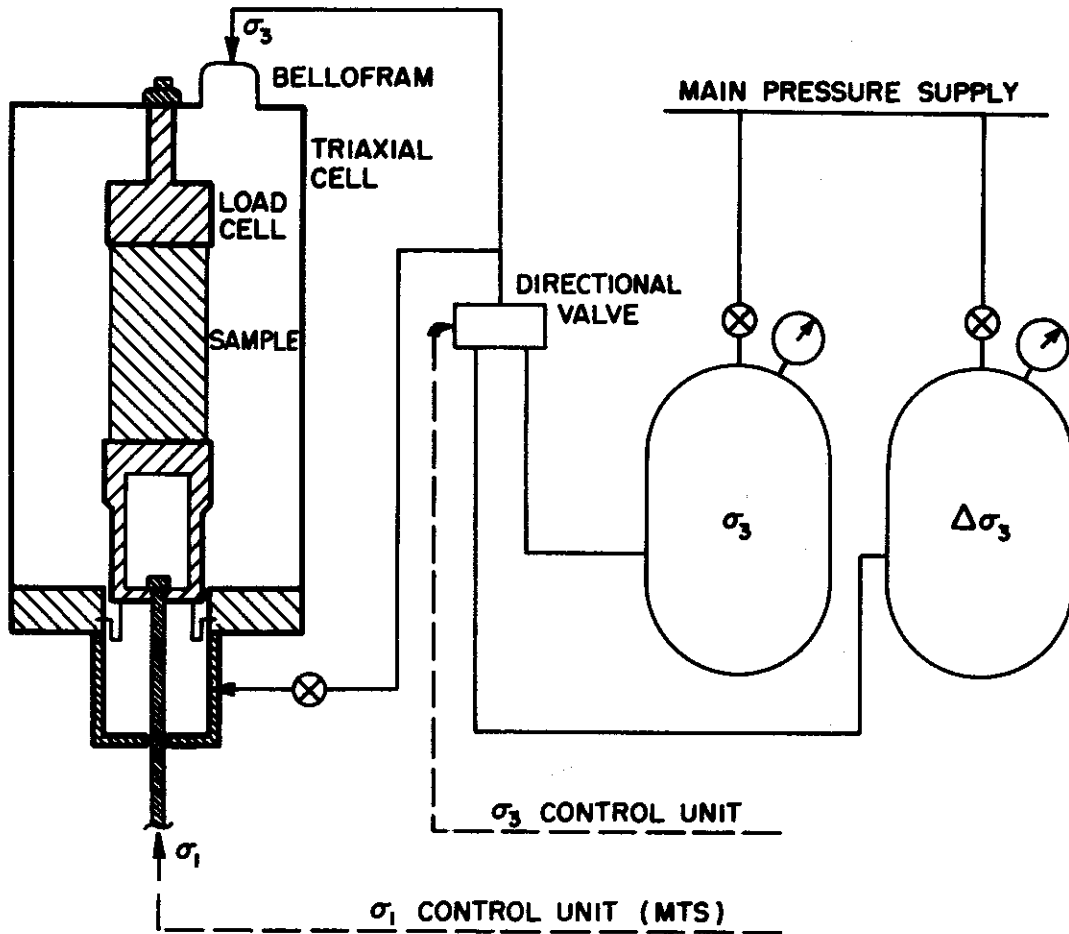


FIGURE 10 - The System Used in Pulsing the Chamber Pressure

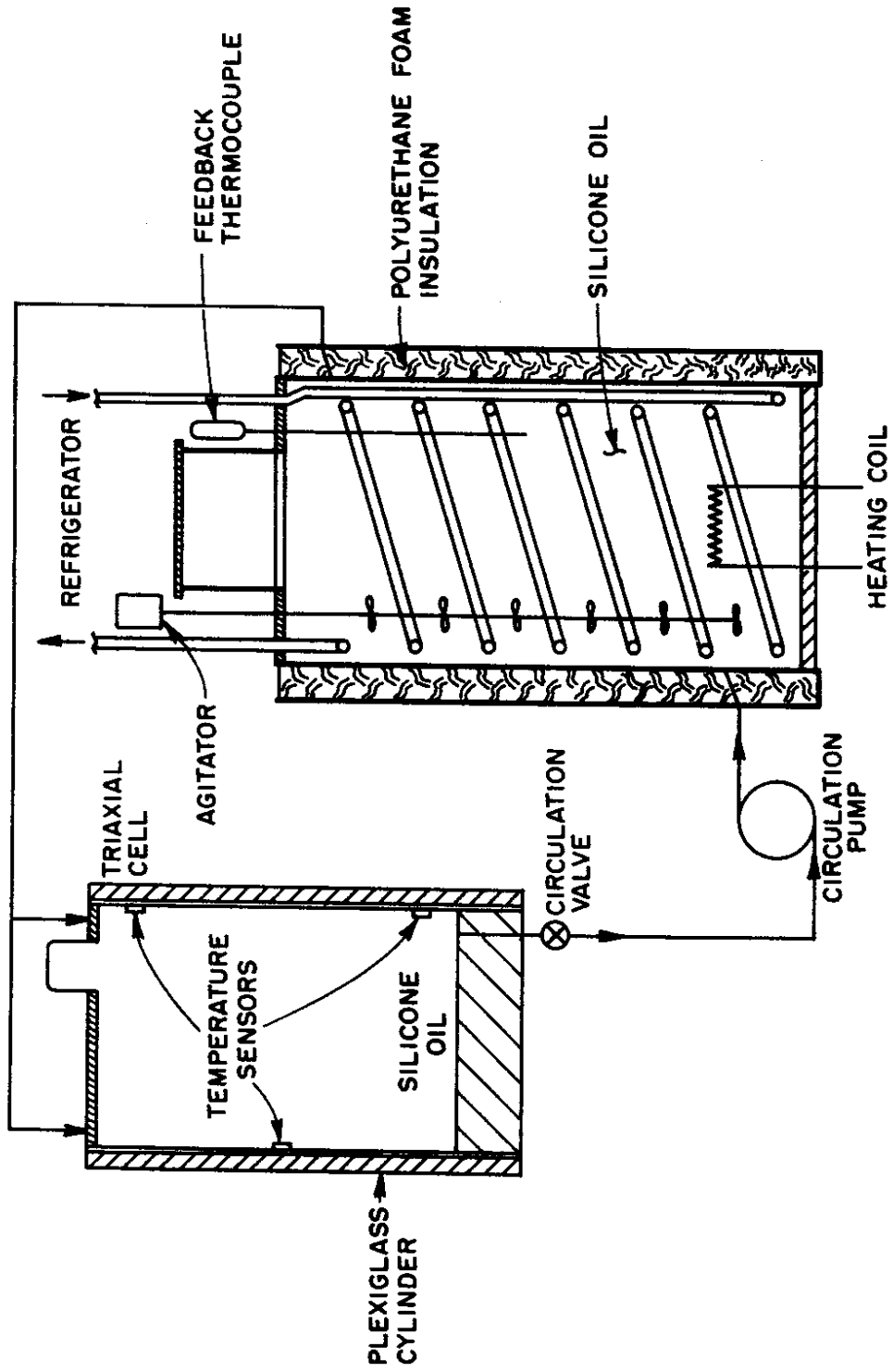


FIGURE 11 - The Temperature Control System

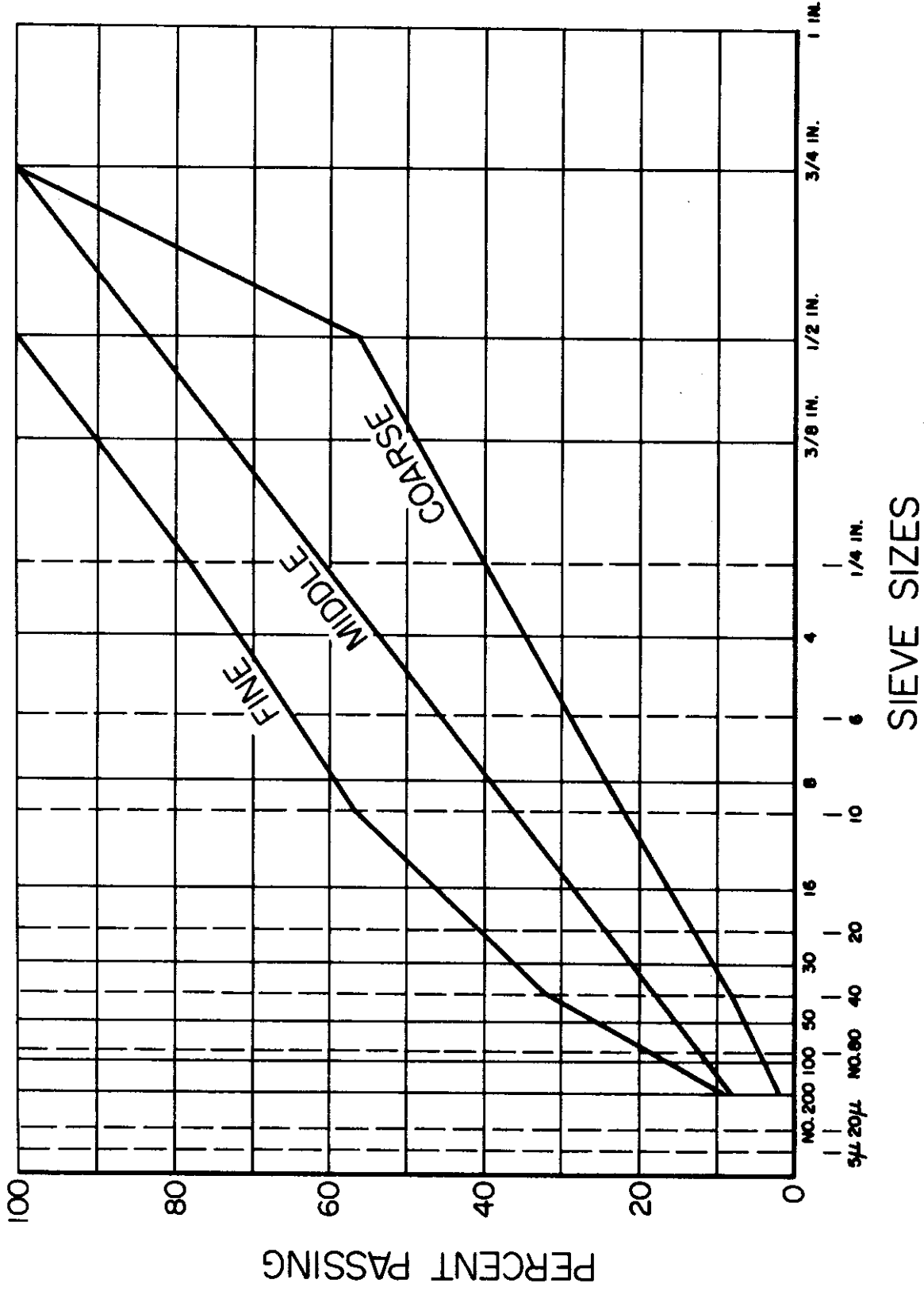


FIGURE 12 - Gradation Chart

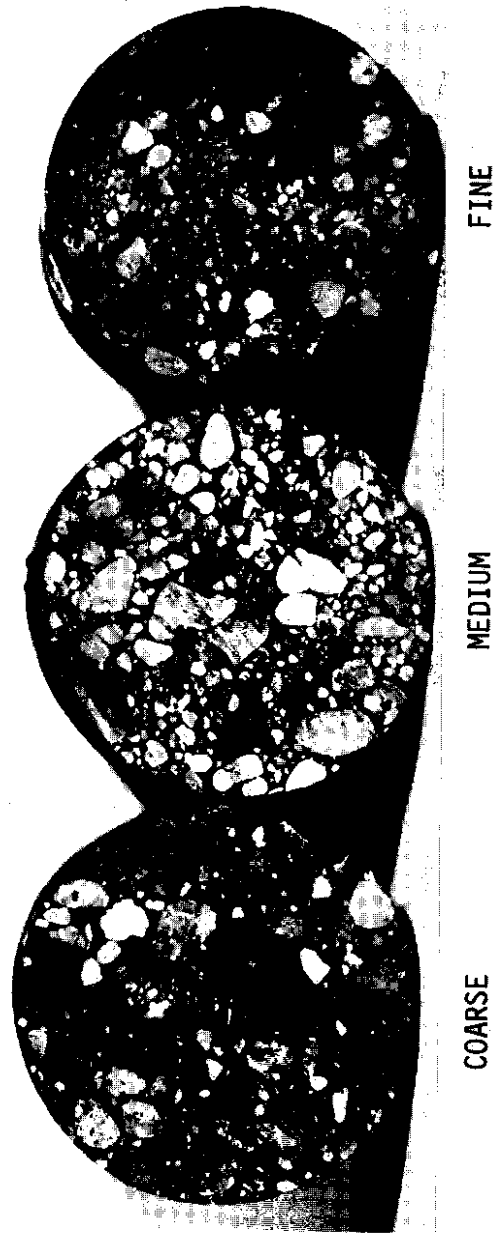


FIGURE 12a - Samples of Laboratory-Compacted Mixtures Illustrating Different Gradations.

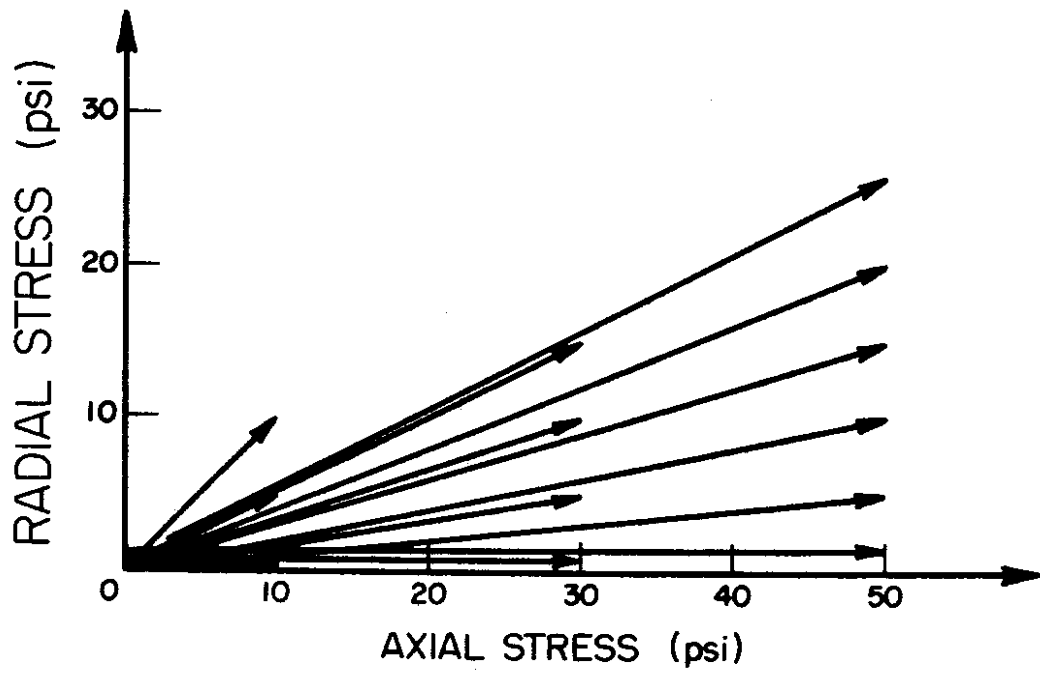


FIGURE 13 - Stress States Applied in the Triaxial Tests

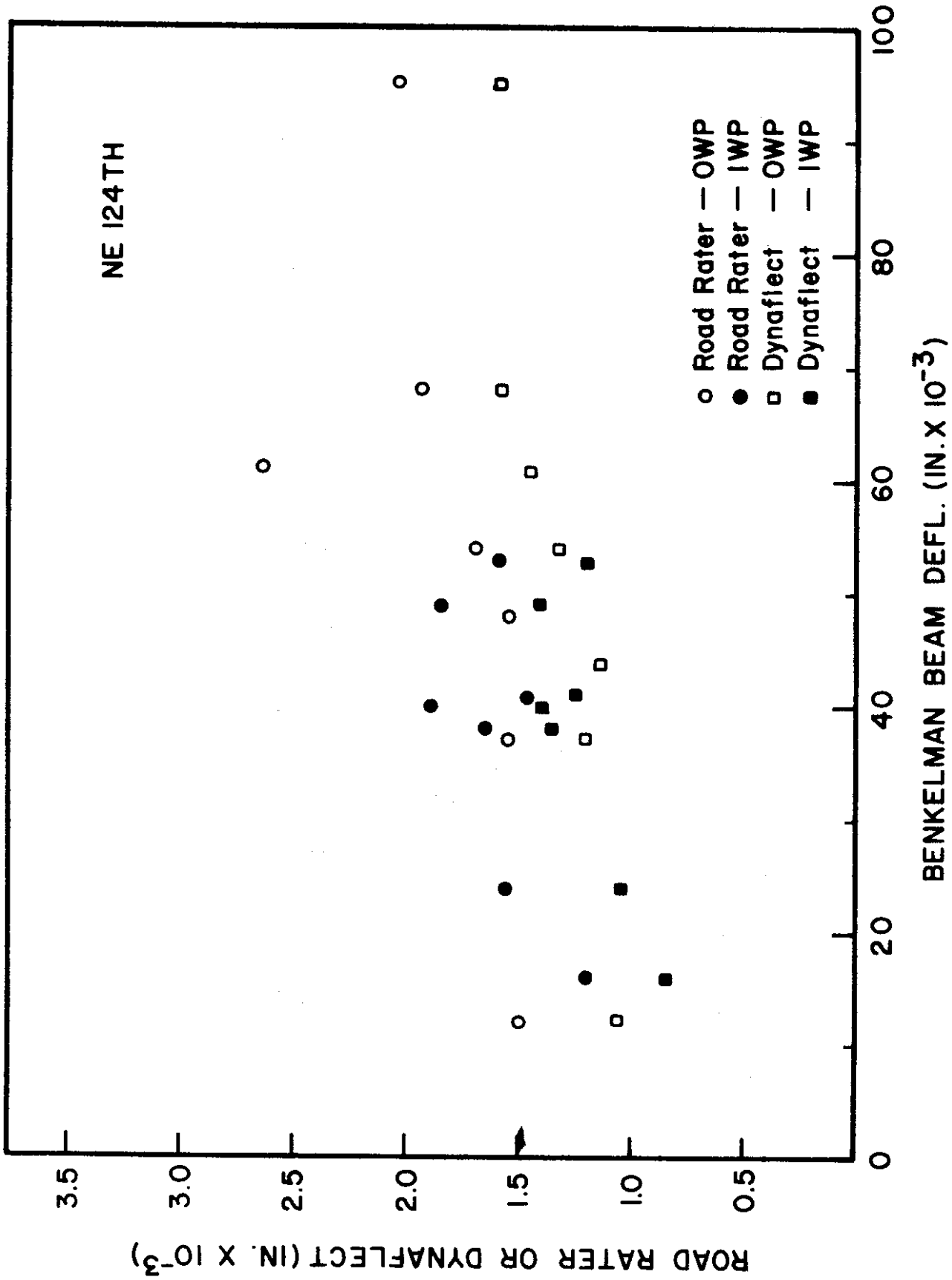
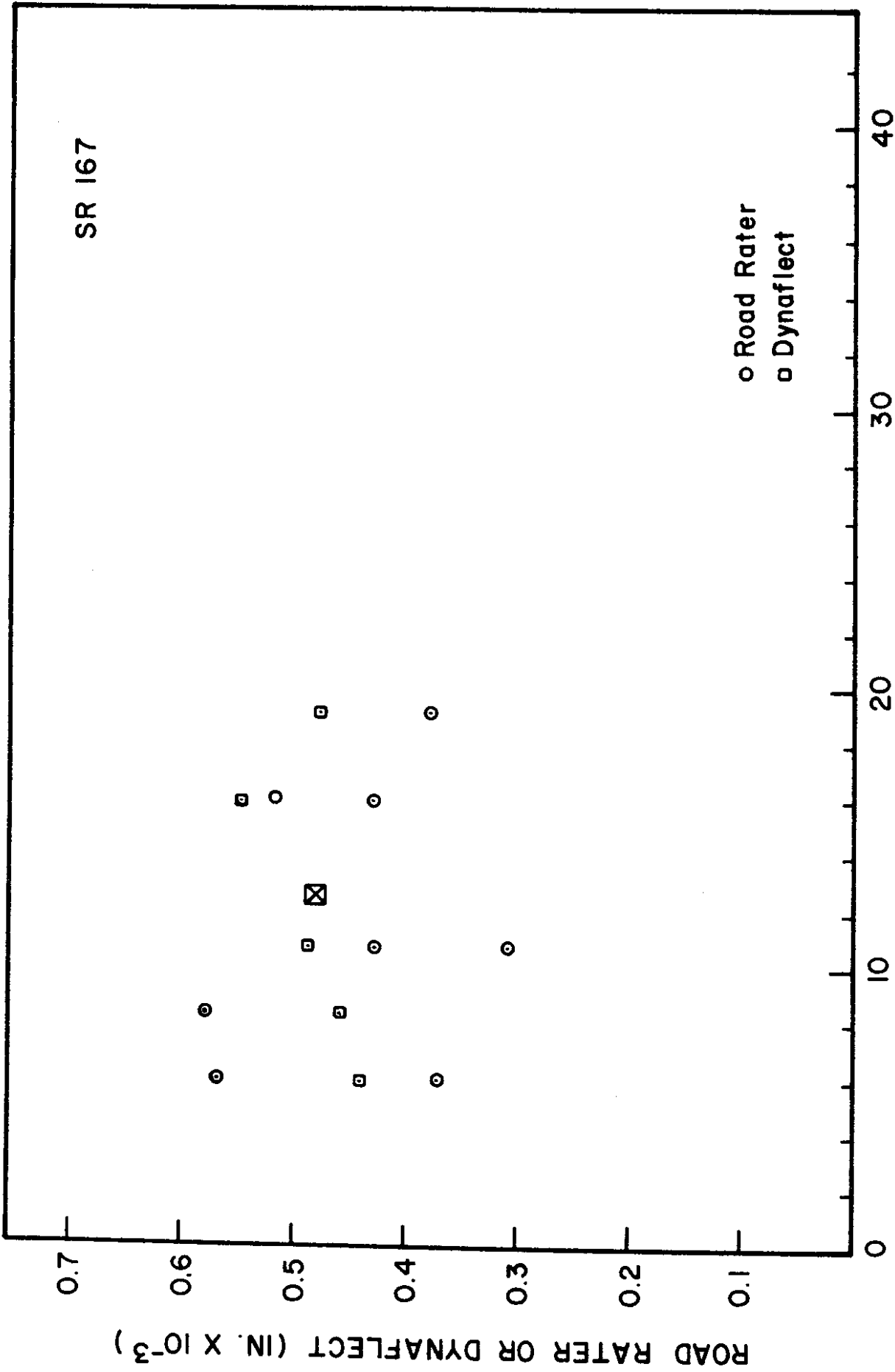


FIGURE 13b - Comparison of Benkelman Beam Deflections with Road Rater and Dynaflect for NE 124th Street



BENKELMAN BEAM DEFL. (IN. X 10⁻³)

FIGURE 13c - Comparison of Benkelman Beam Deflections with Road Rater and Dynaflect for Sign Route 167 Highway

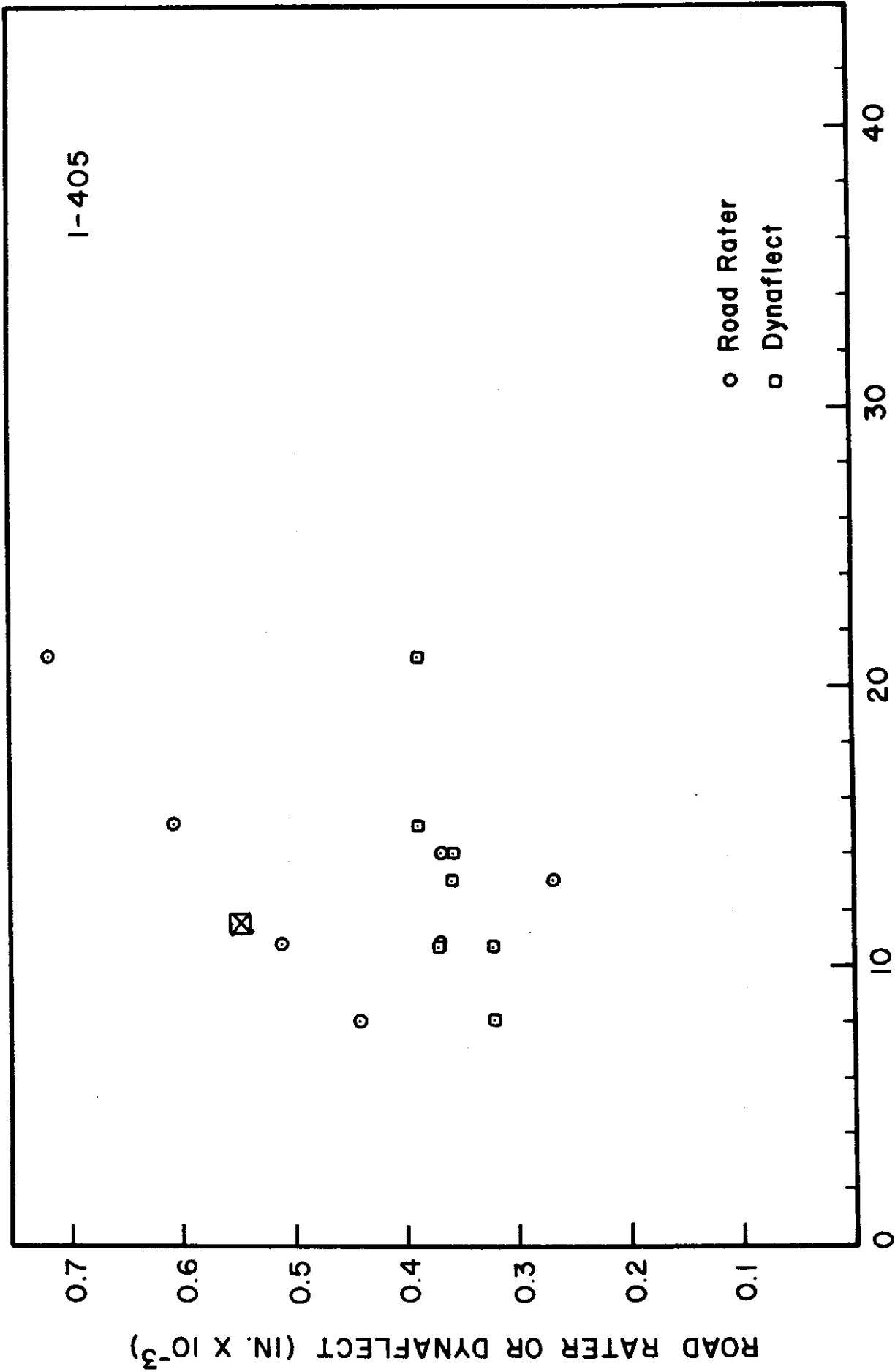


FIGURE 13d - Comparison of Benkelman Beam Deflections with Road Rater and Dynaflect for Interstate 405

FIGURE 13d - Comparison of Benkelman Beam Deflections with Road Rater and Dynaflect for Interstate 405

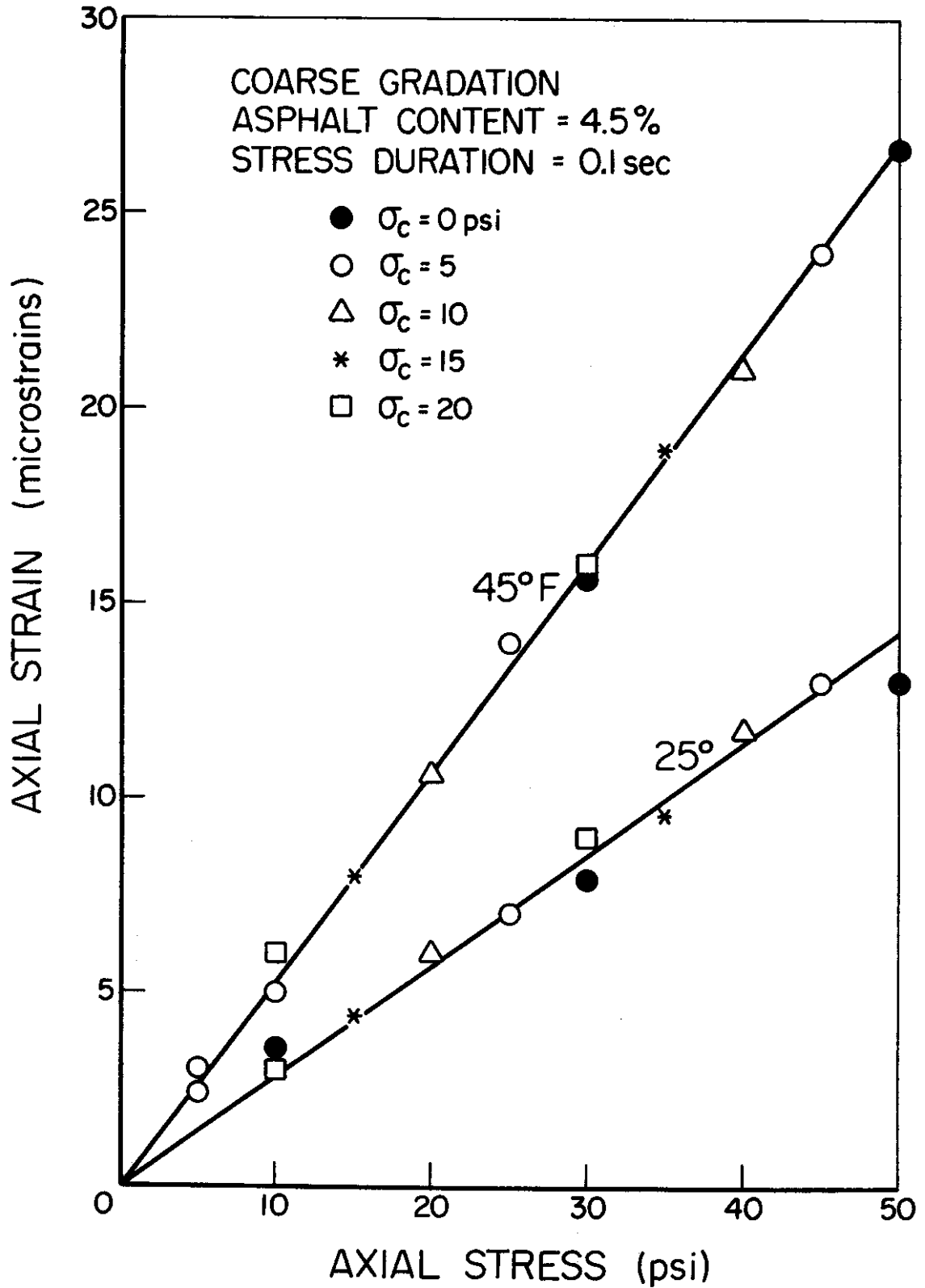


FIGURE 14 - Stress-Strain States Under Sustained Confining Pressures

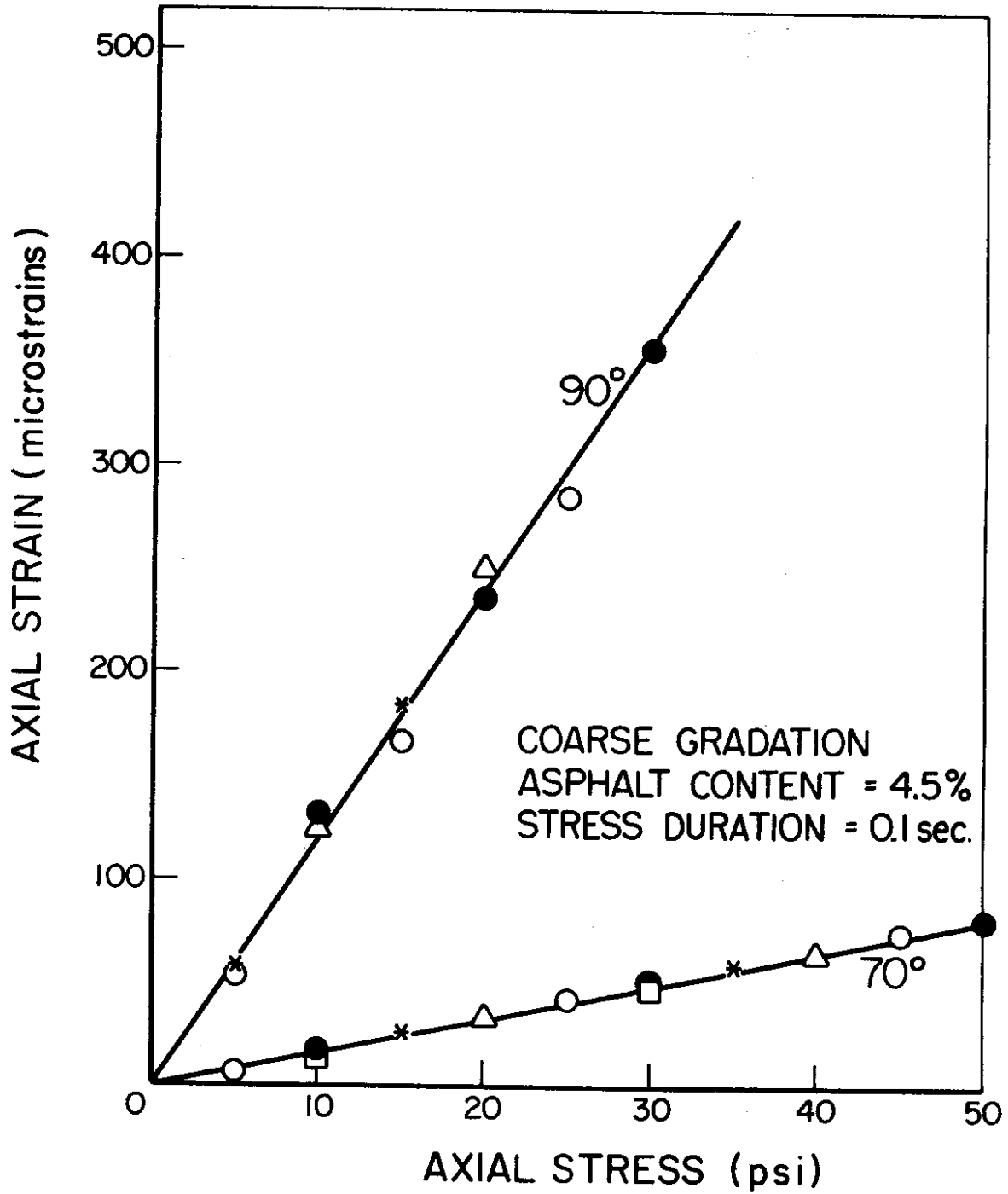


FIGURE 15 - Stress-Strain States Under Sustained Confining Pressures

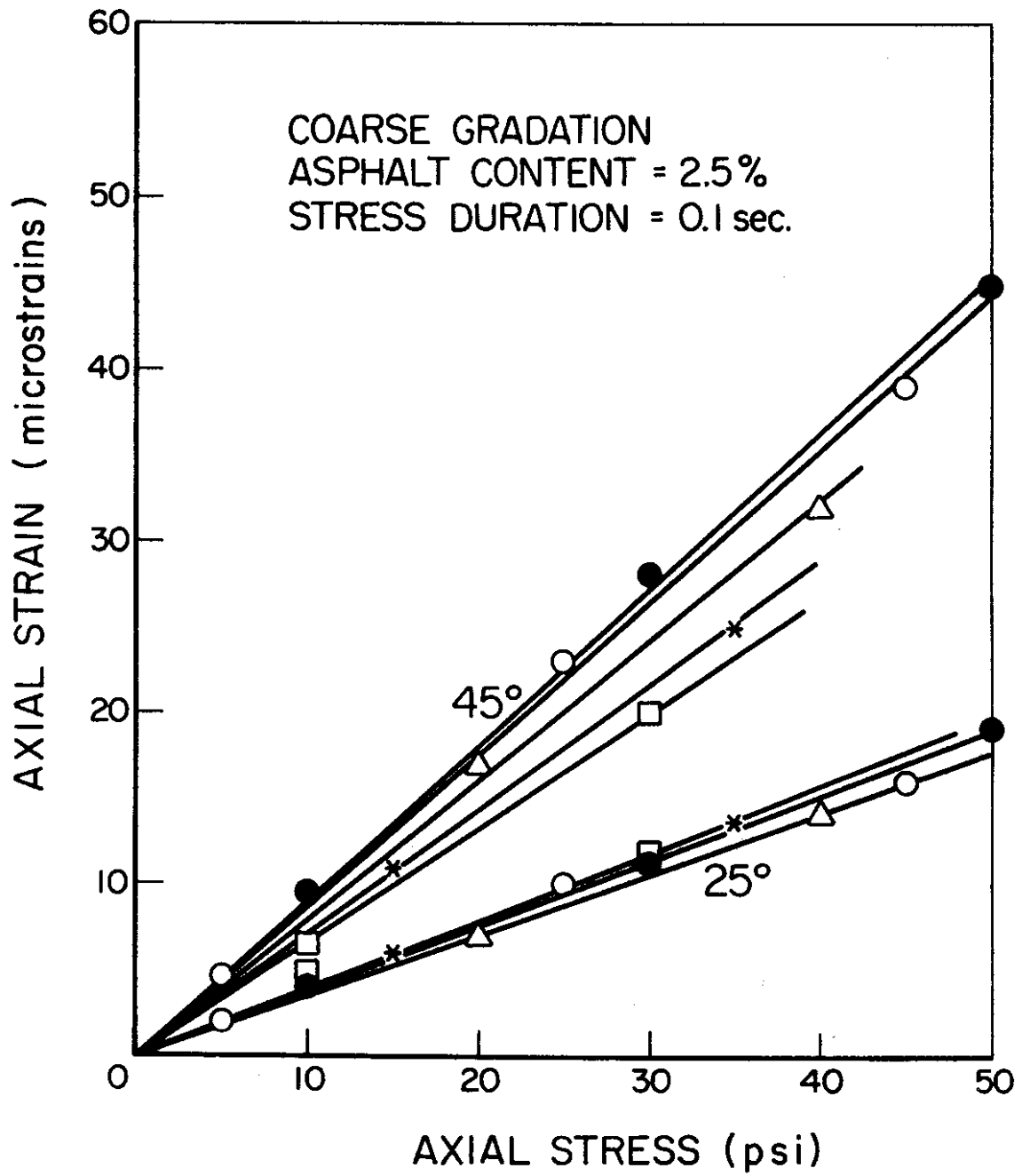


FIGURE 16 - Stress-Strain States Under Sustained Confining Pressures

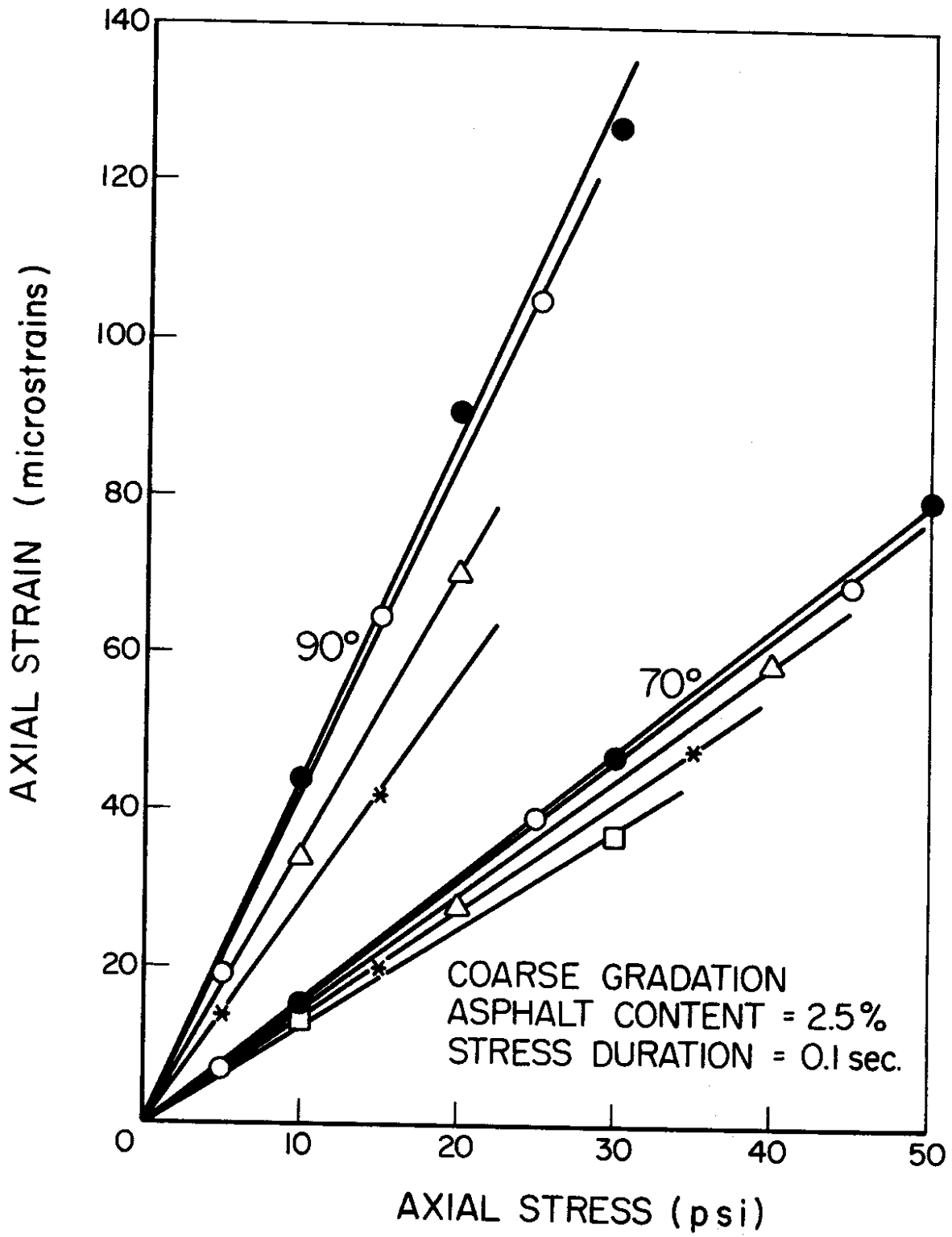


FIGURE 17 - Stress-Strain States Under Sustained Confining Pressures

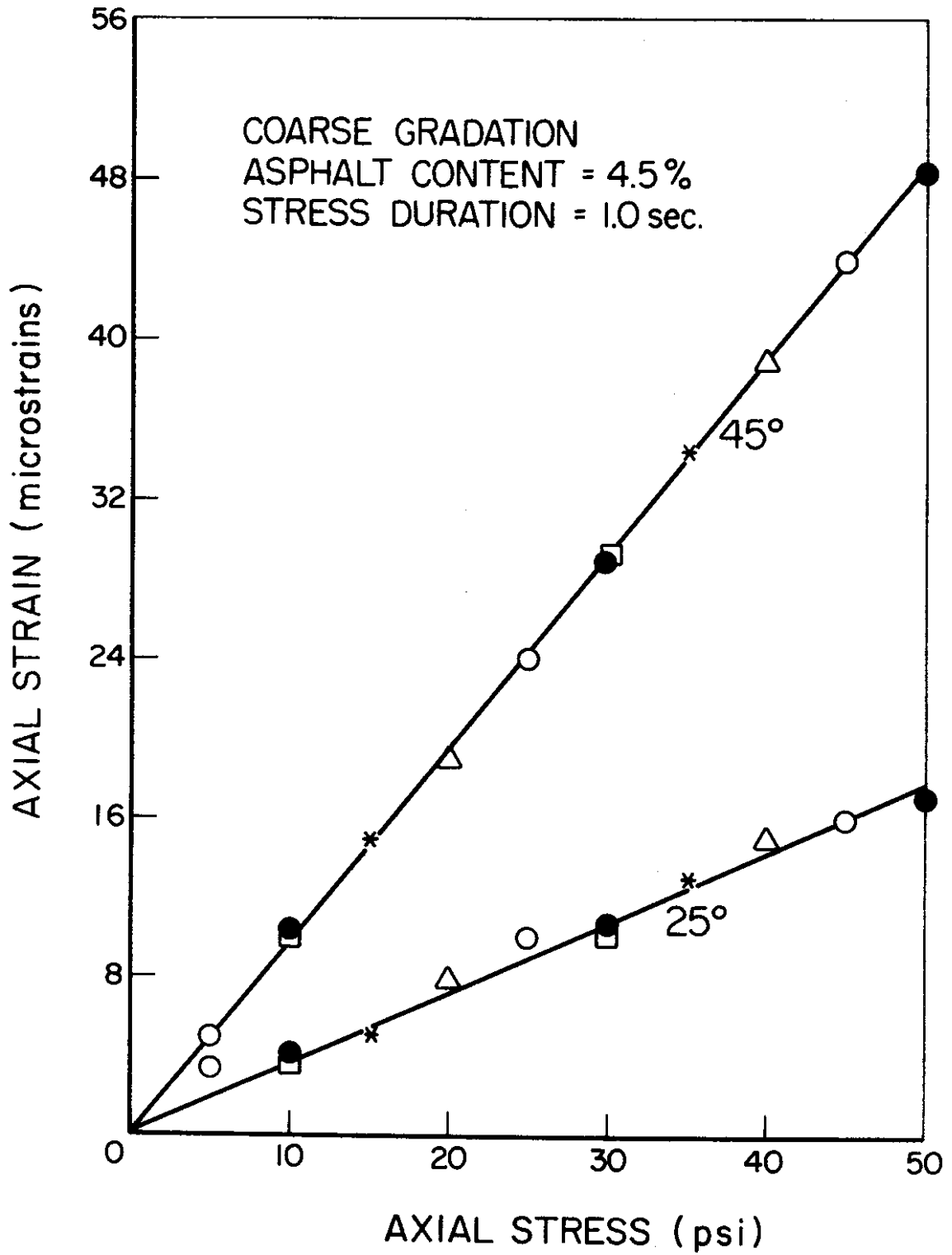


FIGURE 18 - Stress-Strain States Under Sustained Confining Pressures

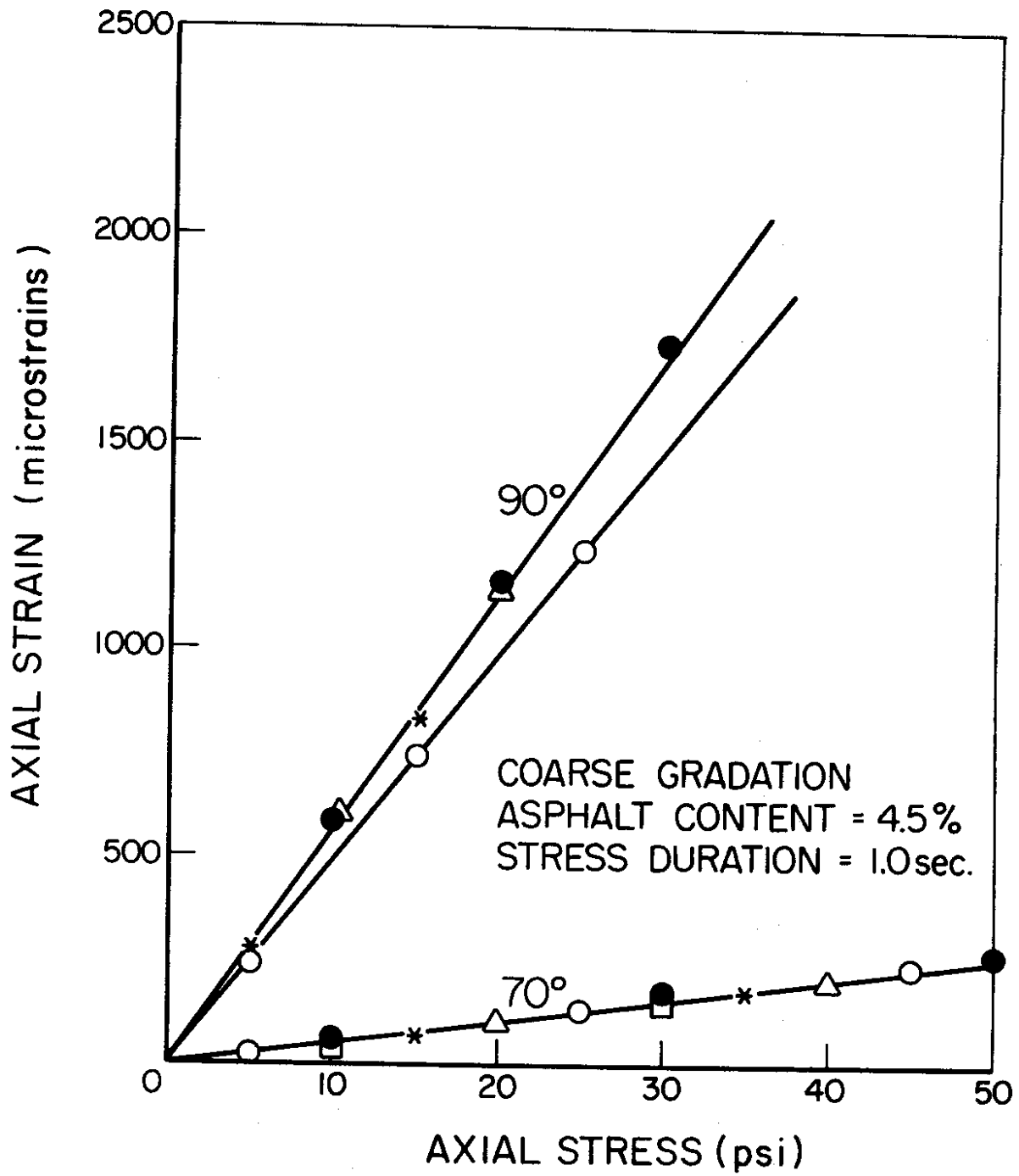


FIGURE 19 - Stress-Strain States Under Sustained Confining Pressures

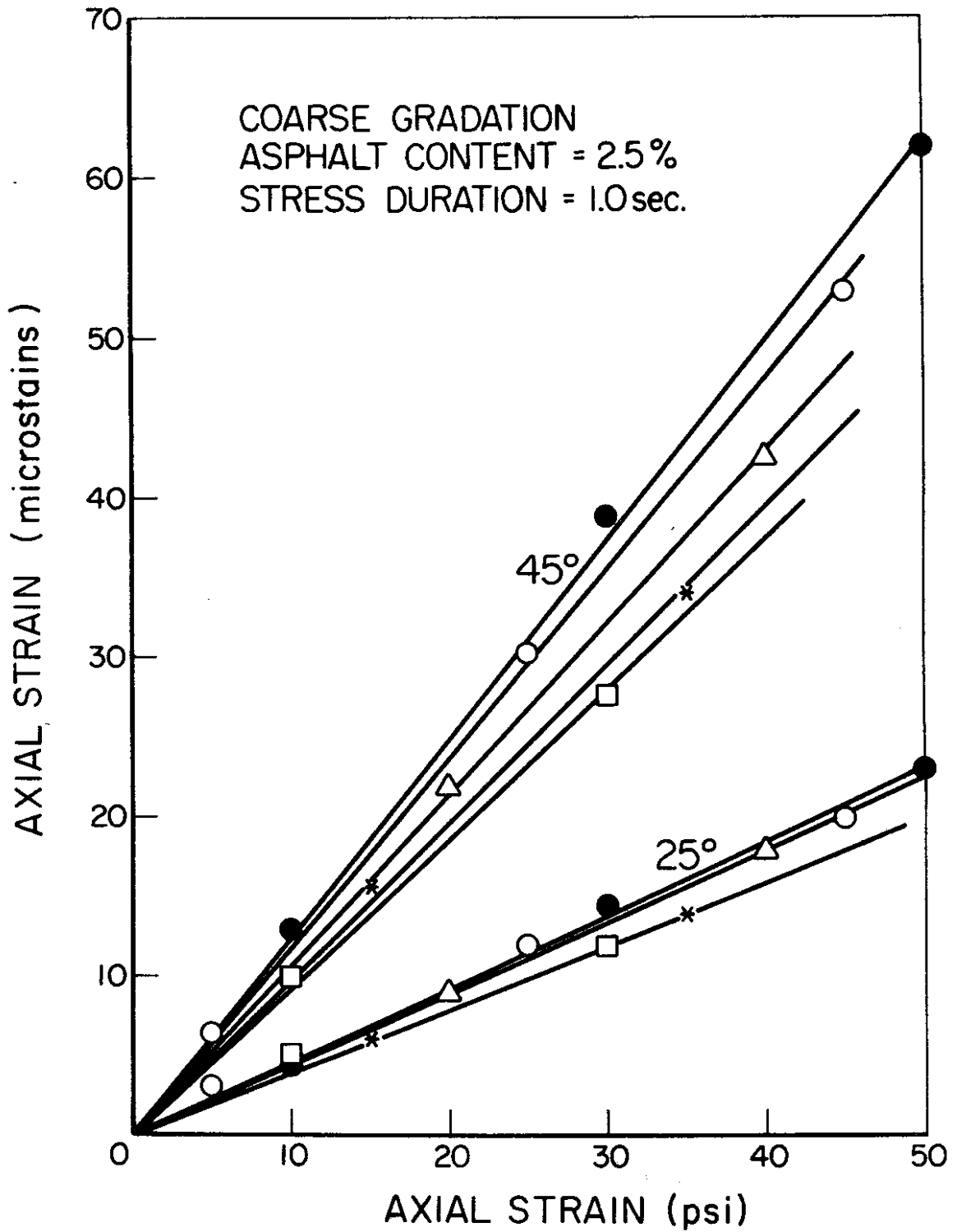


FIGURE 20 - Stress-Strain States Under Sustained Confining Pressures

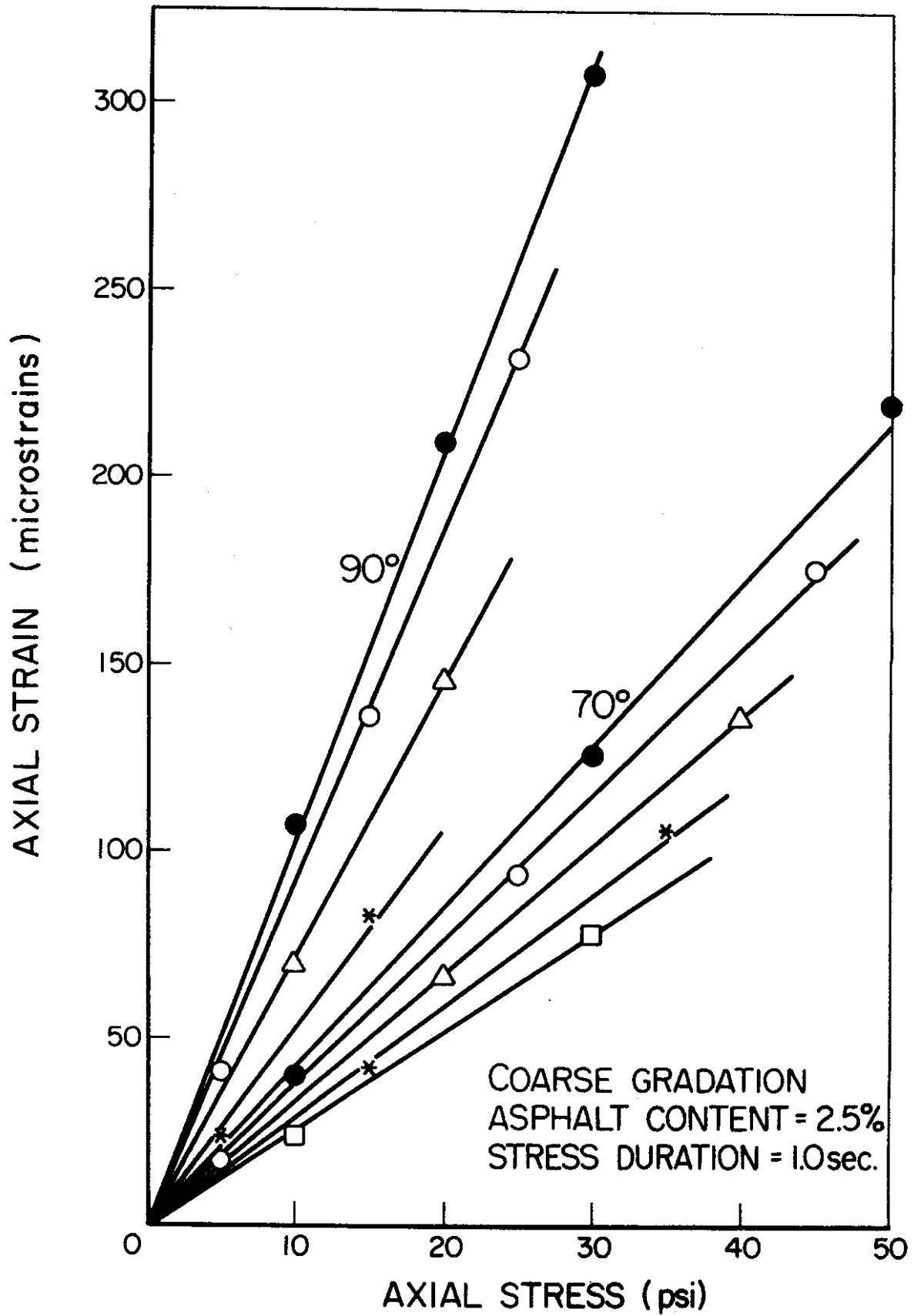


FIGURE 21 - Stress-Strain States Under Sustained Confining Pressures

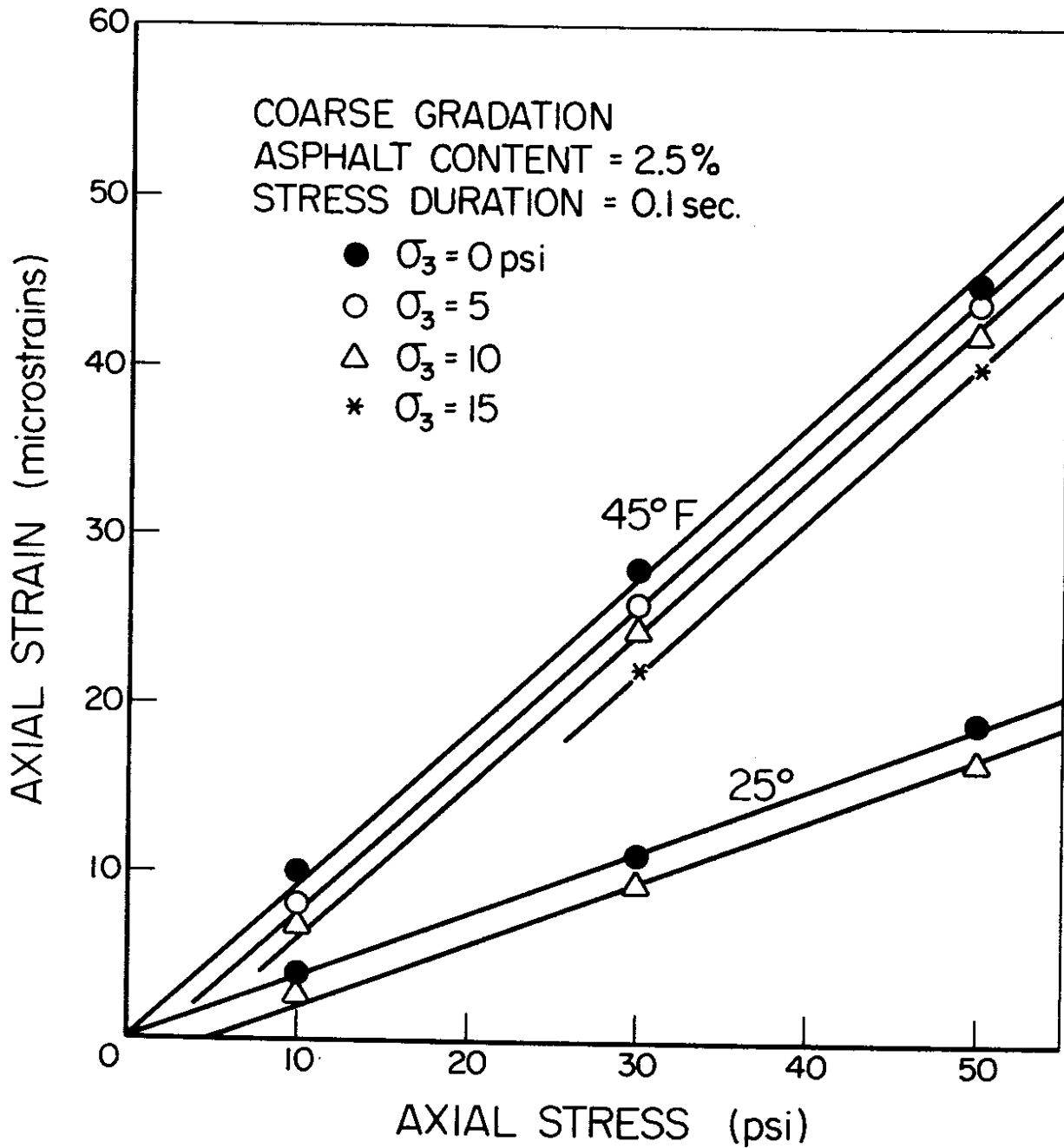


FIGURE 22 - Stress-Strain States Under Cyclic Axial and Radial Stresses

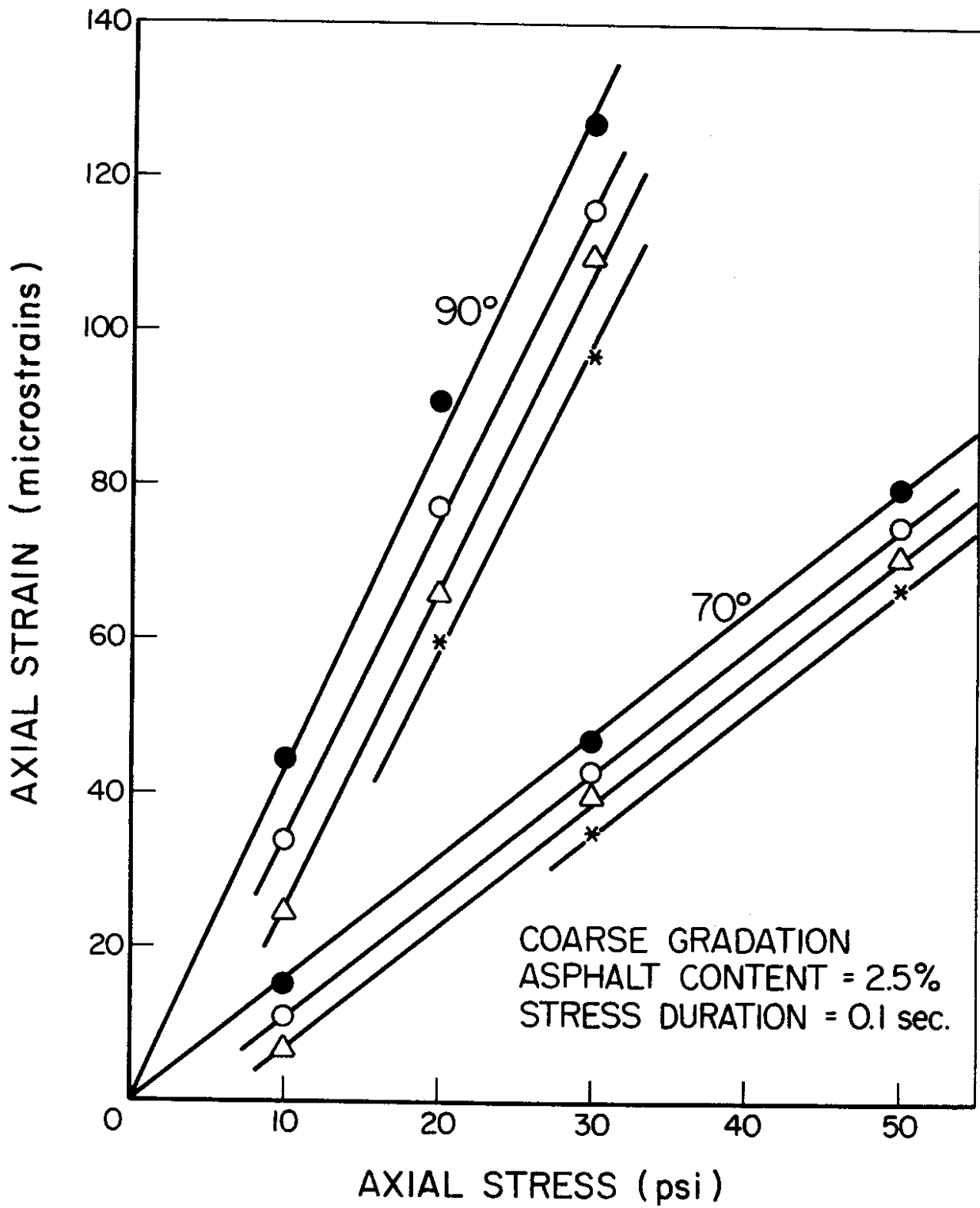


FIGURE 23 - Stress-Strain States Under Cyclic Axial and Radial Stresses

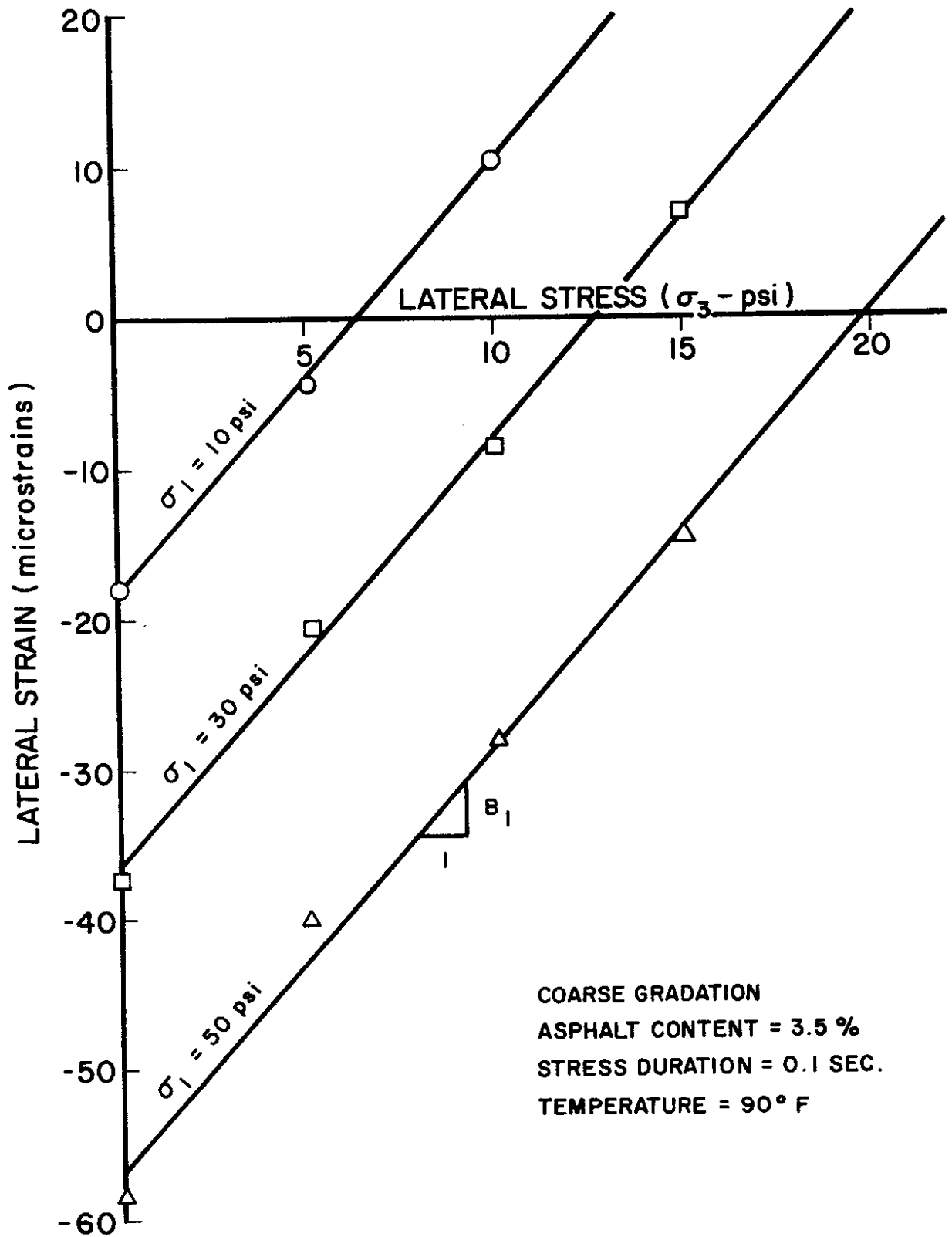


FIGURE 24 - Stress-Strain States Under Cyclic Axial and Radial Stresses

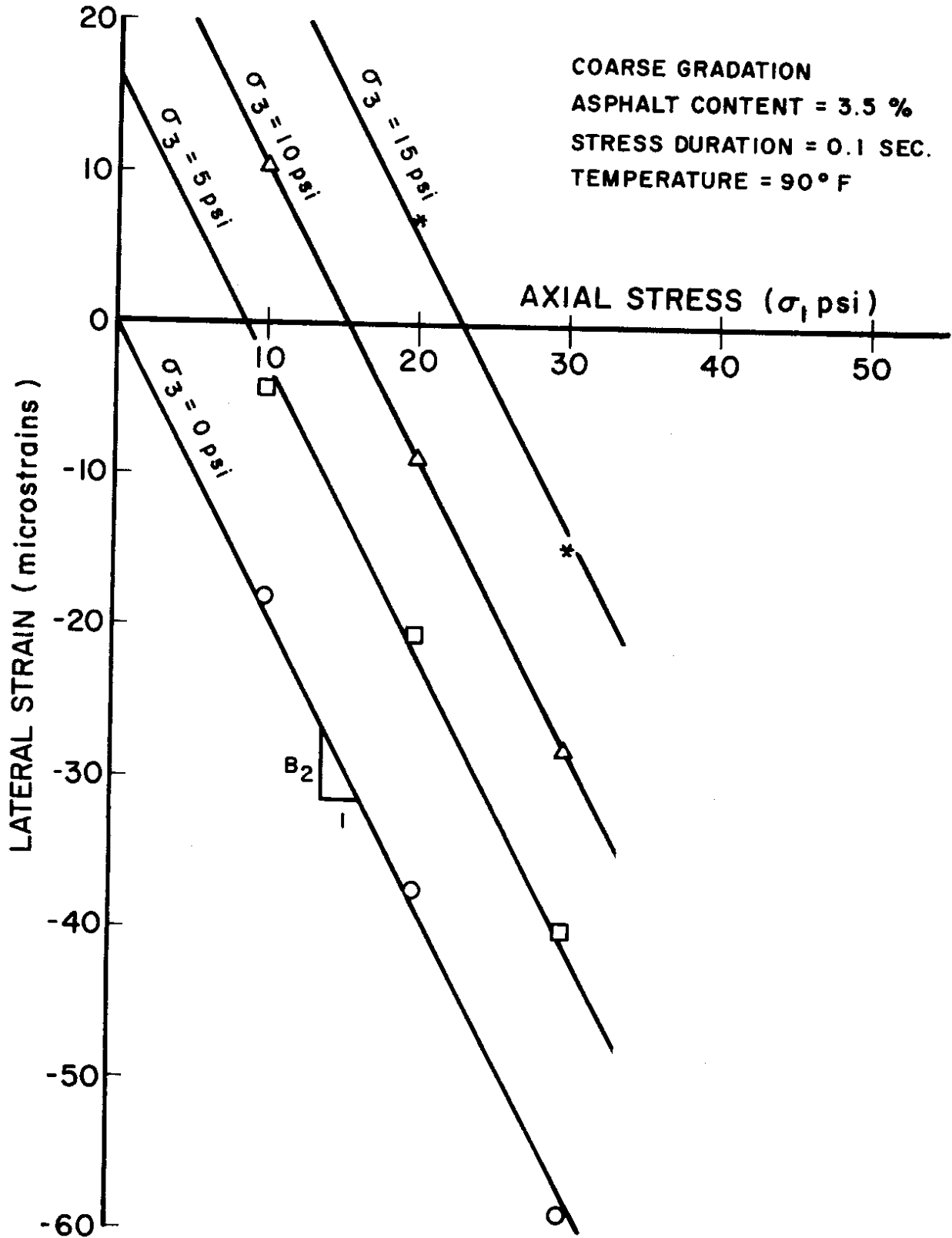


FIGURE 25 - Stress-Strain States Under Cyclic Axial and Radial Stresses

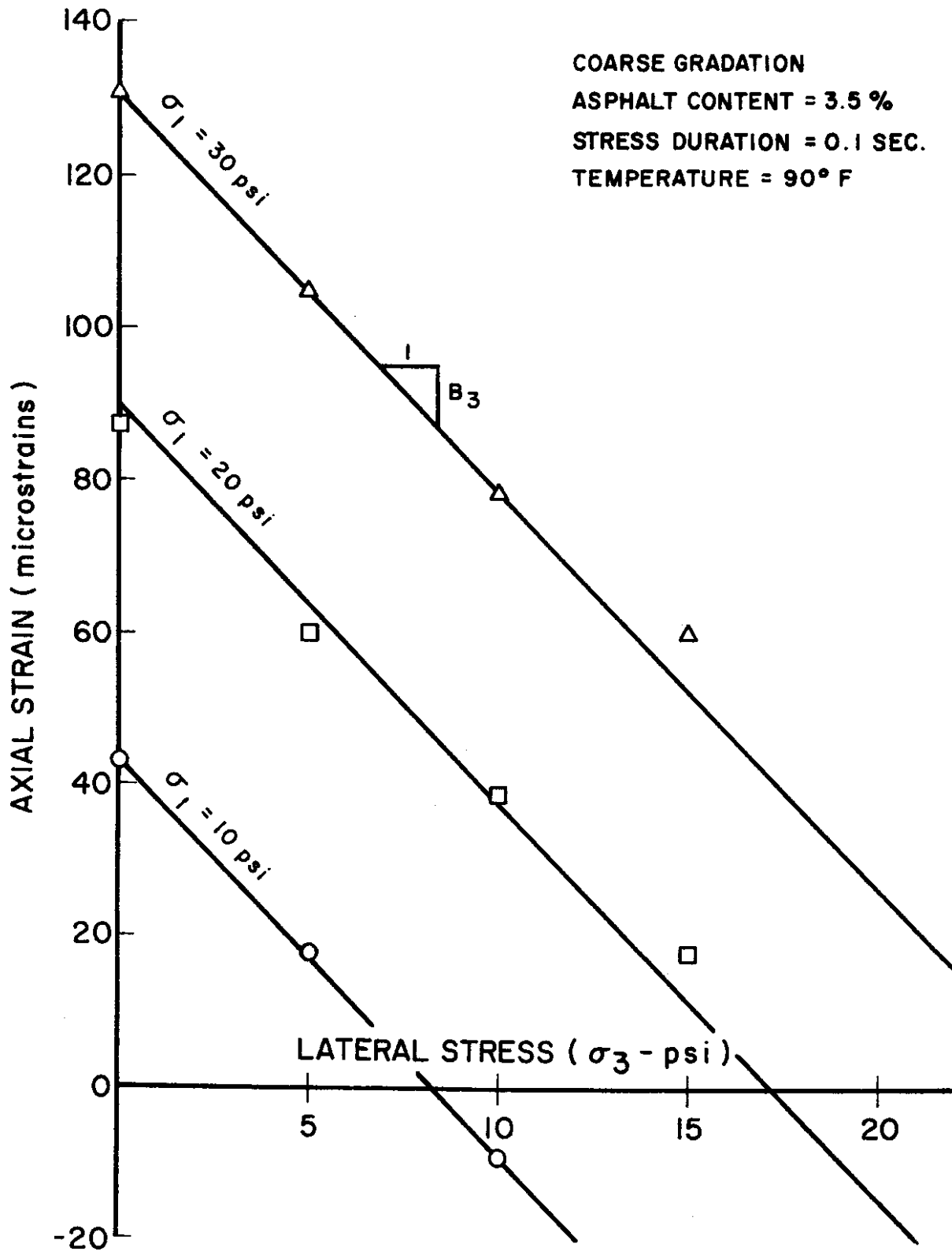


FIGURE 26 - Stress-Strain States Under Cyclic Axial and Radial Stresses

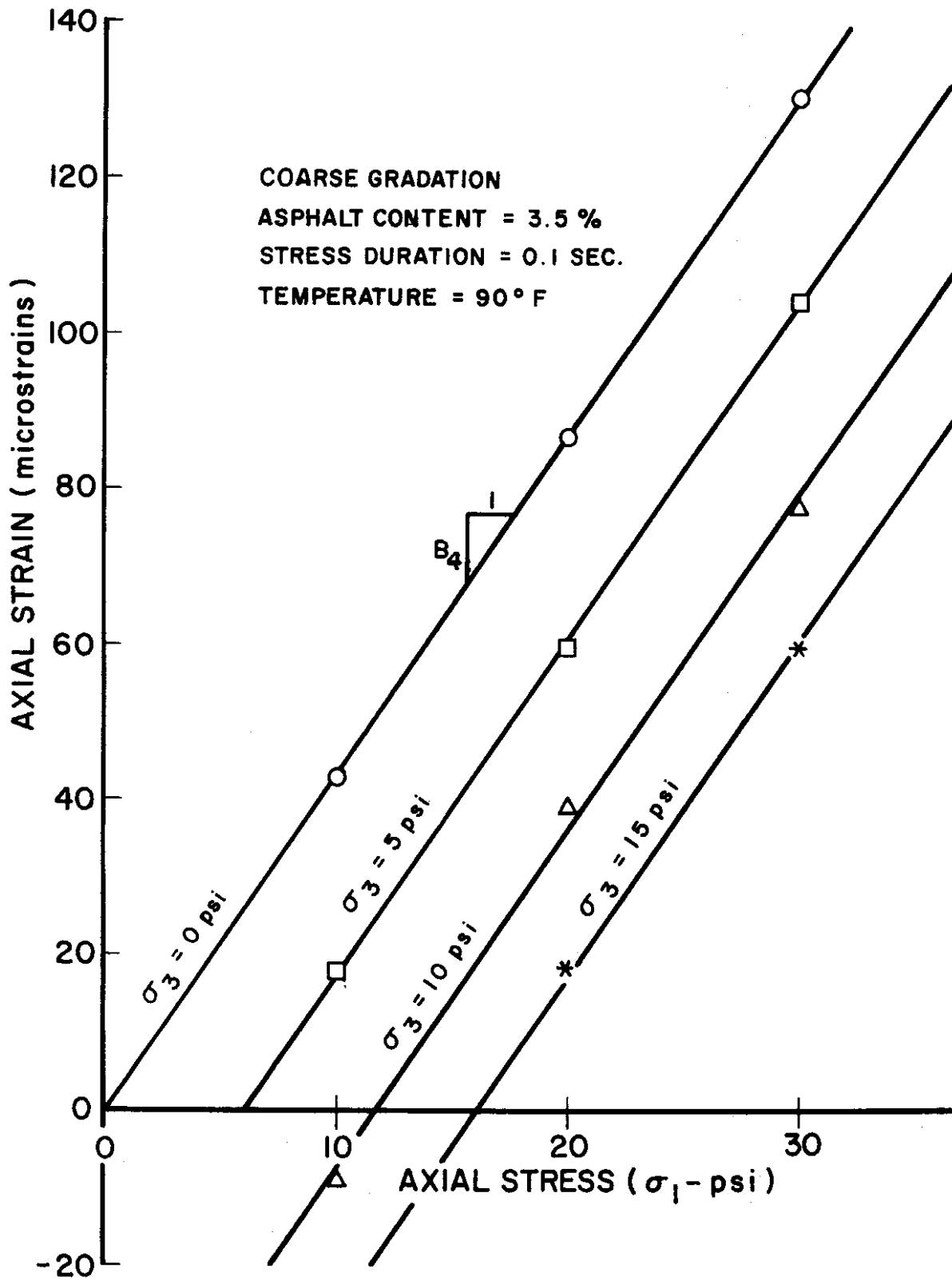


FIGURE 27 - Stress-Strain States Under Cyclic Axial and Radial Stresses

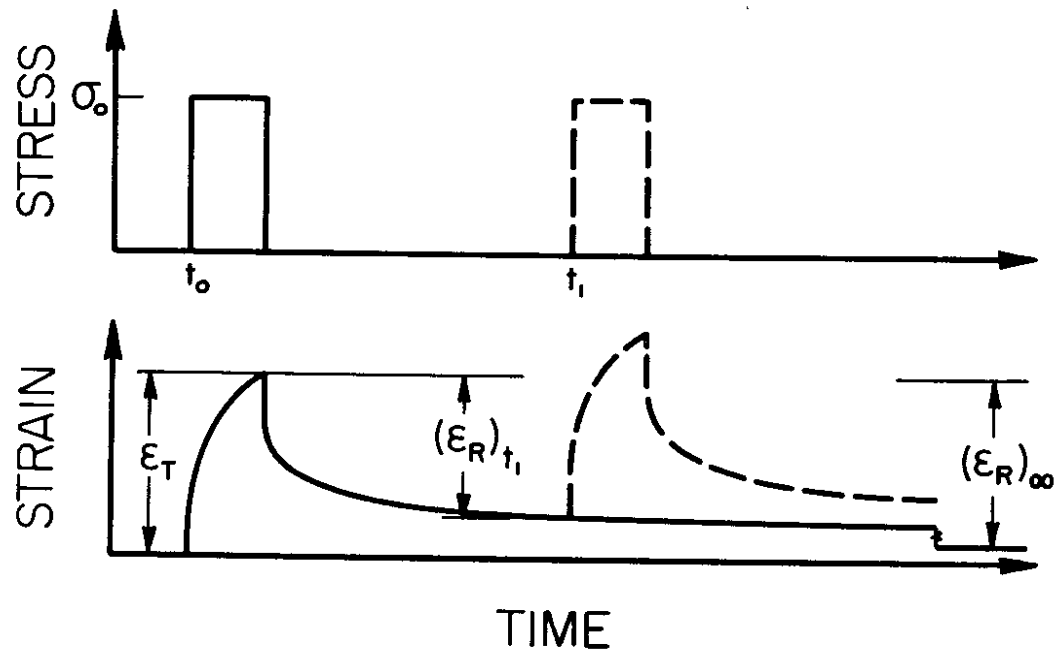


FIGURE 28 - Resilient and Total Strains under Repeated Stress

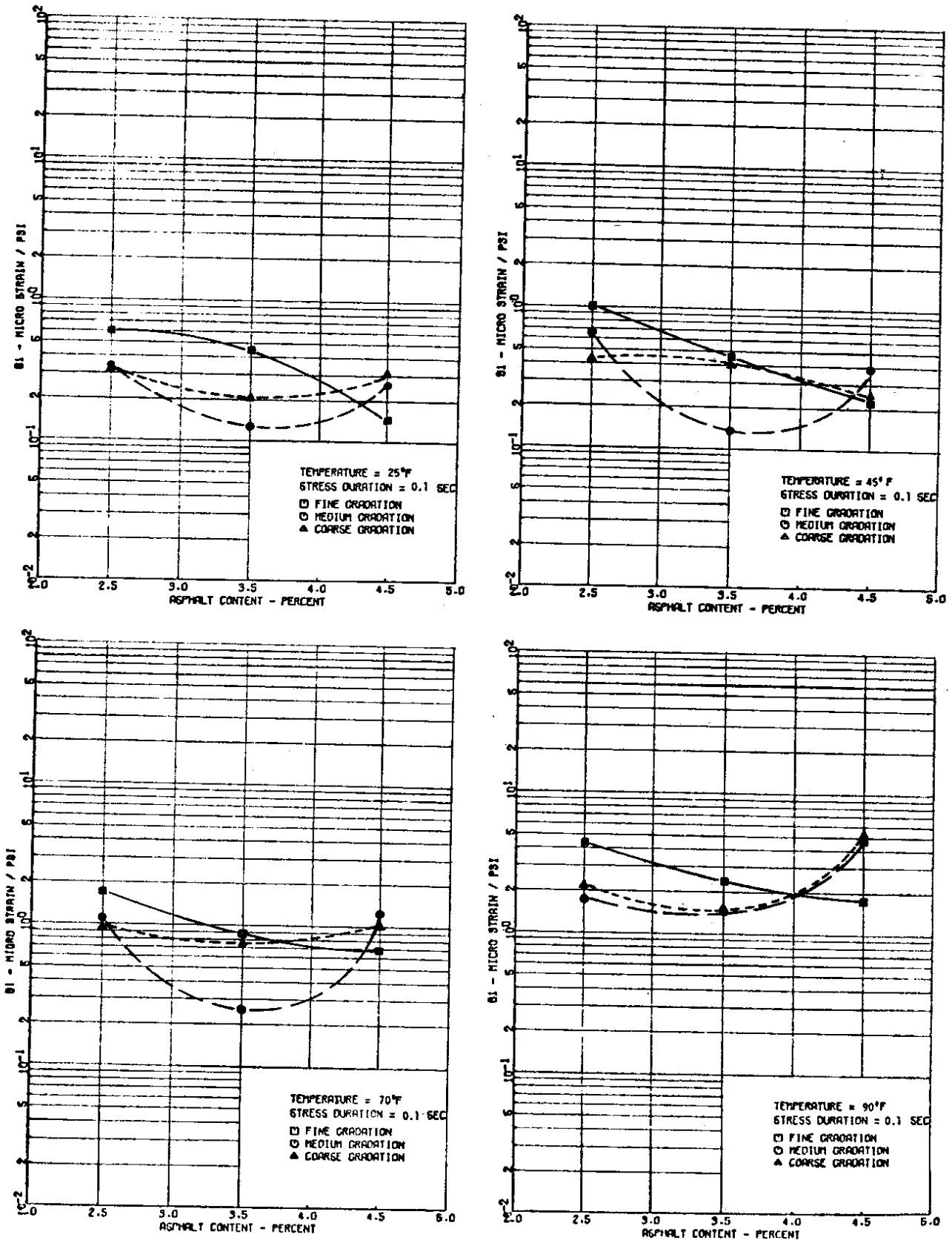


FIGURE 29 - Coefficient B1 Versus Asphalt Content at 25, 45, 70 and 90°F

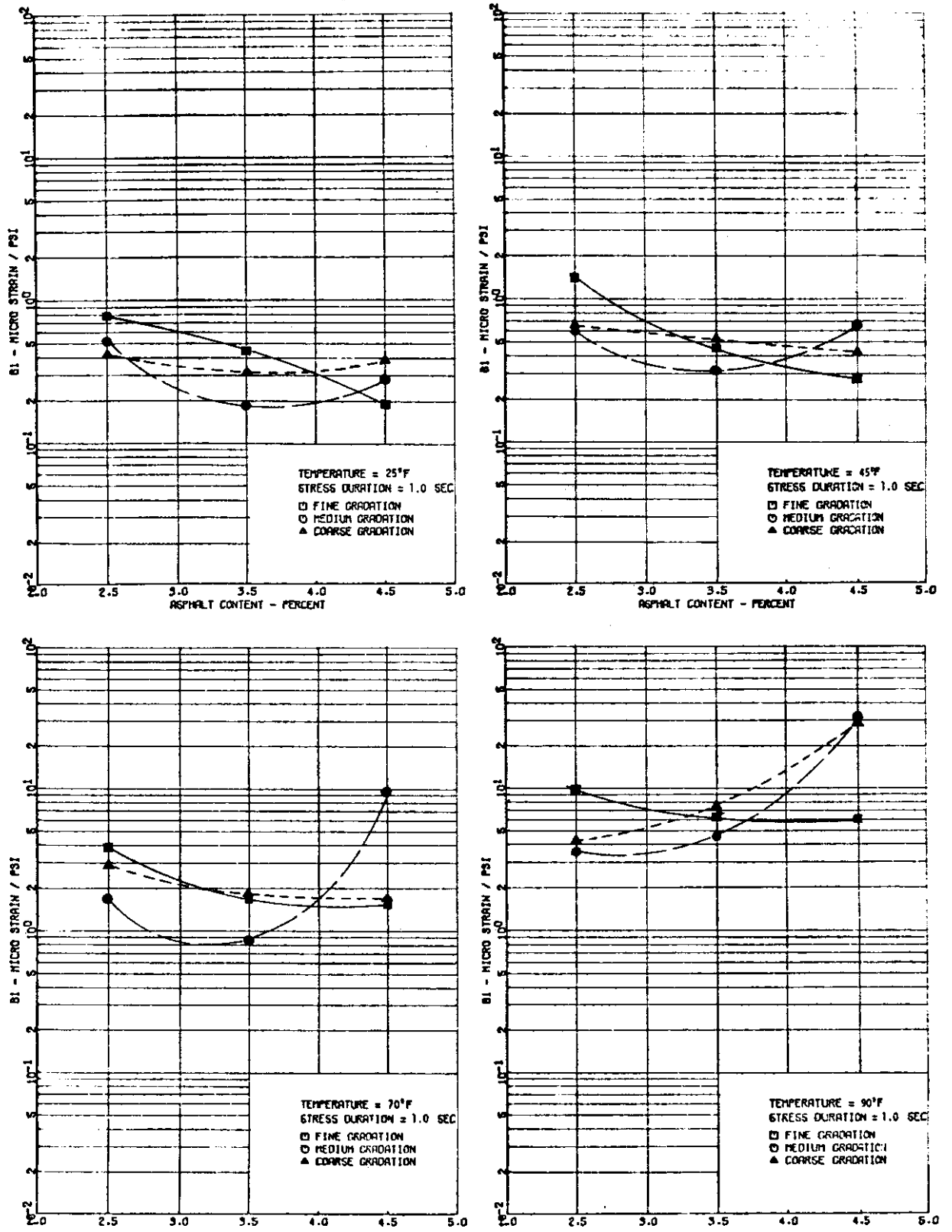


FIGURE 30 - Coefficient B1 Versus Asphalt Content at 25, 45, 70 and 90°F

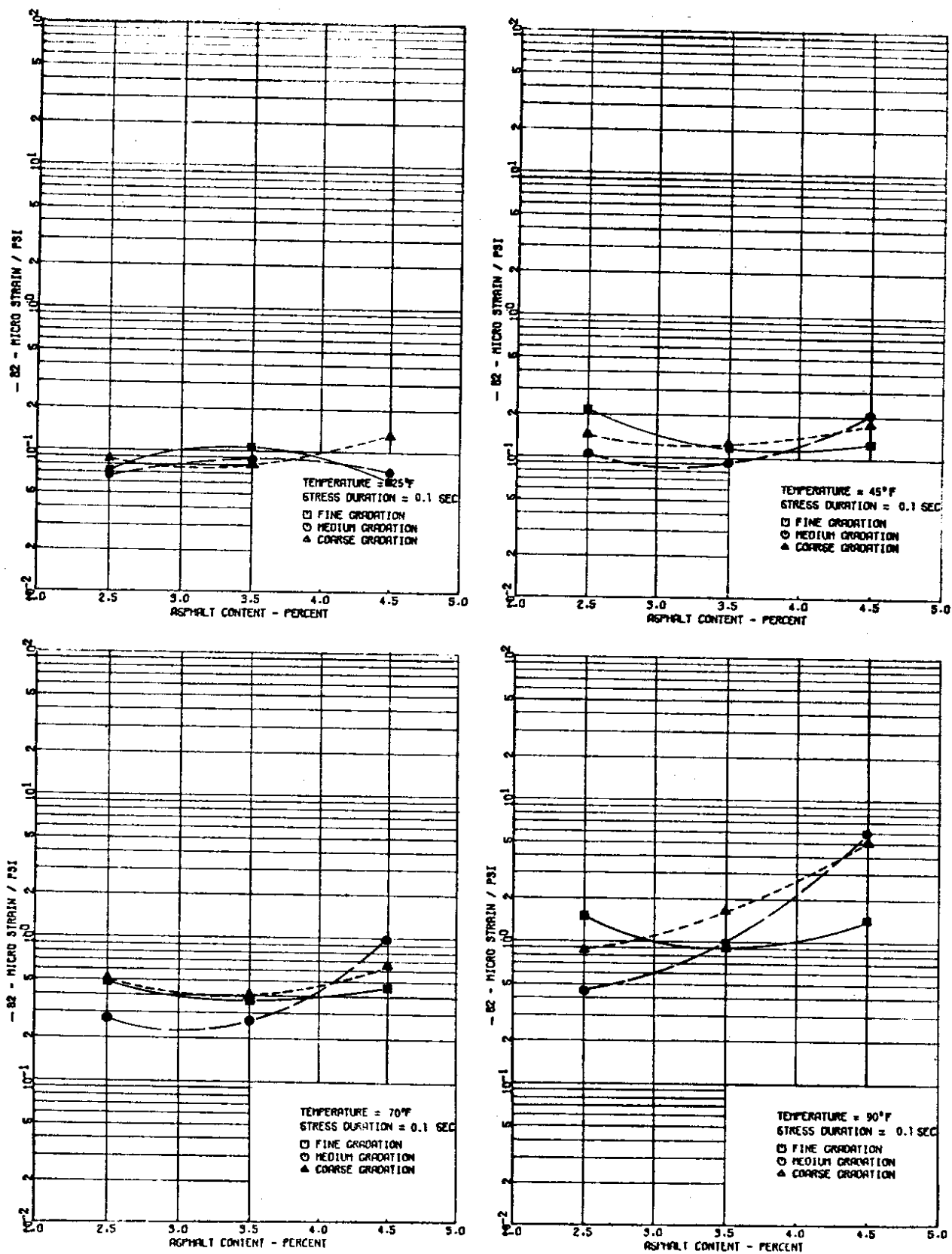


FIGURE 31 - Coefficient B2 Versus Asphalt Content at 25, 45, 70 and 90°F

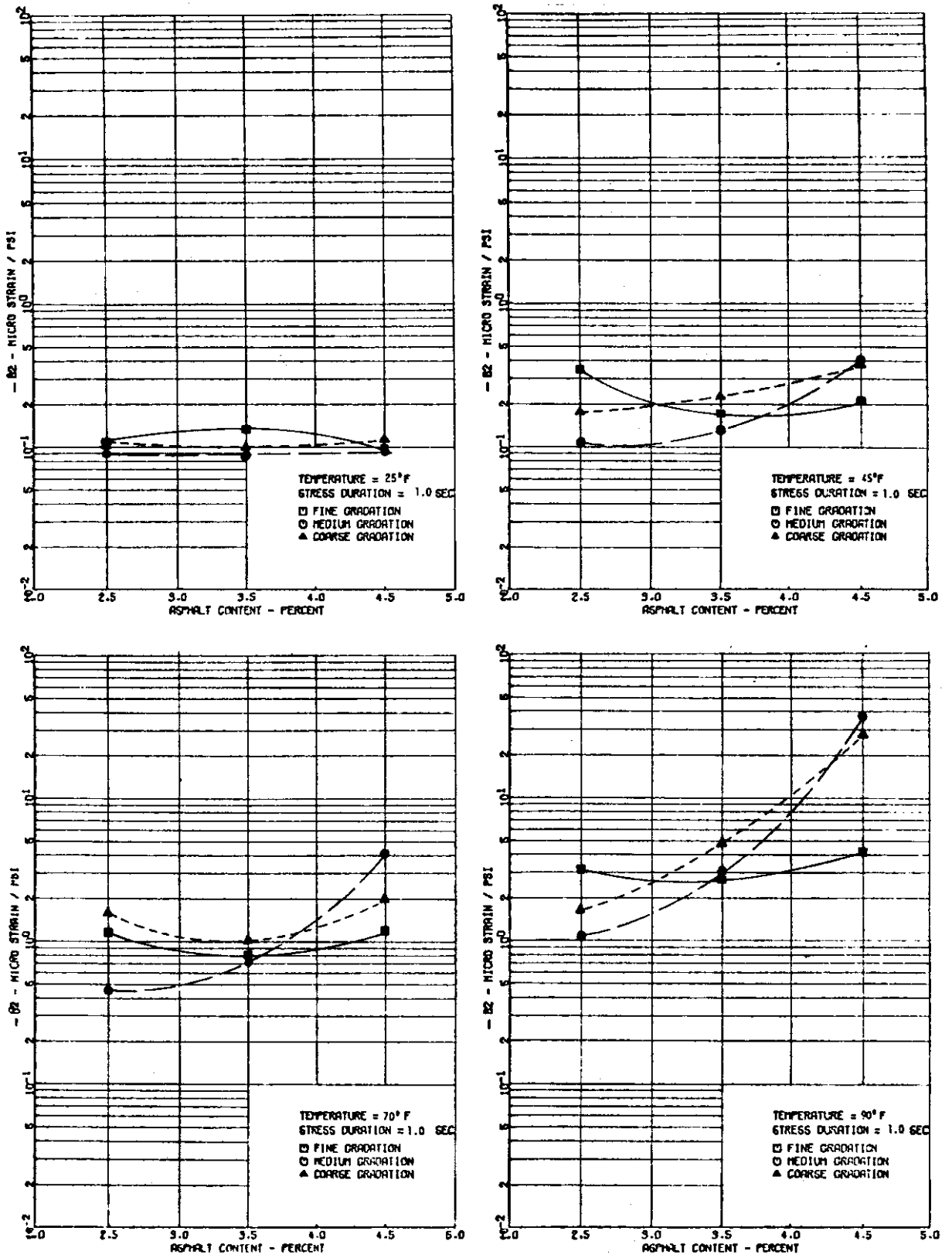


FIGURE 32 - Coefficient B2 Versus Asphalt Content at 25, 45, 70 and 90°F

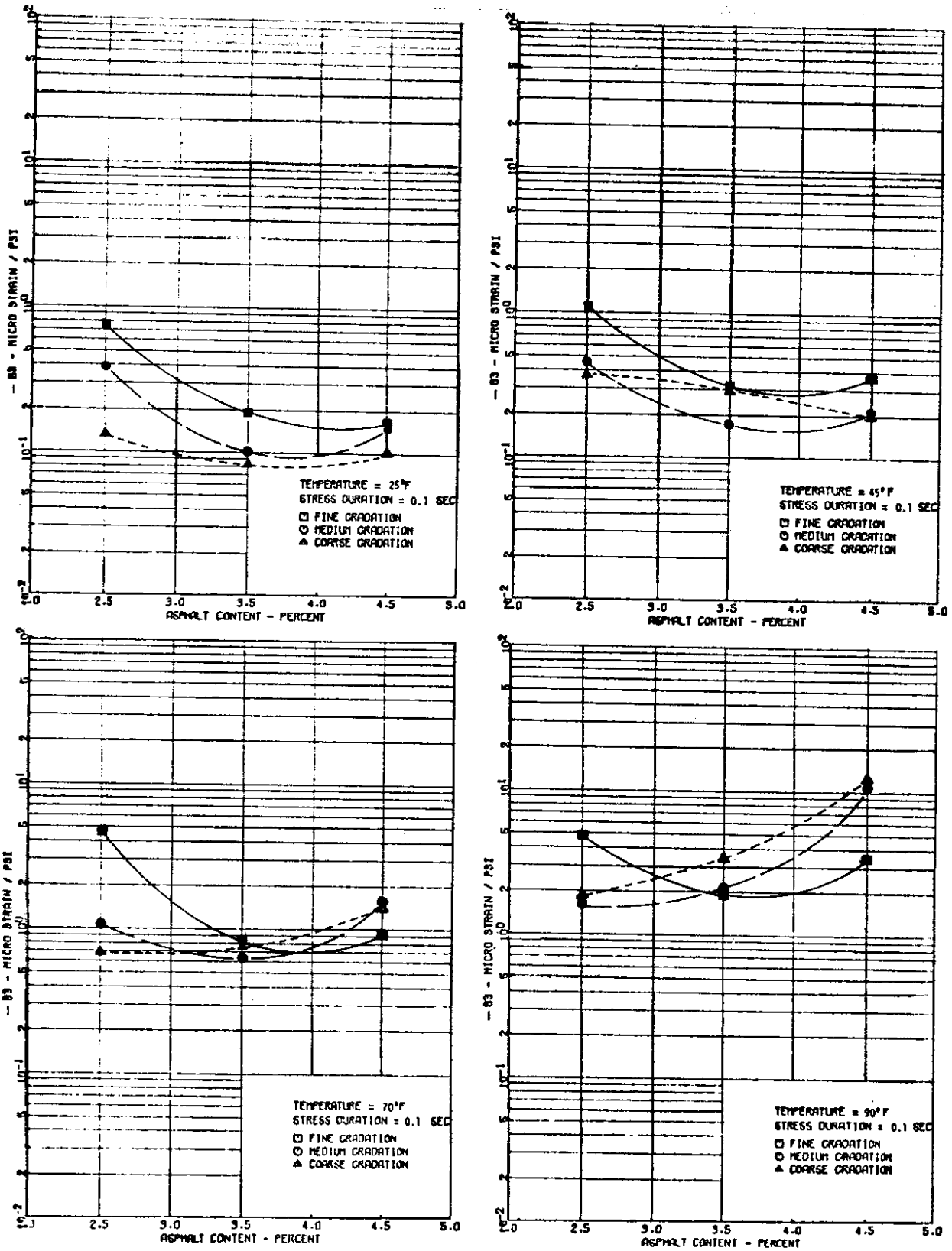


FIGURE 33 - Coefficient B3 Versus Asphalt Content at 25, 45, 70 and 90°F

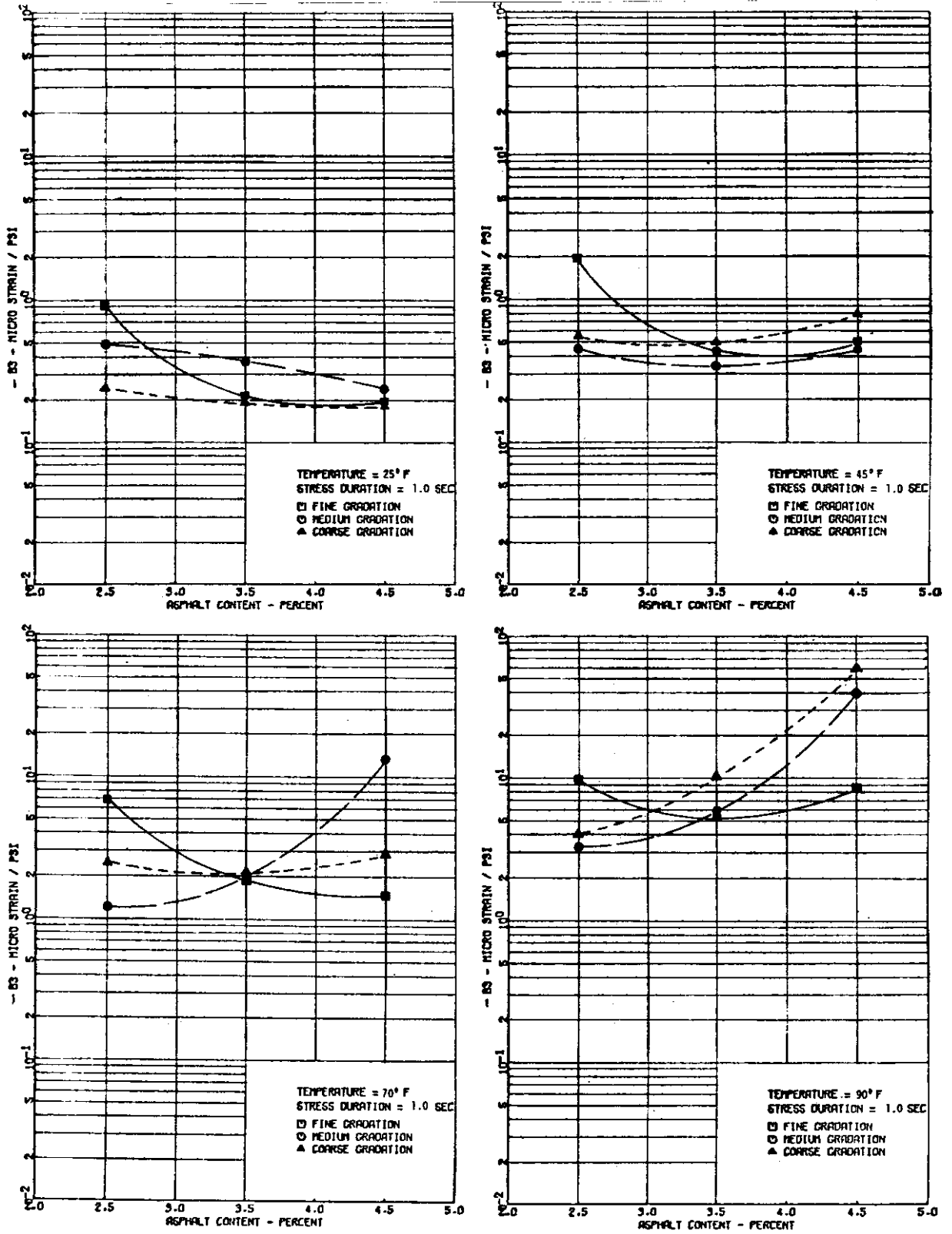


FIGURE 34 - Coefficient B3 Versus Asphalt Content at 25, 45, 70 and 90°F

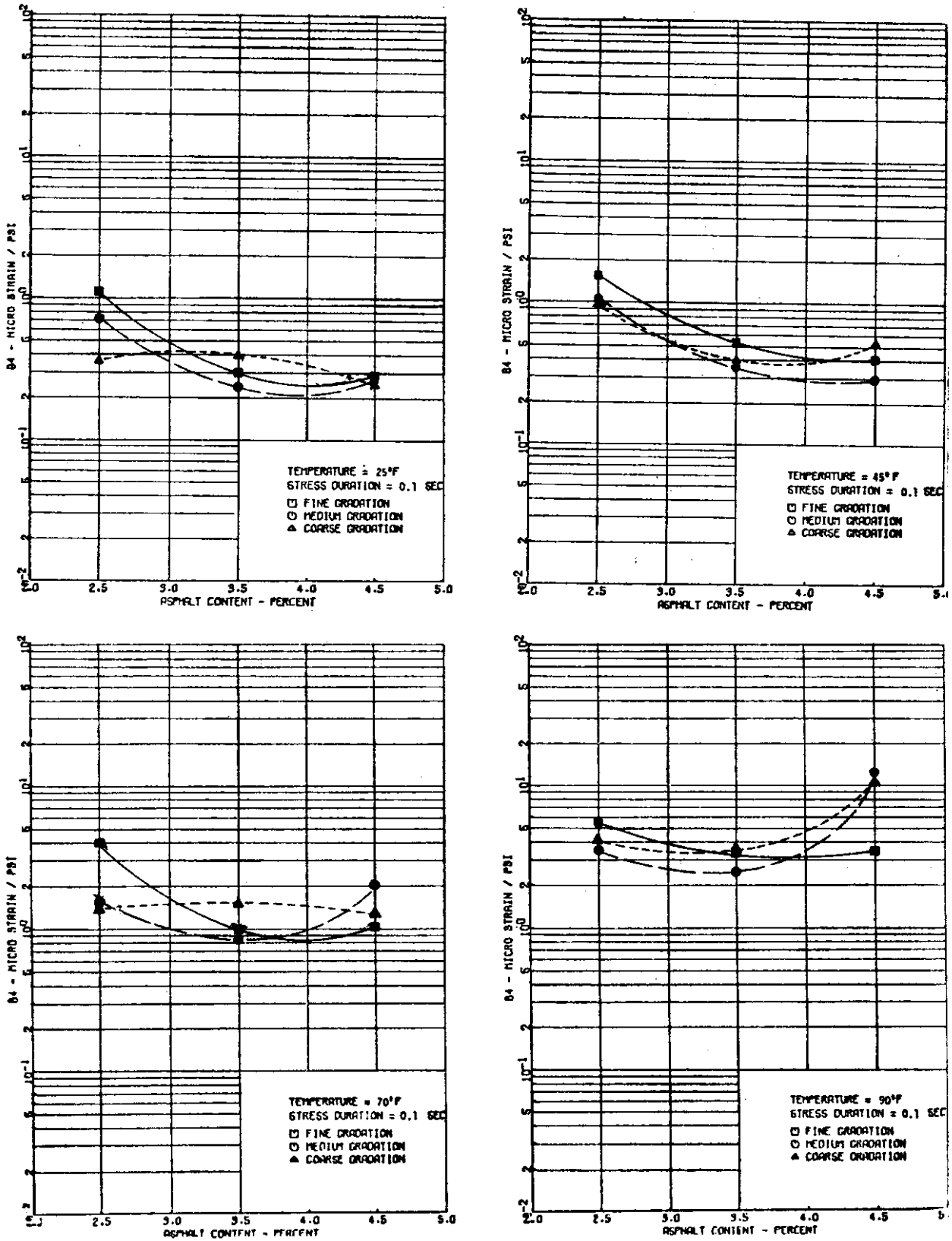


FIGURE 35 - Coefficient B4 Versus Asphalt Content at 25, 45, 70 and 90°F

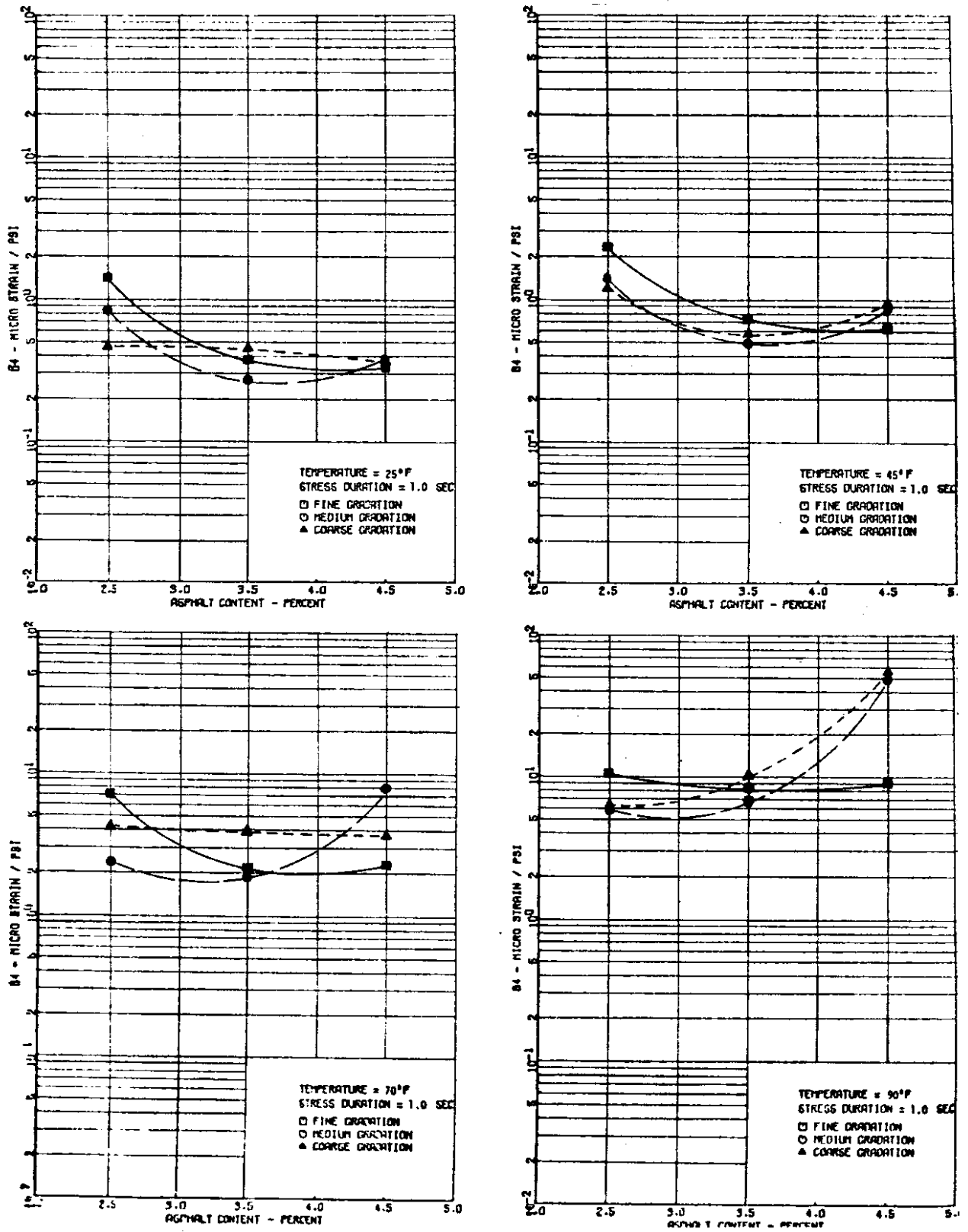


FIGURE 36 - Coefficient B4 Versus Asphalt Content at 25, 45, 70 and 90°F

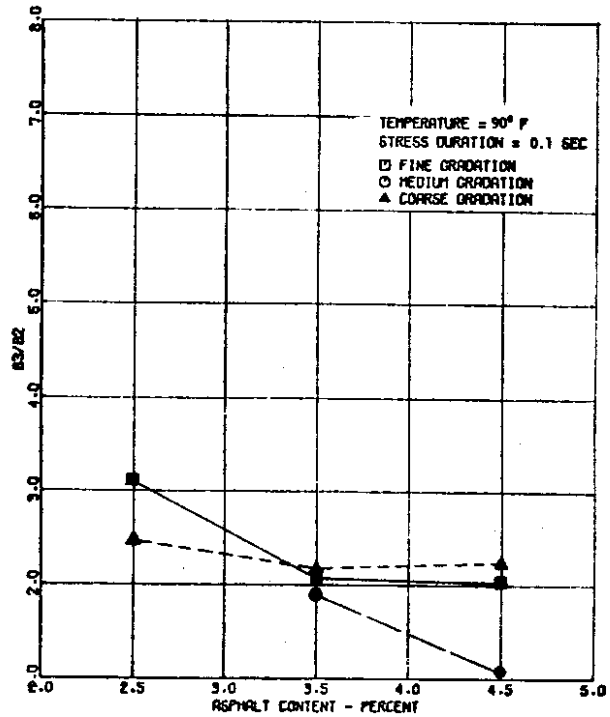
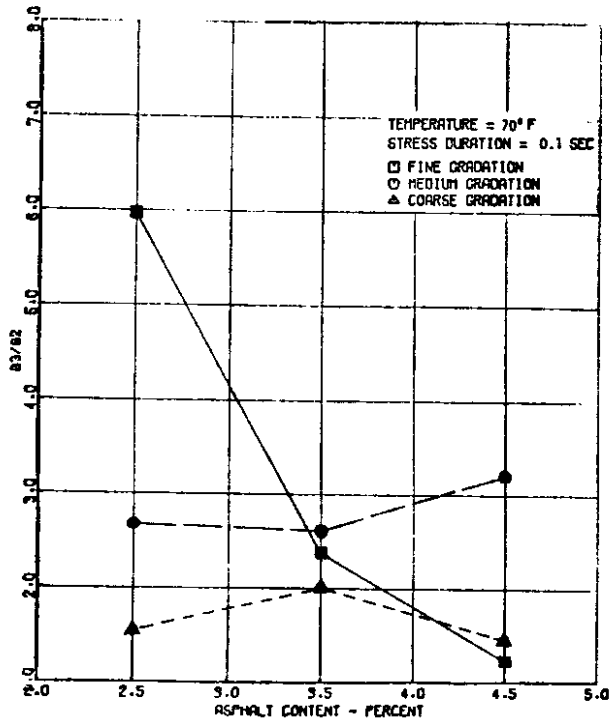
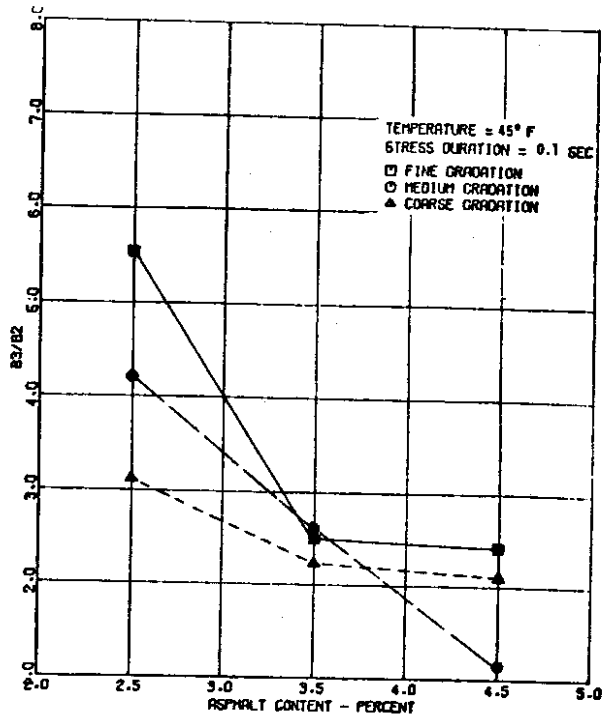
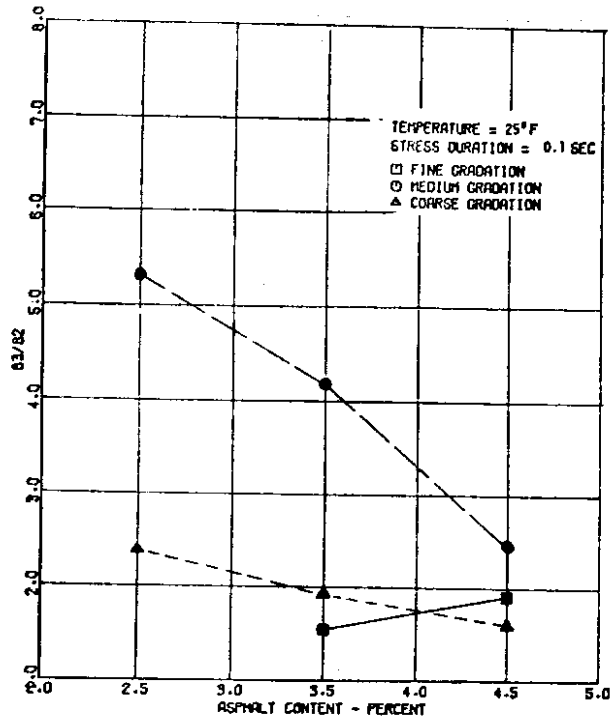


FIGURE 37 - Ratio B3/B2 Versus Asphalt Content at 25, 45, 70 and 90°F

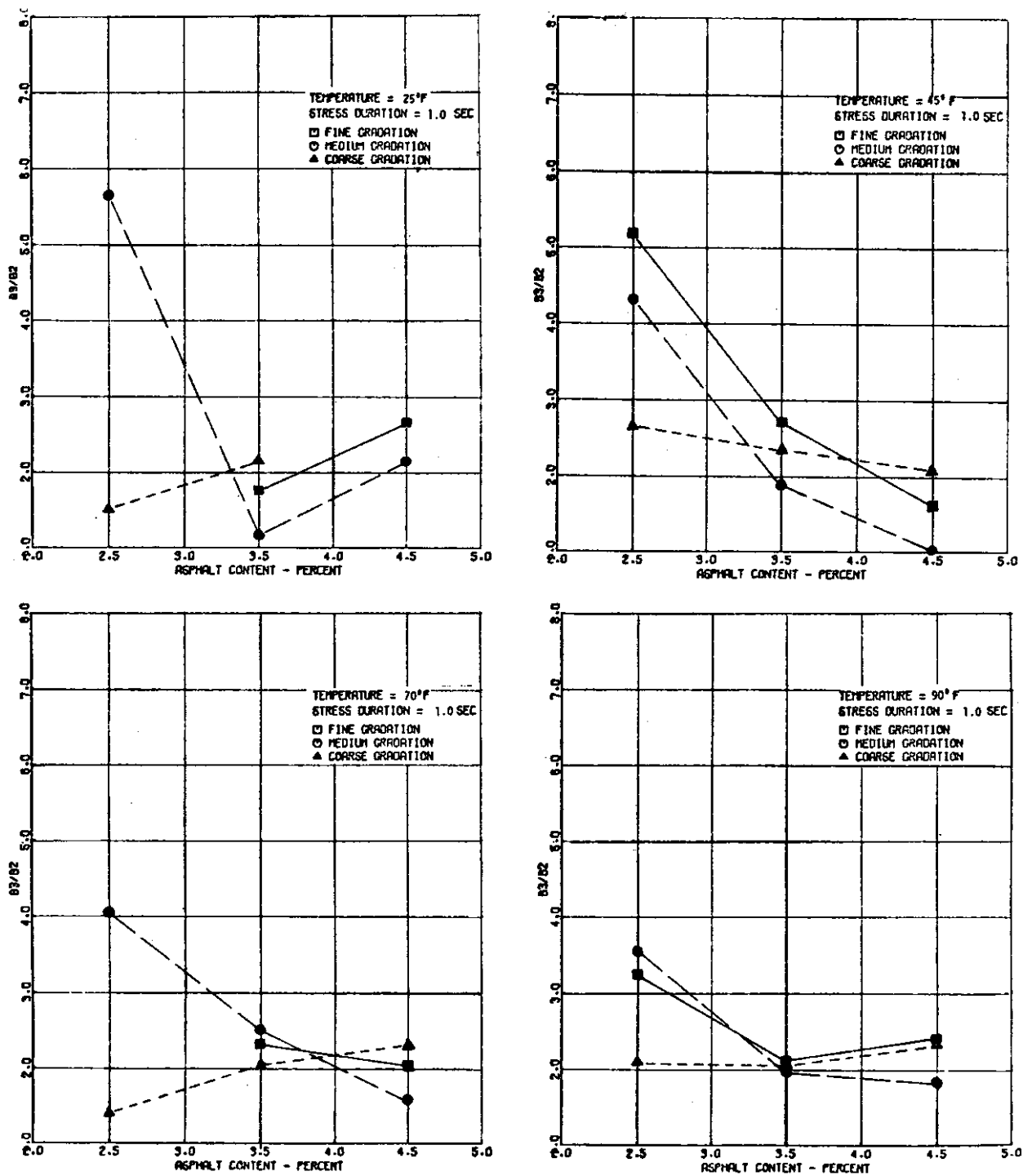


FIGURE 38 - Ratio B3/B2 Versus Asphalt Content at 25, 45, 70 and 90°F

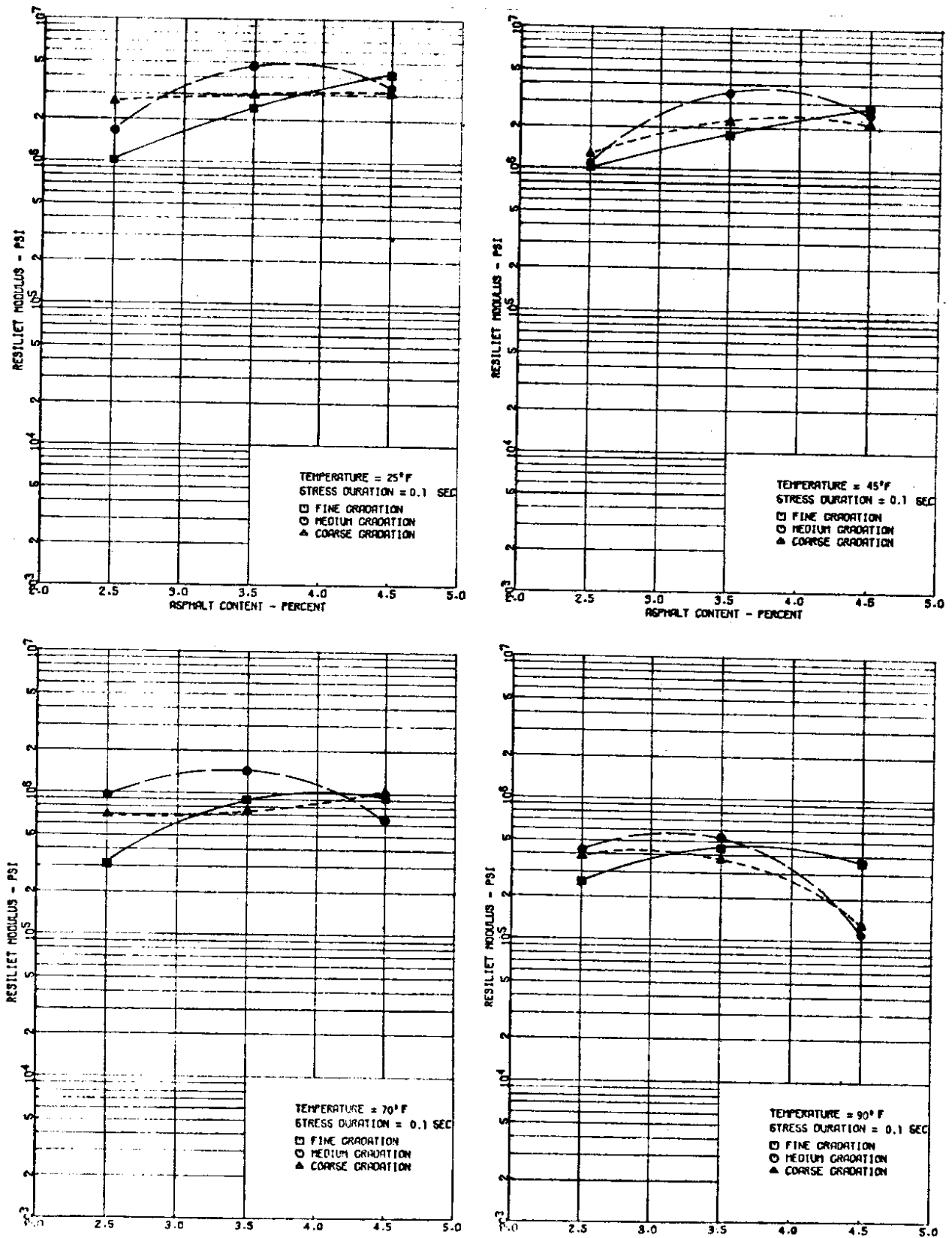


FIGURE 39 - Resilient Modulus Versus Asphalt Content at 25, 45, 70 and 90°F

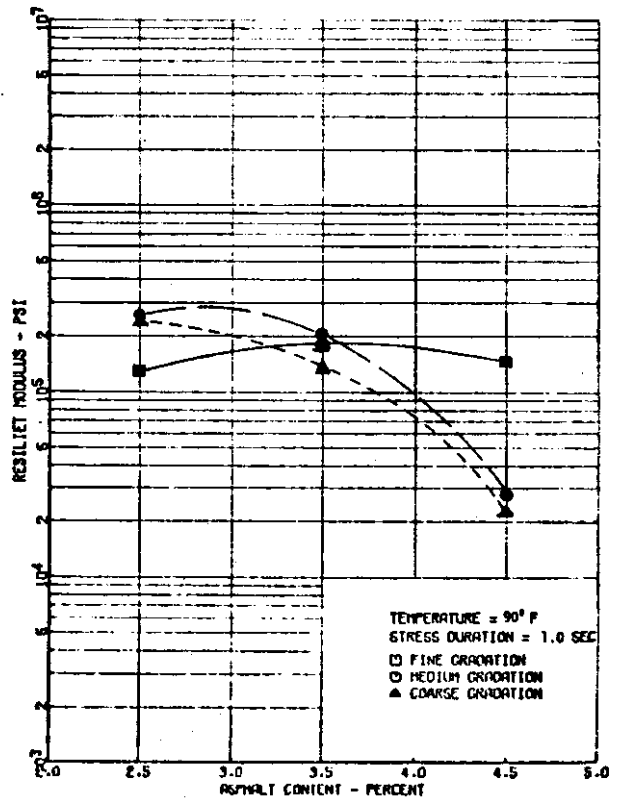
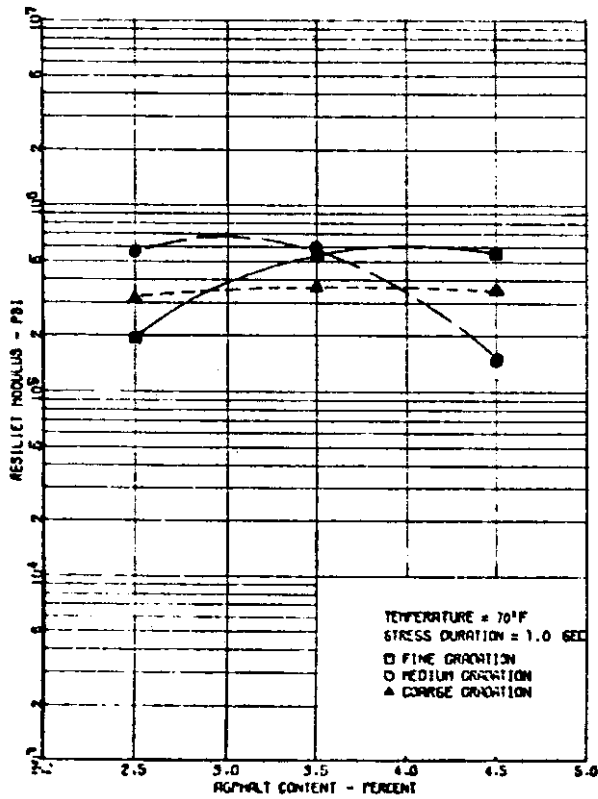
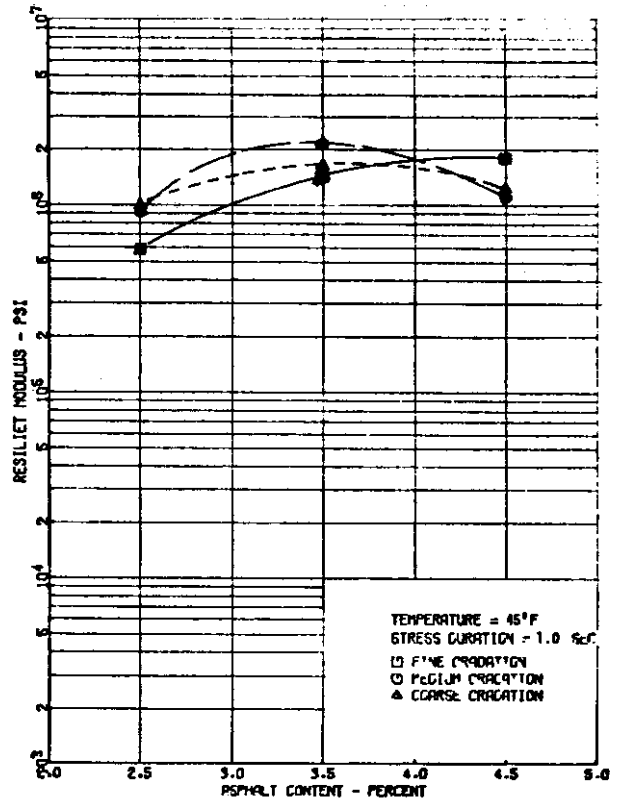
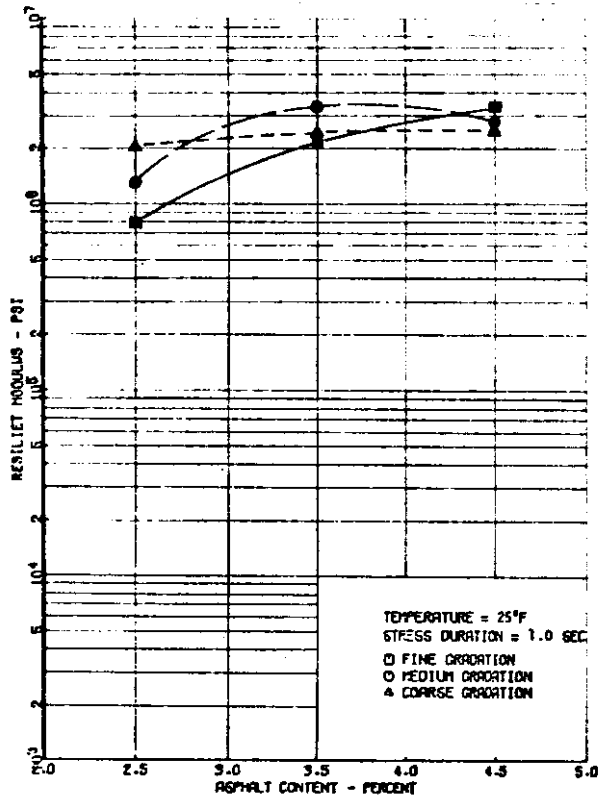


FIGURE 40 - Resilient Modulus Versus Asphalt Content at 25, 45, 70 and 90°F

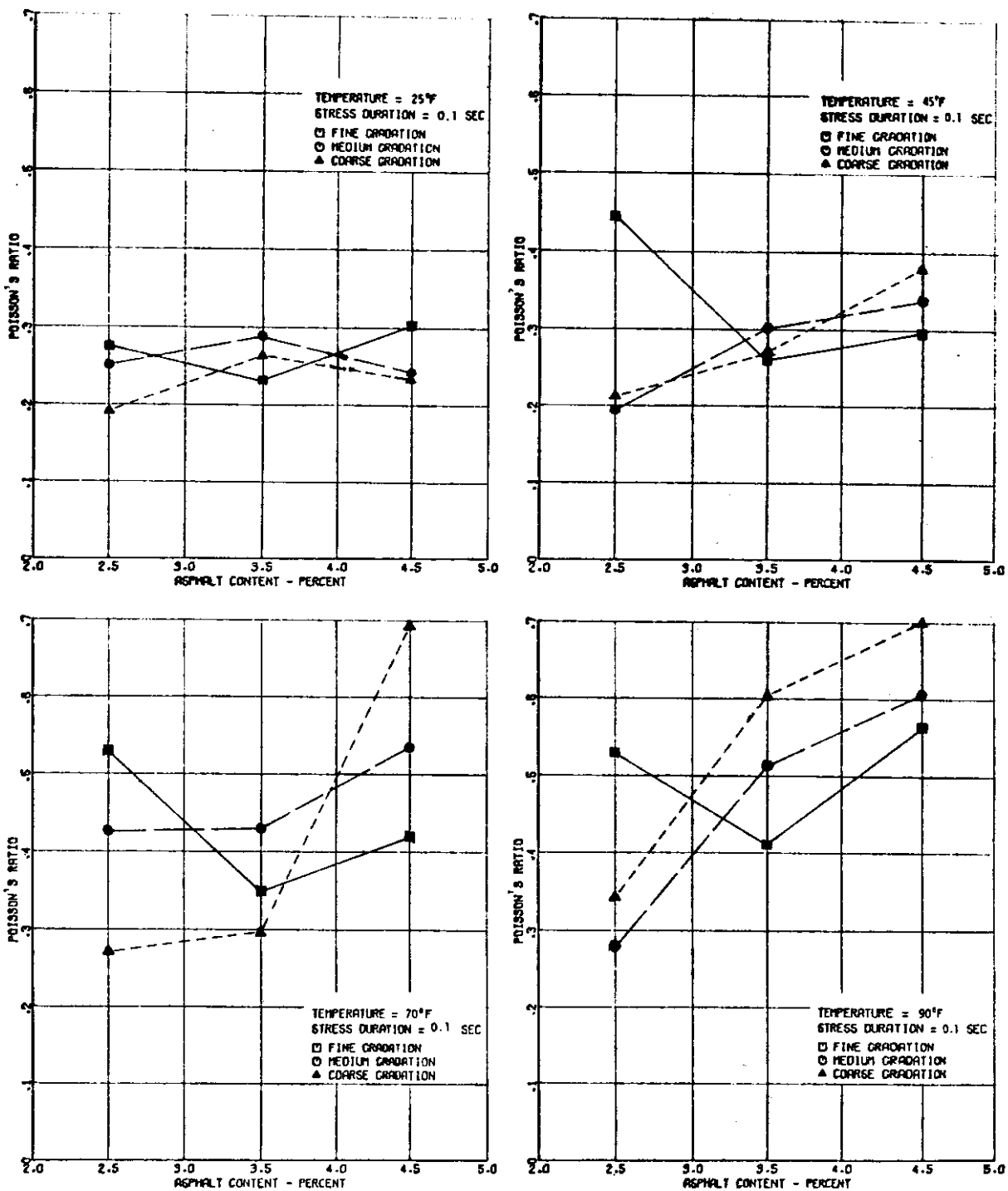


FIGURE 41 - Poisson's Ratio Versus Asphalt Content at 25, 45, 70 and 90°F

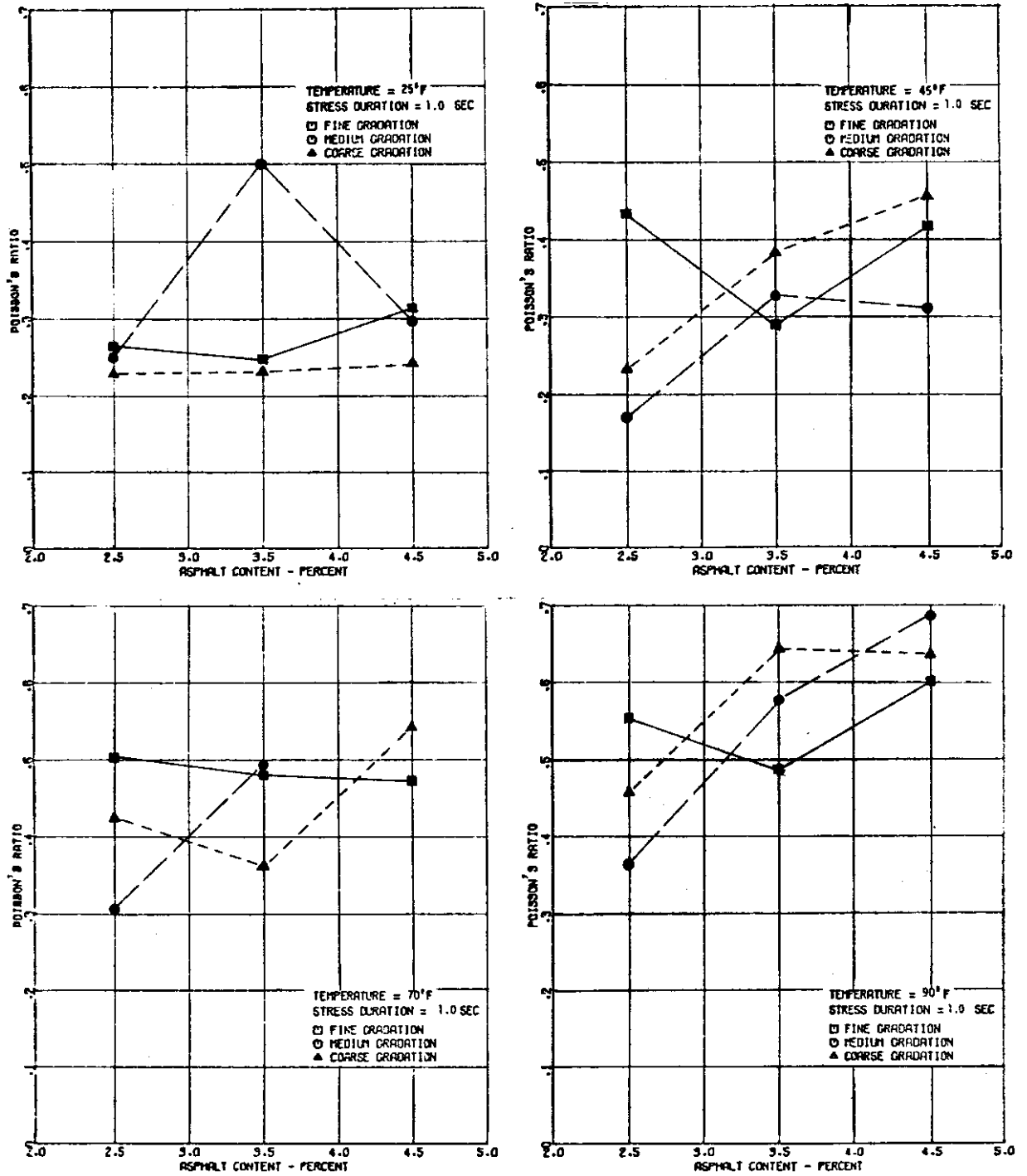


FIGURE 42 - Poisson's Ratio Versus Asphalt Content at 25, 45, 70 and 90°F

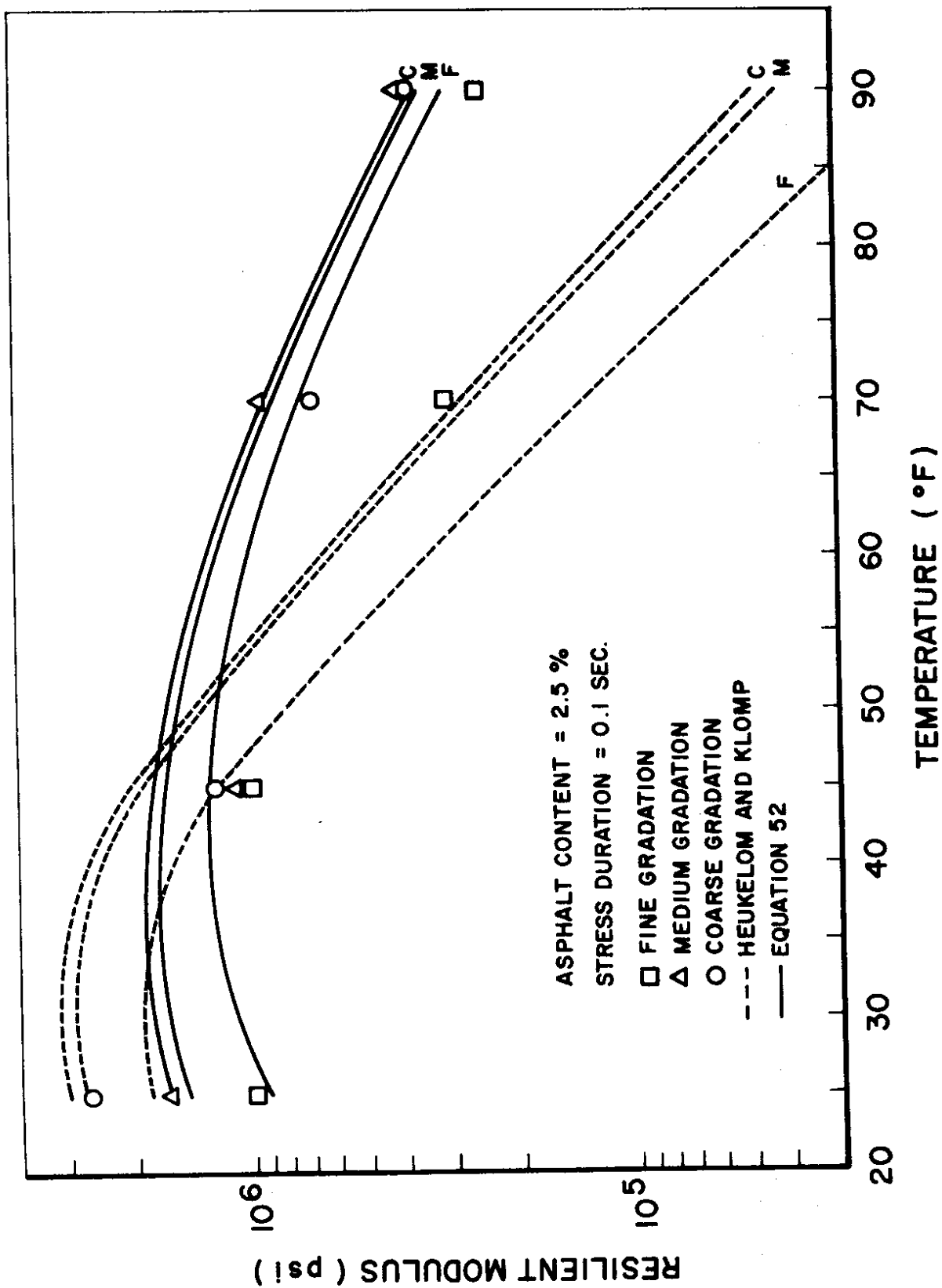


FIGURE 43 - Resilient Modulus Computed from Test Data, Equation 52, and Heukelom and Klomp

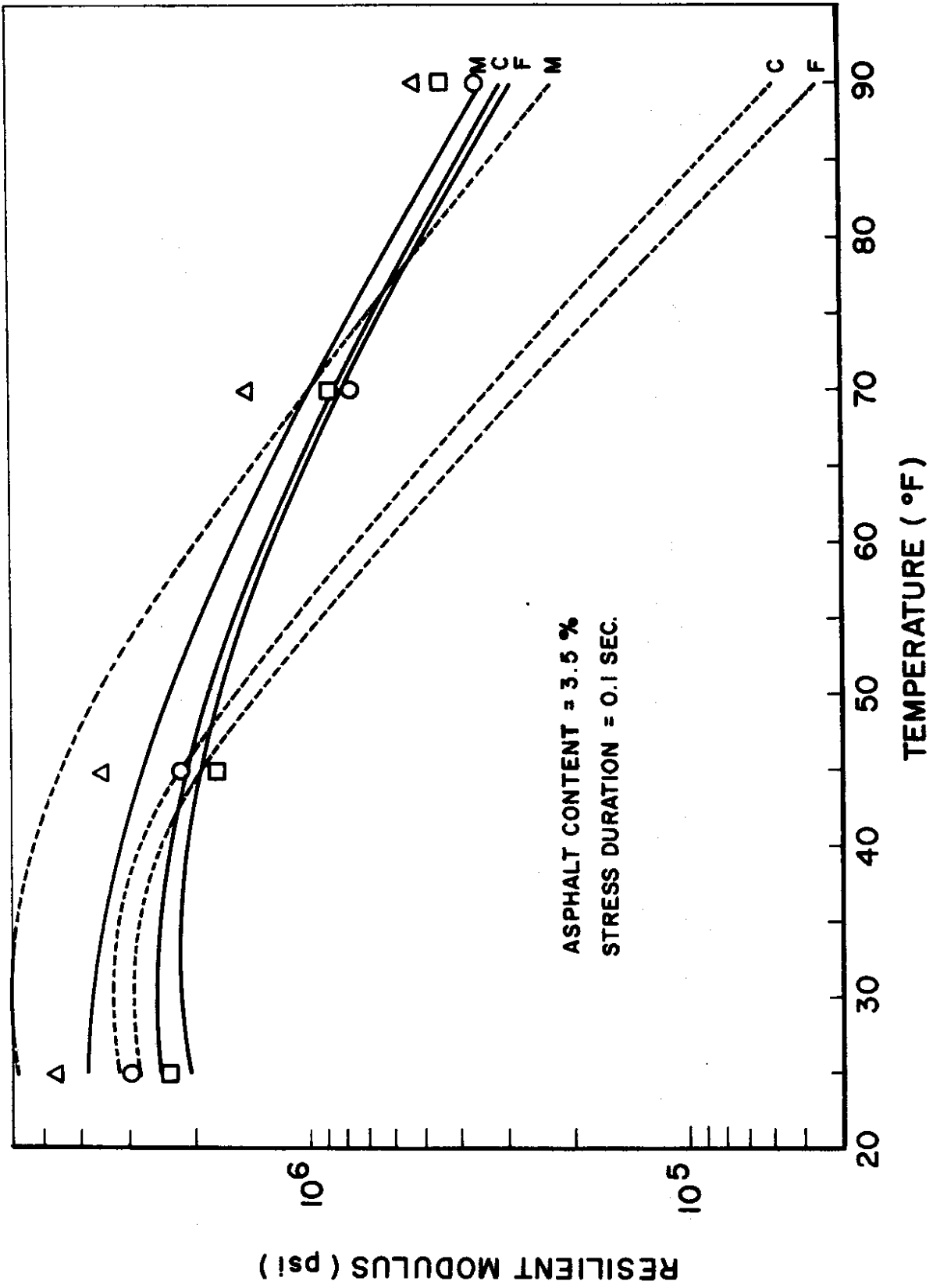


FIGURE 44 - Resilient Modulus Computed from Test Data, Equation 52, and Heukelom and Klomp

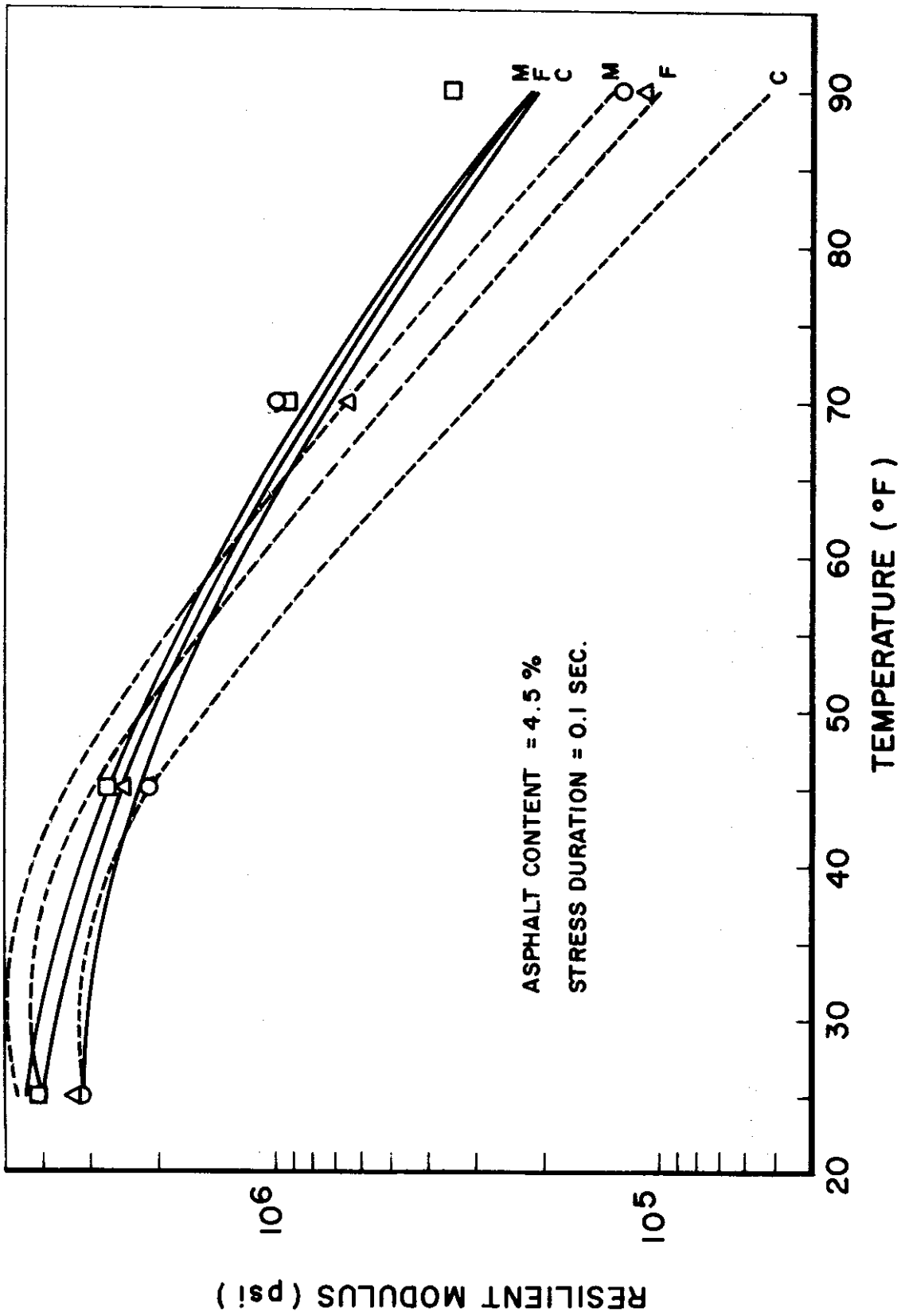


FIGURE 45 - Resilient Modulus Computed from Test Data, Equation 52, and Heukelom and Klomp

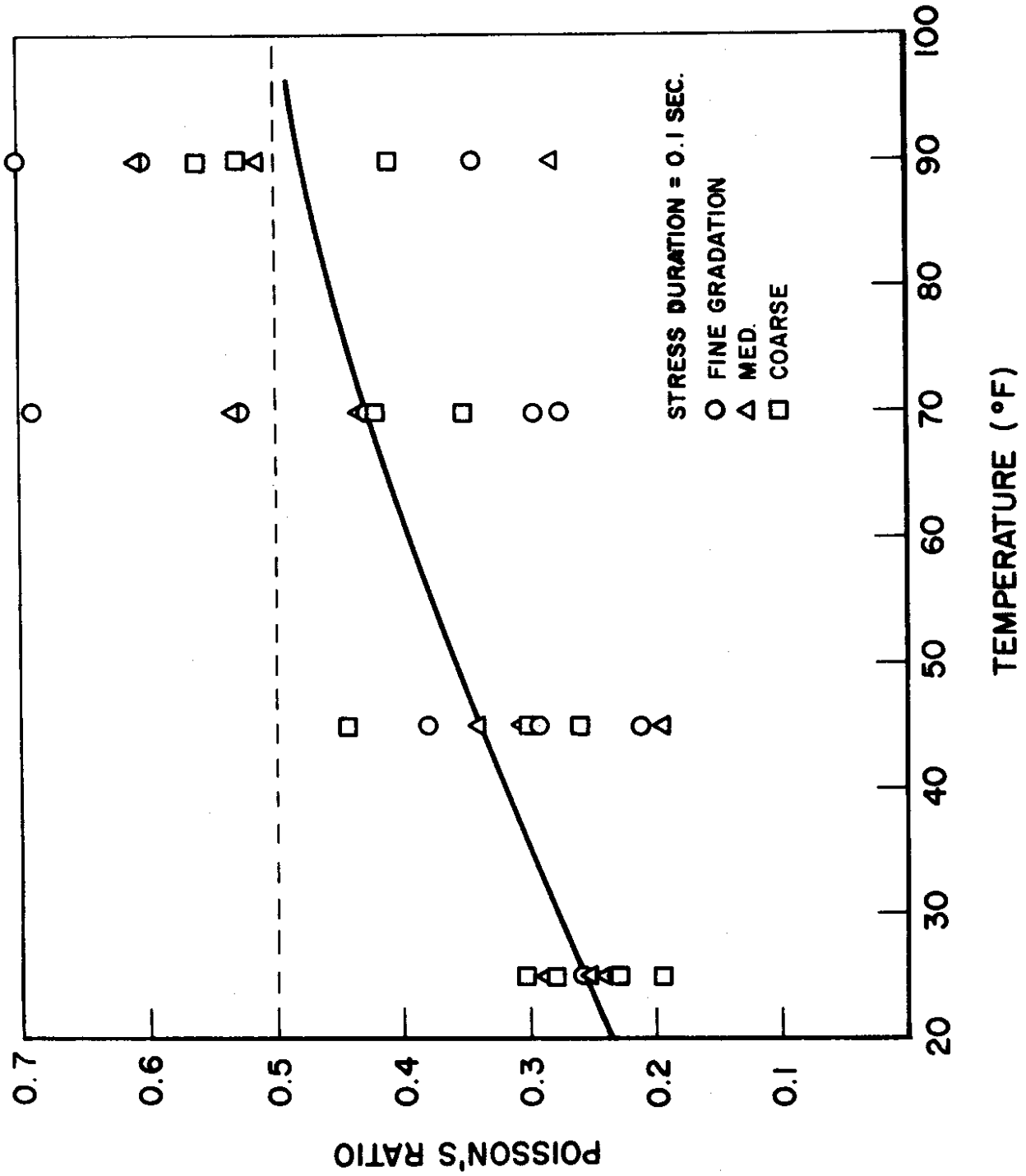


FIGURE 46 - Variation of Poisson's Ratio of Different Mixtures with Temperature

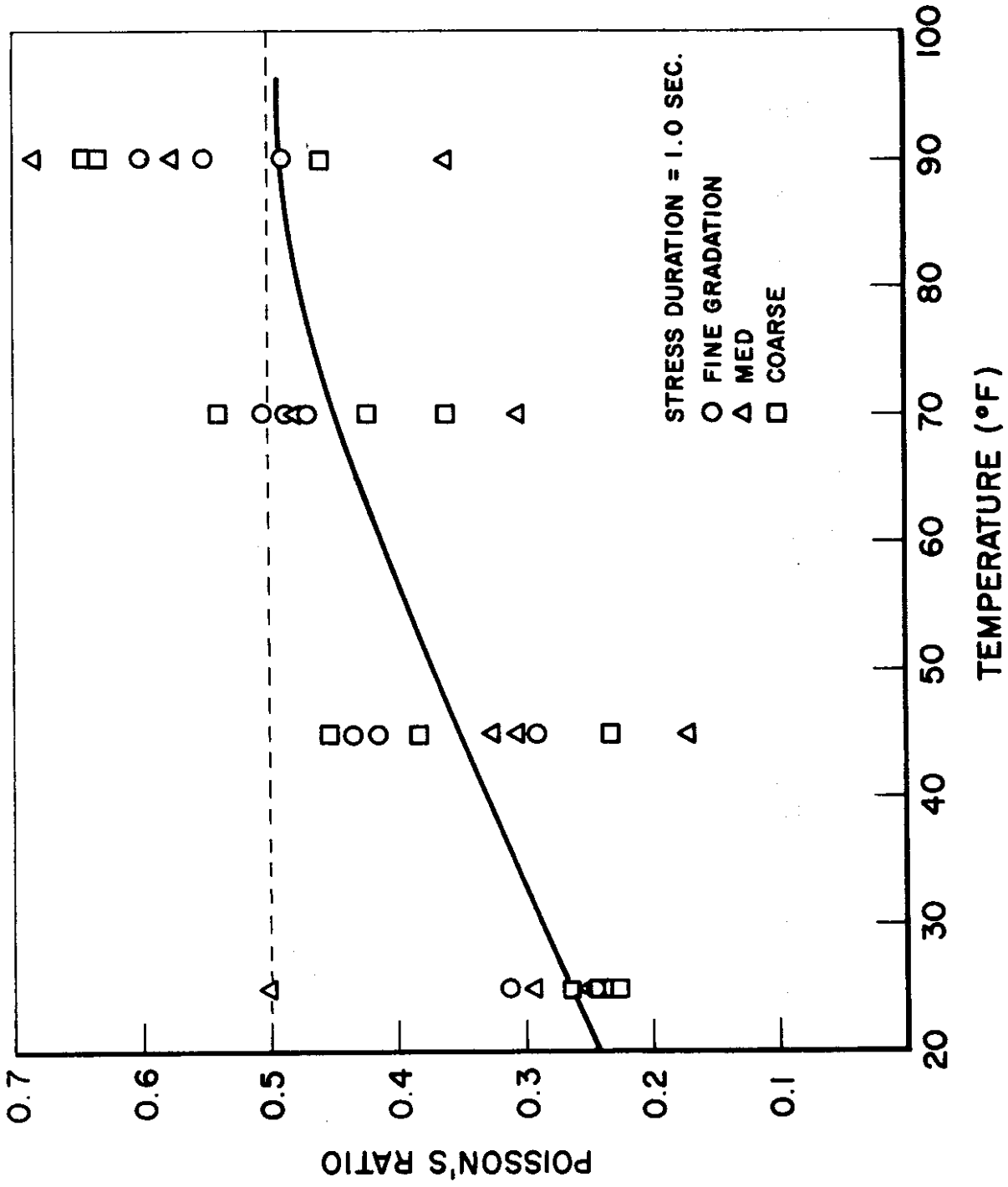


FIGURE 47 - Variation of Poisson's Ratio of Different Mixtures with Temperature

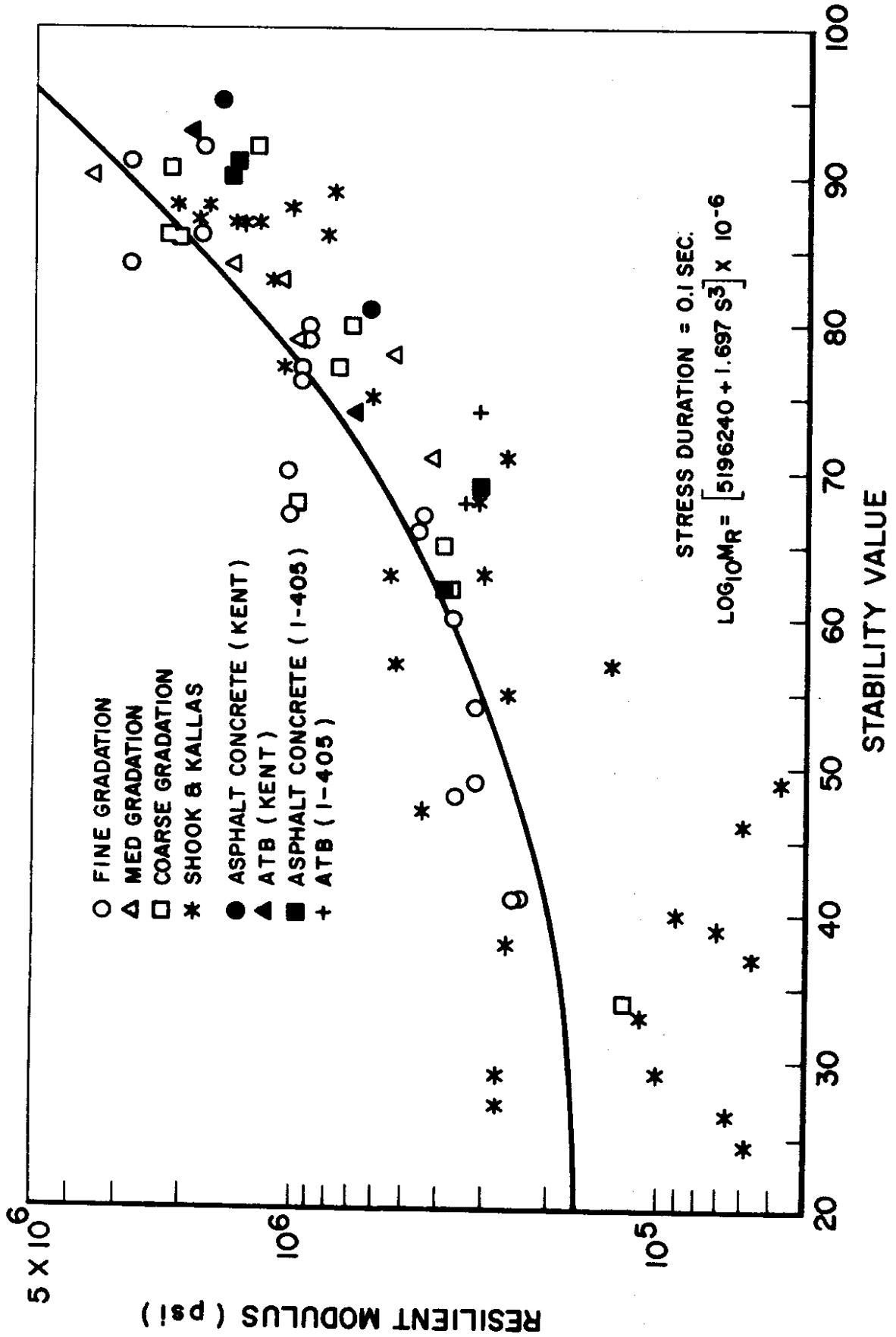


FIGURE 48 - Correlation Between the Stability Value and the Resilient Modulus

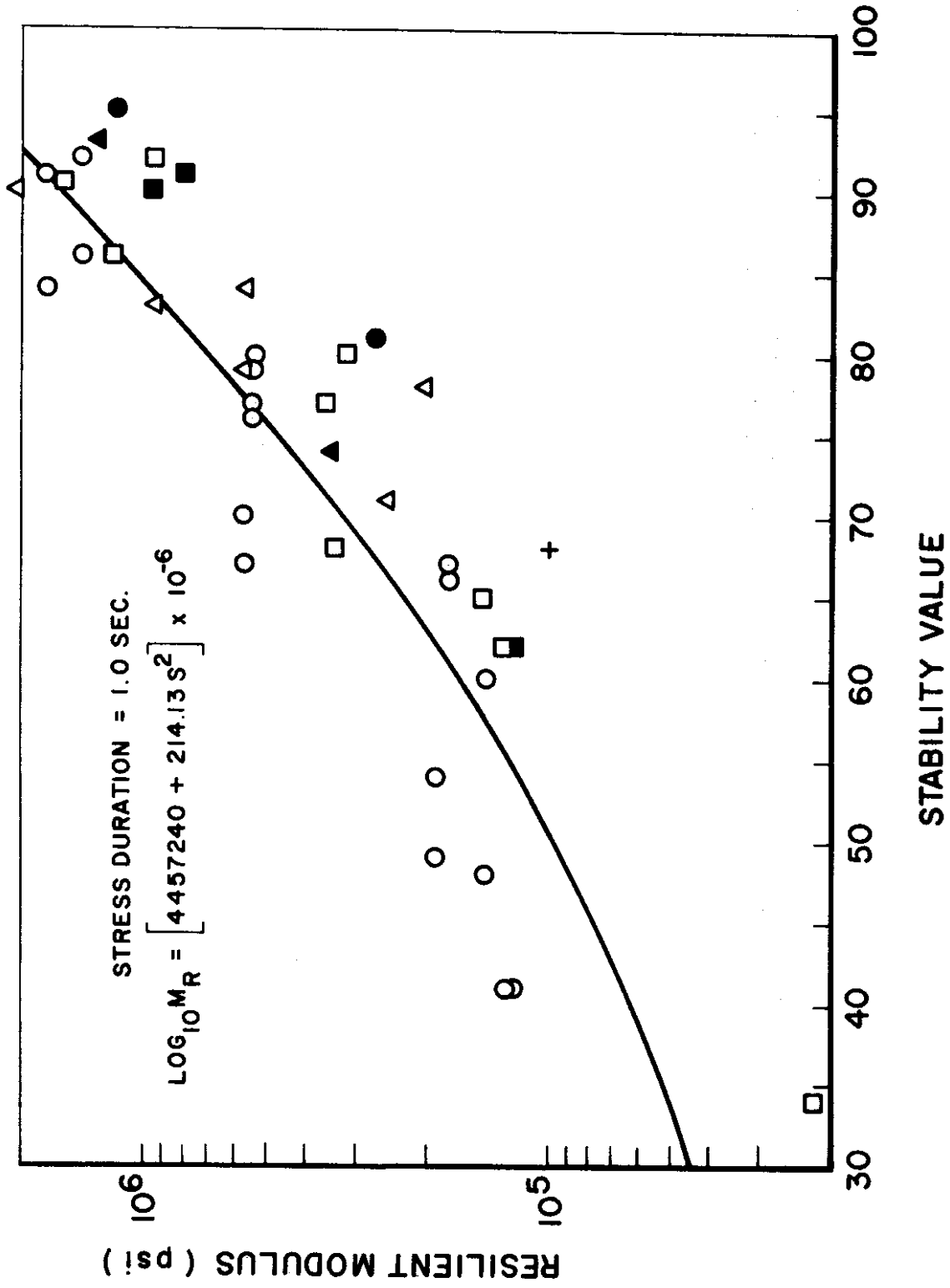


FIGURE 49 - Correlation Between the Stability Value and the Resilient Modulus

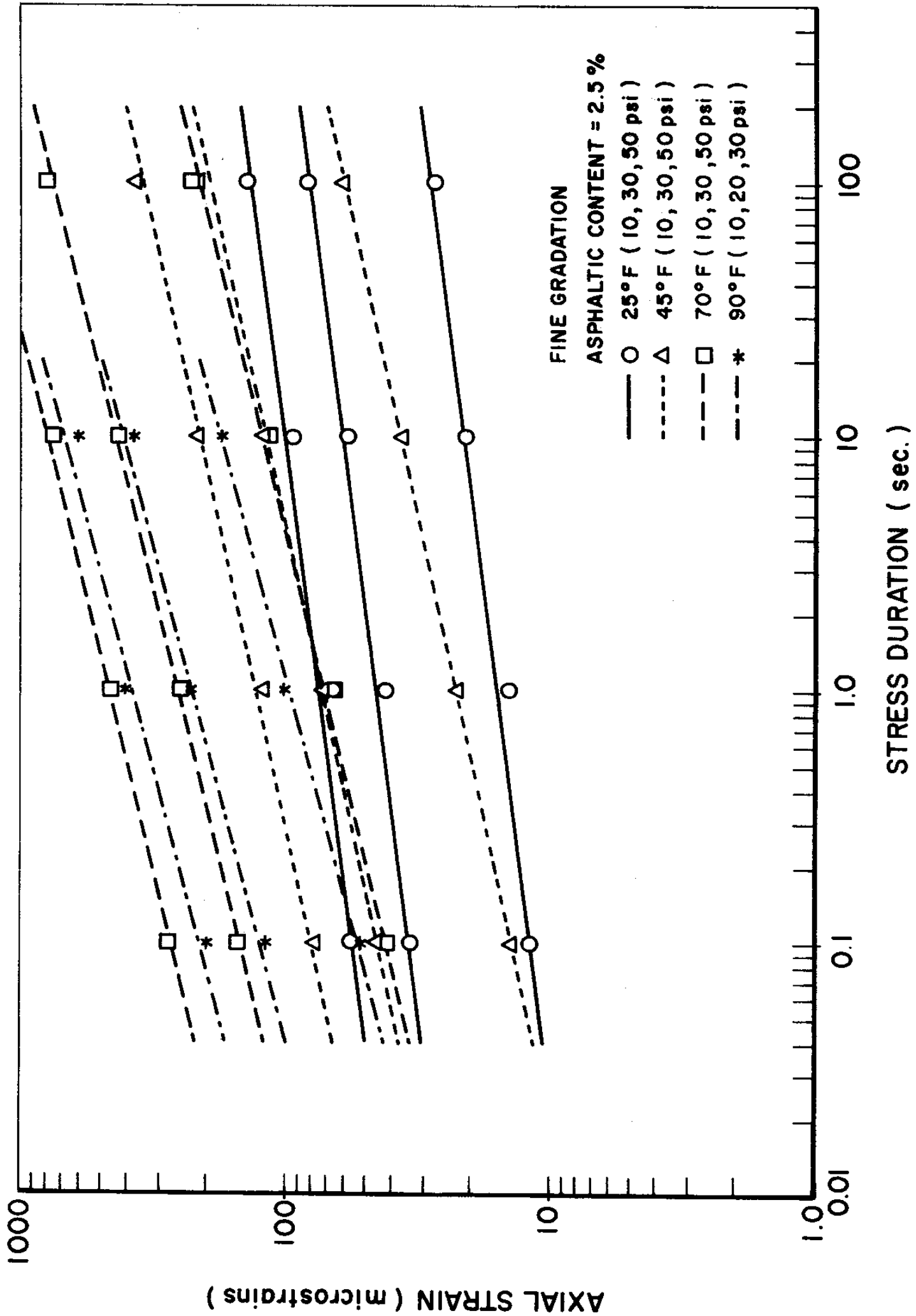


FIGURE 50 - Log Axial Strain Versus Log Stress Duration at Different Temperatures

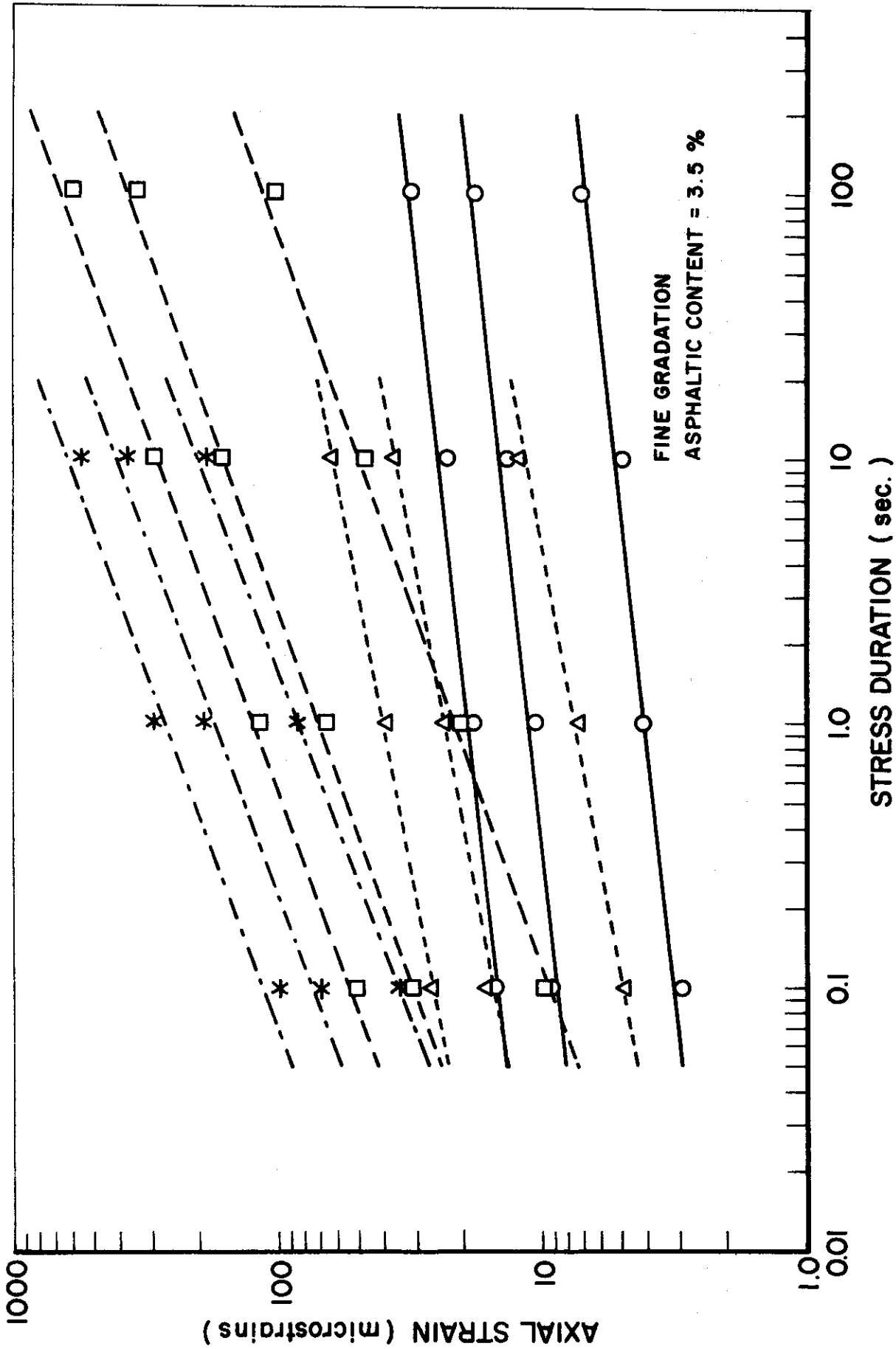


FIGURE 51 - Log Axial Strain Versus Log Stress Duration at Different Temperatures

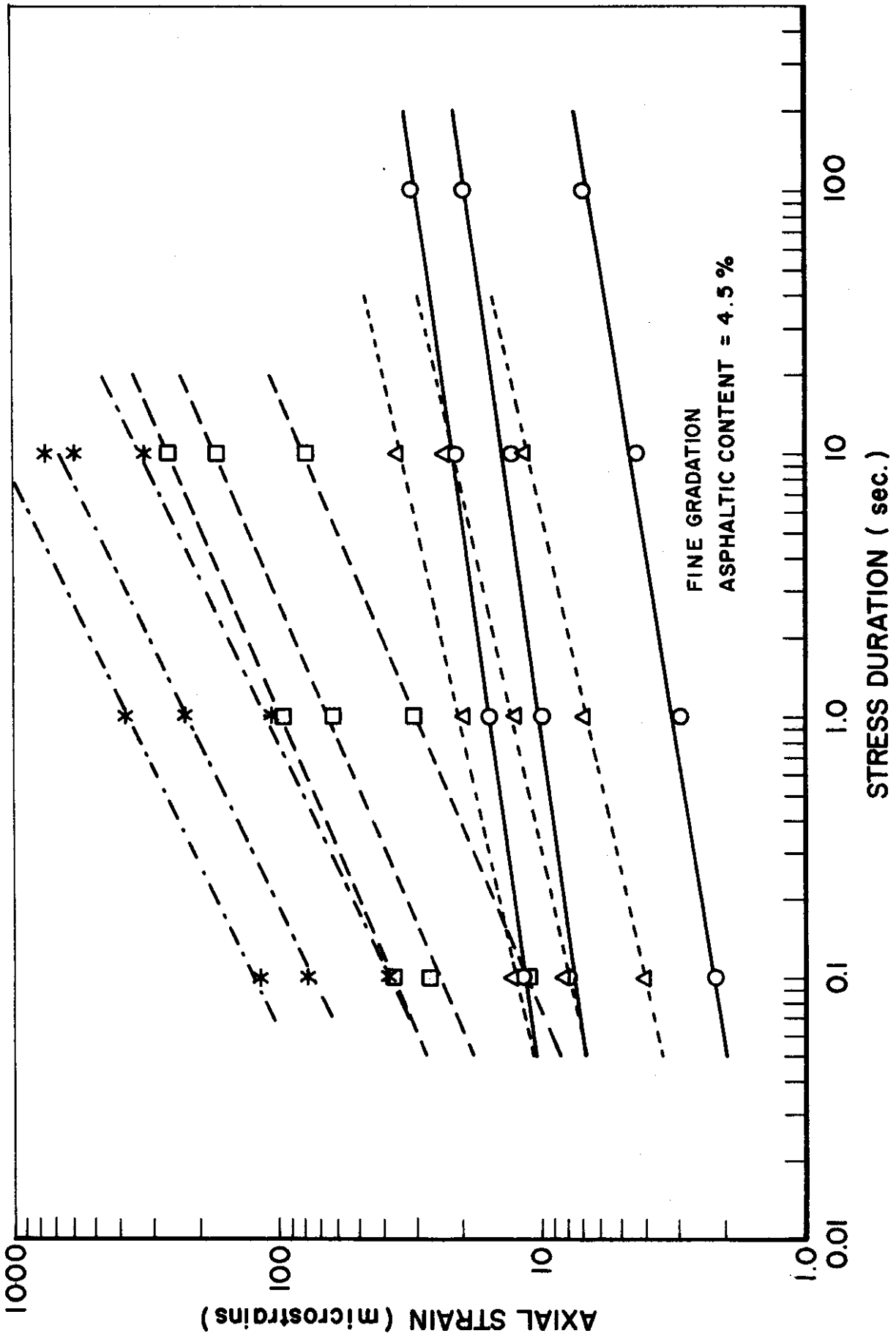


FIGURE 52 - Log Axial Strain Versus Log Stress Duration at Different Temperatures

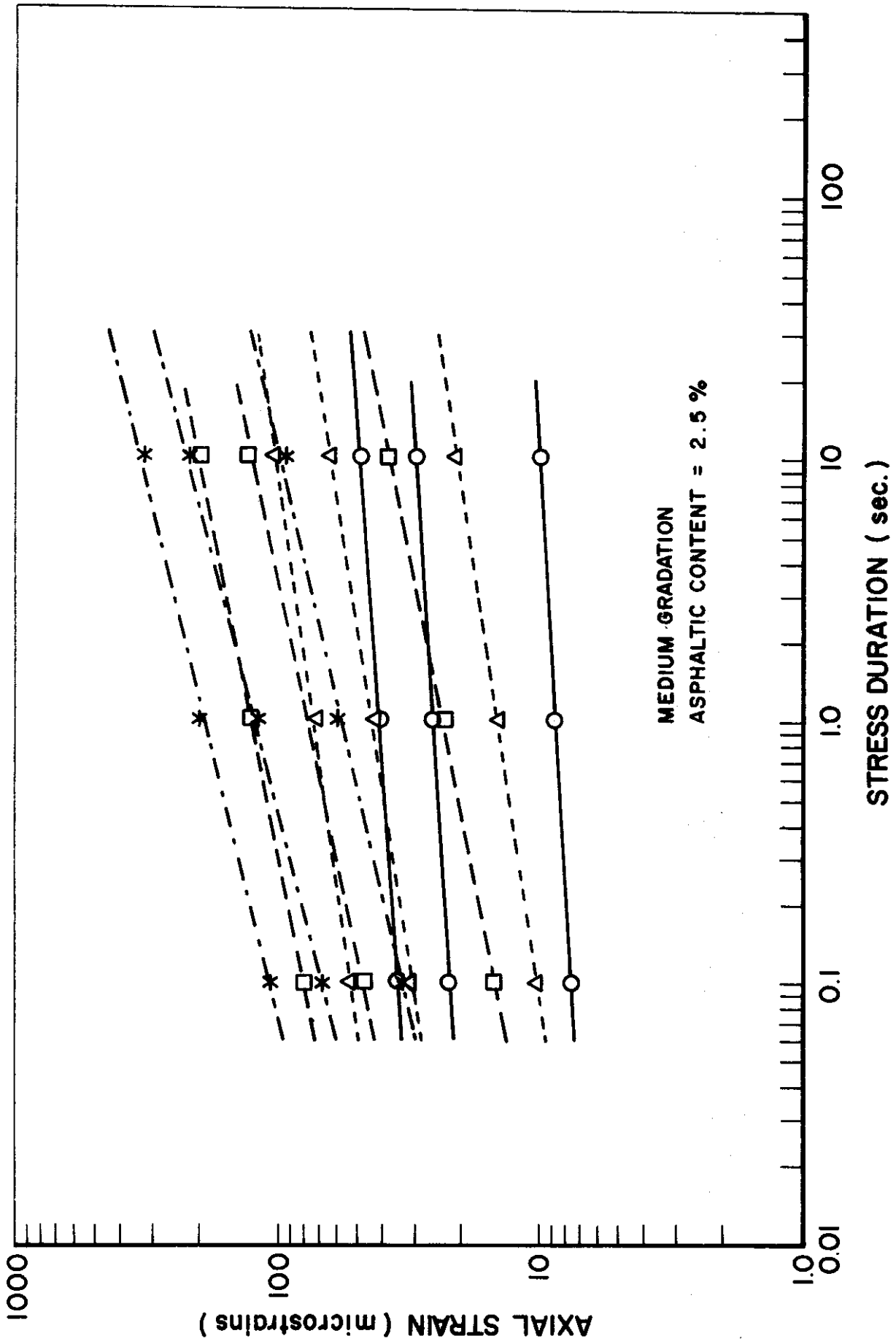


FIGURE 53 - Log Axial Strain Versus Log Stress Duration at Different Temperatures

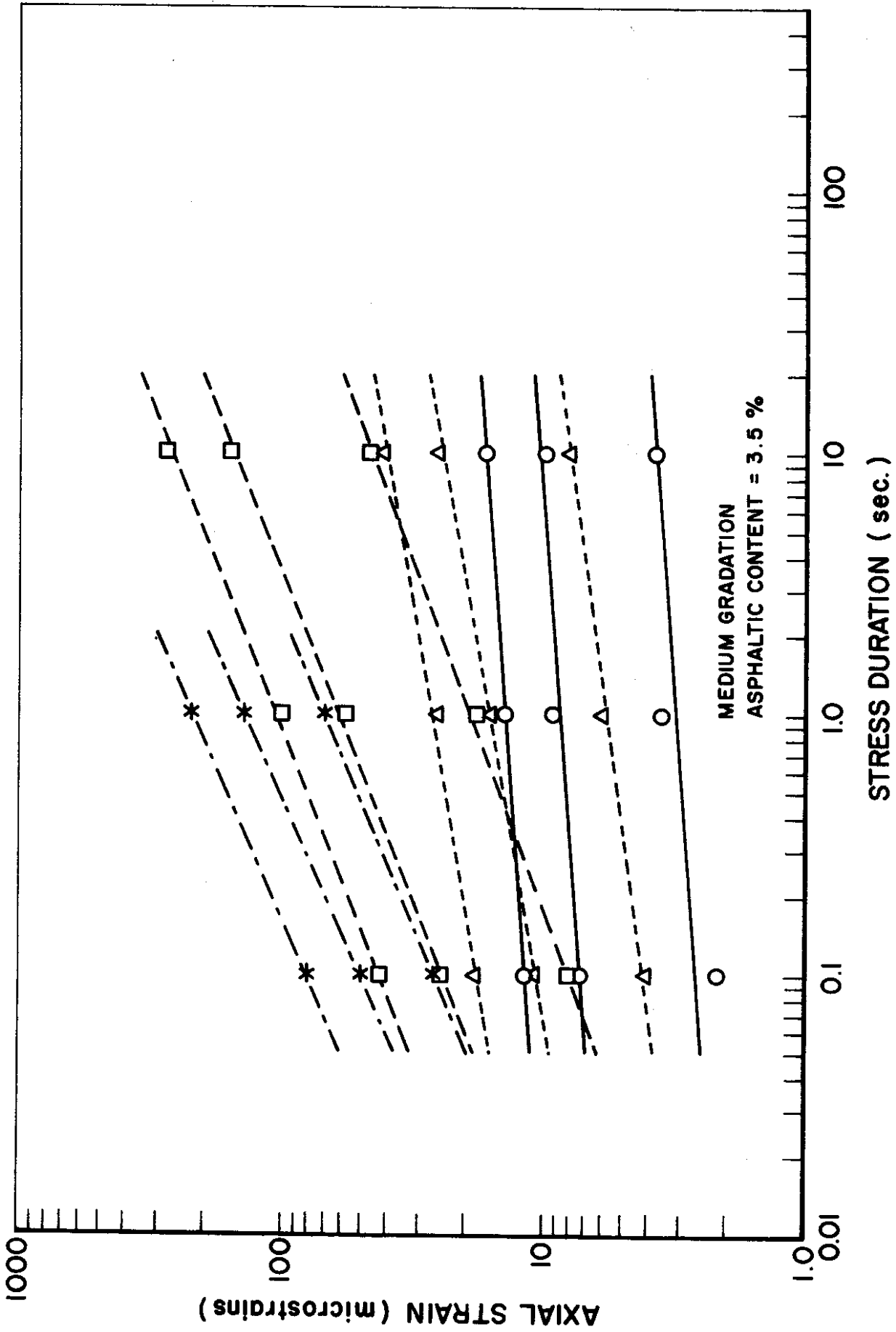


FIGURE 54 - Log Axial Strain Versus Log Stress Duration at Different Temperatures

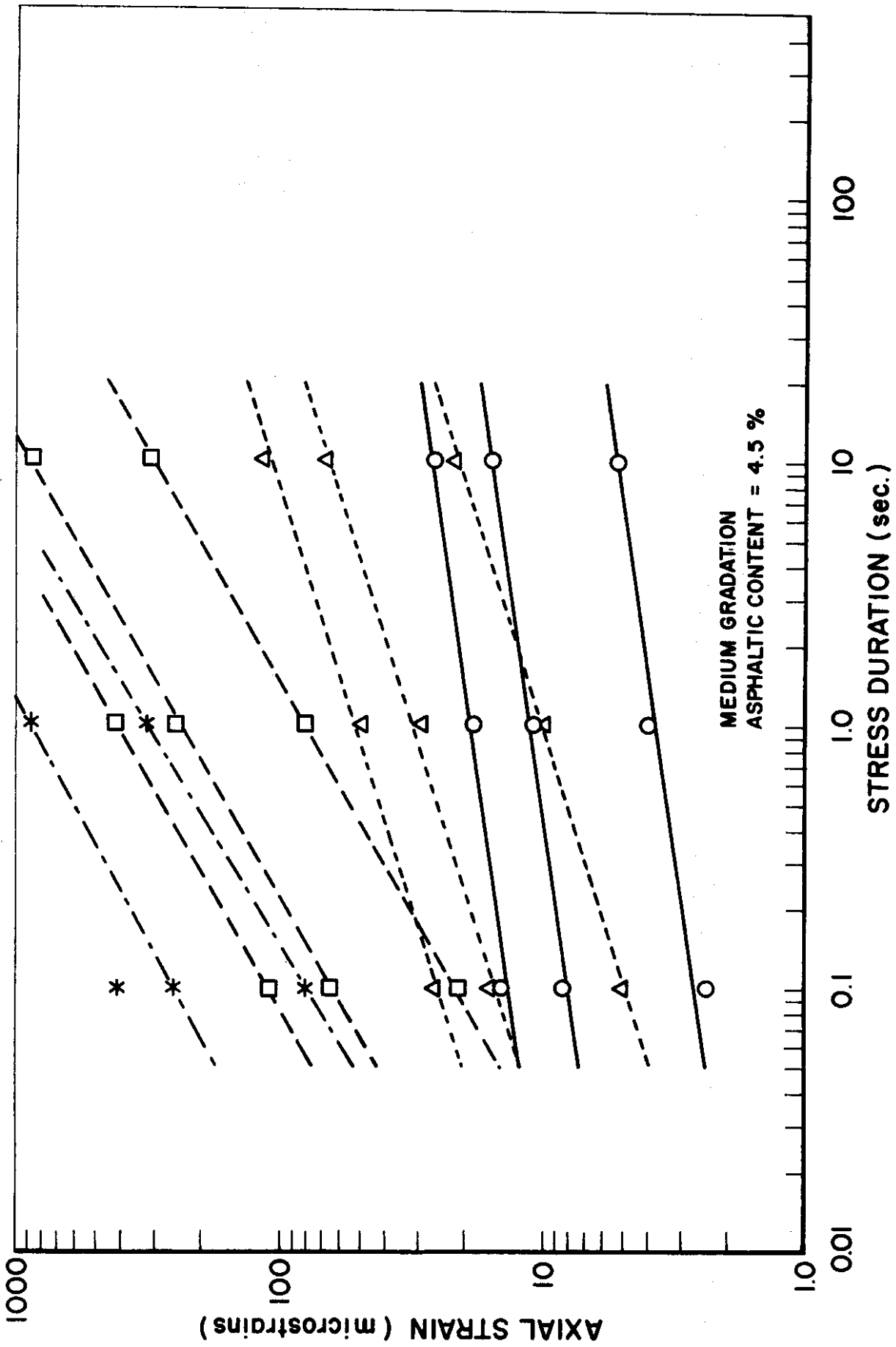


FIGURE 55 - Log Axial Strain Versus Log Stress Duration at Different Temperatures

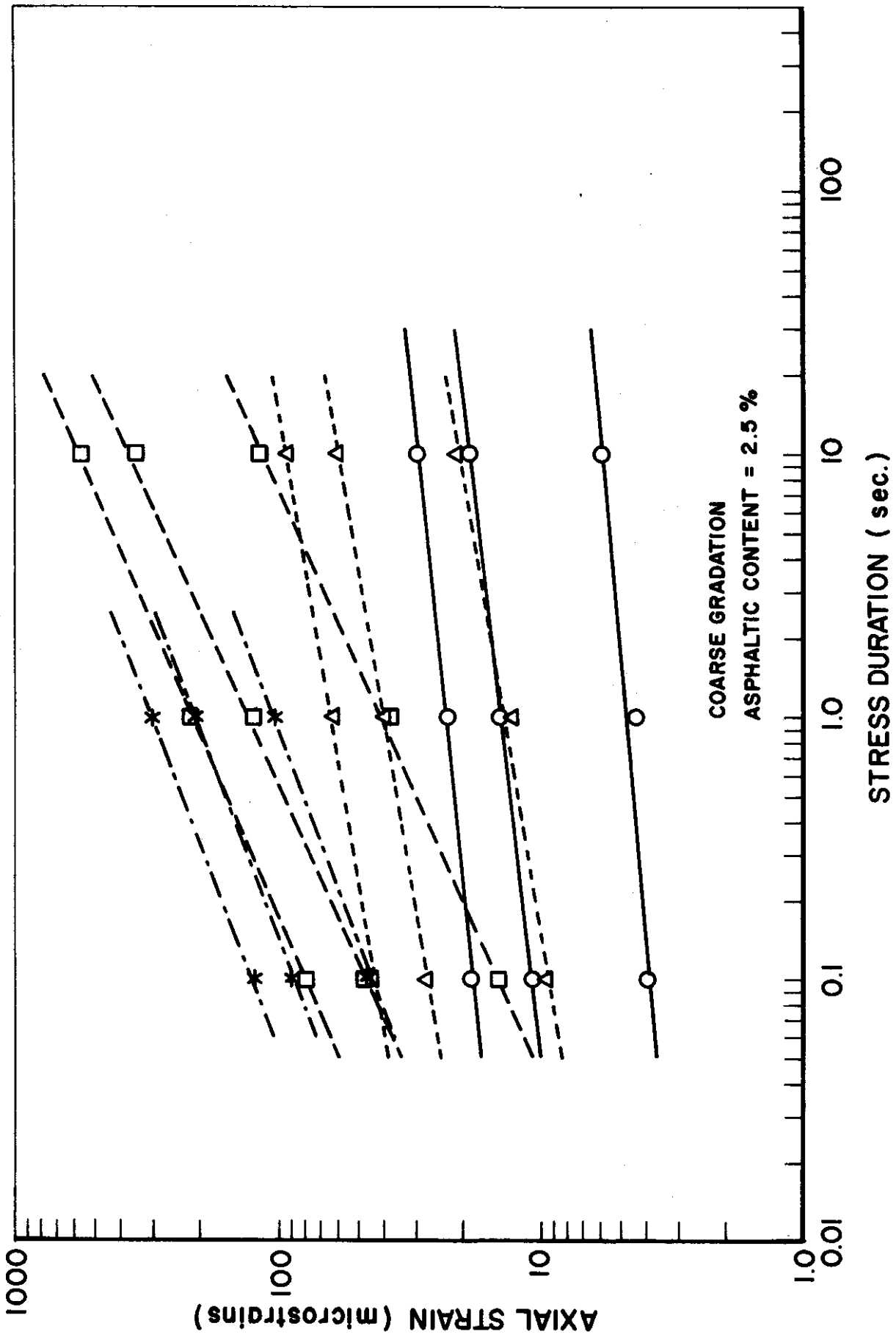


FIGURE 56 - Log Axial Strain Versus Log Stress Duration at Different Temperatures

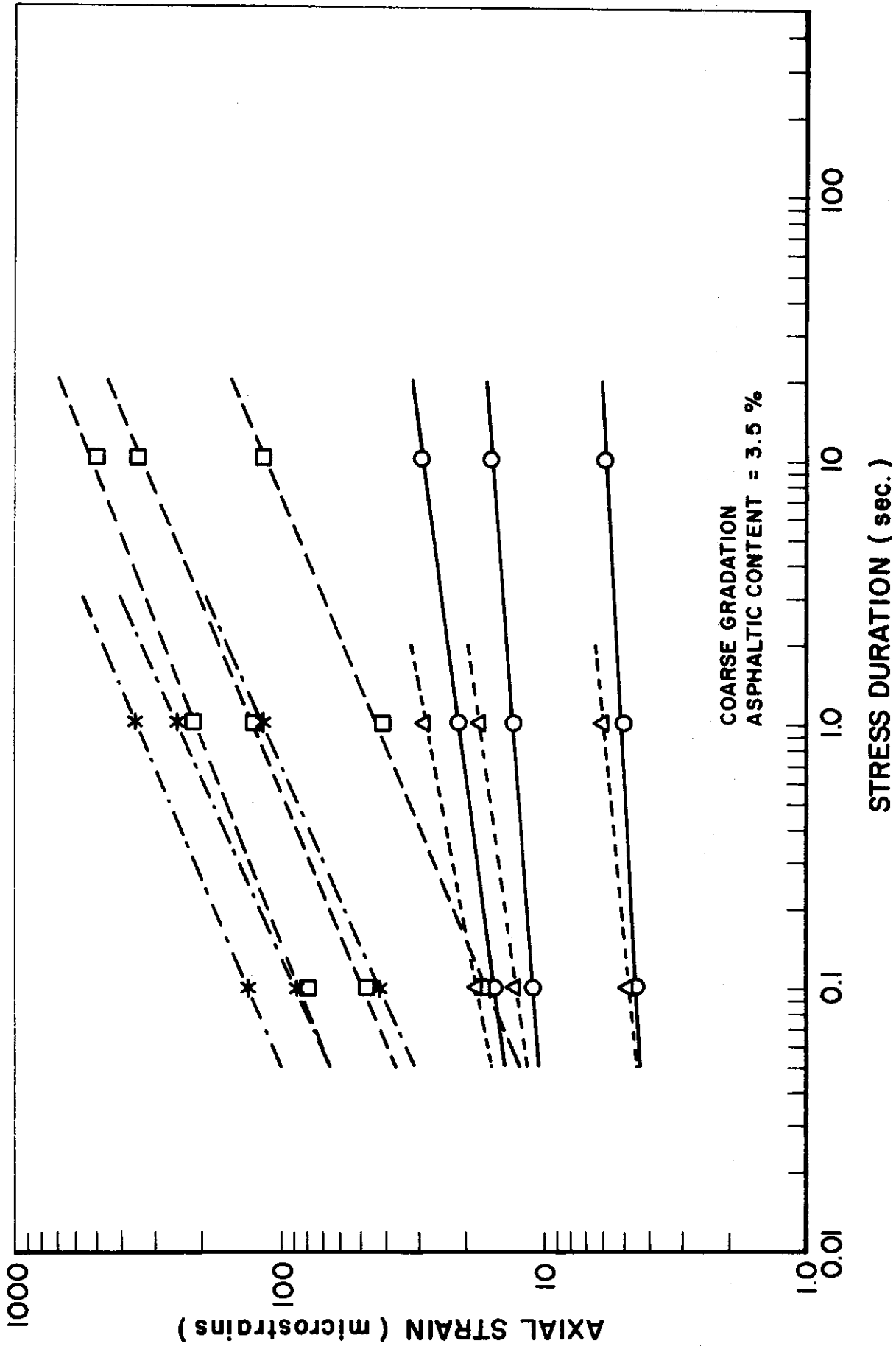


FIGURE 57 - Log Axial Strain Versus Log Stress Duration at Different Temperatures

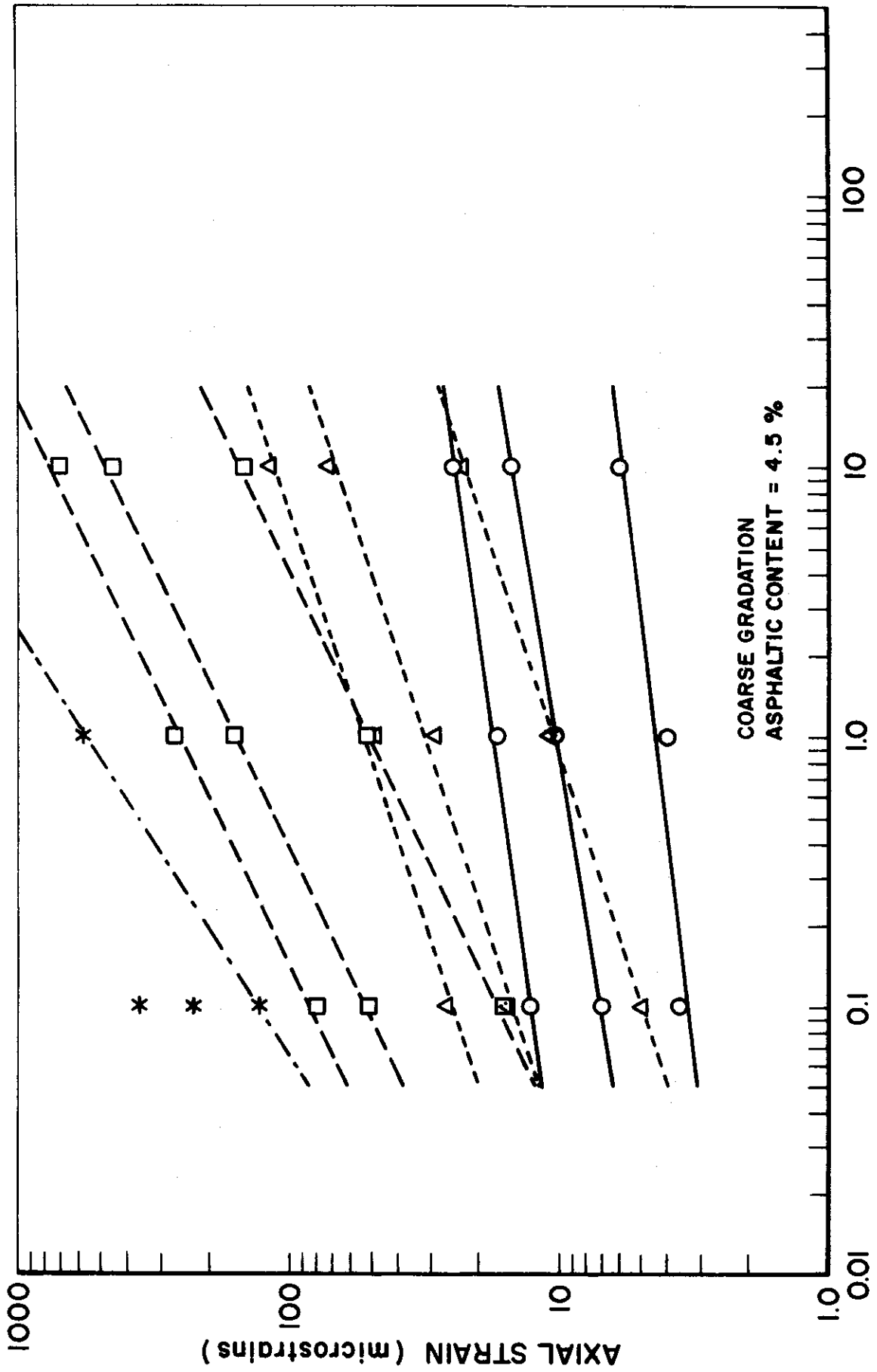


FIGURE 58 - Log Axial Strain Versus Log Stress Duration at Different Temperatures

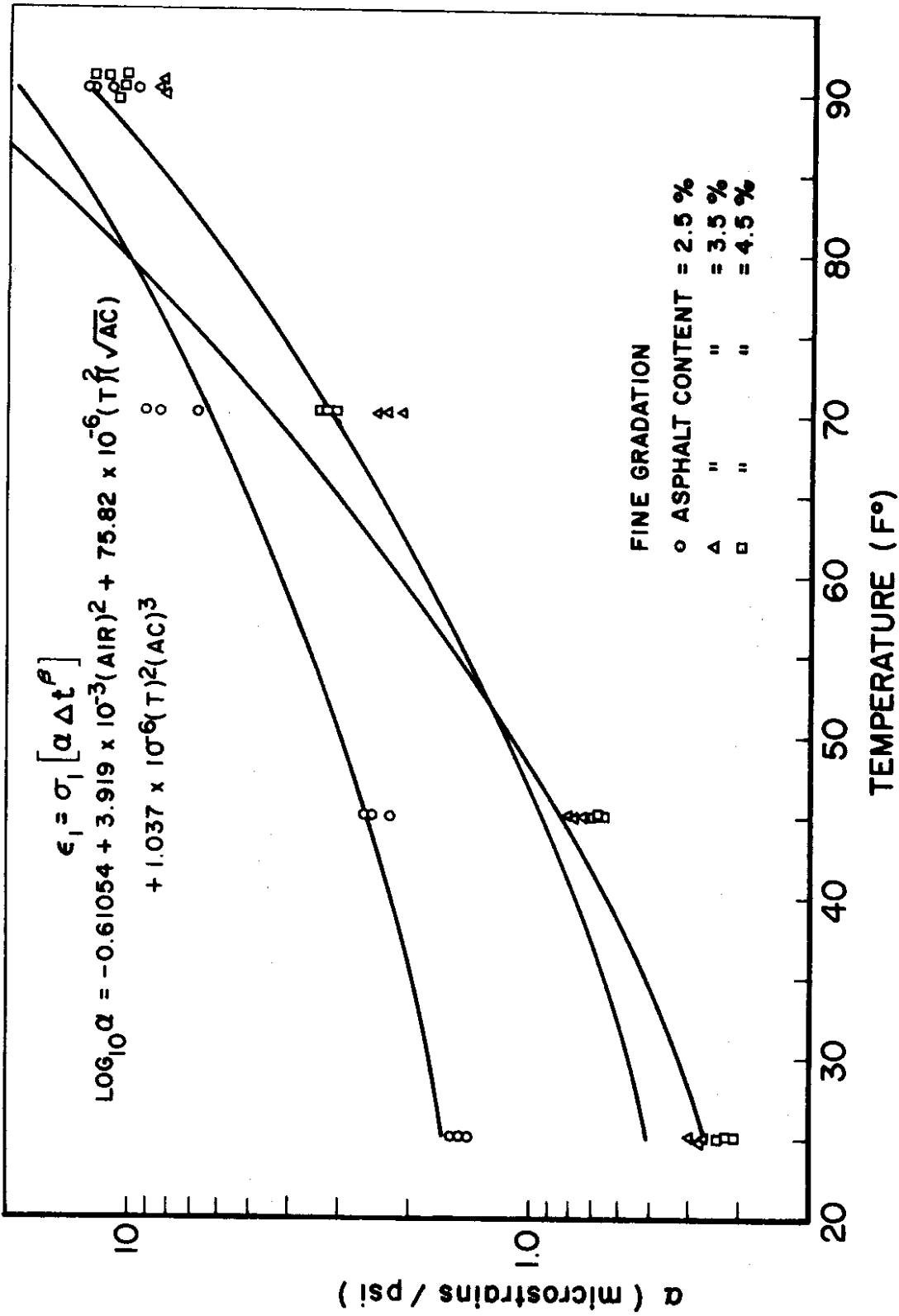


FIGURE 59 - Coefficient α Versus Temperature for Different Asphalt Contents

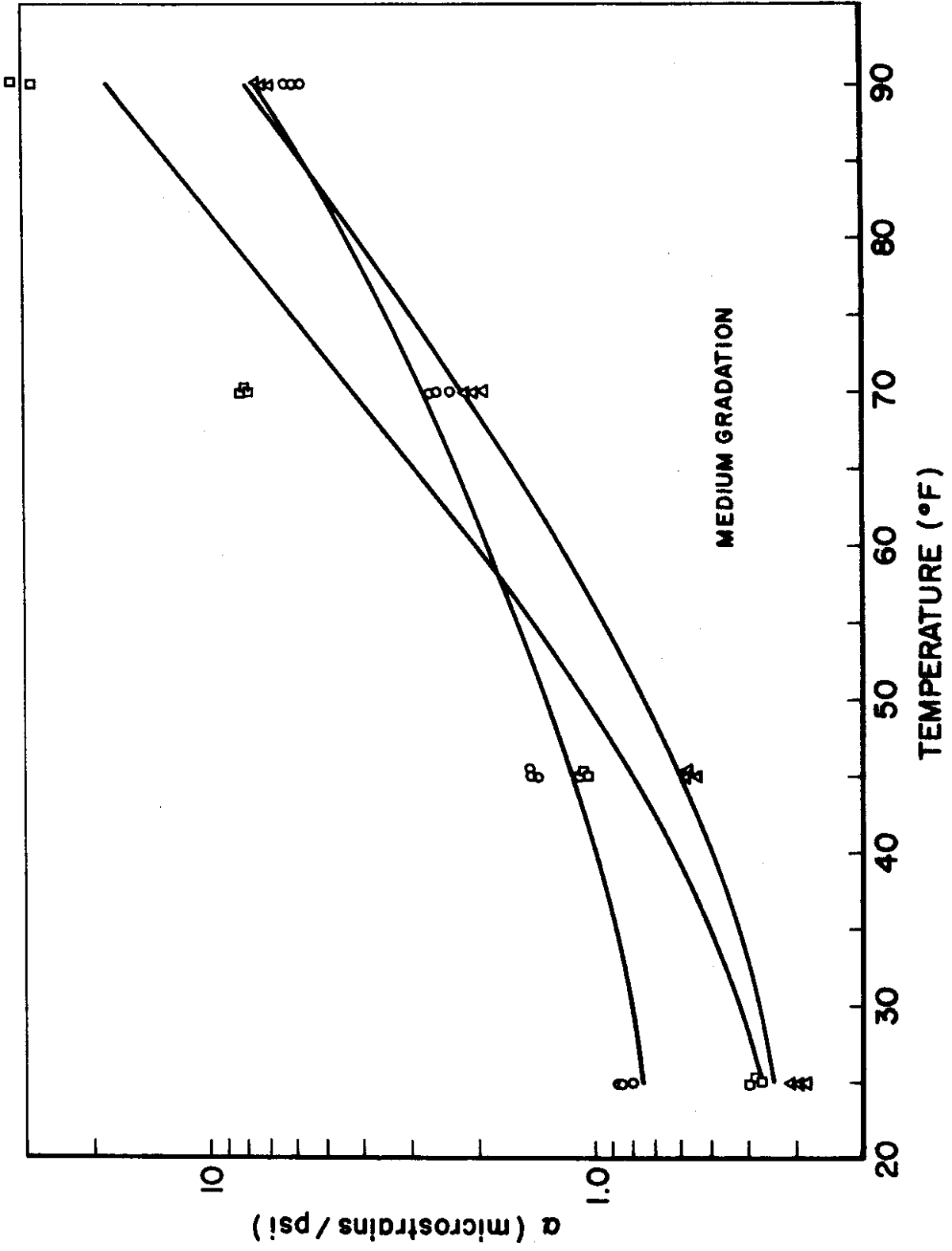


FIGURE 60 - Coefficient α Versus Temperature for Different Asphalt Contents

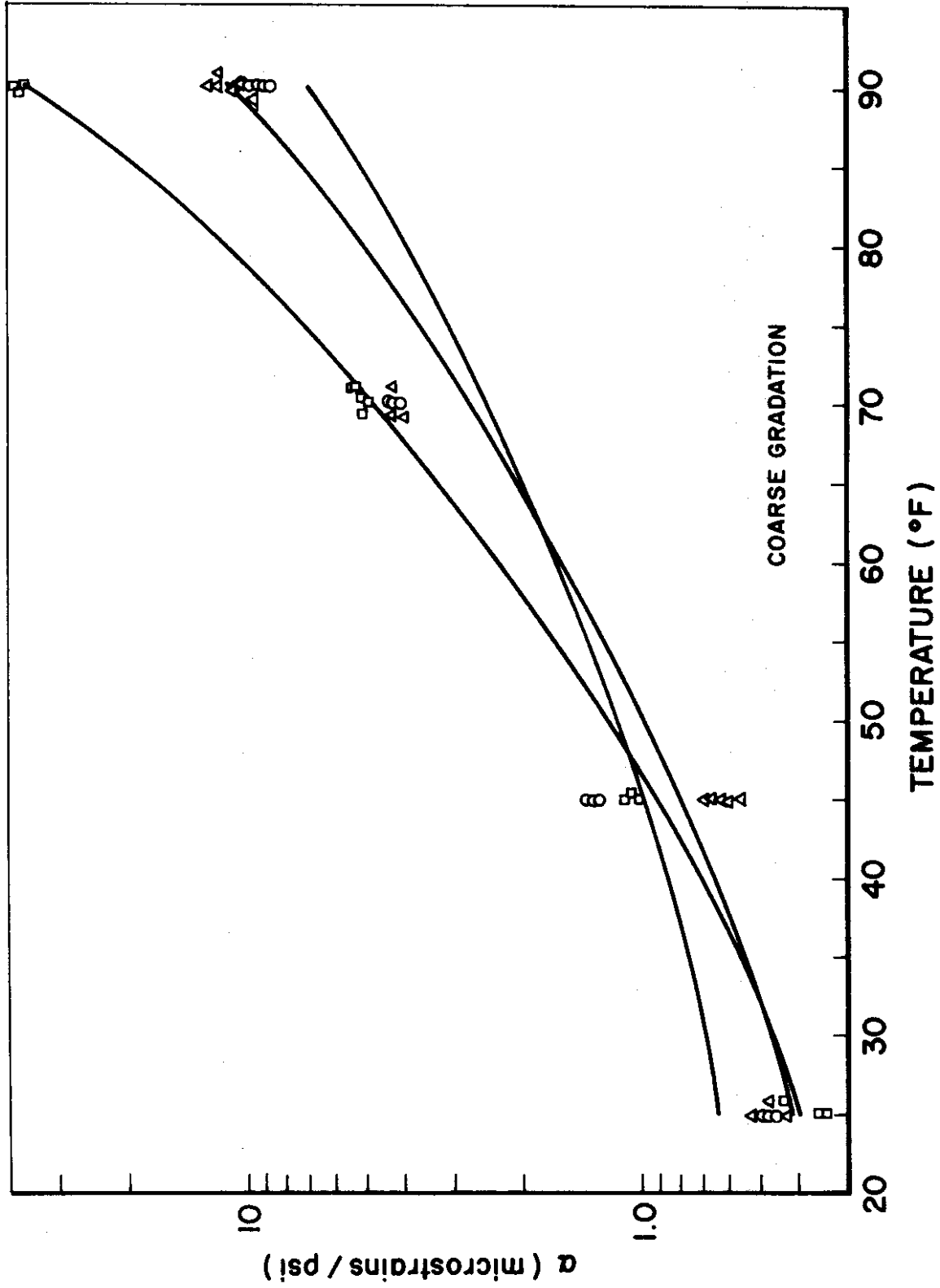


FIGURE 61 - Coefficient α Versus Temperature for Different Asphalt Contents

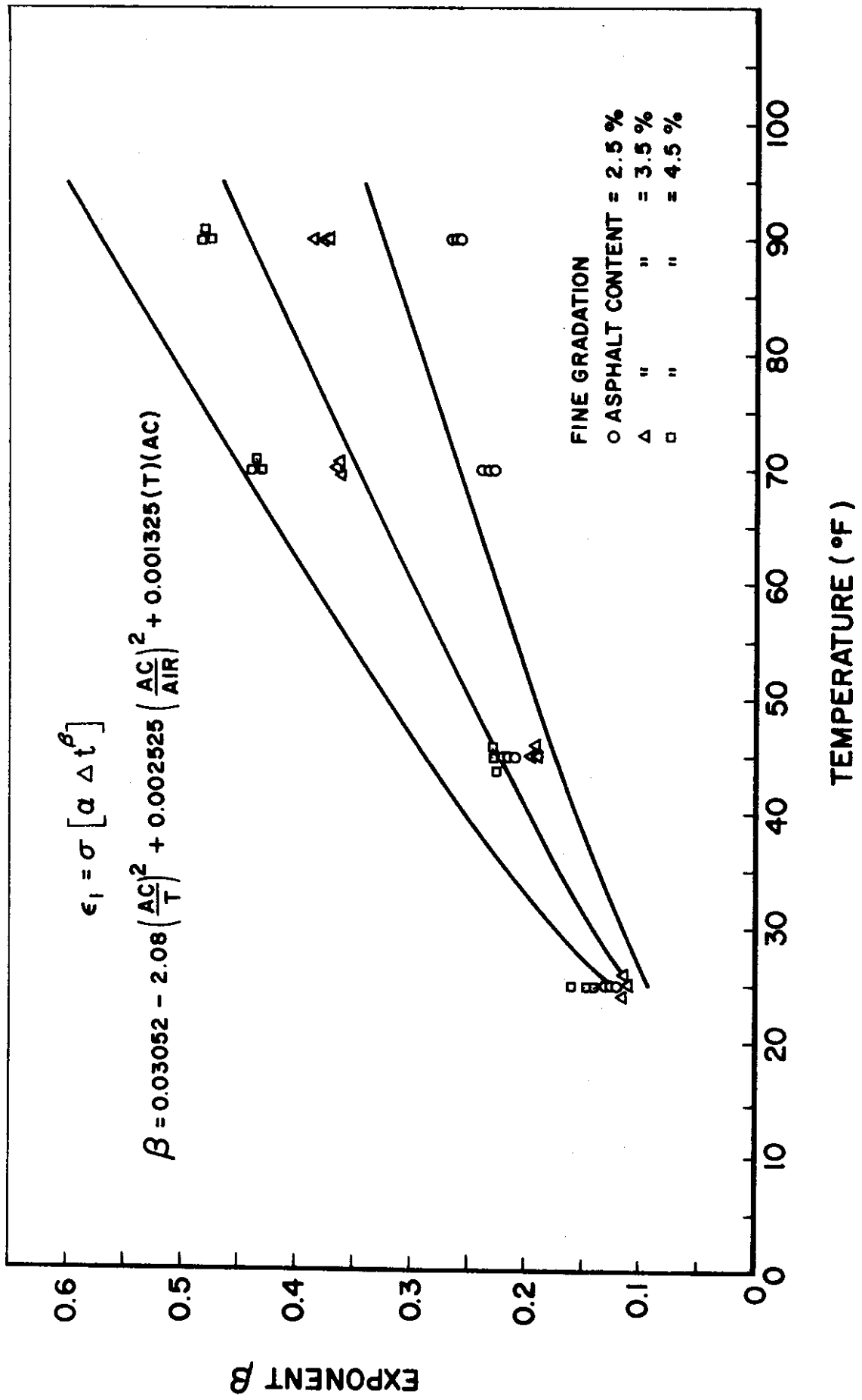


FIGURE 62 - Coefficient β Versus Temperature for Different Asphalt Contents

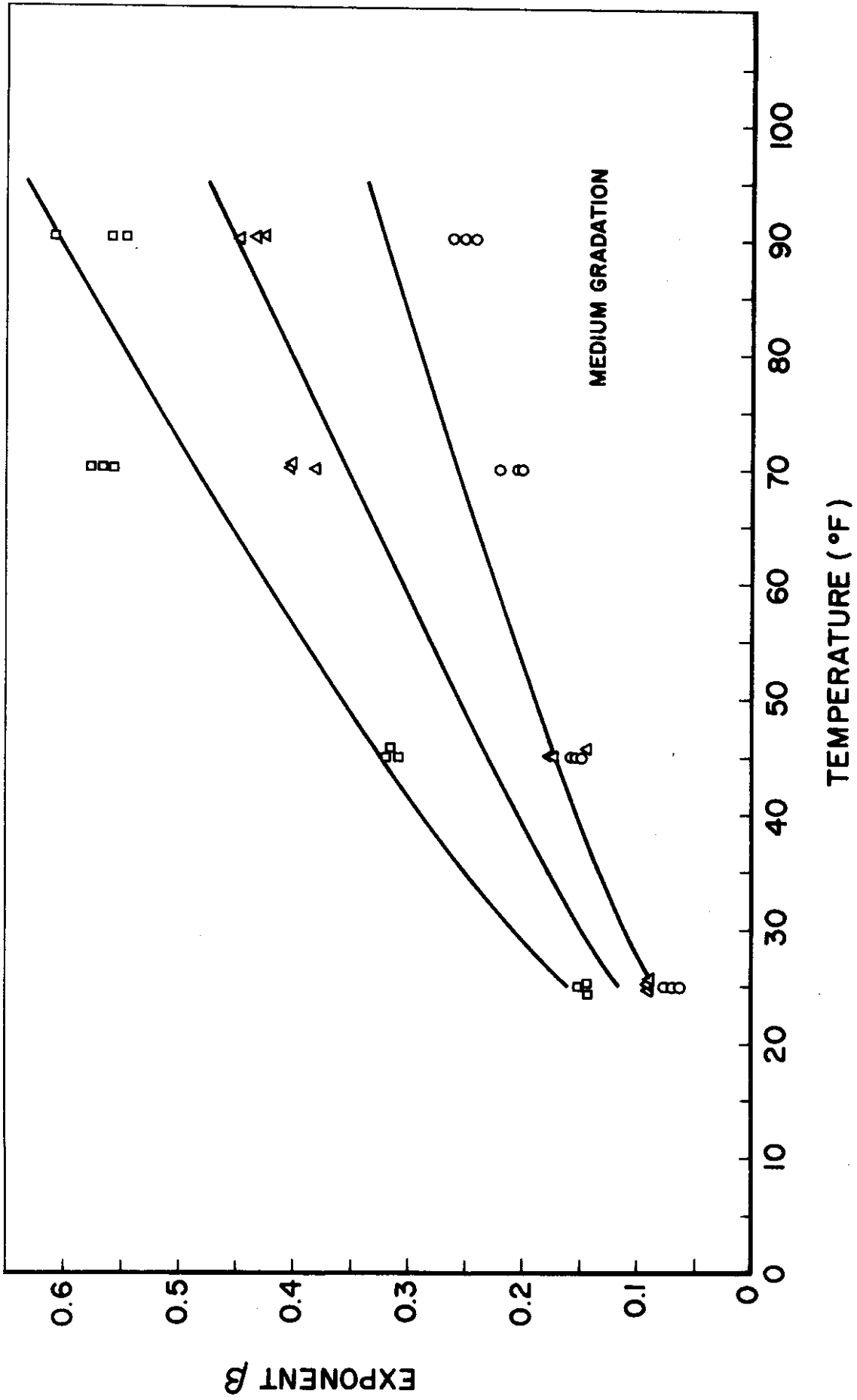


FIGURE 63 - Coefficient β Versus Temperature for Different Asphalt Contents

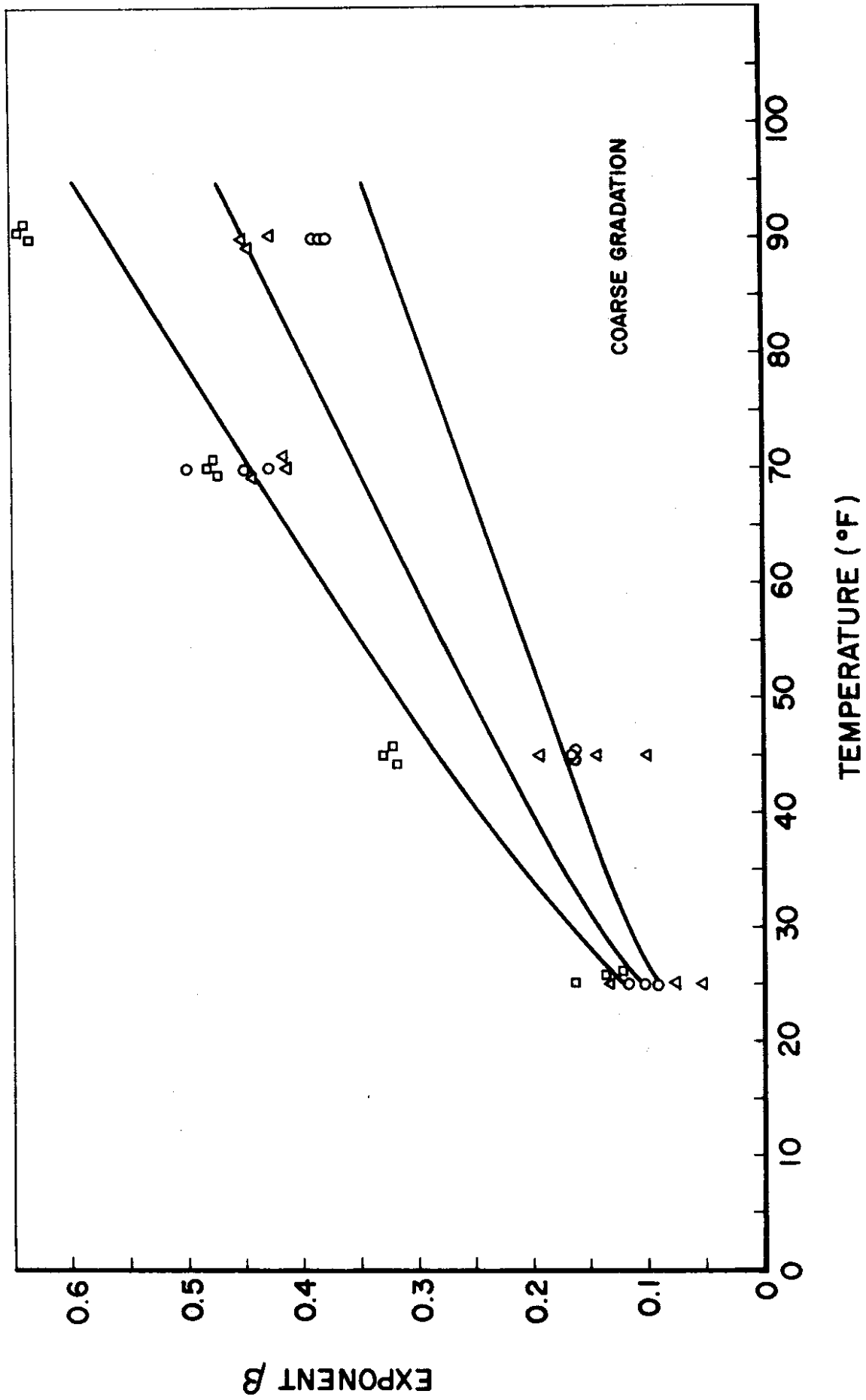


FIGURE 64 - Coefficient β Versus Temperature for Different Asphalt Contents

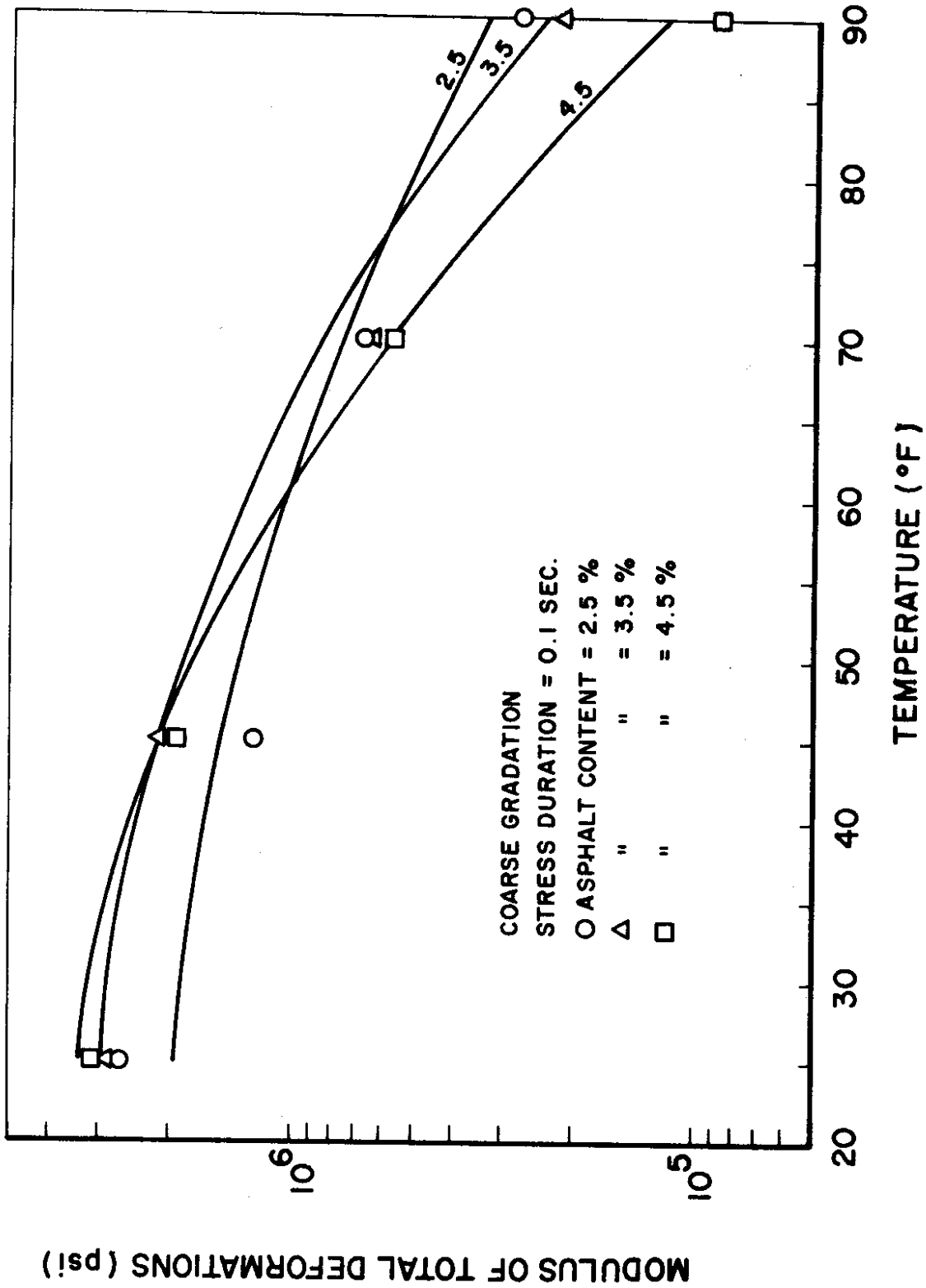


FIGURE 65 - Equation 59 Plotted Against Temperature for Different Asphalt Contents

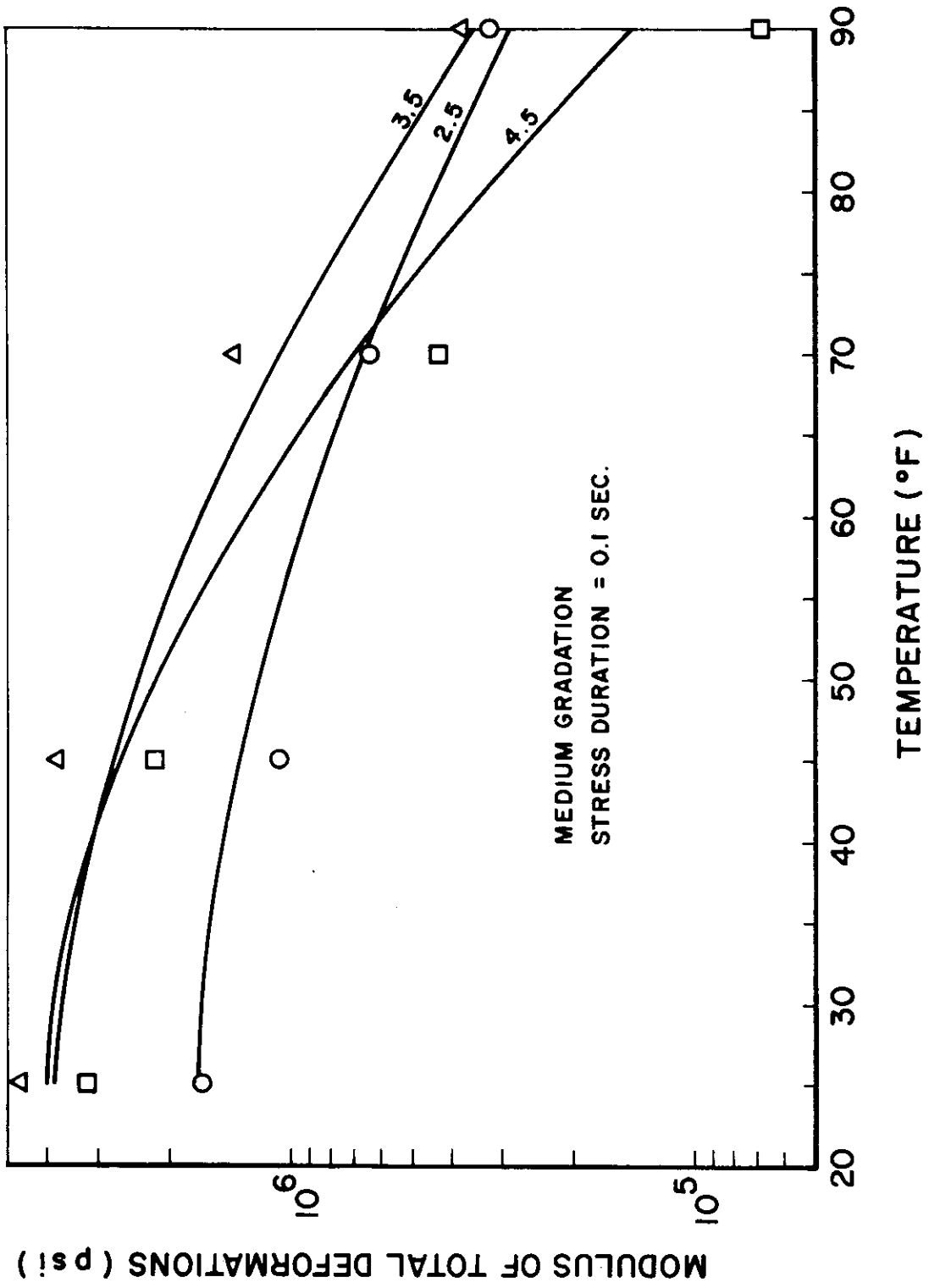


FIGURE 66 - Equation 59 Plotted Against Temperature for Different Asphalt Contents

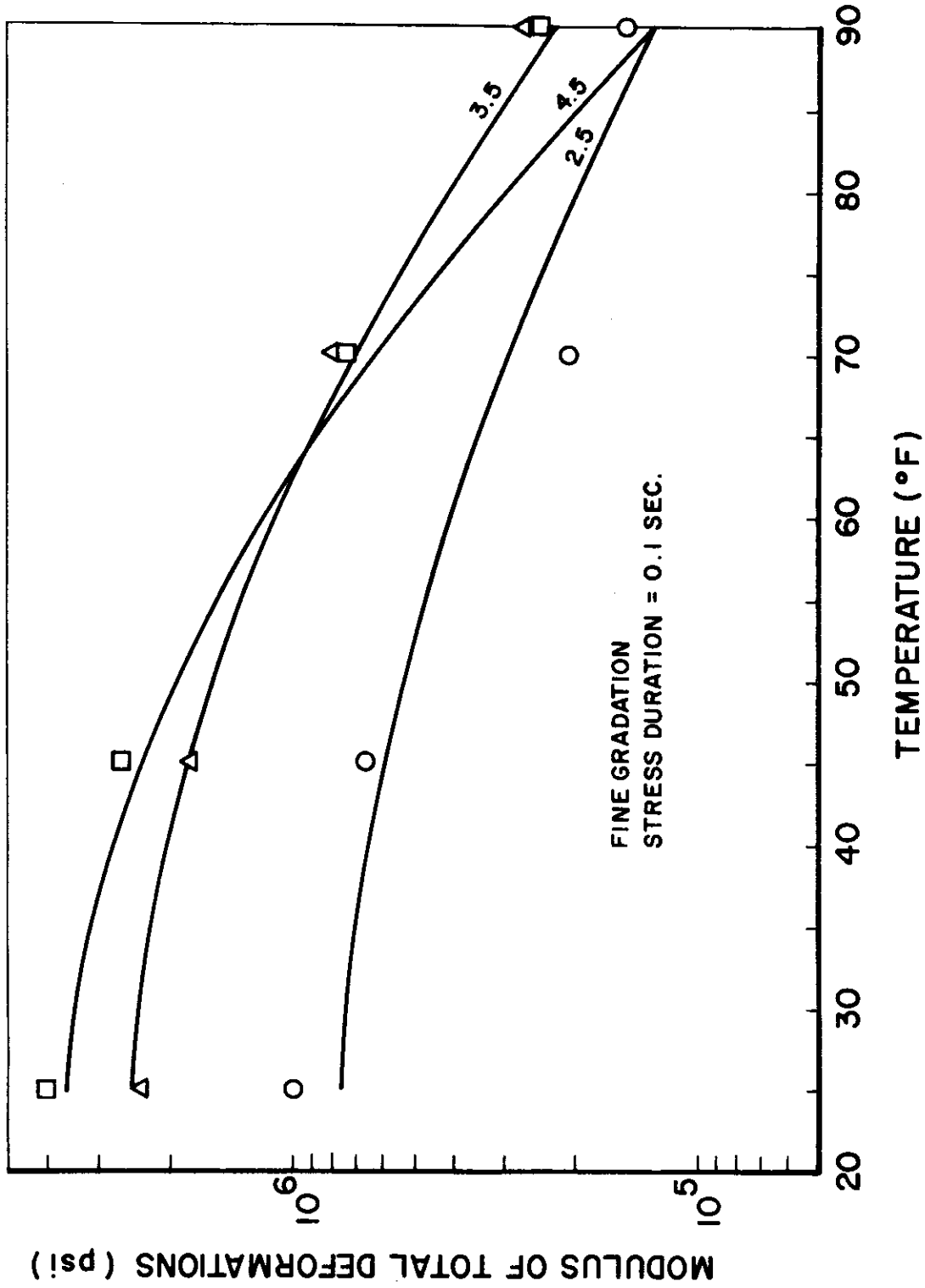


FIGURE 67 - Equation 59 Plotted Against Temperature for Different Asphalt Contents

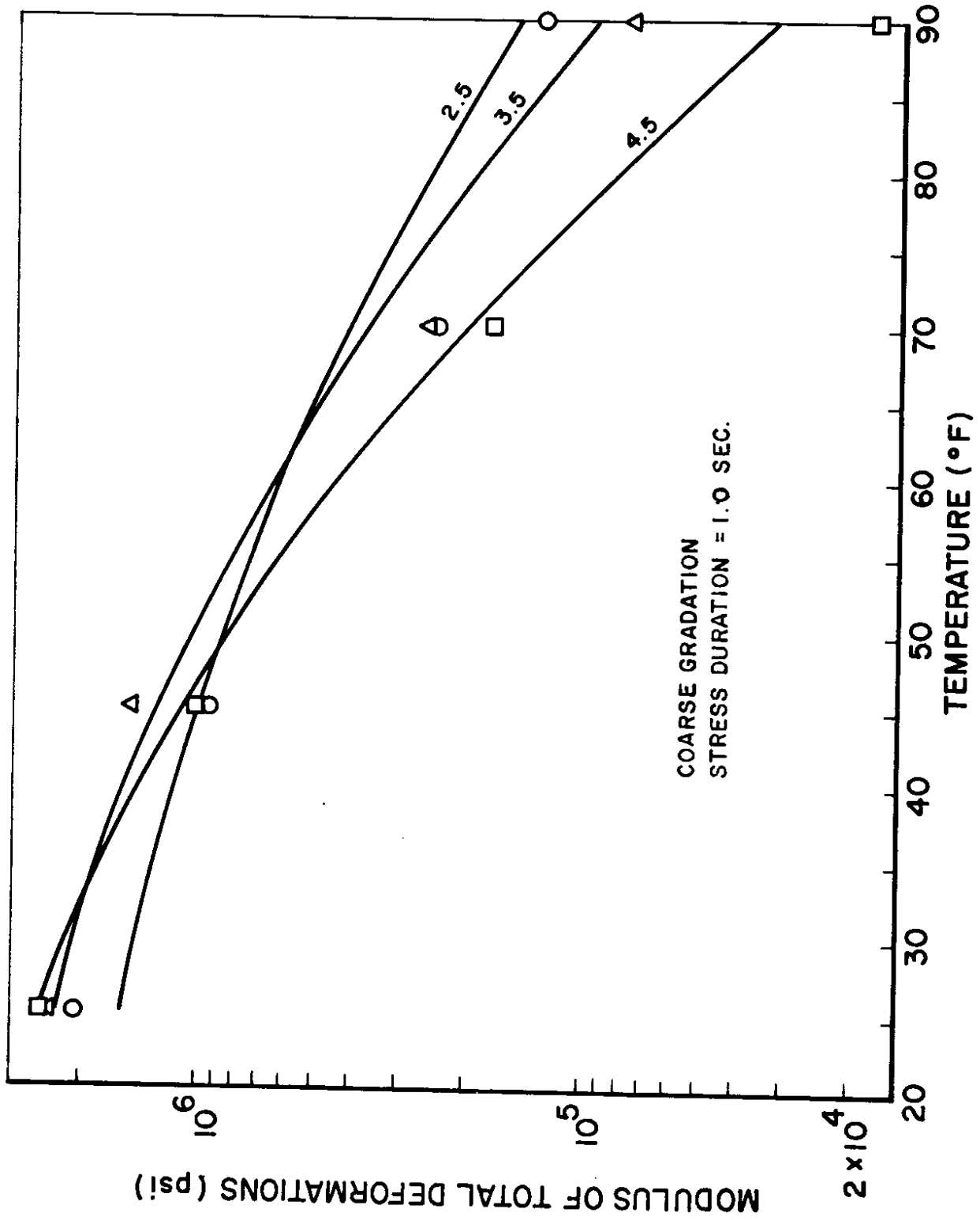


FIGURE 68 - Equation 59 Plotted Against Temperature for Different Asphalt Contents

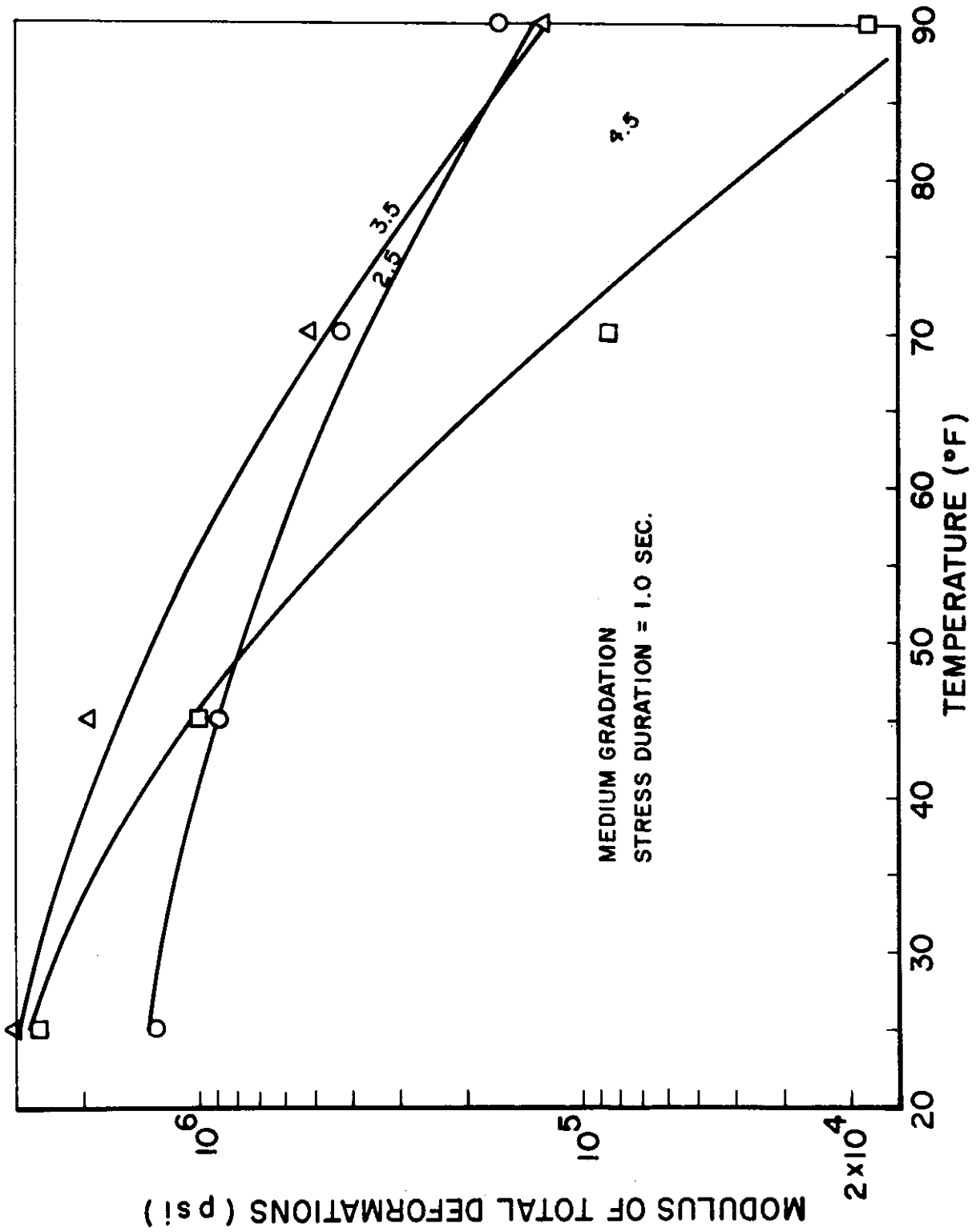


FIGURE 69 - Equation 59 Plotted Against Temperature for Different Asphalt Contents

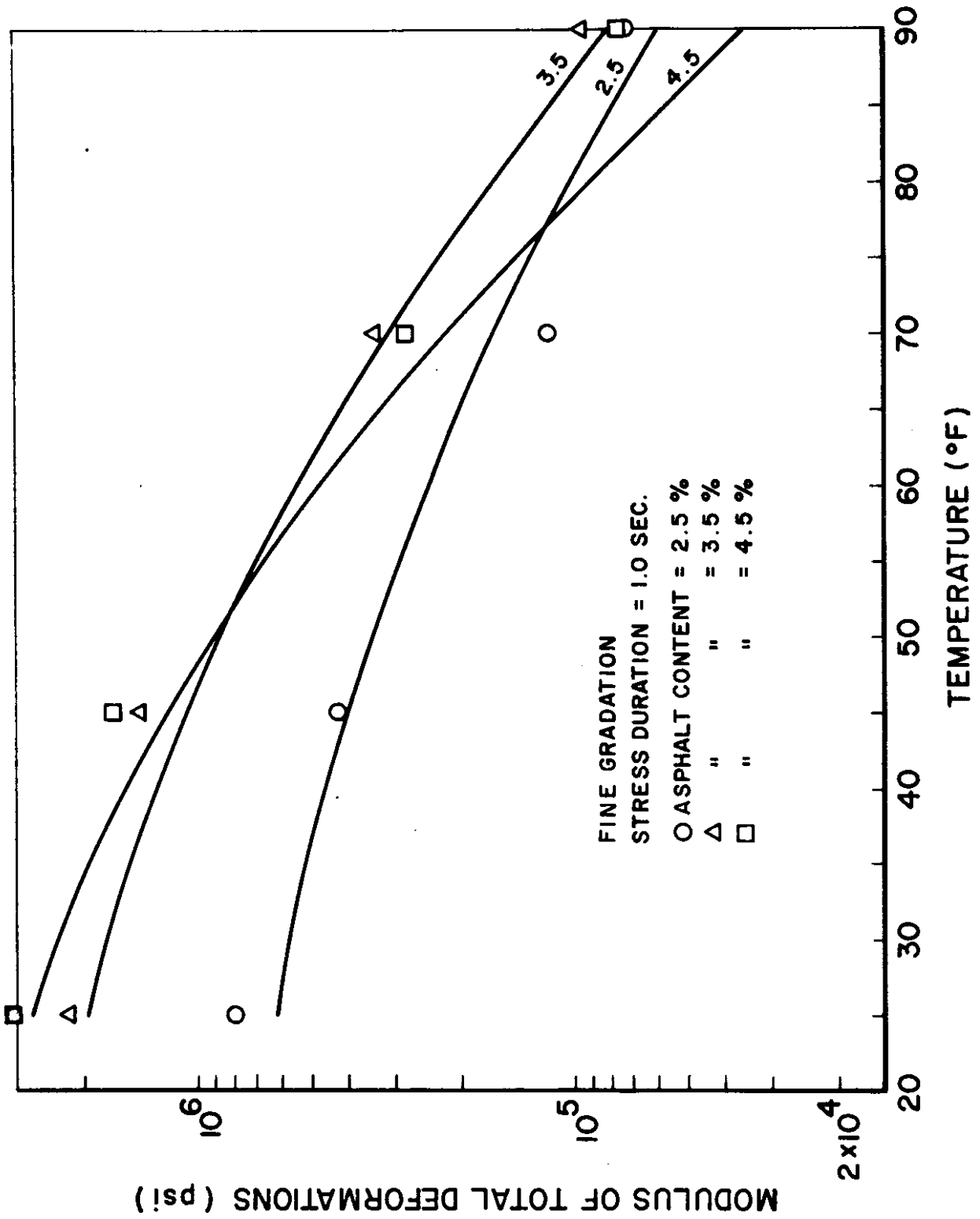


FIGURE 70 - Equation 59 Plotted Against Temperature for Different Asphalt Contents

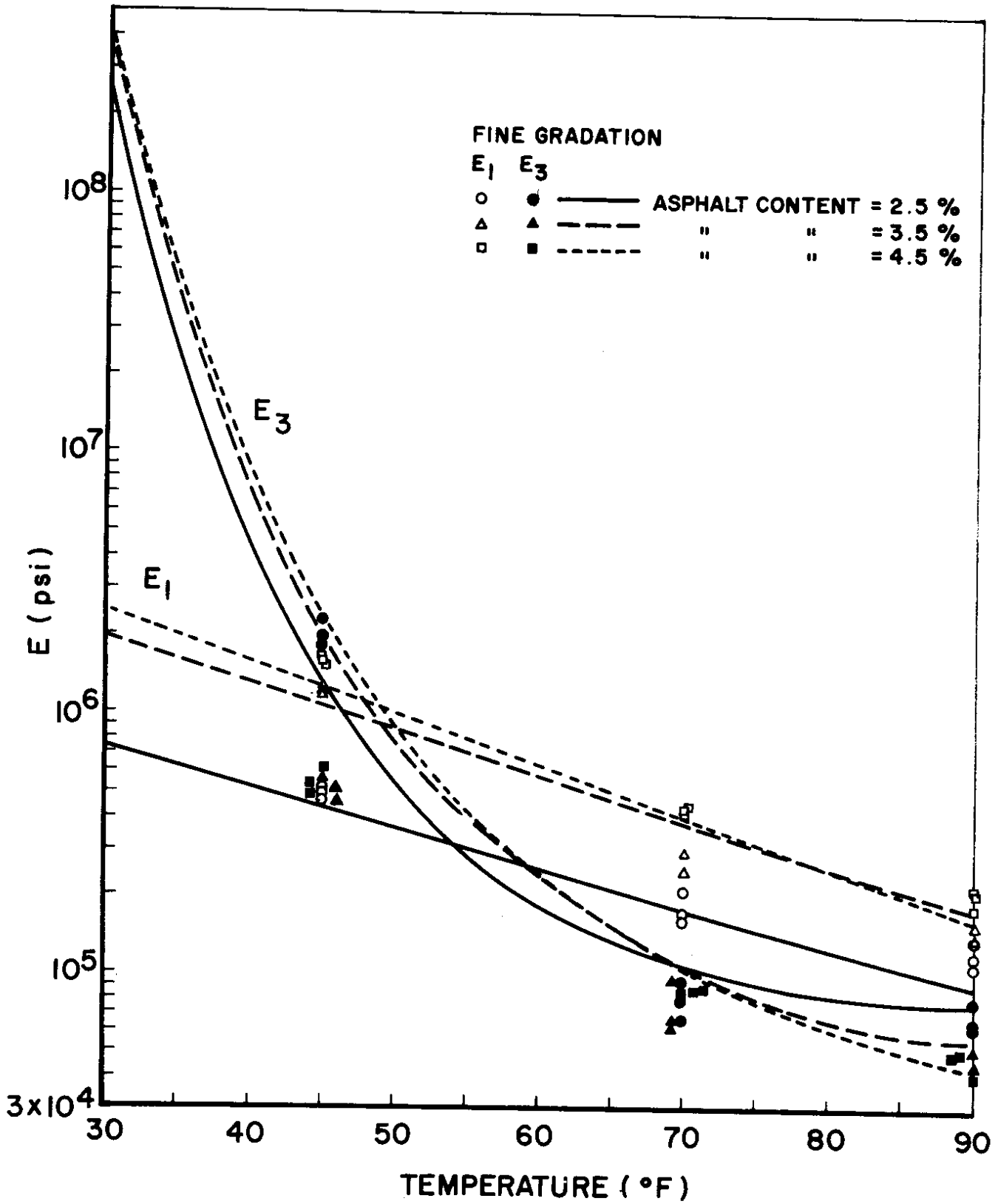


FIGURE 71 - Variation of the Four-Element Model Parameters with Temperature

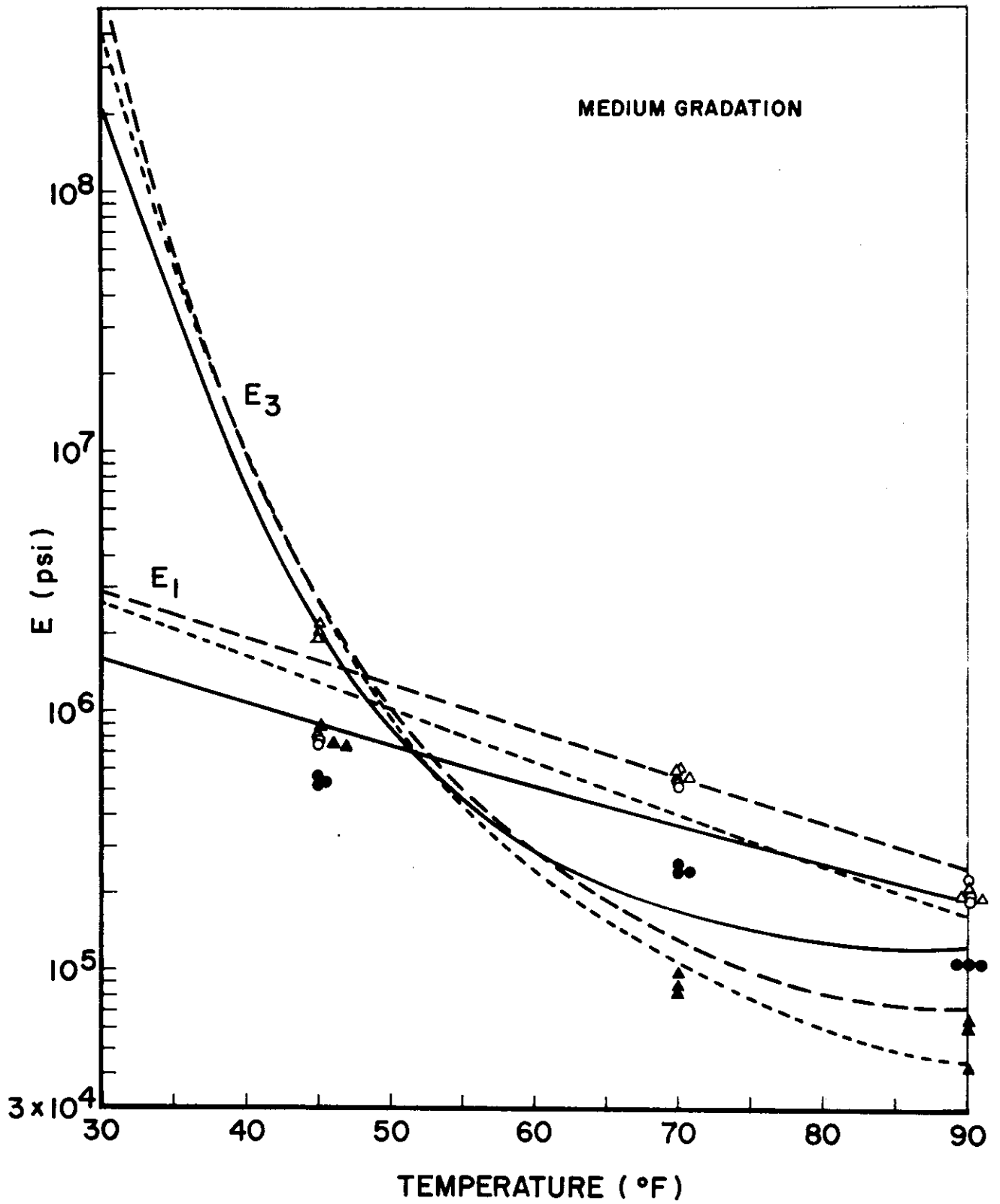


FIGURE 72 - Variation of the Four-Element Model Parameters with Temperature

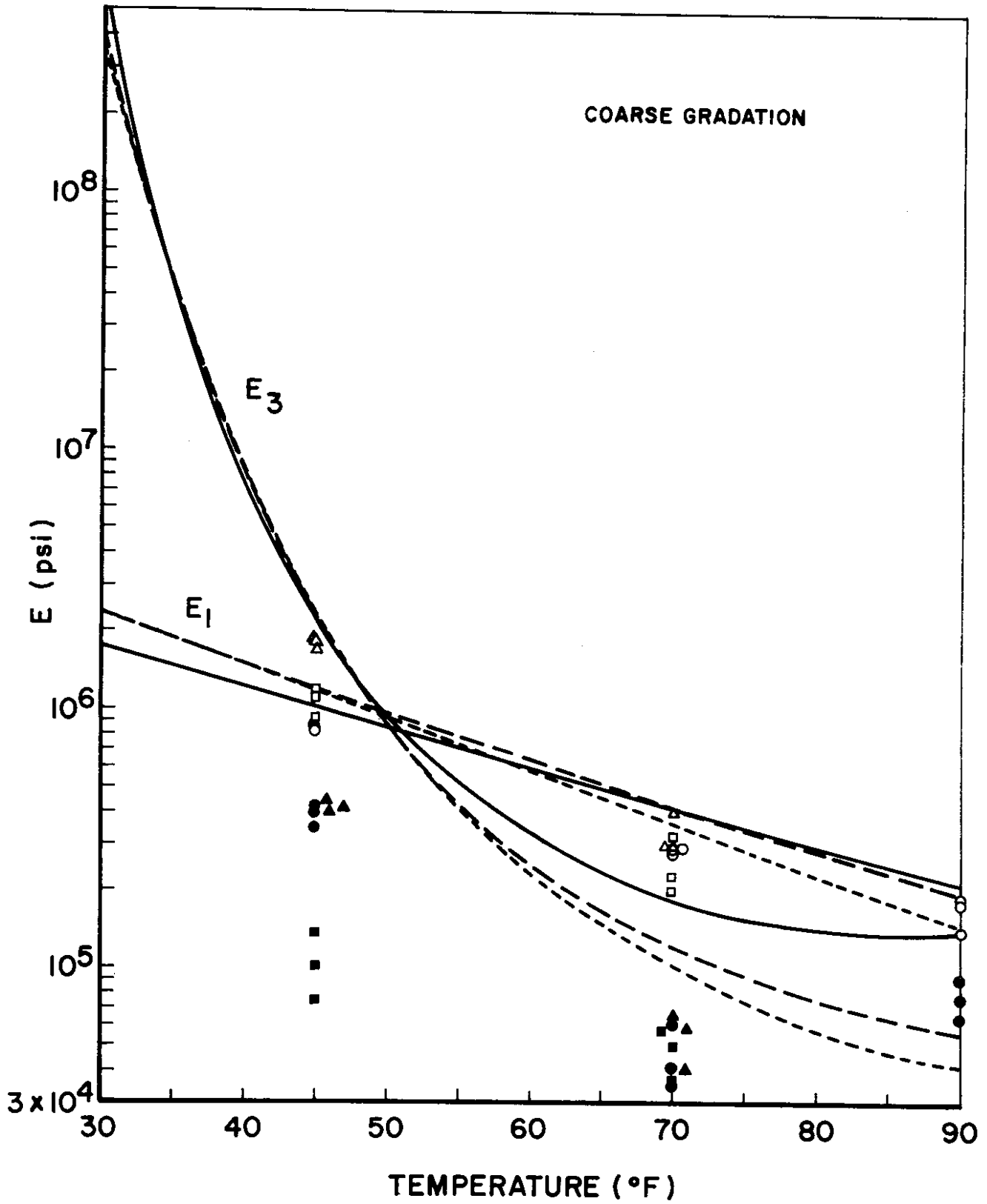


FIGURE 73 - Variation of the Four-Element Model Parameters with Temperature

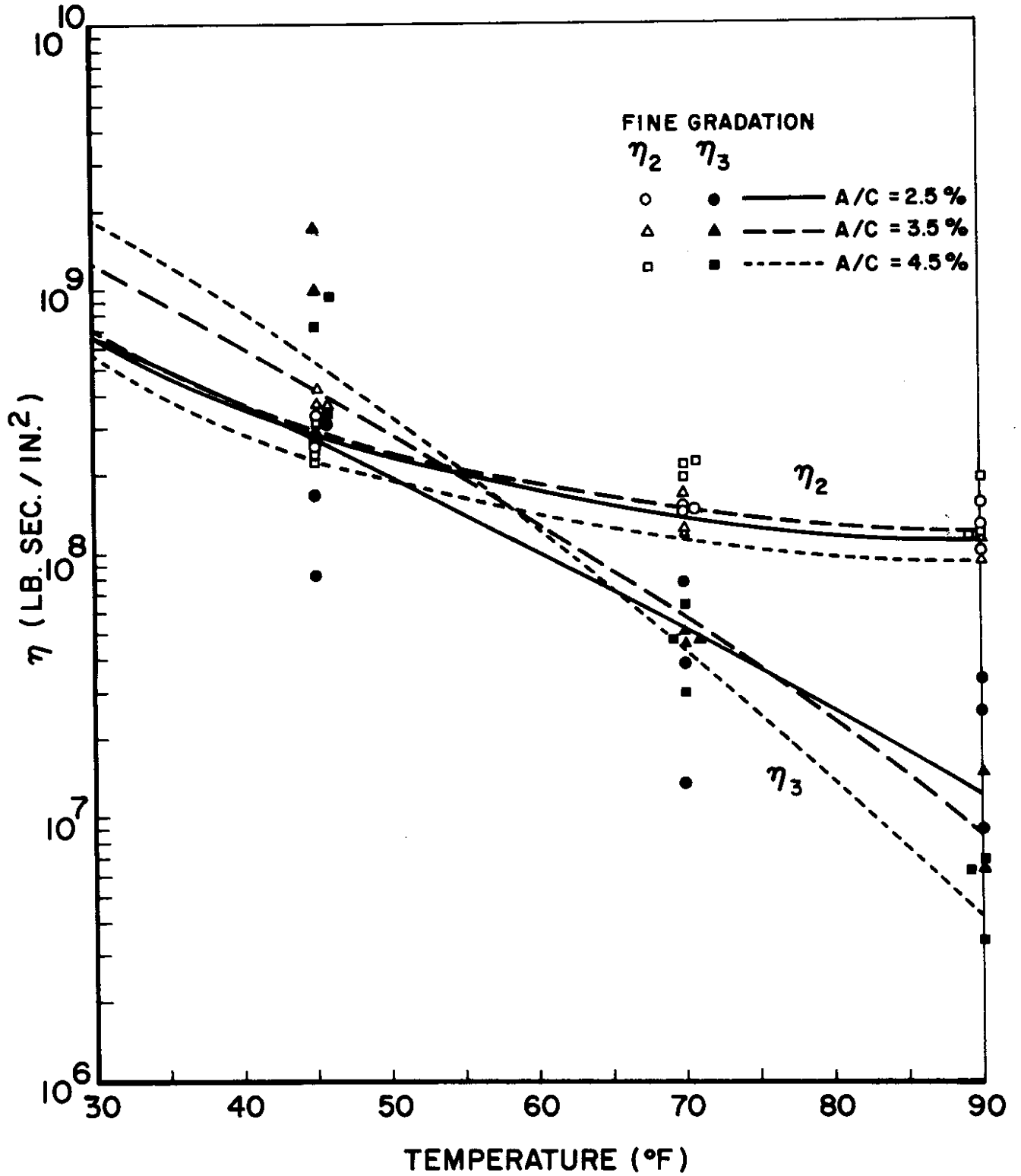


FIGURE 74 - Variation of the Four-Element Model Parameters with Temperature

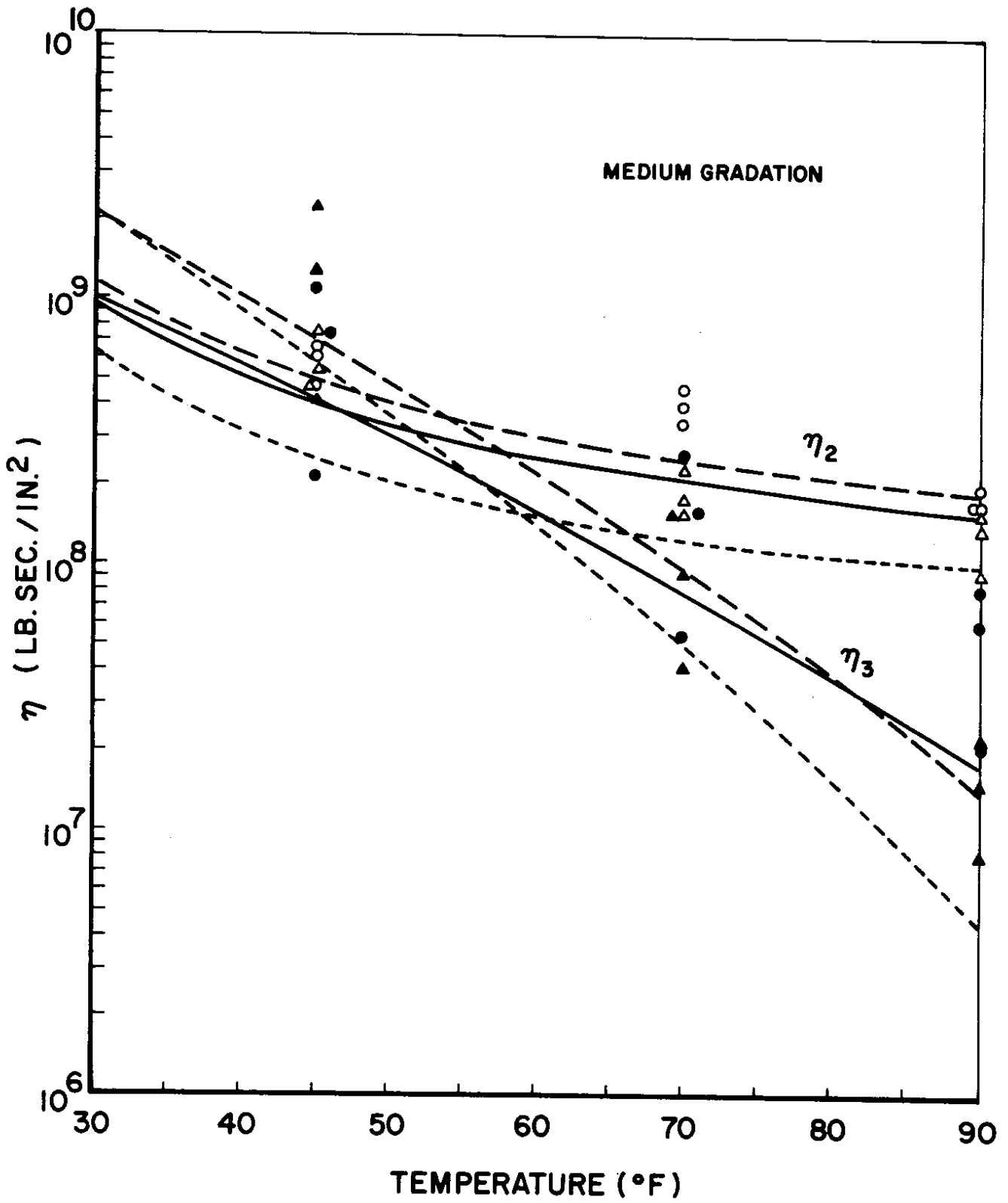


FIGURE 75 - Variation of the Four-Element Model Parameters with Temperature

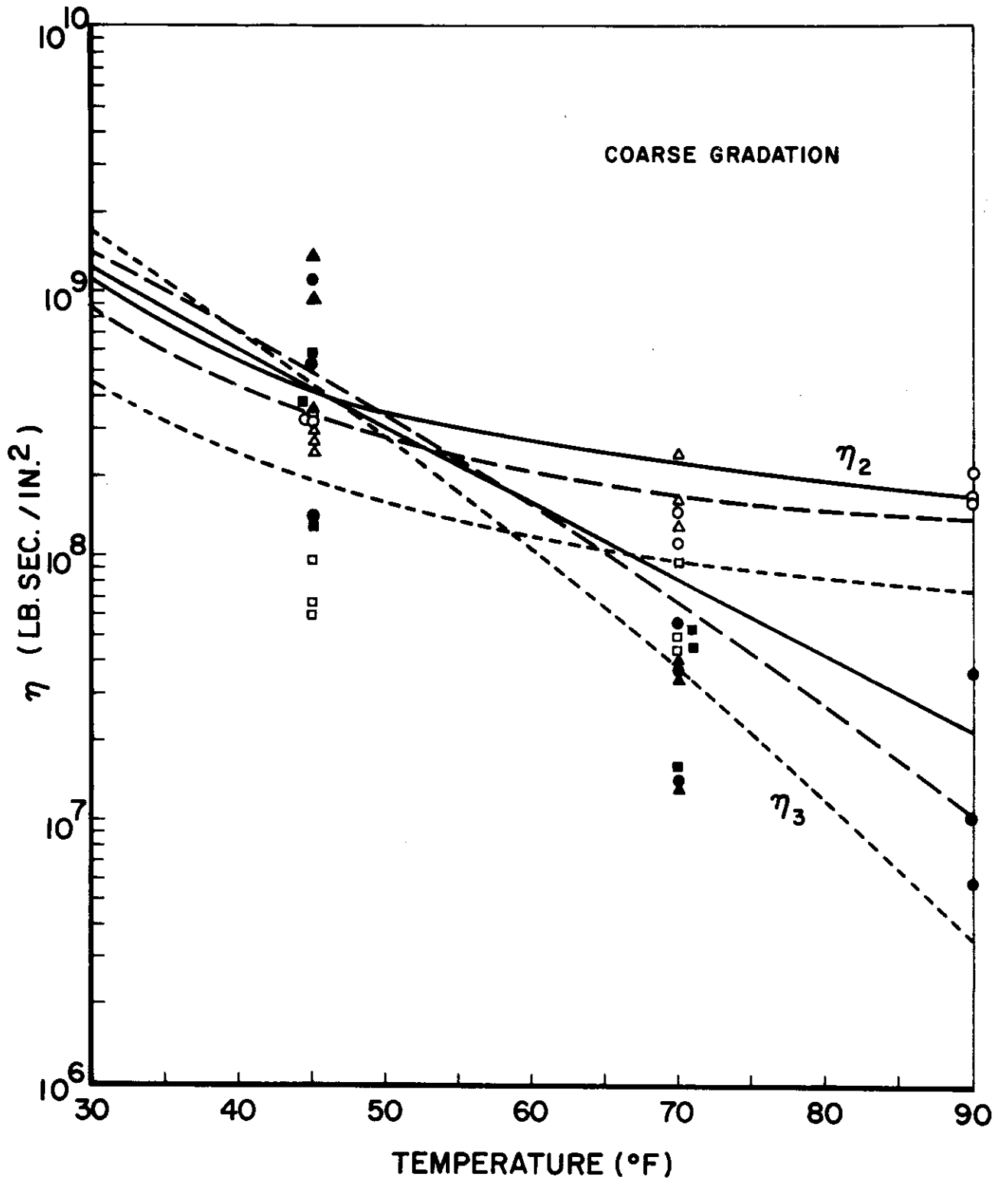


FIGURE 76 - Variation of the Four-Element Model Parameters with Temperature

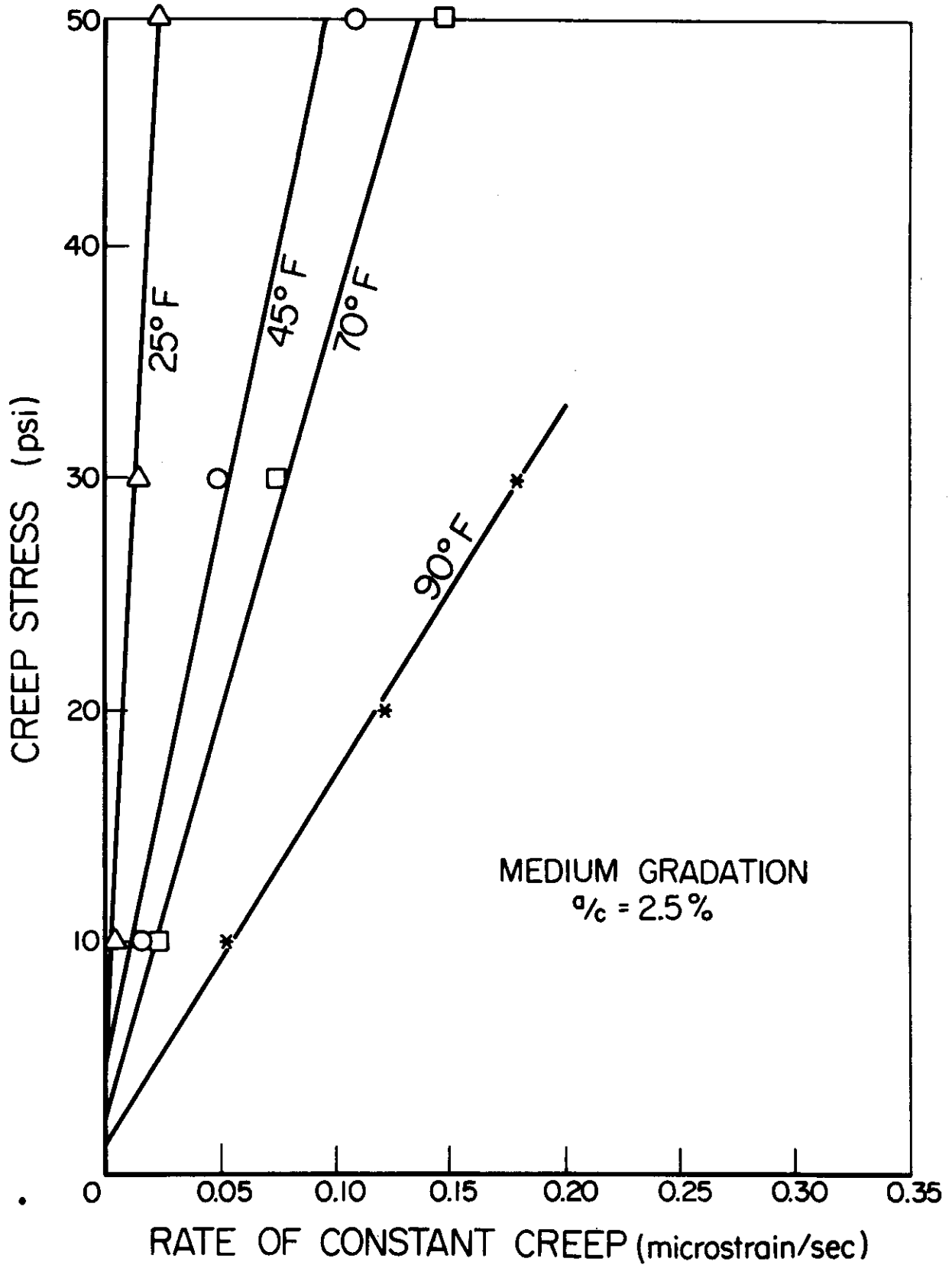


FIGURE 77 - Creep Stress Versus Rate of Constant Creep at Different Temperatures

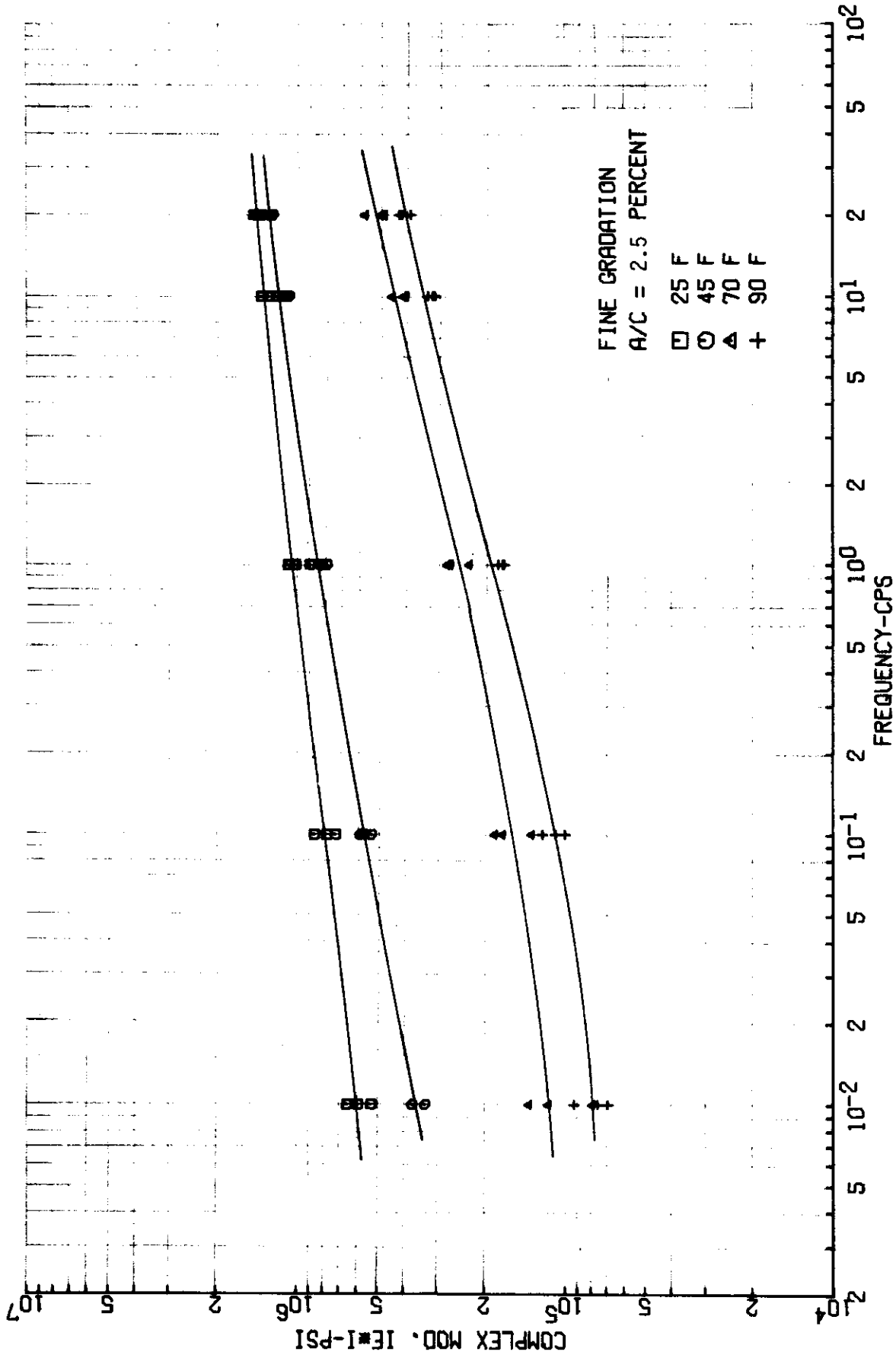


FIGURE 78 - Complex Modulus Versus Frequency at Different Temperatures

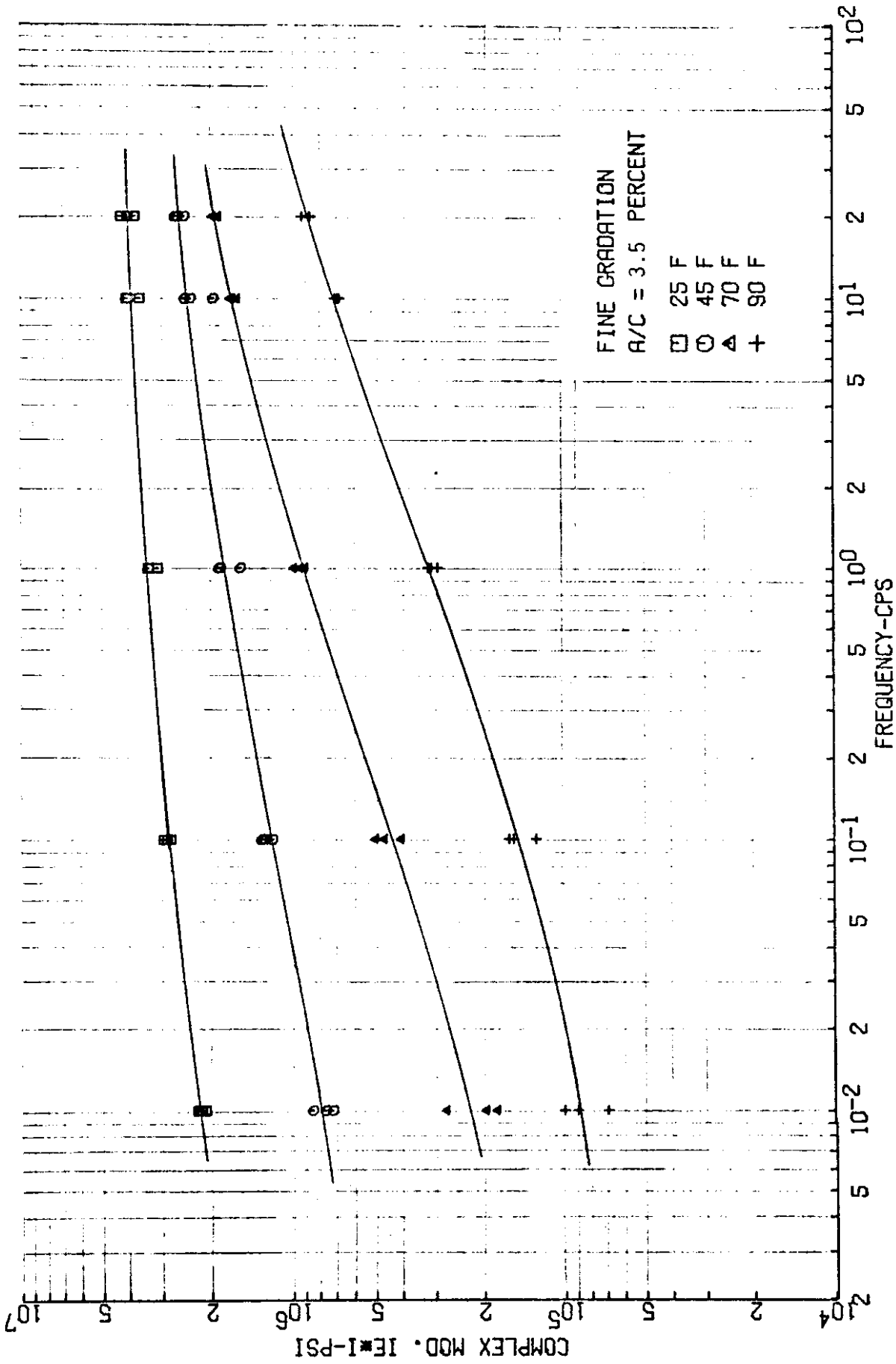


FIGURE 79 - Complex Modulus Versus Frequency at Different Temperatures

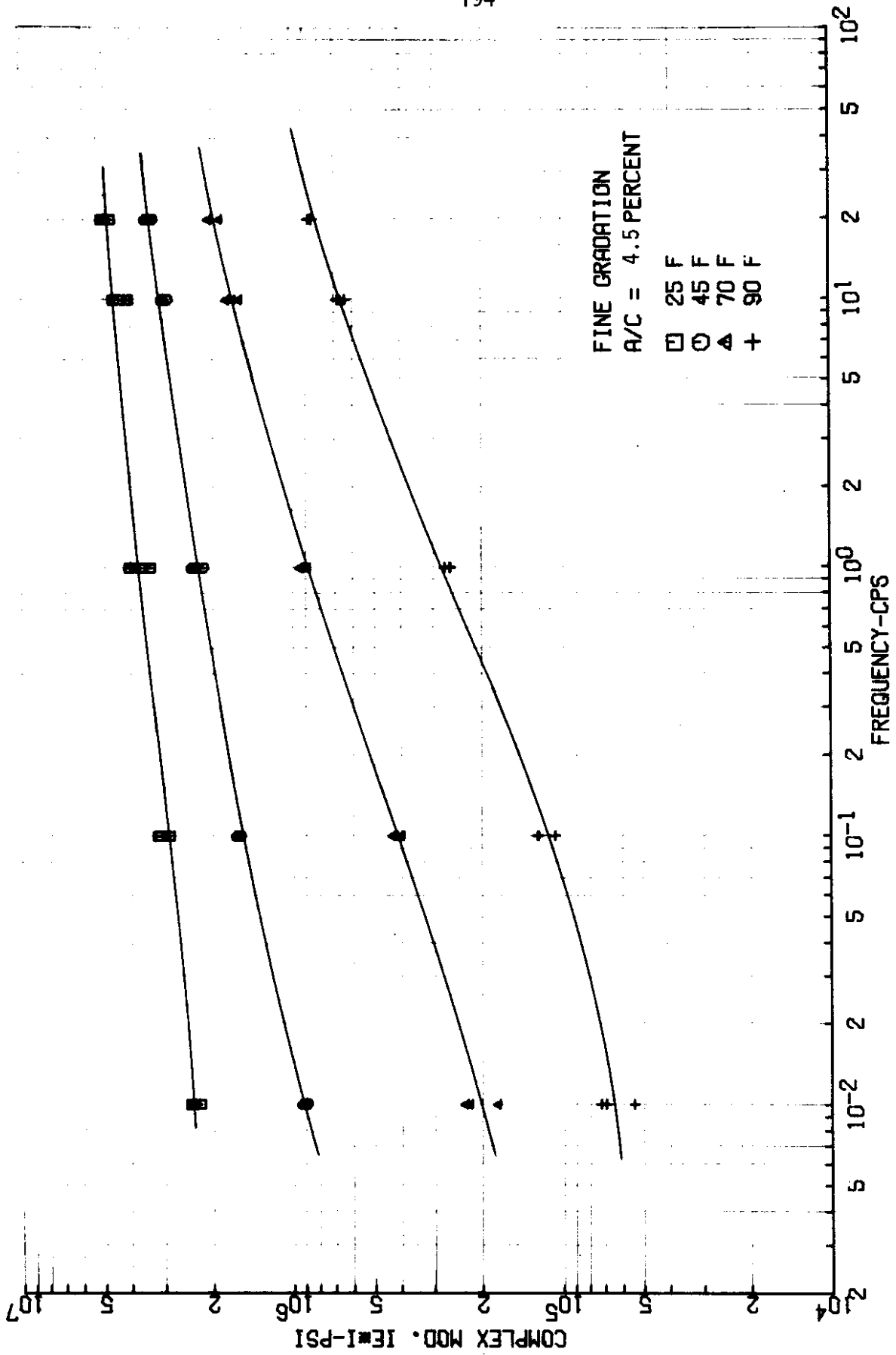


FIGURE 80 - Complex Modulus Versus Frequency at Different Temperatures

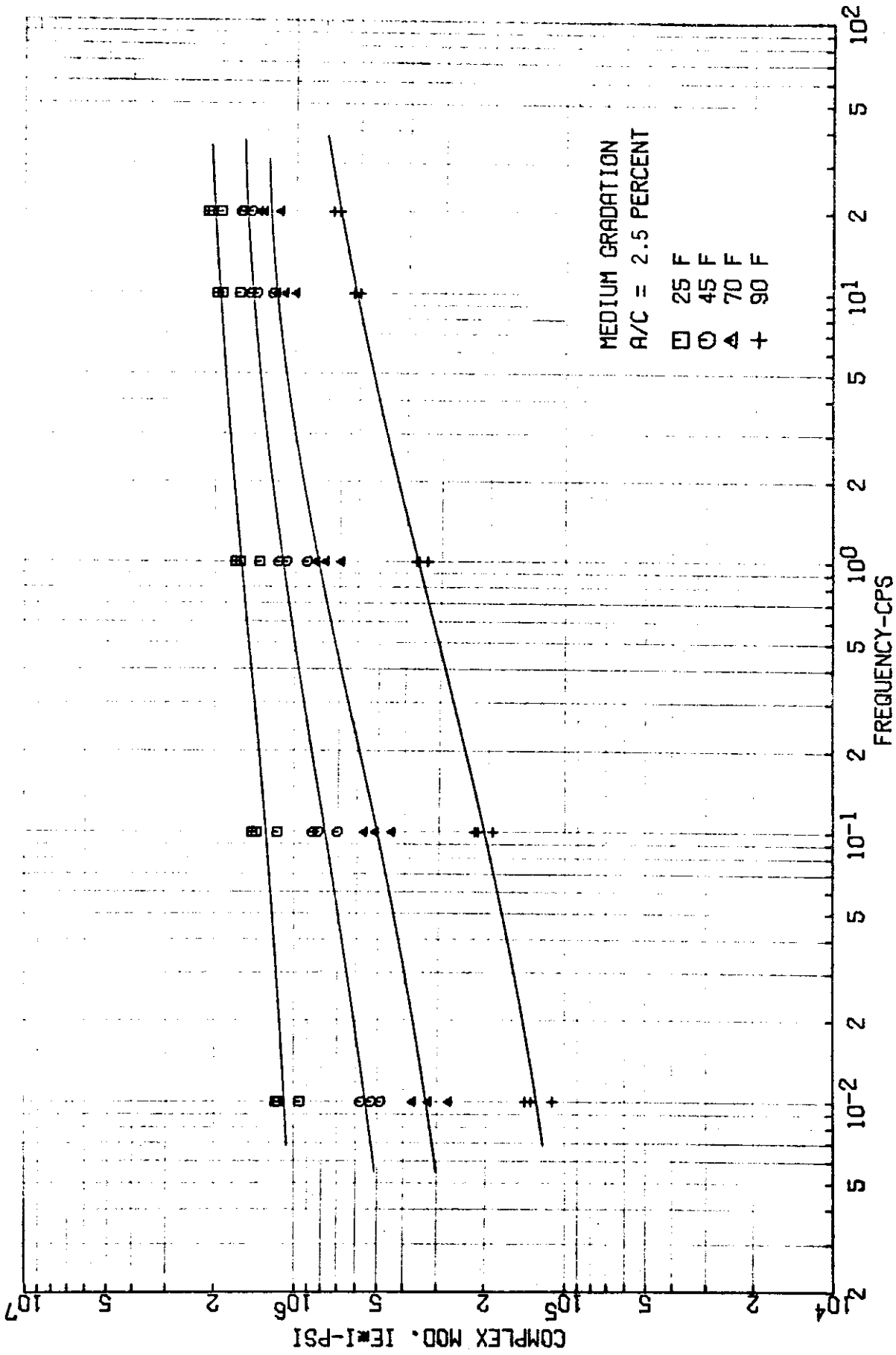


FIGURE 81 - Complex Modulus Versus Frequency at Different Temperatures

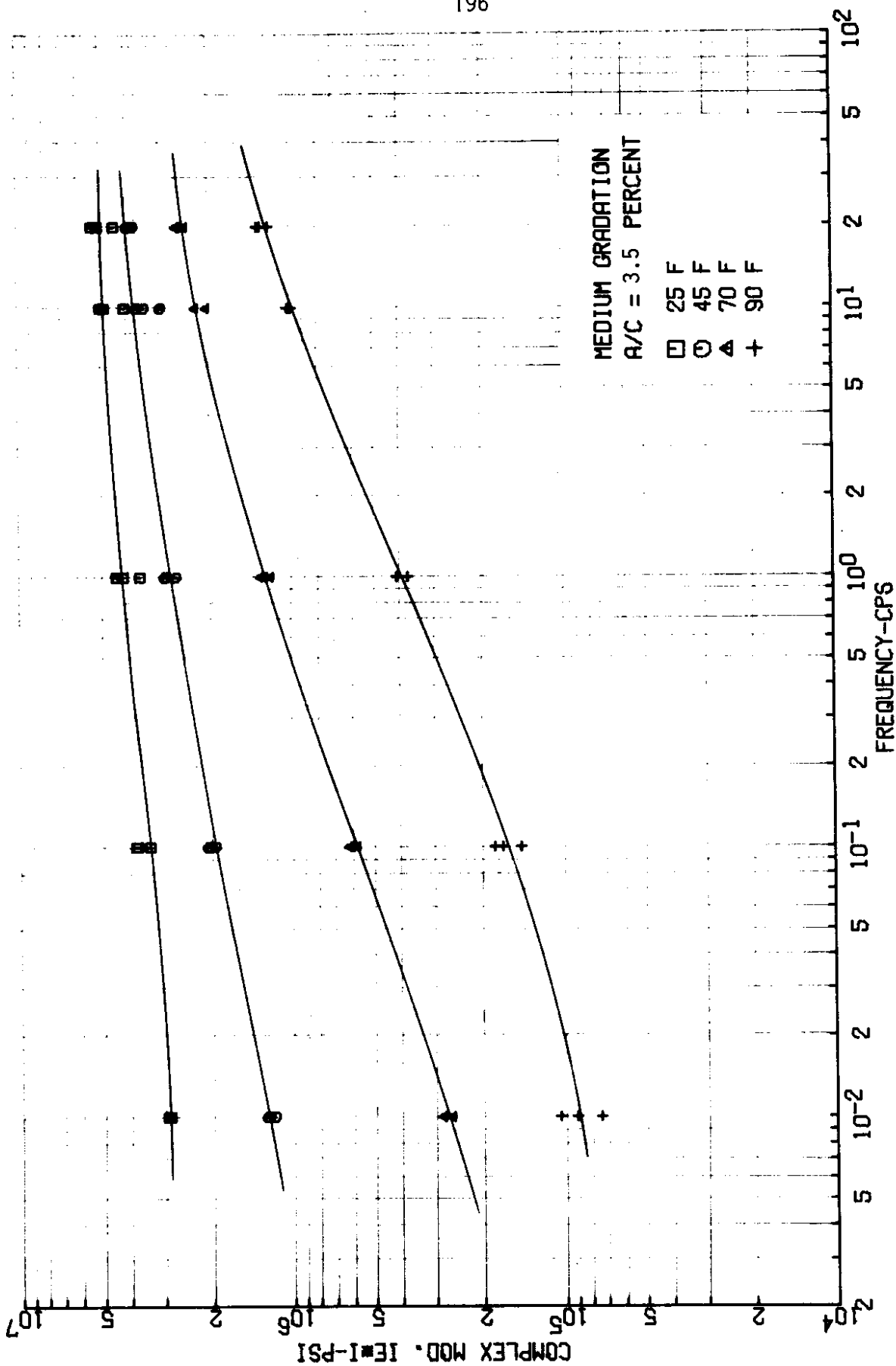


FIGURE 82 - Complex Modulus Versus Frequency at Different Temperatures

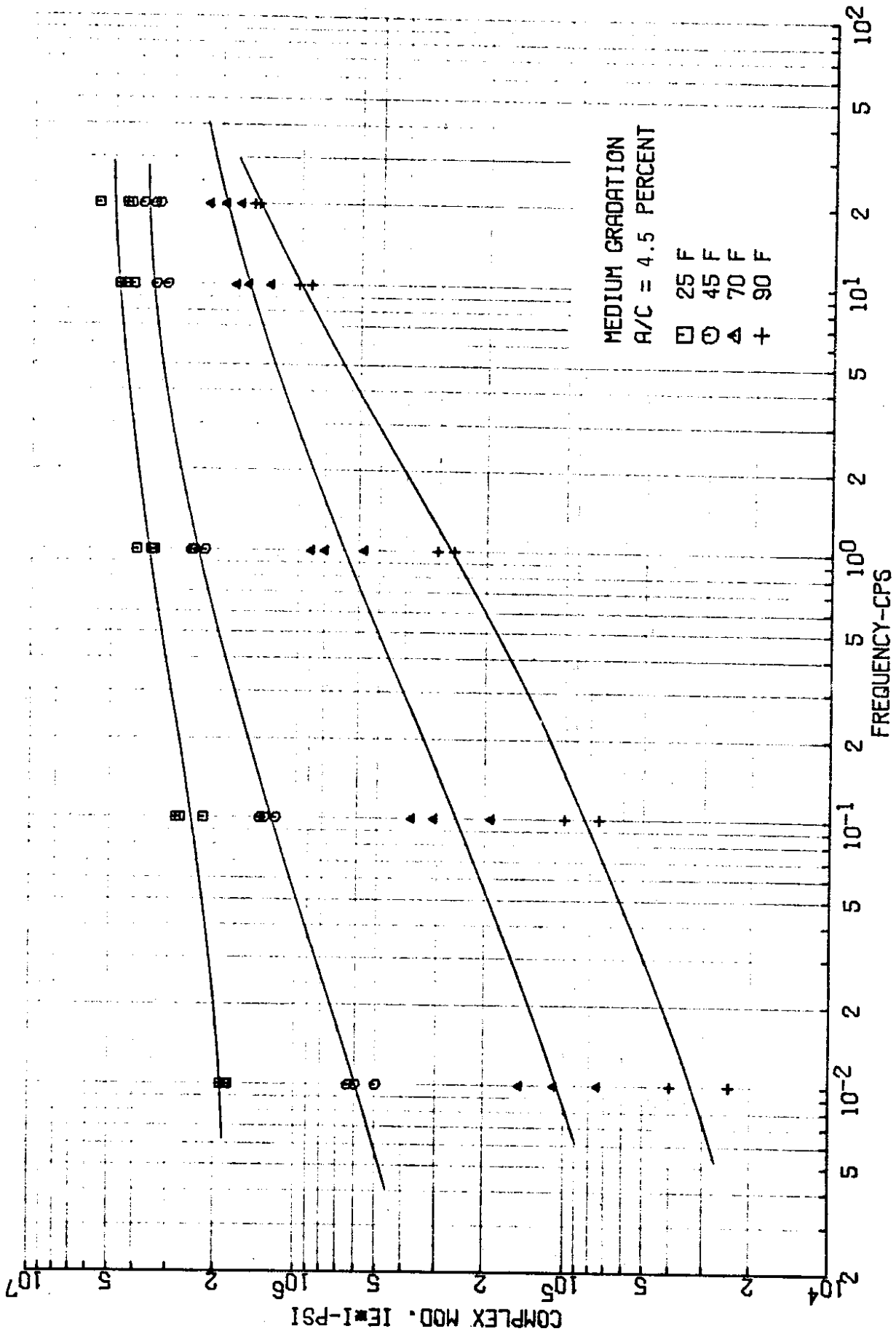


FIGURE 83 - Complex Modulus Versus Frequency at Different Temperatures

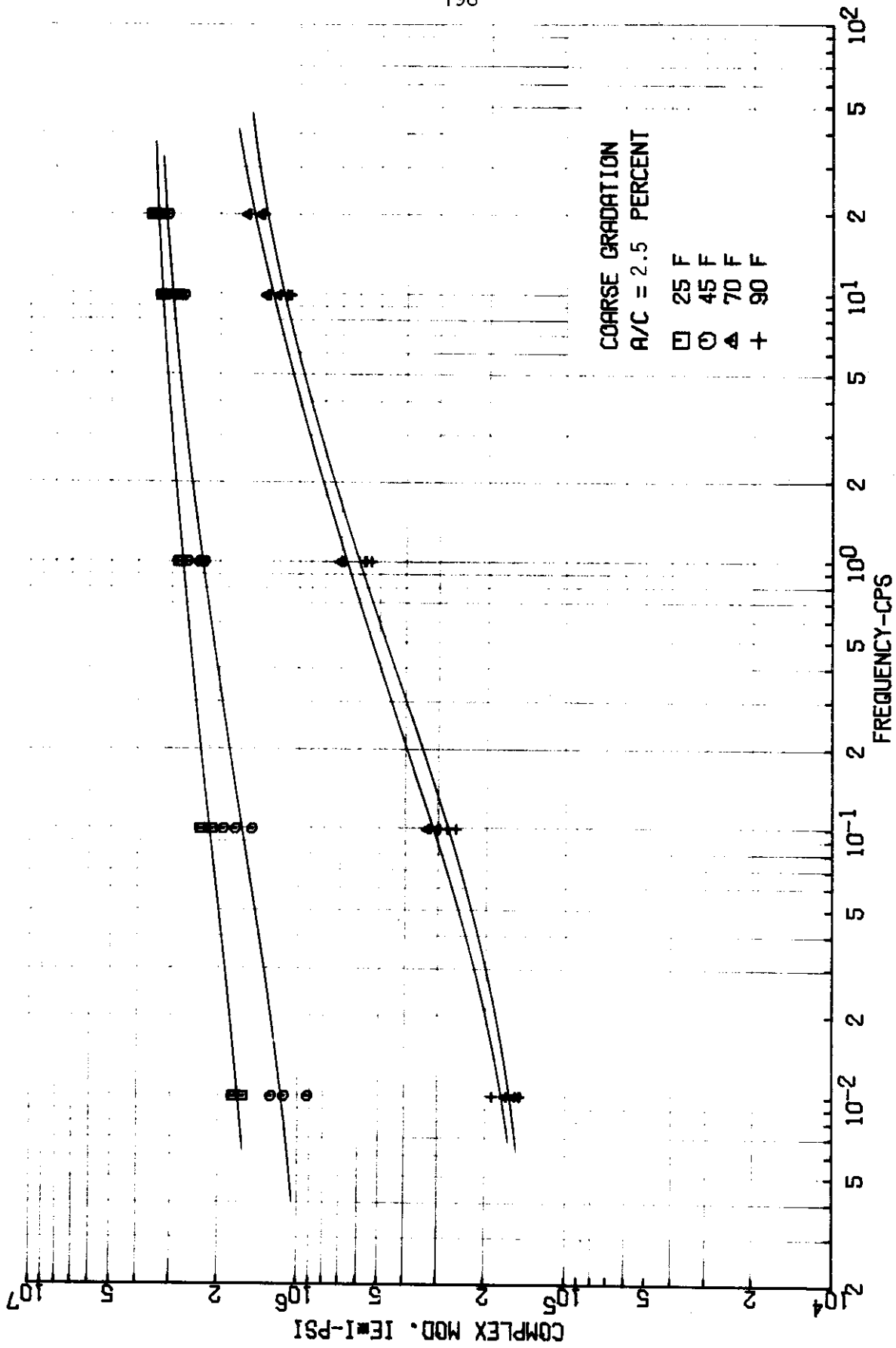


FIGURE 84 - Complex Modulus Versus Frequency at Different Temperatures

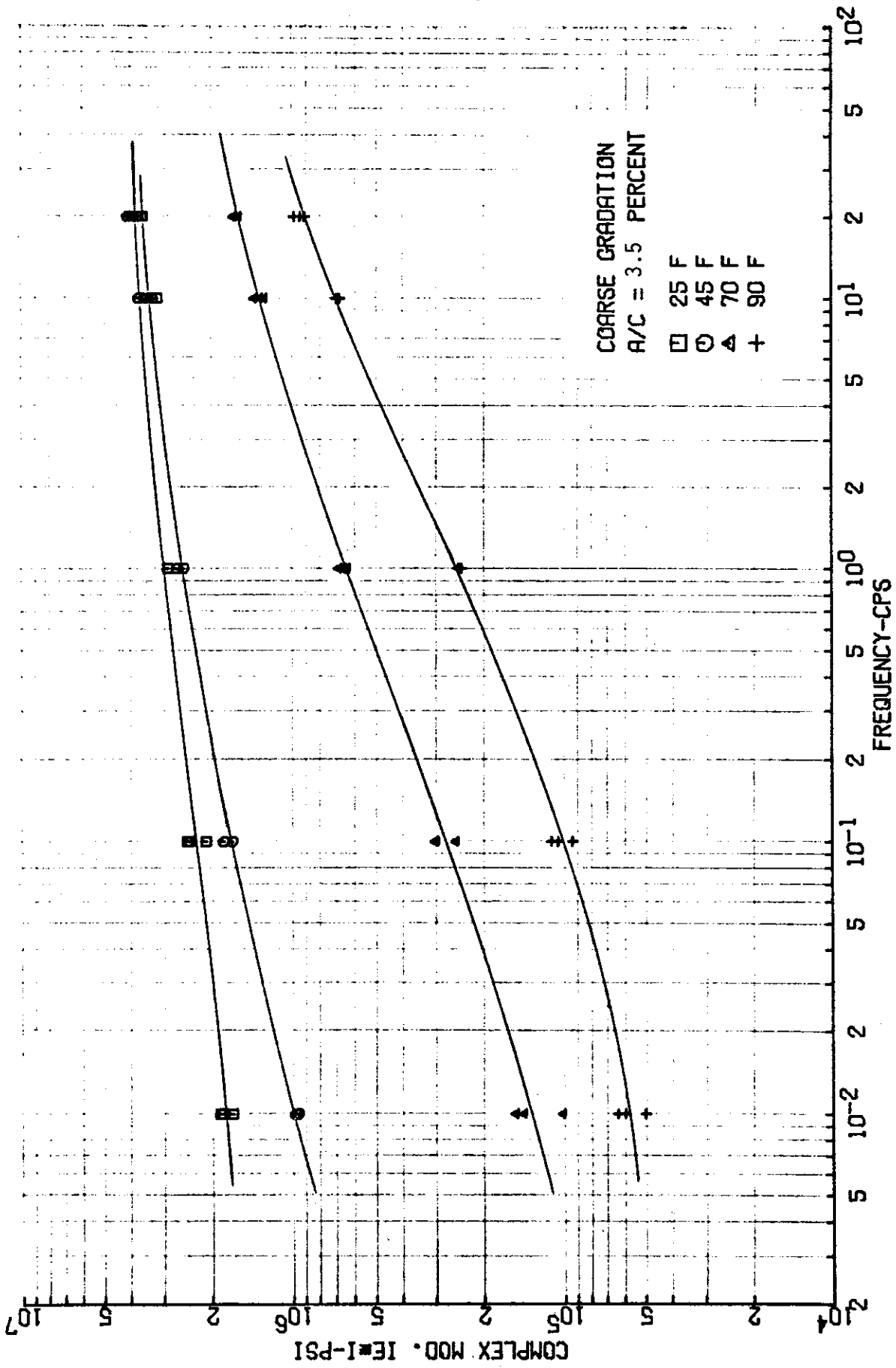


FIGURE 85 - Complex Modulus Versus Frequency at Different Temperatures

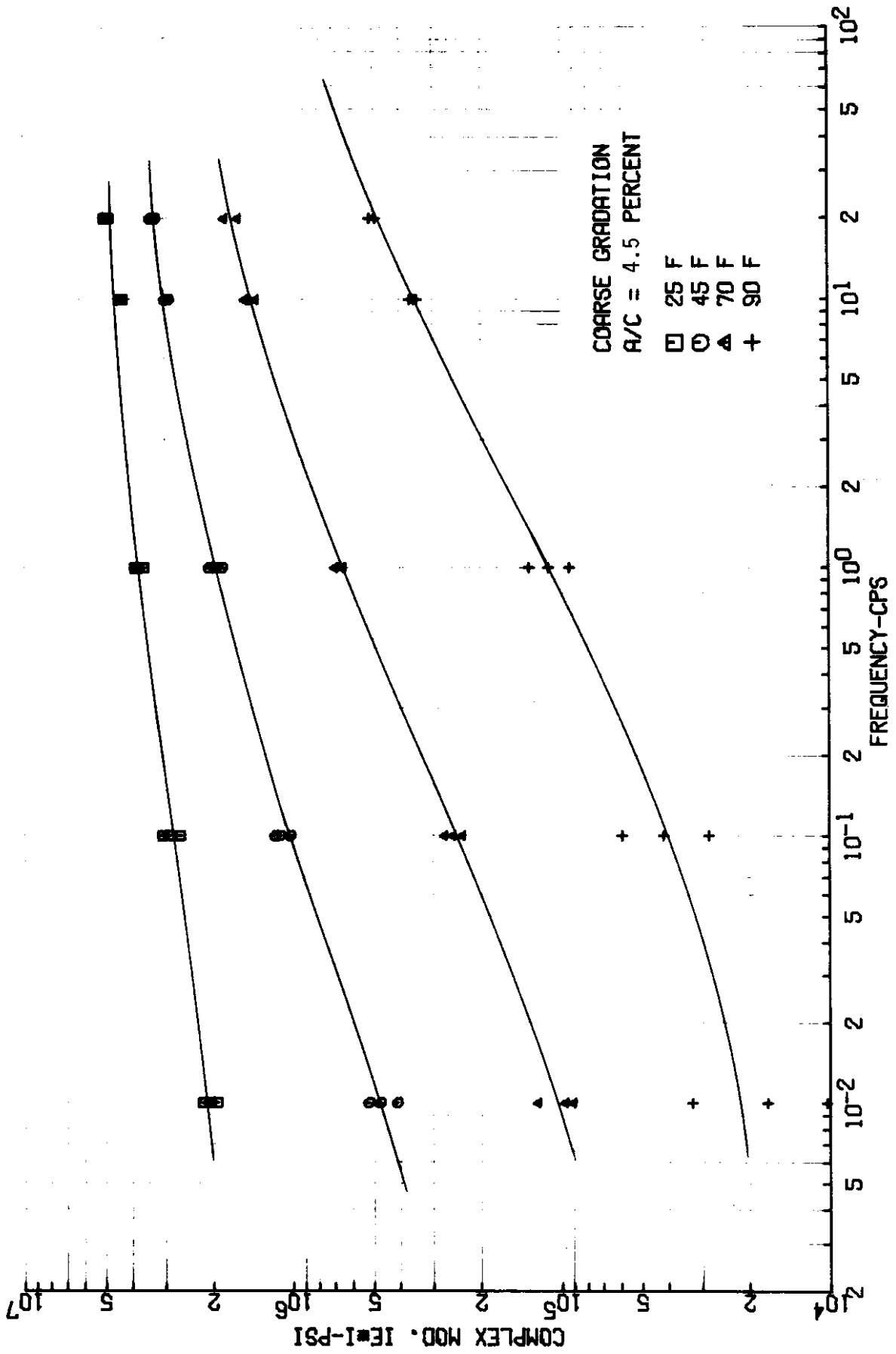


FIGURE 86 - Complex Modulus Versus Frequency at Different Temperatures

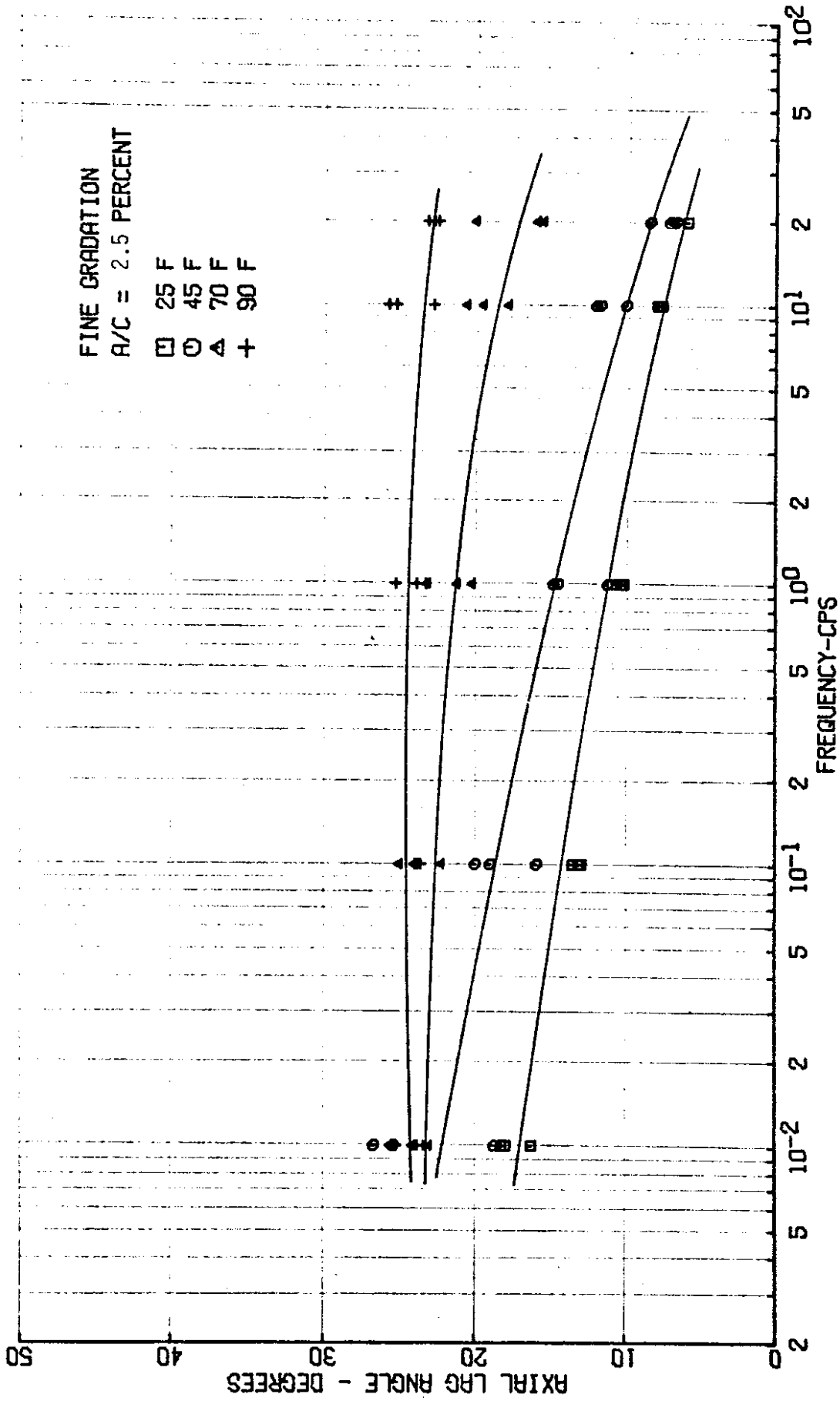


FIGURE 87 - Axial Lag Angle ϕ_1 Versus Frequency at Different Temperatures

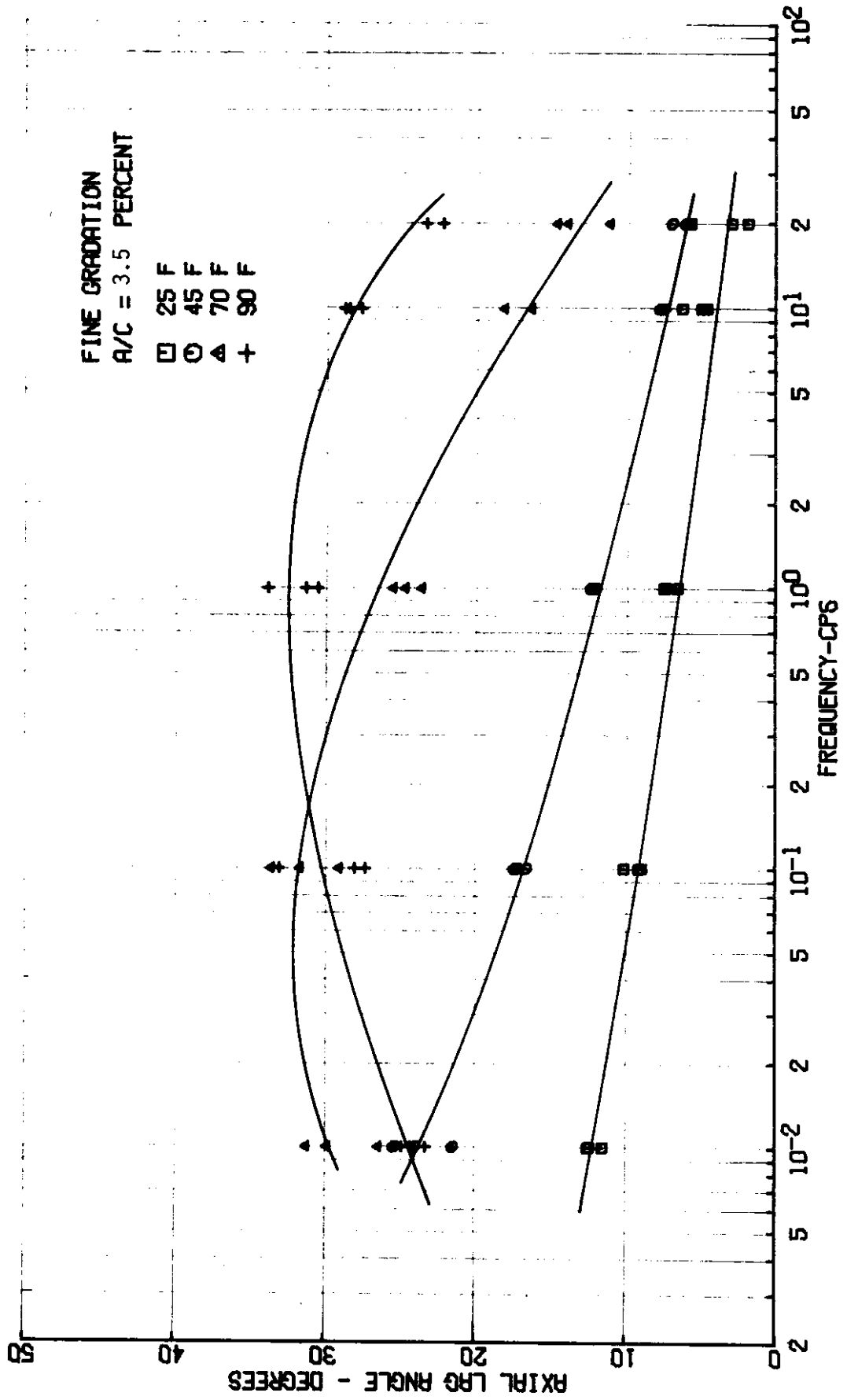


FIGURE 88 - Axial Lag Angle ϕ_1 Versus Frequency at Different Temperatures

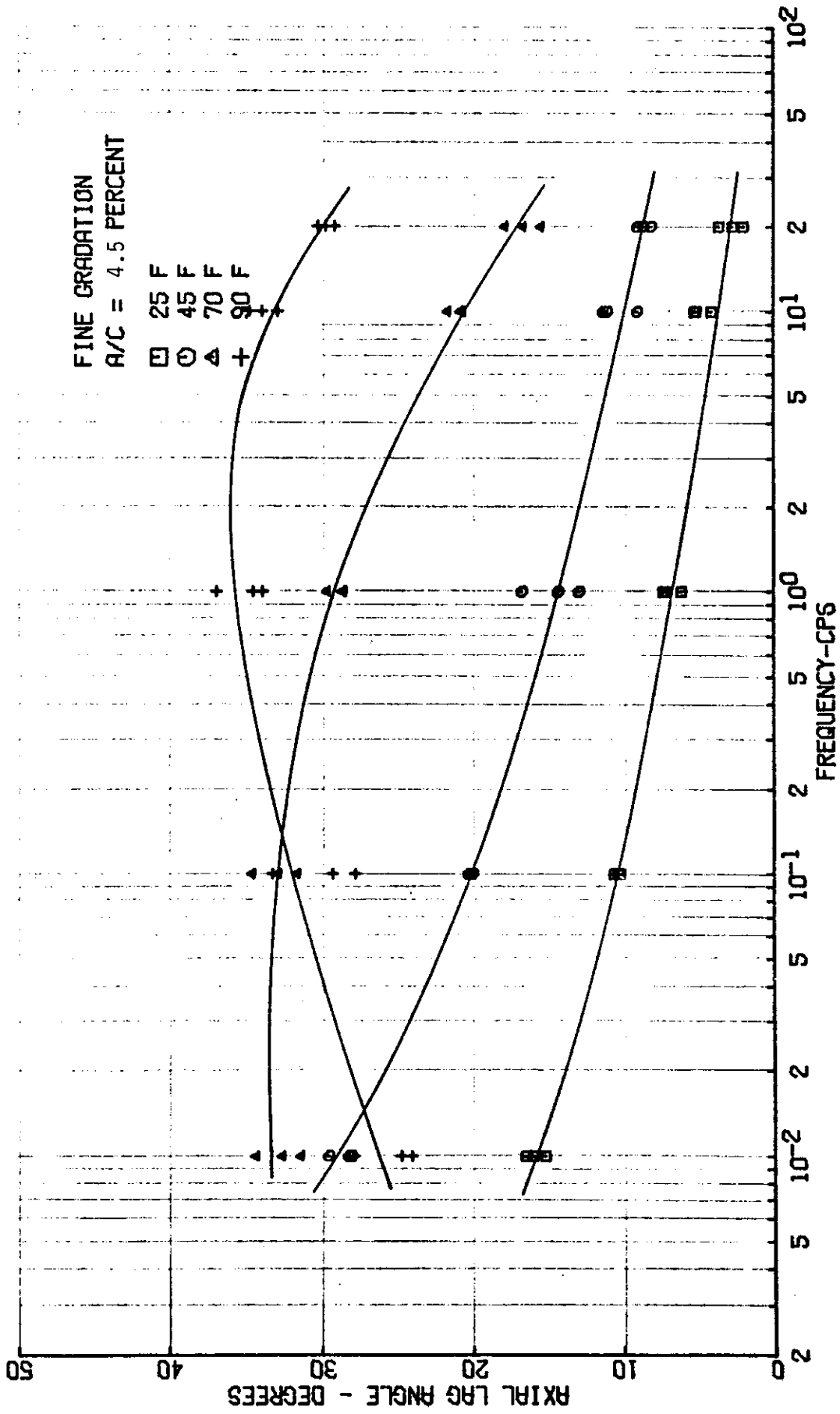


FIGURE 89 - Axial Lag Angle ϕ_1 Versus Frequency at Different Temperatures

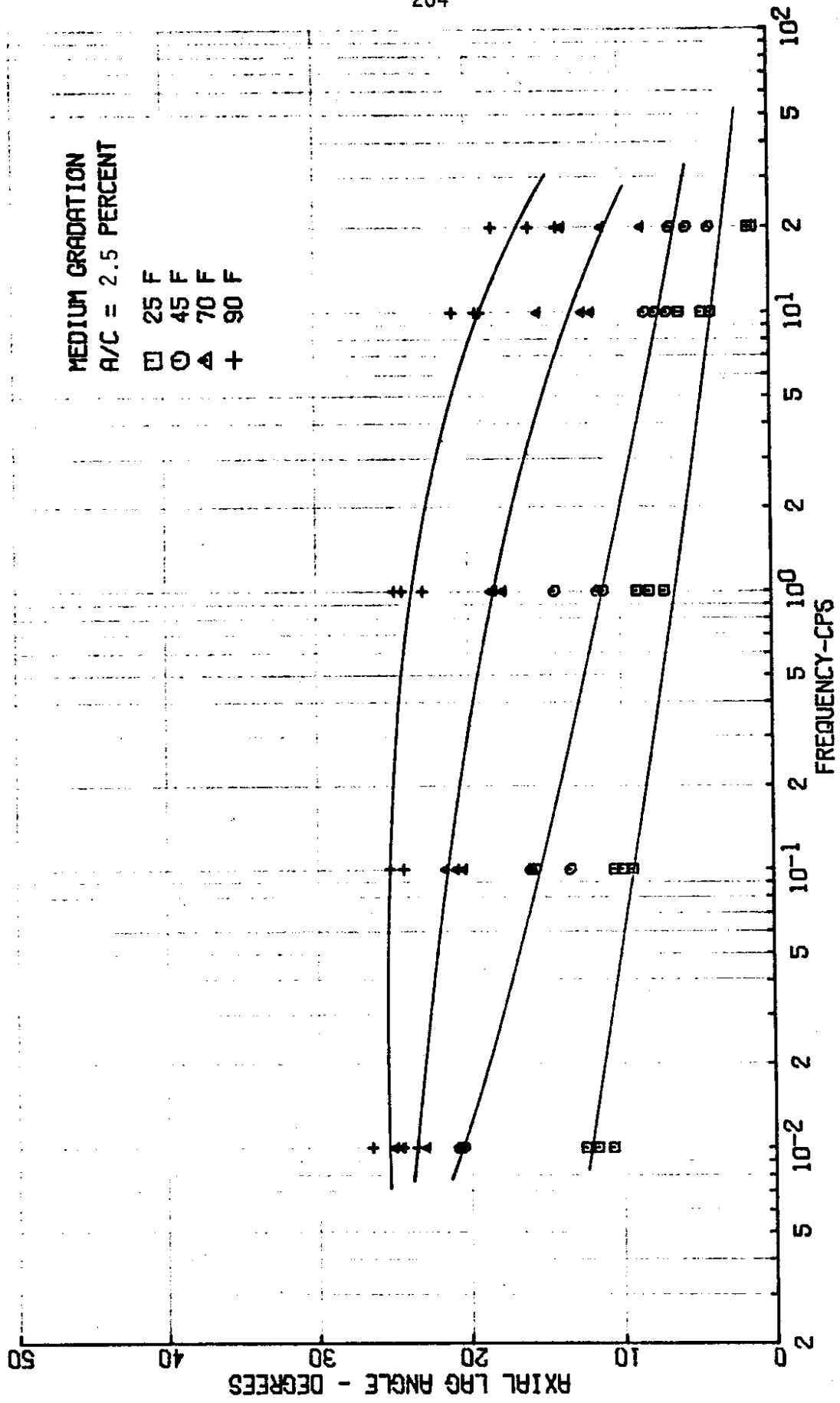


FIGURE 90 - Axial Lag Angle ϕ_1 Versus Frequency at Different Temperatures

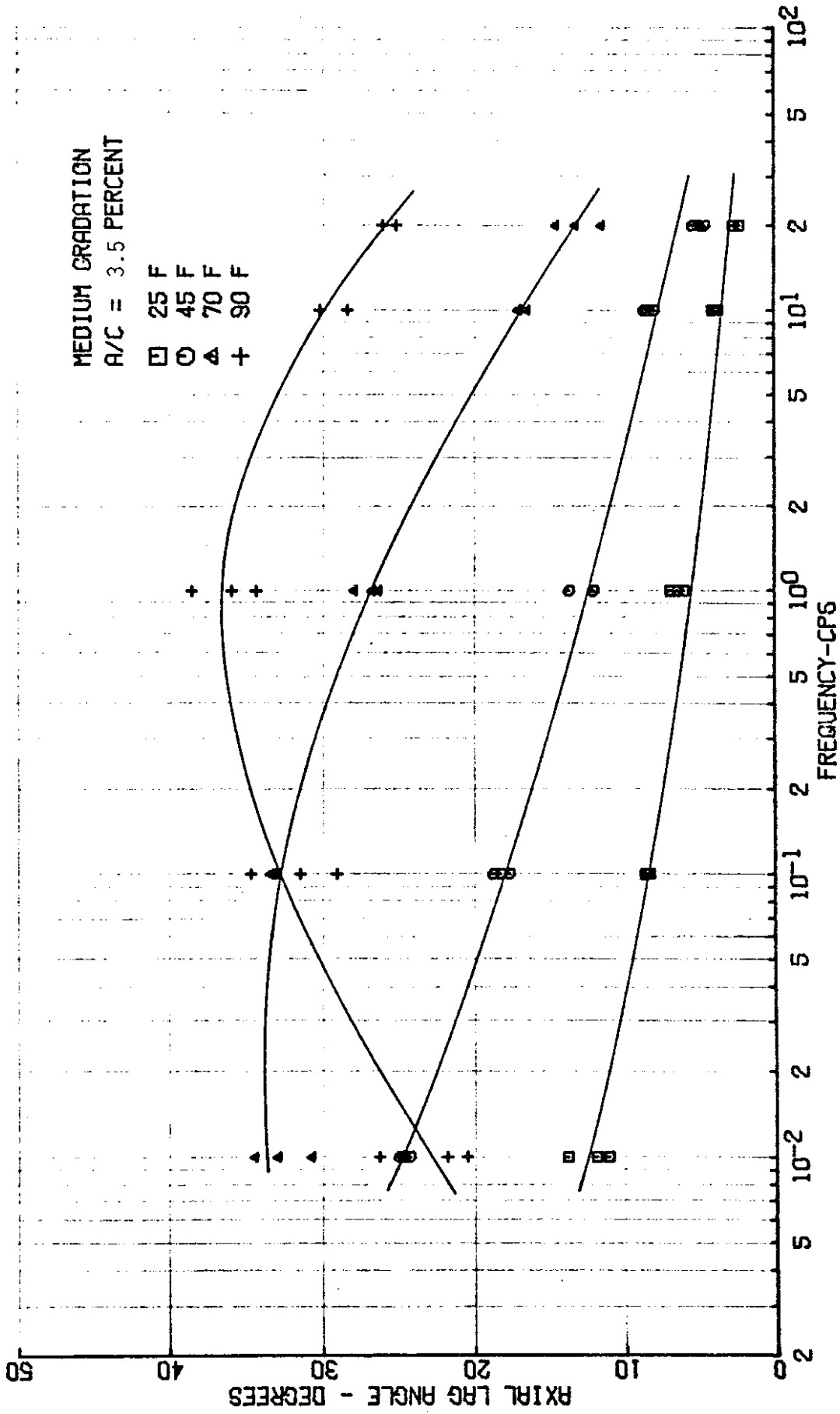


FIGURE 91 - Axial Lag Angle ϕ_1 Versus Frequency at Different Temperatures

MEDIUM GRADATION
A/C = 4.5 PERCENT

□ 25 F
○ 45 F
△ 70 F
+ 90 F

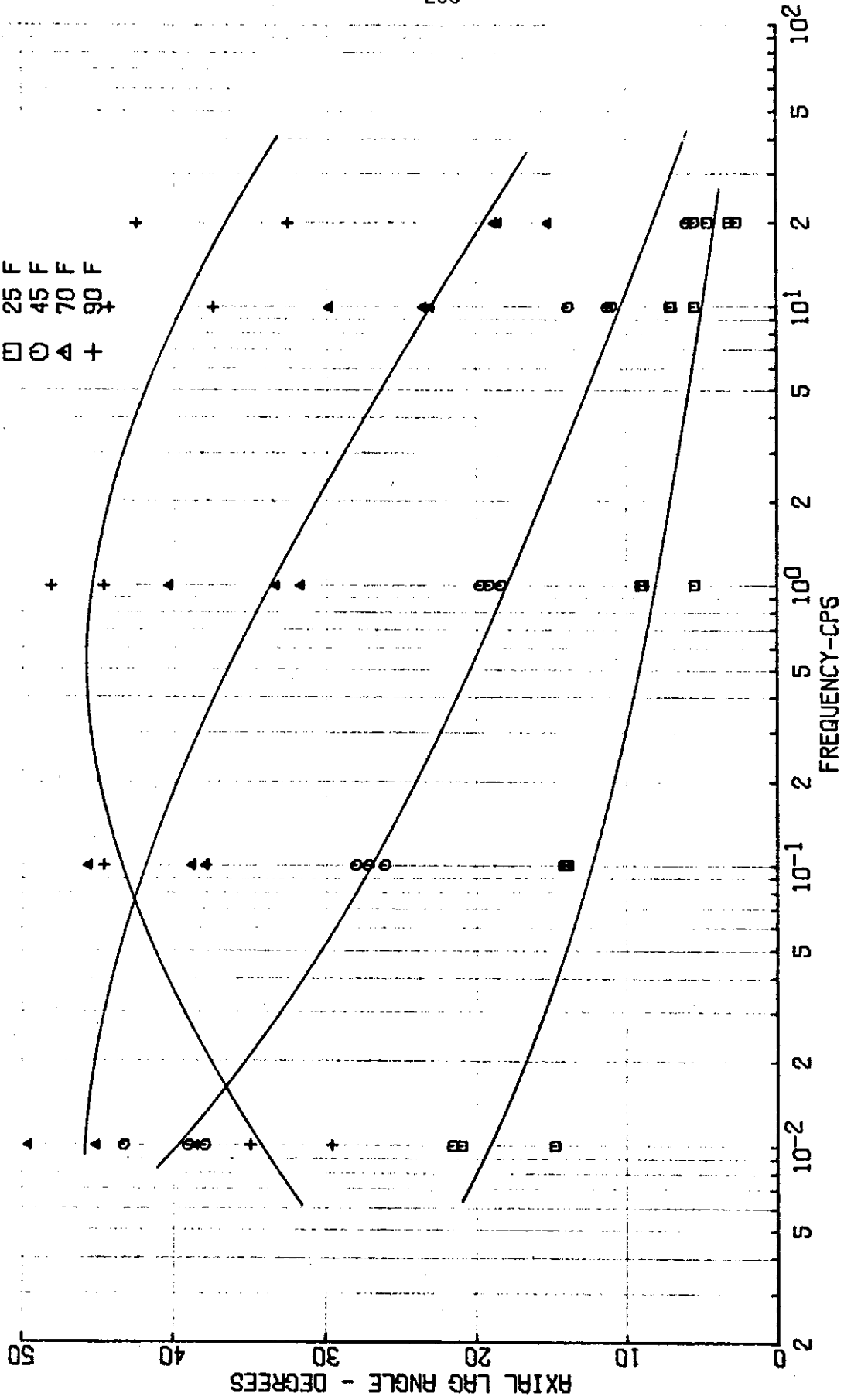


FIGURE 92 - Axial Lag Angle ϕ_1 Versus Frequency at Different Temperatures

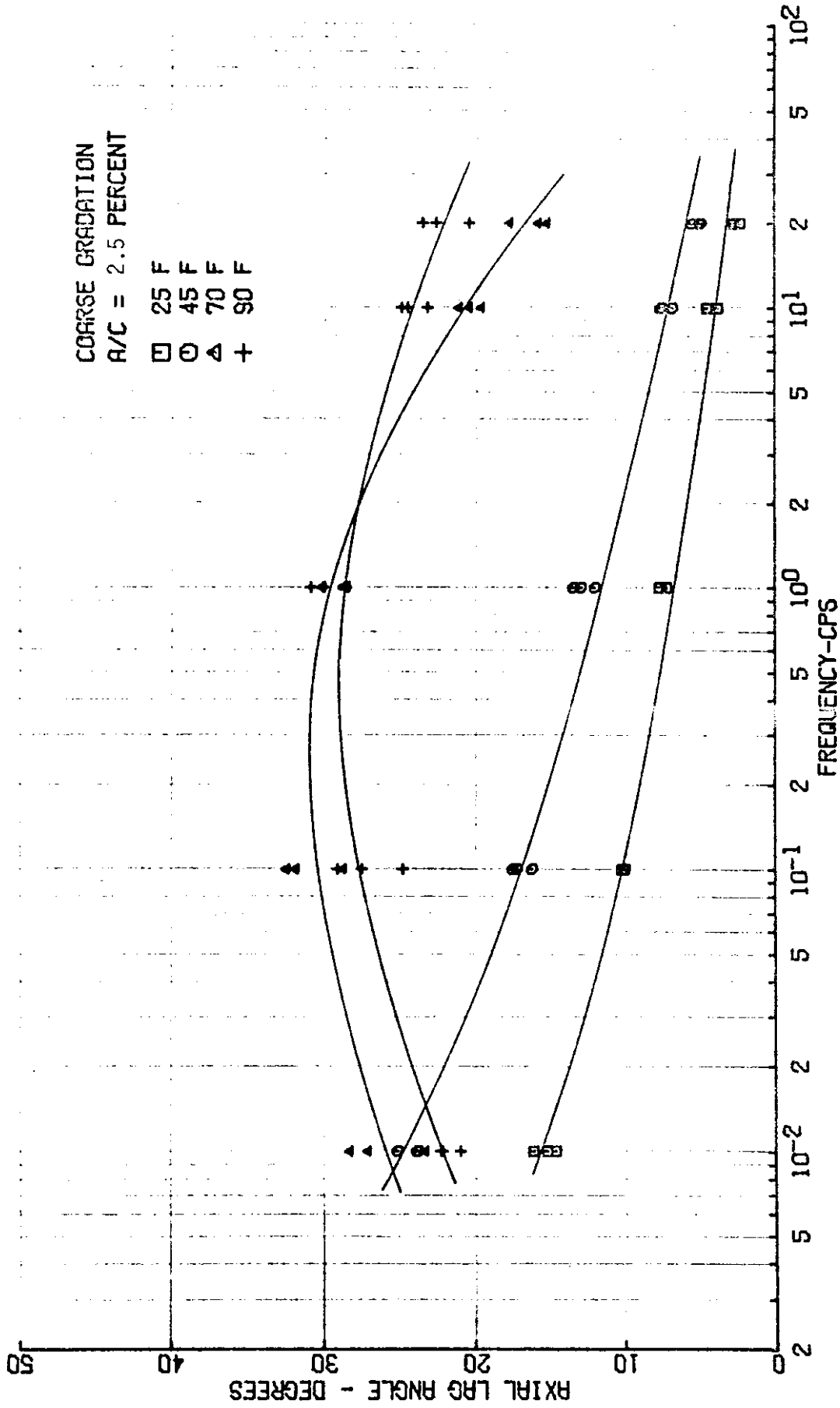


FIGURE 93 - Axial Lag Angle ϕ_1 Versus Frequency at Different Temperatures

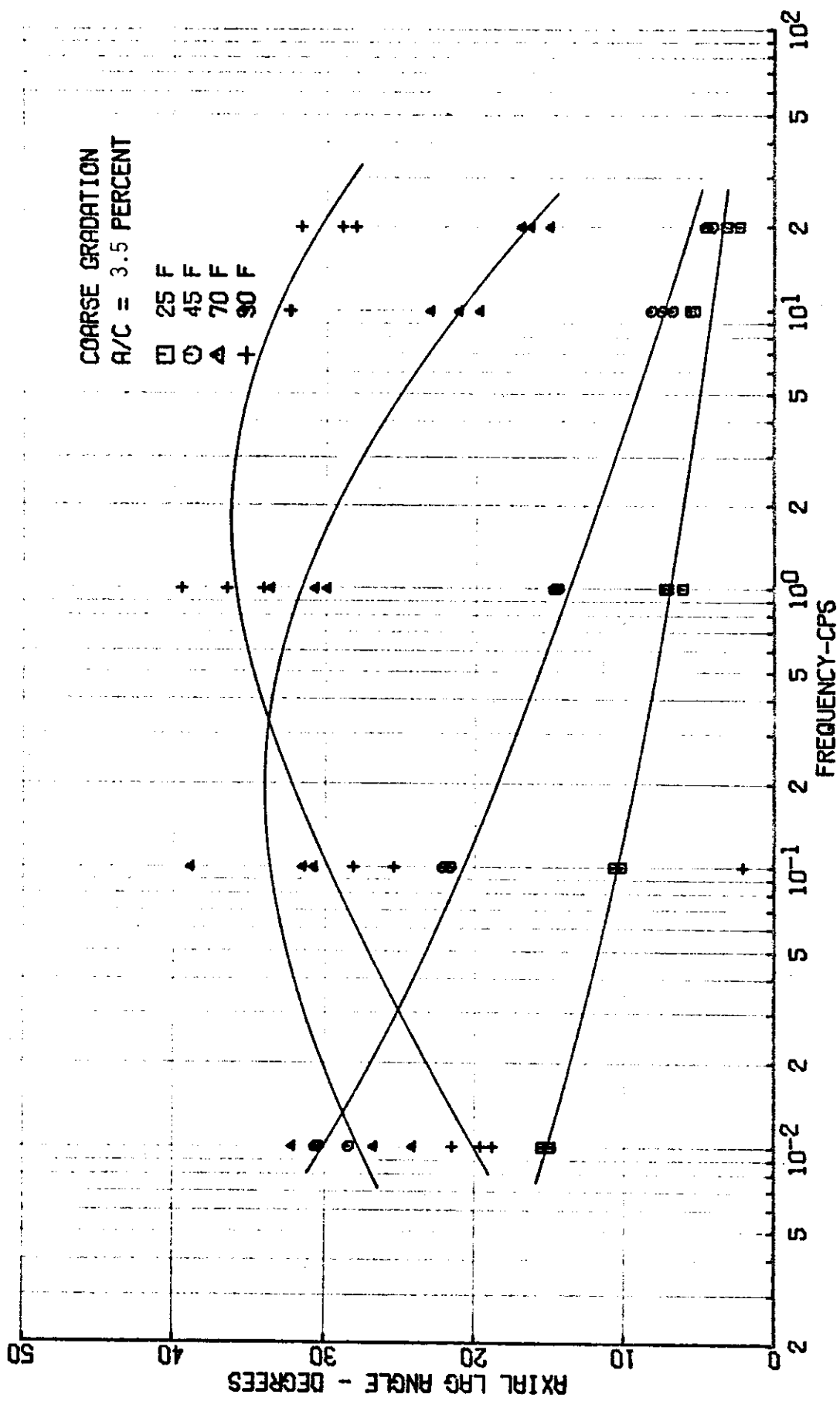


FIGURE 94 - Axial Lag Angle ϕ_1 Versus Frequency at Different Temperatures

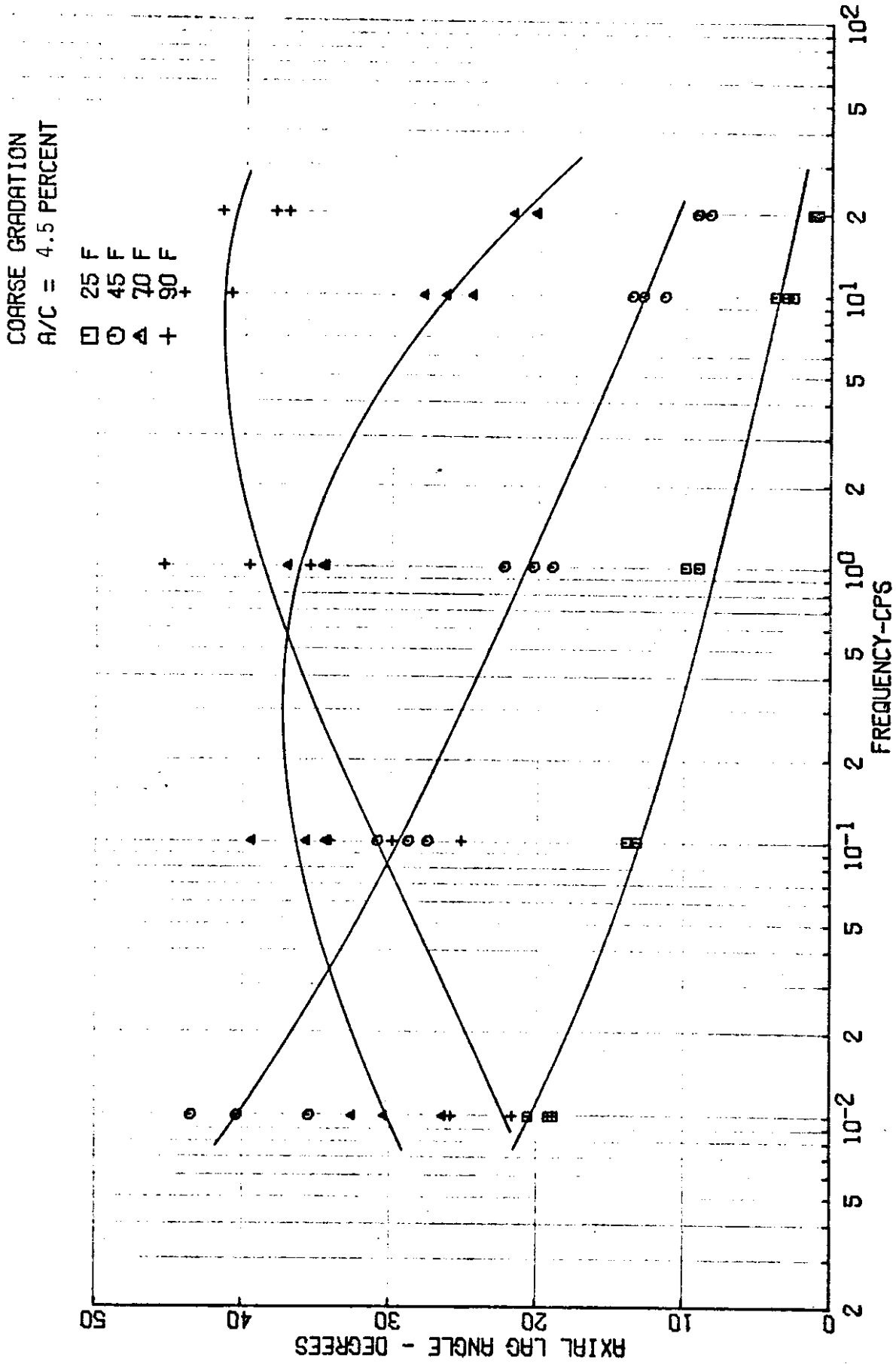


FIGURE 95 - Axial Lag Angle ϕ_1 Versus Frequency at Different Temperatures

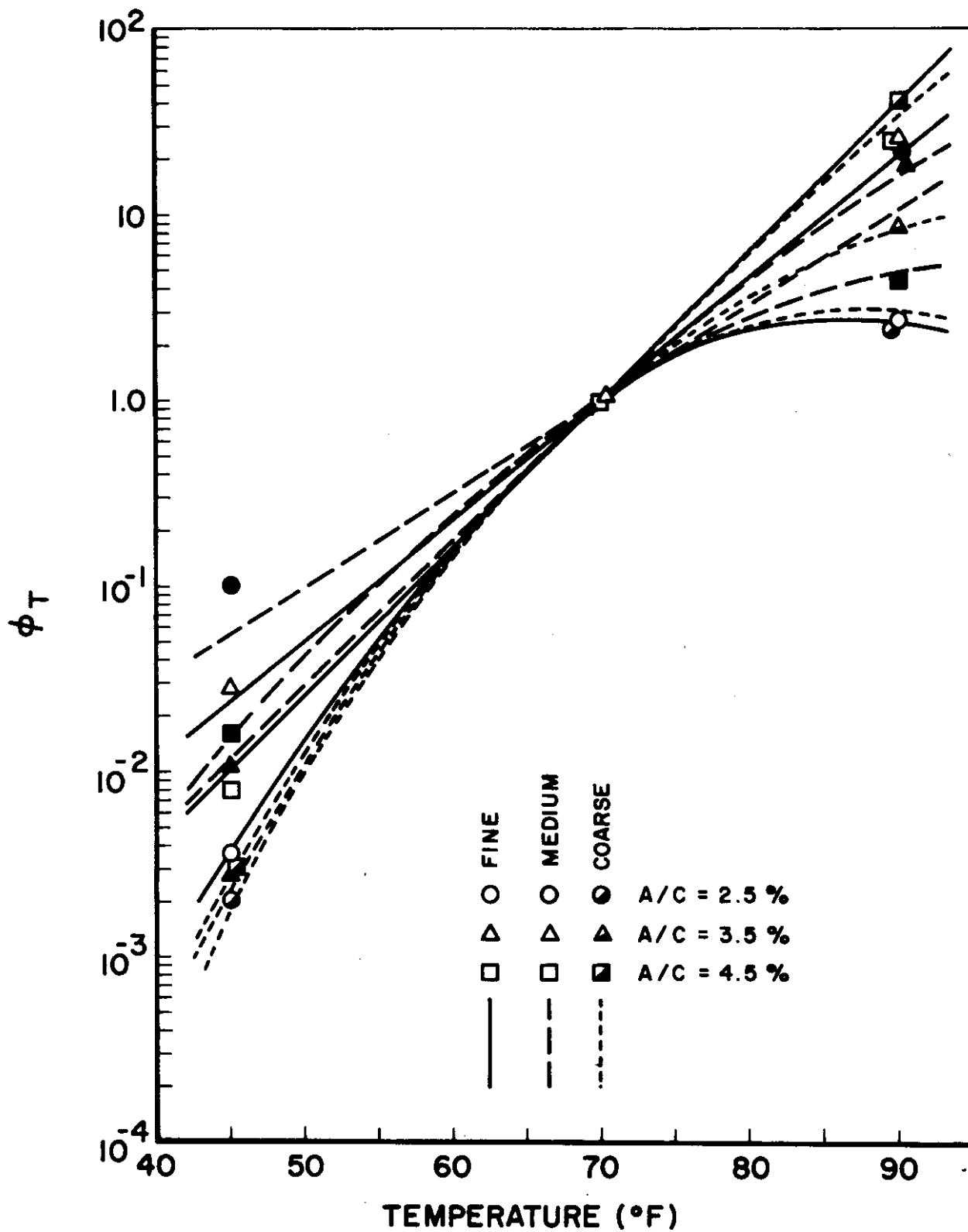


FIGURE 96 - Shift Factor Versus Temperature
(Reference Temperature = 70°F)

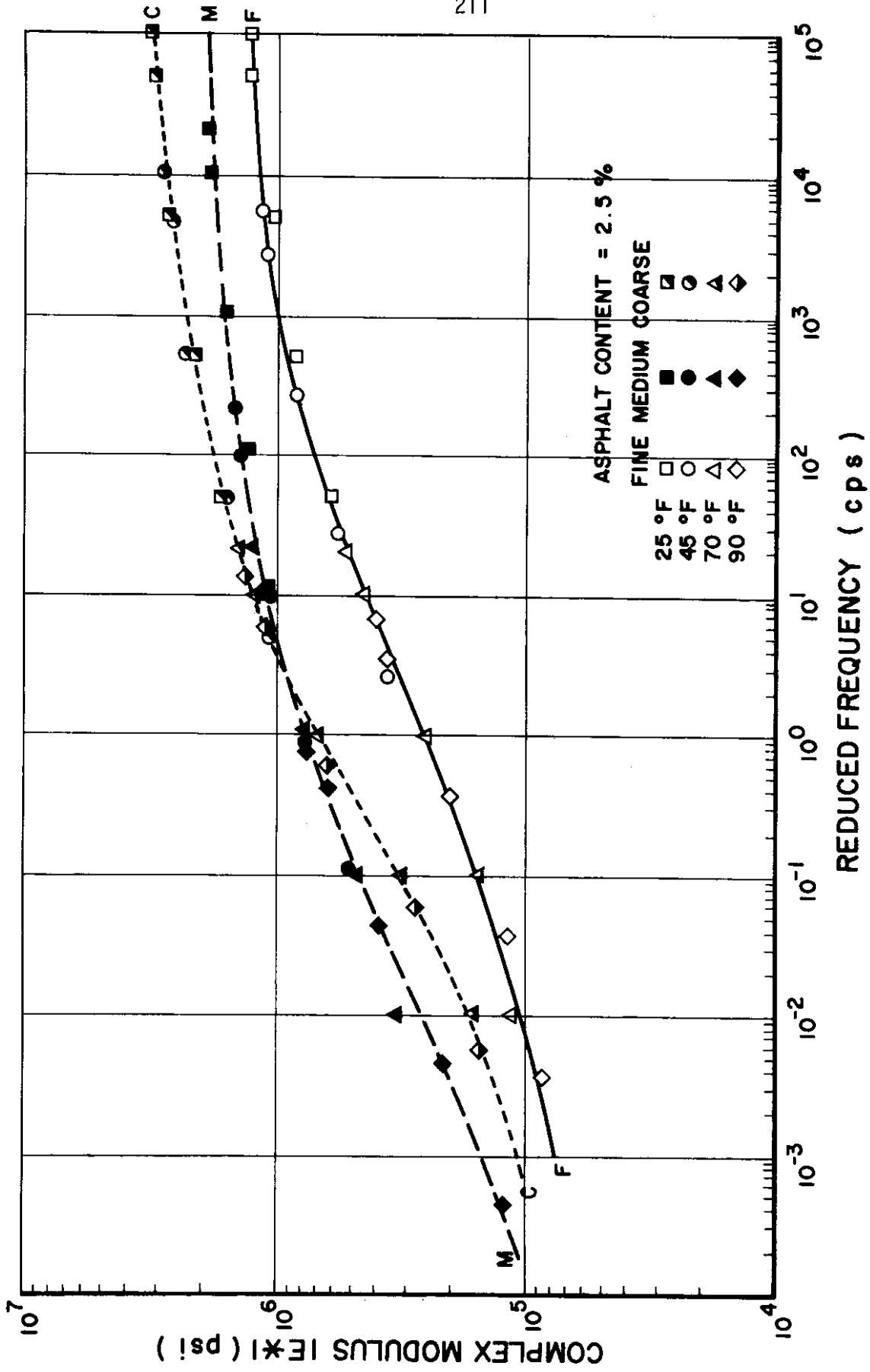


FIGURE 97 - Master Complex Modulus $|E^*|$ at Reference Temperature = 70°F

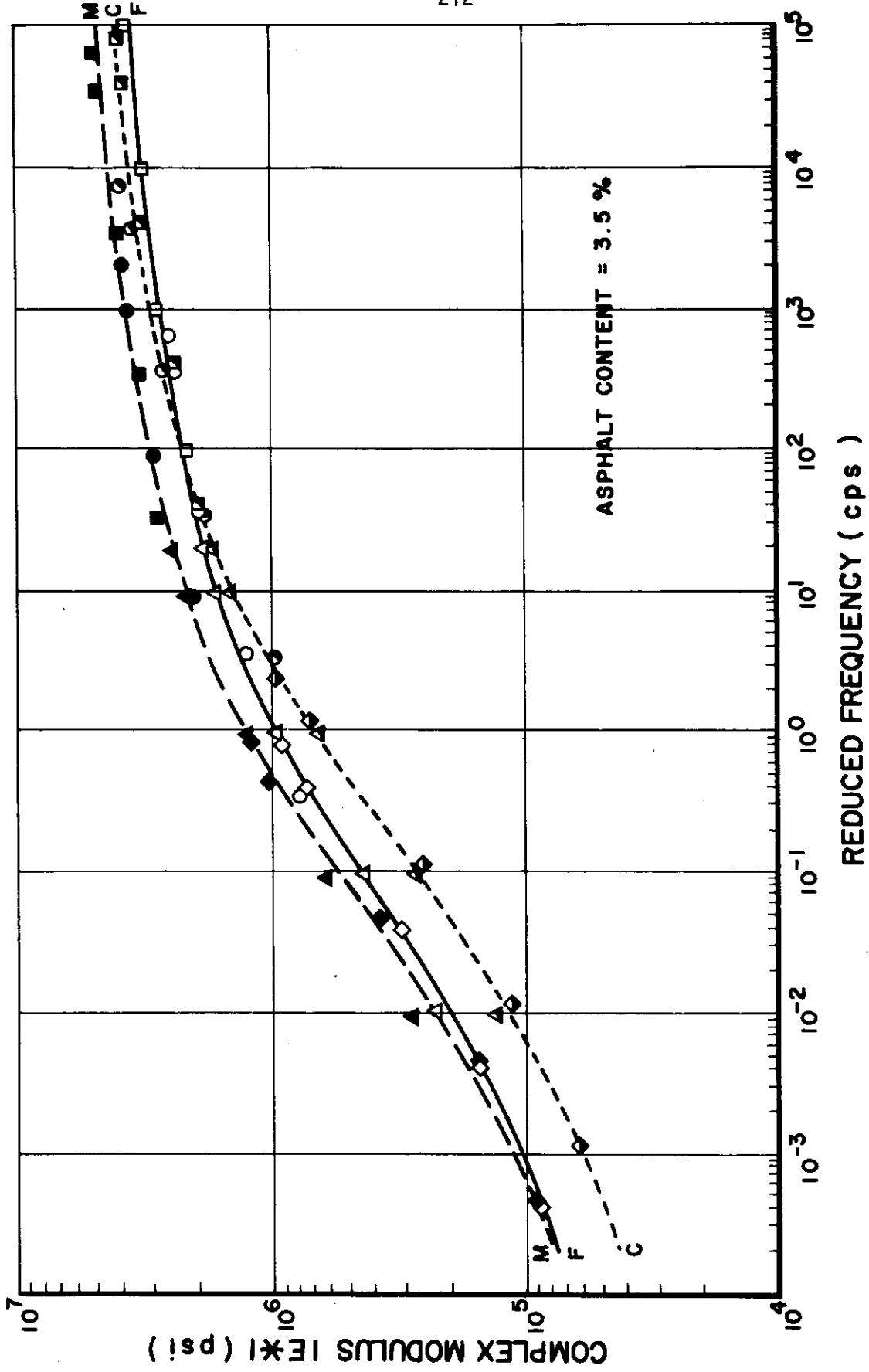


FIGURE 98 - Master Complex Modulus $|E^*|$ at Reference Temperature = 70°F

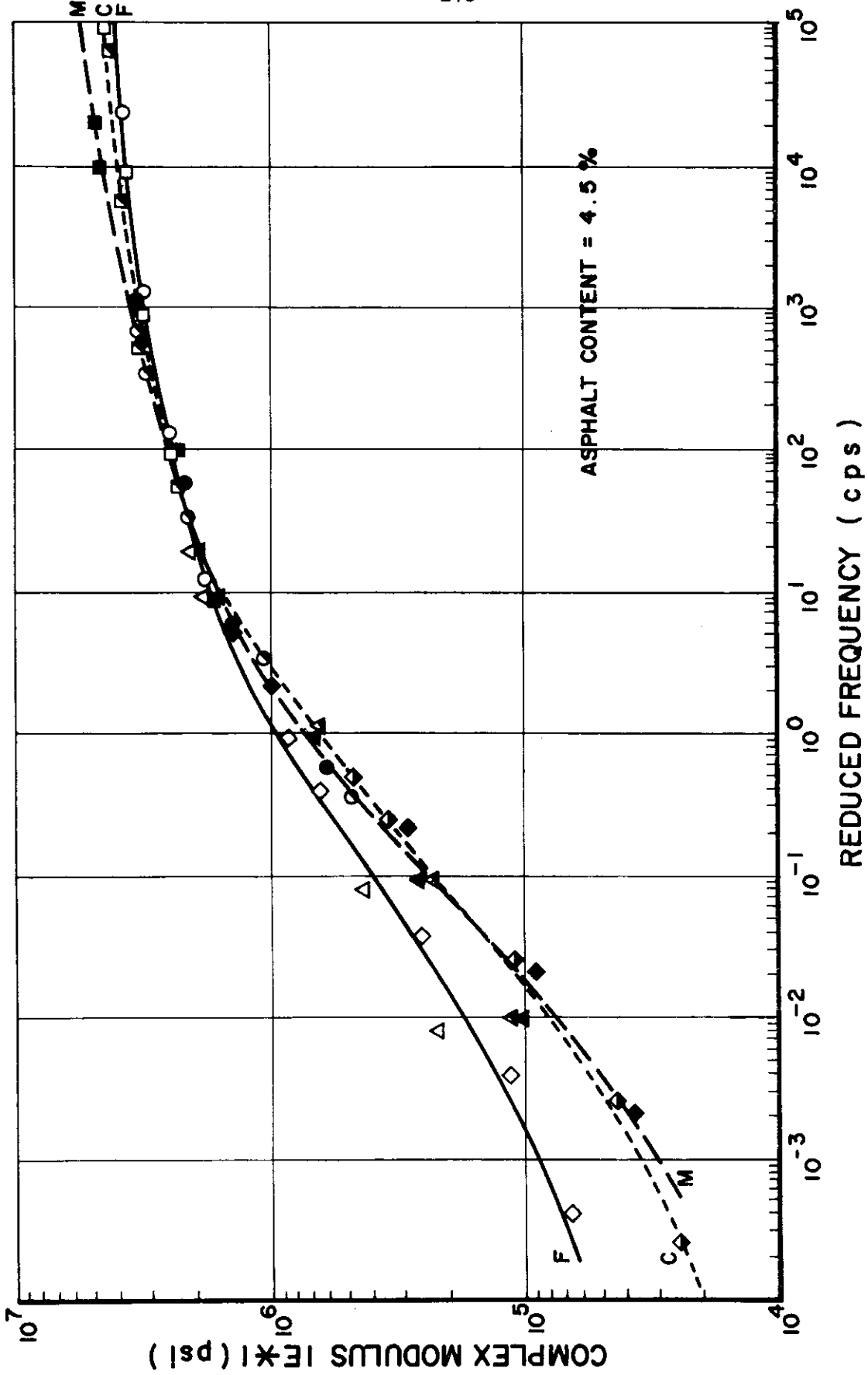


FIGURE 99 - Master Complex Modulus $|E^*|$ at Reference Temperature = 70°F

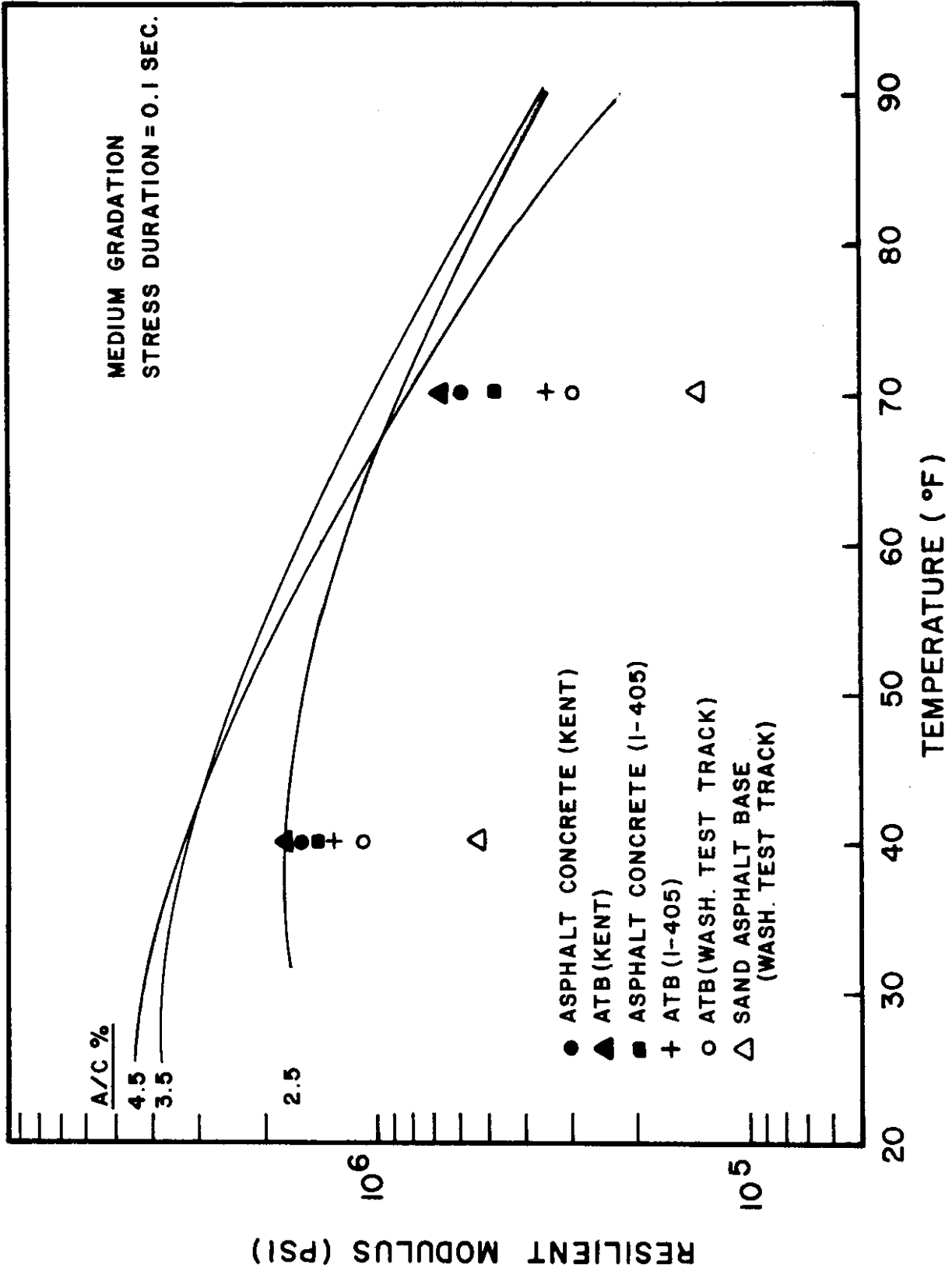
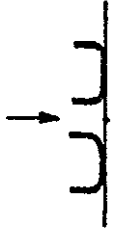


FIGURE 100 - Comparison of Laboratory Prepared Mixtures with Cores of ATB Sampled from WSU Test Track and In-Service Pavements

P = 9000 lbs.
 $\Delta t = 30$ sec.

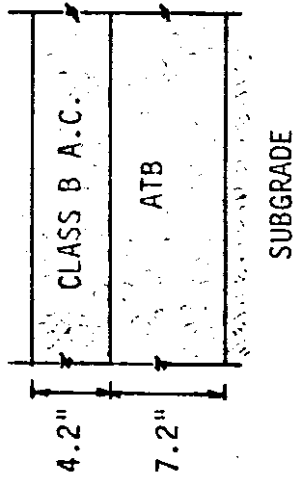


P = 1000 lbs.
 8 cps



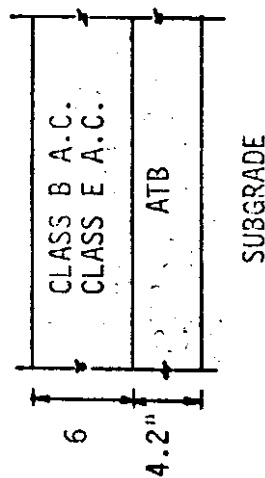
I-405

TEMPERATURE = 74°F



SR 167

TEMPERATURE = 61°F



BENKELMAN BEAM			DYNAFLECT		
RESILIENT MODULUS	POISSON'S RATIO	% DEFORMATION WITHIN LAYER	RESILIENT MODULUS	POISSON'S RATIO	% DEFORMATION WITHIN LAYER
25,000	0.32	6.5	600,000	0.3	-0.25
40,000	0.33	15.5	450,000	0.22	1.5
42,000	0.4	78	42,000	0.4	98.75
MEASURED DEFORMATION = 14×10^{-3} IN. COMPUTED DEFORMATION = 11.6×10^{-3} IN.			MEASURED DEFORMATION = 36.6×10^{-5} IN. COMPUTED DEFORMATION = 55×10^{-5} IN.		
200,000	0.325	5.5	1300,000	0.3	-1.5
280,000	0.48	7	1300,000	0.38	2
52,500	0.4	87.5	52,500	0.4	99.5
MEASURED DEFORMATION = 12.5×10^{-3} IN. COMPUTED DEFORMATION = 5.4×10^{-3} IN.			MEASURED DEFORMATION = 48.5×10^{-5} IN. COMPUTED DEFORMATION = 32×10^{-5} IN.		

FIGURE 101 - Summary of Material Properties and Deflections for WSU Test Track Comparison